DOC.20071220.0004

QA: QA

MDL-MGR-GS-000006 REV 00

December 2007

Redistribution of Tephra and Waste by Geomorphic Processes Following a Potential Volcanic Eruption at Yucca Mountain, Nevada

Prepared for:
U.S. Department of Energy
Office of Civilian Radioactive Waste Management
Office of Repository Development
1551 Hillshire Drive
Las Vegas, Nevada 89134-6321

Prepared by:
Sandia National Laboratories
OCRWM Lead Laboratory for Repository Systems
1180 Town Center Drive
Las Vegas, Nevada 89144

Under Contract Number
DE-AC04-94AL85000

DISCLAIMER

This report was prepared as an account of work sponsored by an agency of the United States Government. Neither the United States Government nor any agency thereof, nor any of their employees, nor any of their contractors, subcontractors or their employees, makes any warranty, express or implied, or assumes any legal liability or responsibility for the accuracy, completeness, or any third party's use or the results of such use of any information, apparatus, product, or process disclosed, or represents that its use would not infringe privately owned rights. Reference herein to any specific commercial product, process, or service by trade name, trademark, manufacturer, or otherwise, does not necessarily constitute or imply its endorsement, recommendation, or favoring by the United States Government or any agency thereof or its contractors or subcontractors. The views and opinions of authors expressed herein do not necessarily state or reflect those of the United States Government or any agency thereof.

QA: QA

Redistribution of Tephra and Waste by Geomorphic Processes Following a Potential Volcanic Eruption at Yucca Mountain, Nevada

MDL-MGR-GS-000006 REV 00

December 2007

Model Signature Page/Change History

Complete only applicable items.

1. Total Pages: 316

2. Type of Mathematical Model

☒ Process Model ☐ Abstraction Model ☐ System Model

Describe Intended Use of Model

This report describes a model for estimating the redistribution of waste-contaminated tephra by fluvial and hillslope processes following a volcanic eruption that releases waste onto the landscape. The model is directly integrated into TSPA.

3. Title

Redistribution of Tephra and Waste by Geomorphic Processes Following a Potential Volcanic Eruption at Yucca Mountain, Nevada

4. DI (including Revision No. and Addendum No.):

MDL-MGR-GS-000006 REV 00

	Printed Name	Signature	Date
5. Originator	Joshua S. Stein	Joshua S. Stein	12/17/07
6. Independent Technical Reviewer	Peter Swift	Peter Swift	12/17/07
7. Checker	Jim Schreiber	James D. Schreiber	12/17/2007
8. QCS/Lead Lab QA Reviewer	Sounia Kassabian-Darnell	Sounia K. Darnell	12/17/07
9. Responsible Manager/Lead	Geoff Freeze	Geoff Freeze	12/17/07
10. Responsible Manager	M. Kathryn Knowles	M. Kathryn Knowles	12/17/07

11. Remarks

Change History

12. Revision No. and Addendum No.	13. Description of Change
REV 00	Initial issue. • CR-6016 raises issues that are resolved in this model report. Section 5 includes a justification for excluding eolian erosion and deposition and sediment transport via sheetwash. Section 6.5.8 provides a transparent discussion of how the Cs-137 data is interpreted.

REV 00 (continued)	• CR-10603 identified compliance issues with the Scientific Notebook SN-M&O-SCI-051-V1. All the concerns raised in this CR are addressed in this report. Specifically, all direct inputs to this model development activity are documented in this report. All of the DTNs noted in the CR that listed incorrect references have been superseded or replaced. • CR-10604 identified compliance issues with the Scientific Notebook SN-M&O-SCI-050-V1. All the concerns raised in this CR are addressed in this report. Specifically, all data from scientific notebooks was submitted to TDMS, including the soils-geomorphic map, which is considered product output. All of the DTNs noted in the CR that listed incorrect references have been superseded or replaced. • CR-10792 identified problems with the reproducibility of DTN: MO0704DEMSOURC.000. These problems were corrected by superseding the DTN with DTN: SN0707DEMSOURC.001, which was independently reviewed for transparency, traceability, and reproducibility.

ACKNOWLEDGMENTS

The model described in this report was primarily developed by Professor Jon Pelletier, Ph.D., and two of his graduate students (Michael Cline and Steve DeLong) at the University of Arizona, Tucson. Following the model development phase, a new team assumed responsibility for the model and associated documentation. This team included Joshua S. Stein, Ph.D., as the "originator" for the model report. Sandra Dalvit-Dunn provided key technical contributions to the report. In addition, Tim Vogt, Terry Crump, and Michael Cline provided important technical support. William Statham assumed responsibility of the FAR software for TSPA and ran all FAR simulations presented in this report.

INTENTIONALLY LEFT BLANK

CONTENTS

Page

ACKNOWLEDGMENTS v

ACRONYMS AND ABBREVIATIONS xvii

1. PURPOSE 1-1
   1.1 SCOPE 1-4
   1.2 MODEL LIMITATIONS 1-4

2. QUALITY ASSURANCE 2-1

3. USE OF SOFTWARE 3-1
   3.1 SOFTWARE TRACKED BY SOFTWARE CONFIGURATION MANAGEMENT 3-1
   3.2 EXEMPT SOFTWARE 3-2

4. DIRECT INPUT 4-1
   4.1 DATA, PARAMETERS, AND OTHER MODEL INPUTS 4-1
      4.1.1 Repository Layout Data 4-1
      4.1.2 Digital Orthophotos 4-2
      4.1.3 Critical Slope Data 4-2
      4.1.4 Permeable Depth Data 4-3
      4.1.5 Cesium-137 Data 4-4
      4.1.6 Geomorphic Field Observation Data 4-7
      4.1.7 DEM and Watershed Boundary Grid 4-16
      4.1.8 Scour Depth Data 4-16
   4.2 CRITERIA 4-17
   4.3 CODES, STANDARDS, AND REGULATIONS 4-17

5. ASSUMPTIONS 5-1
   5.1 GENERAL MODEL ASSUMPTIONS 5-1
      5.1.1 Effects of Future Climate Changes 5-1
      5.1.2 Spatial Distribution of Fluvial Activity across the Fortymile Wash Alluvial Fan 5-2
      5.1.3 Floodplain Sedimentation 5-3
      5.1.4 Channel Geomorphology 5-3
      5.1.5 Concentrating Processes 5-4
   5.2 ASSUMPTIONS IN THE INITIAL MOBILIZATION AND REDISTRIBUTION OF THE TEPHRA AND CONTAMINANT 5-6
      5.2.1 Rate of Hillslope and Fluvial Redistribution to the RMEI Location 5-6
      5.2.2 Eolian Redistribution to the RMEI Location 5-7
      5.2.3 Mode of Sediment Transport 5-11
      5.2.4 RMEI Domain Is Not a Perfect Depozone 5-12
      5.2.5 Mass of Radionuclide Contaminant Is Directly Proportional to the Mass of Tephra Initially Deposited 5-12

CONTENTS (Continued)

Page

5.3 POST-REDEPOSITION DIFFUSIVE TRANSPORT IN THE RMEI DOMAIN 5-13
5.3.1 No Advection 5-13
5.3.2 No Further Mixing or Transport Occurs after Initial Deposition 5-13
5.3.3 Migration of Different Radionuclide Species in the Soil Profile at the RMEI Location 5-14

6. MODEL DEVELOPMENT 6-1
6.1 FEATURES, EVENTS, AND PROCESSES 6-1
6.2 CONCEPTUAL MODEL DESCRIPTION 6-1
6.2.1 Physical Process Description of Tephra Redistribution 6-1
6.2.2 FAR Conceptual Model Description 6-4
6.3 MATHEMATICAL MODEL DESCRIPTION 6-10
6.3.1 Nomenclature 6-10
6.3.2 Initial Conditions and Input Parameters 6-10
6.3.3 Algorithm Description 6-11
6.4 MODEL IMPLEMENTATION IN FAR V.1.2 6-34
6.5 DEVELOPMENT OF MODEL INPUTS FOR TSPA 6-36
6.5.1 Digital Elevation Model of the Fortymile Wash Drainage Basin 6-36
6.5.2 Critical Slope 6-37
6.5.3 Drainage Density 6-40
6.5.4 Area of Fortymile Wash Alluvial Fan and Channel Fraction Area 6-45
6.5.4.1 Area of Fortymile Wash, *A* 6-46
6.5.4.2 Channel Fraction Area, *F* 6-46
6.5.5 Permeable Depth on Divides and in Channels 6-46
6.5.5.1 Permeable Depth on Divides 6-46
6.5.5.2 Permeable Depth in Channels 6-47
6.5.6 Scour Depth at the Fortymile Wash Fan Apex 6-48
6.5.7 Volcanic Vent Parameters 6-50
6.5.7.1 Vent Location 6-50
6.5.7.2 Vent Radius 6-52
6.5.8 Diffusivity of Radionuclides on Divides and in Channels 6-52
6.5.8.1 Diffusivity of Radionuclides on Divides 6-54
6.5.8.2 Diffusivity of Radionuclides in Channels 6-55
6.5.9 Miscellaneous Input Parameters 6-56
6.5.9.1 The Output Time Step (Δt) 6-56
6.5.9.2 Model Duration (T) 6-56
6.5.9.3 *oflag* 6-56
6.5.10 Summary of Model Parameter Values for TSPA 6-56
6.6 PARAMETER SENSITIVITY ANALYSIS 6-57
6.6.1 Parameter Sensitivity for the Hillslope and Fluvial Redistribution of Tephra in the Upper Drainage Basin 6-58
6.6.2 Parameter Sensitivity for the Diffusion of Radionuclides at the RMEI Location 6-59

CONTENTS (Continued)

Page

6.6.3 Sensitivity Analysis Conclusions 6-64

7. MODEL VALIDATION 7-1
7.1 VALIDATION OF INPUT 7-1
7.1.1 Grids of Tephra Thickness and Waste Concentration 7-1
7.1.2 DEMs and DOQQs 7-1
7.1.3 Field Data 7-2
7.2 VALIDATION DURING MODEL DEVELOPMENT 7-13
7.2.1 Bilinear Interpolation on Input ASHPLUME Tephra and Waste Concentration Grids and Rectification to DEM (Step 1) 7-13
7.2.2 Fill Pits and Flats in the Input DEM (Step 2) 7-15
7.2.3 Compute Slope, Contributing Area, and Scour Depth Grids (Step 3) 7-17
7.2.4 Calculate Total Mass of Mobilized Tephra/Dilution Factor (Step 4) 7-23
7.2.5 Transfer of Tephra from the Upper Basin to the RMEI Domain and the Calculation of Initial Radionuclide Concentrations on Divides and in Channels (Step 5) 7-26
7.2.6 Compute Diffusion of Radionuclides into Soil (Step 6) 7-30
7.2.7 Test Cases for the FAR Model 7-37
7.2.8 Distribution of Tephra Mass 7-37
7.2.8.1 Topographic Classification of Tephra on Landscape 7-38
7.2.8.2 Calculation of Mobilized Tephra Mass 7-38
7.2.8.3 Transfer of Tephra Mass to RMEI Location 7-39
7.2.8.4 Summary of Tephra Mass Distribution 7-40
7.2.9 Confidence Building from Sensitivity Studies 7-40
7.3 POST-DEVELOPMENT MODEL VALIDATION 7-41
7.3.1 Corroboration of Model Results with Relevant Information Published in Refereed Journal 7-41
7.3.1.1 Lathrop Wells Site Description 7-42
7.3.1.2 Field Data 7-43
7.3.1.3 Lathrop Wells Scour-Dilution-Mixing Model 7-47
7.3.1.4 Lathrop Wells Input Data and Model Results 7-48
7.3.1.5 Summary of Lathrop Wells Corroboration 7-50
7.3.1.6 Publication of Diffusion Model for Radionuclide Migration into Soil 7-51
7.3.2 Critical Review 7-51
7.3.2.1 Originator's General Response to Dr. Mayer's Critical Review 7-52
7.3.2.2 Originator's General Response to Dr. Hackett's Critical Reviews 7-56
7.3.2.3 Summary of Critical Reviews 7-57

CONTENTS (Continued)

Page

8. CONCLUSIONS 8-1
8.1 MODEL SUMMARY 8-1
8.1.1 Technical Product Output 8-2
8.2 MODEL LIMITATIONS AND UNCERTAINTIES 8-3
8.3 YUCCA MOUNTAIN REVIEW PLAN CRITERIA ASSESSMENT 8-3

9. INPUTS AND REFERENCES 9-1
9.1 DOCUMENTS CITED 9-1
9.2 CODES, STANDARDS, REGULATIONS, AND PROCEDURES 9-7
9.3 SOURCE DATA, LISTED BY DATA TRACKING NUMBER 9-7
9.4 DEVELOPED AND PRODUCT OUTPUT DATA, LISTED BY DATA TRACKING NUMBER 9-8
9.5 SOFTWARE CODES 9-8

APPENDIX A: GEOMORPHIC CHARACTERIZATION OF THE FORTYMILE WASH ALLUVIAL FAN A-1

APPENDIX B: YUCCA MOUNTAIN REVIEW PLAN (NUREG-1804) ACCEPTANCE CRITERIA B-1

APPENDIX C: CRITICAL REVIEWS C-1

APPENDIX D: NOMENCLATURE USED D-1

APPENDIX E: VERIFICATION OF THE SOLUTION TO AN INITIAL-VALUE PROBLEM E-1

FIGURES

Page

1-1. Location Map of the Yucca Mountain Region Centered on the RMEI Location 1-2
1-2. Map Showing the Upper Drainage Basin Domain (colored by elevation), the RMEI Location (pink), and the Hypothetical Vent Location 1-3
5-1. USGS Orthophoto Mosaic of the Fortymile Wash Alluvial Fan 5-10
6.2-1. Schematic Diagram of Tephra Redistribution Model 6-5
6.3.3-1. Geometry Conventions Used for Polar Coordinate Bilinear Interpolation 6-12
6.3.3-2. Rectified ASHPLUME Output Grid Displayed over the Upper Drainage Basin Domain and Centered at the Vent Location 6-13
6.3.3-3. Local Slope Calculated in the Upper Drainage Basin Domain 6-16
6.3.3-4. Illustration of the Moving Window Used to Calculate the 5 × 5 Grid-cell Average Slope 6-17
6.3.3-5. Map of Contributing Area for the Upper Drainage Basin Domain Calculated Using the Bifurcation Routing Method 6-19
6.3.3-6. Scour Depth Predicted by the FAR for the Upper Drainage Basin Domain 6-22
6.3.3-7. Tephra Classification Scheme Based on Slope and Stream Power 6-23
6.3.3-8. Dilution Factor Calculated within the Channel Network for an Example Run of the FAR Model 6-26
6.3.3-9. Example Model Output for Southern Part of Drainage Basin 6-27
6.3.3-10. Plot of Normalized Concentration versus Depth in the Channels for a Range of Times Following an Eruption 6-31
6.3.3-11. Flow Chart for Tephra Redistribution Model 6-33
6.5.2-1. Distribution Curve for Grid Cell Slope Values within the Watershed of the Upper Drainage Basin Domain 6-39
6.5.2-2. Maps Showing Areas (red) Where the Local Slope Exceeds a Critical Slope Value for the Upper Drainage Basin Domain 6-40
6.5.3-1. Upper Fortymile Drainage Basin Shaded Relief Map Showing the Location of the 34 Selected Channel Heads near the Top of Yucca Mountain 6-42
6.5.3-2. Close-up View of the Top of Yucca Mountain Showing the Location of 34 Channel Heads Identified on the DOQQ Imagery 6-43
6.5.3-3. Plot Showing the Average Distance between Observed and Predicted Channel Heads for Various Values of Stream Power for 34 Selected Channels on the East Slope of Yucca Mountain 6-45
6.5.6-1. Scour Measurements a) Pre-flood Emplacement, b) Maximum Scour in the Channel (H), and c) Post-flood Fill Emplacement 6-48
6.6.1-1. Plot of 100 Realization LHS Results against Critical Slope Value 6-58
6.6.1-2. Plot of 100 Realization LHS Results against Scour Depth Value 6-59
6.6.1-3. Plot of 100 Realization LHS Results against Drainage Density Value 6-59
6.6.2-1. Surface Concentration on Divides versus Time for Various Values of D_d 6-61
6.6.2-2. Integrated Waste to the B Depth on Divides versus Time for Various Values of D_d 6-61
6.6.2-3. Surface Concentration in Channels versus Time for Various Values of D_c 6-62
6.6.2-4. Integrated Waste to the B Depth in Channels versus Time for Various Values of D_c 6-62

FIGURES (Continued)

Page

6.6.2-5. Surface Concentration on Divides versus Time for Various Values of L_d 6-63
6.6.2-6. Integrated Waste to the B Depth on Divides versus Time for Various values of L_d 6-63
7.1.3-1. Plot of Normalized Concentration versus Depth in the Channels for a Range of Times Following an Eruption 7-5
7.1.3-2. Example Scour Depth Predicted by the FAR Model for Fortymile Wash between the Narrows and the Fan Apex 7-8
7.1.3-3. Plot of Normalized Concentration versus Depth for the Divide Sample Point Cs-071702-E at a Time of 50 Years after Deposition of the Cesium and the Maximum Range of Calculated Diffusivities Based on Measurement Error 7-11
7.1.3-4. Plot of Normalized Concentration versus Depth for the Channel Sample Point Cs-071702-B at a Time of 50 Years after Deposition of the Cesium and the Maximum Range of Calculated Diffusivities Based on Measurement Error 7-12
7.1.3-5. Plot of Diffusivity versus an Assumed Fraction of ^{137}Cs below the Lower Sample Zones Maximum Depth of 6 cm for Sample Point Cs-071702-B 7-13
7.2.1-1. Comparison between ASHPLUME Tephra Thickness and Interpolated Tephra Thickness Values for an Example Eruption 7-15
7.2.2-1. Map Showing the Location of Grid Cells Filled with the "Fill Pits and Flats" Routine 7-16
7.2.2-2. Histograms Showing the Frequency of Elevation Changes Made to Fill Pits and Flats 7-17
7.2.3-1. Histogram of the Difference in Cell Values of Slope Calculated Using the Four-Direction Method Used by FAR and the Steepest Descent Method Implemented Using ArcGIS Tools 7-18
7.2.3-1. Plot of Observed Scour Depth versus Unit Discharge 7-20
7.2.3-2. Difference in Scour Depth Predicted by Equations 6.3-12 and 6.3-14 for Two Bounding Values of Average Channel Width 7-22
7.2.4-1. Channel Maps for Two Values of Drainage Density: (a) 20 km^{-1}, (b) 33 km^{-1} 7-24
7.2.4-2. Maps of Tephra Thickness Stored under Scour Depth for an Example ASHPLUME Result Shown with Two Values of Drainage Density: Left: 20 km^{-1} and Right: 33 km^{-1} 7-25
7.2.5-1. Plot of Stream Flow Velocity versus Particle Size Suspended 7-27
7.2.5-2. Example Dilution Factor Results near Fan Apex 7-29
7.2.6-1. Total Activity of ^{137}Cs as a Function of Depth for Chernobyl 7-35
7.2.6-2. Total Activity of ^{137}Cs as a Function of Depth for Harwell Airfield 7-36
7.3.1-1. Location Map of the Study Areas in Amargosa Valley, Nevada 7-43
7.3.1-2. Sample Location Map, Tephra Concentration, and Model Results for Lathrop Wells Site 7-45
7.3.1-3. Field Photos Illustrating the Three-dimensional Pattern of Contaminant Dilution near Lathrop Wells Tephra Sheet 7-46
7.3.1.3-4. Model Prediction for Tephra Concentration and Scour/mixing Depth Downstream from the Tephra Sheet of the Lathrop Wells Volcanic Center 7-49
A-1. Fortymile Wash Alluvial Fan as Seen on Digital Orthophoto Quadrangles A-3

FIGURES (Continued)

Page

A-2. Locations of Field Observations Shown on Fortymile Wash Alluvial Fan (points) as Seen on Digital Orthophoto Quadrangles A-5
A-3. Transparent Geomorphic Map of the Fortymile Wash Alluvial Fan Shown with Field Observations (points) Overlain on Digital Orthophoto Quadrangles A-9
A-4. Geomorphic Map of the Fortymile Wash Alluvial Fan A-10
A-5. Detail Geomorphic Map 1 of the Fortymile Wash Alluvial Fan A-11
A-6. Detail Geomorphic Map 2 of the Fortymile Wash Alluvial Fan A-12
A-7. Detail Geomorphic Map 3 of the Fortymile Wash Alluvial Fan A-13

INTENTIONALLY LEFT BLANK

TABLES

Page

3.1-1. Qualified Software 3-1
3.2-1. Exempt Software 3-2
4.1-1. Direct Input Data Sources 4-1
4.1-2. DOQQs Used in This Report 4-2
4.1-3. Critical Slope Measurements for Tephra Mobilization from Sunset Crater Area near Flagstaff, AZ 4-2
4.1-4. Summary of Permeable Depth Data 4-4
4.1-5. Cesium-137 Measurements 4-5
4.1-6. Geomorphic Field Observations 4-7
4.1-7. Summary of Scour Depth Data 4-17
6.4-1. Input Parameters for the FAR V.1.2 Tephra Redistribution Model 6-34
6.5.2-1. Critical Slope Measurements from Sunset Crater Area near Flagstaff, AZ 6-38
6.5.3-1. Distances between Observed and Predicted Channel Heads for 34 Selected Channels on the East Slope of Yucca Mountain 6-44
6.5.5-1. Summary of Permeable Depth Data 6-47
6.5.6-1. Summary of Scour Depth Data 6-50
6.5.7-1. Bounding Box Corner Coordinates for Waste Emplacement Area (State Plane) 6-51
6.5.7-2. Bounding Box Coordinates for Waste Emplacement Area (UTM) 6-51
6.5.8-1. Calculated Values for D_d 6-55
6.5.8-2. Calculated Values for D_C 6-56
6.5.10-1. Summary of Developed Parameter Values for the TSPA Tephra Redistribution Model 6-57
6.6.2-1. Diffusion Sensitivity Analysis FAR V.1.2 Simulations 6-60
7.2.3-1. Data for Discharge and Scour Depth in Low-order Ephemeral Streams at Walnut Gulch Experimental Watershed 7-20
7.2.6-1. ^{137}Cs Measurements as a Function of Depth near Chernobyl in 1997 7-32
7.2.6-2. ^{137}Cs Measurements as a Function of Depth near Chernobyl in 1999 7-33
7.2.6-3. ^{137}Cs Measurements as a Function of Depth at Harwell Airfield, England 7-34
7.2.8-1. List of FAR V.1.2 Simulations Used in Mass Balance Calculation 7-38
7.2.8-2. Summary of Tephra Mass Fraction Partitioning 7-38
7.2.8-3. Summary of Mobilized Tephra Mass Balance Results 7-39
7.2.8-4. Summary of Tephra Transfer to RMEI Location 7-40
7.3.1-1. Basaltic Sediment Percentages (by volume) of Channels Draining Lathrop Wells Tephra Sheet 7-44
8.1-1. Product Output Intended for Use in the TSPA Model 8-2
8.1-2. Product Output Not Directly Used by the TSPA Model 8-2
A-1. DOQQs Used to Develop Geomorphic Map of the Fortymile Wash Alluvial Fan A-2
A-2. Geomorphic Features of the Alluvial Units A-8
A-3. Combined Area of Each Geomorphic Map Unit A-14

INTENTIONALLY LEFT BLANK

ACRONYMS AND ABBREVIATIONS

COTS	commercial, off-the-shelf software
DEM	digital elevation model
DIRS	Document Input Reference System
DLL	dynamic link library
DOQQ	digital orthophoto quarter quadrangle
DTN	data tracking number
FAR	Fortymile Wash ash redistribution (model)
FEPs	features, events, and processes
GIS	Geographic Information System
LHS	Latin Hypercube Sample
NRC	U.S. Nuclear Regulatory Commission
RMEI	reasonably maximally exposed individual

Soil Geomorphic units:

Qa3	Oldest unit in the field area; it is Middle to Late Pleistocene alluvium
Qa4	Late Pleistocene alluvium
Qa5	the Latest Pleistocene to Holocene alluvium
Qa6	Middle to Late Holocene alluvium
Qa7	Active alluvium in channels (youngest soil)
Qd	Disturbed area

SRRC	standardized rank regression coefficient
STN	software tracking number
TSPA	total system performance assessment
TWP	technical work plan
USGS	U.S. Geological Survey
UTM	Universal Transverse Mercator
YMP	Yucca Mountain Project
YMRP	*Yucca Mountain Review Plan, Final Report*

INTENTIONALLY LEFT BLANK

1. PURPOSE

This model report documents the development and validation of the Fortymile Wash ash redistribution (FAR) model (V.1.2), a conceptual, mathematical, and numerical model intended to estimate the redistribution (mobilization, transport, dilution, deposition, and diffusion) of waste-contaminated tephra deposited on the landscape surrounding Yucca Mountain, Nevada, by a potential volcanic eruption through the repository. Specifically, the FAR tephra redistribution model is intended to provide an estimate, including quantification of uncertainties, of the waste concentration as a function of time since an eruption at a compliance point located approximately 18 km south of the repository on the Fortymile Wash alluvial fan (Figure 1-1). This location represents where a hypothetical person called the reasonably maximally exposed individual (RMEI) lives. The radiological dose to this hypothetical person is calculated within the total system performance assessment (TSPA), using inputs provided by the FAR tephra redistribution model and the biosphere model (SNL 2007 [DIRS 177399]). The initial extent and thickness of the tephra deposit is provided to the FAR tephra redistribution model by the ASHPLUME model (SNL 2007 [DIRS 177431]), which considers volcanic source factors such as eruptive power, wind direction and speed, etc., that influence the nature of the initial tephra deposit. The ASHPLUME, FAR, and biosphere models are integrated within TSPA, which uses Monte Carlo simulations to estimate dose to the RMEI for a volcanic eruptive scenario, including uncertainty associated with each component (SNL 2007 [DIRS 178871], Sections 6.3.11 and 6.5.2).

The FAR tephra redistribution model quantifies the redistribution of volcanic tephra and associated waste within the Fortymile Wash drainage basin (the major drainage network in the western part of the Nevada Test Site) by hillslope and fluvial processes, and quantifies diffusive redistribution of waste in soil profiles at the RMEI location on the Fortymile Wash alluvial fan. The model domain is divided into two sections: (1) an upper drainage basin, characterized by flats and relatively steep terrain that drains into an incised and well defined channel network, and (2) an alluvial fan downstream of the upper drainage basin having considerably less slope, and less deeply incised channels, representing the RMEI location (Figure 1-2).

The tephra redistribution model uses a spatially distributed Geographic Information System (GIS) framework to calculate tephra redistribution in three steps. Specifically, the model calculates:

(1) **mobilization** by hillslope and fluvial processes of waste-contaminated tephra deposited in the upper drainage basin domain,

(2) **transport and mixing** (dilution) of waste-contaminated tephra within the channels of the upper drainage basin domain, and

(3) **emplacement and diffusion** of waste-contaminated sediments within the alluvial fan at the RMEI location.

These three steps are implemented in the FAR V.1.2 software package, which is run within the TSPA GoldSim environment.

The work described in this report was conducted under *Technical Work Plan for: Igneous Activity Assessment for Disruptive Events* (SNL 2007 [DIRS 182219]).

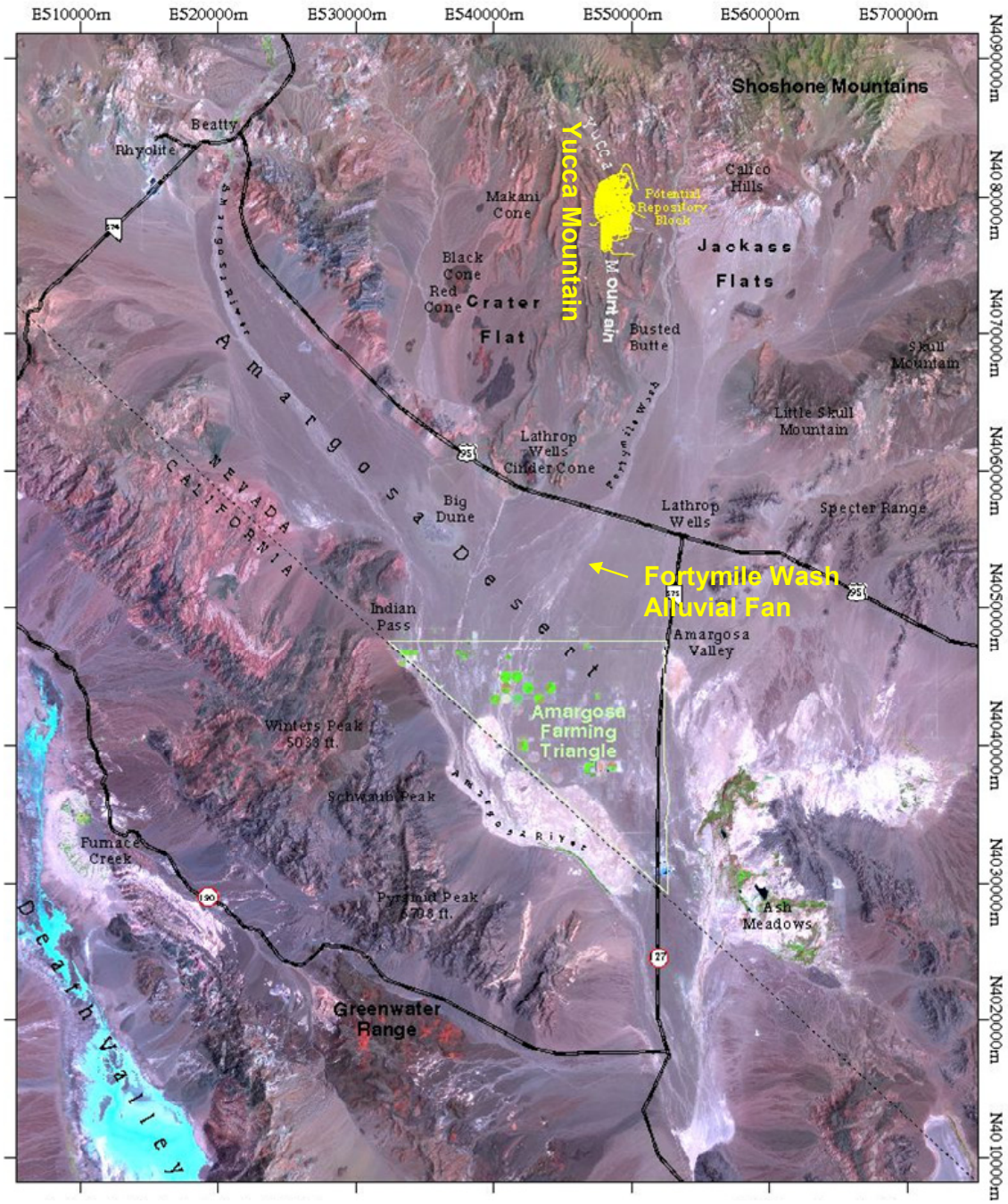

NOTE: Names of specific geographical points are not necessary to understand the technical content of this document. This figure is for illustration purposes.

Figure 1-1. Location Map of the Yucca Mountain Region Centered on the RMEI Location

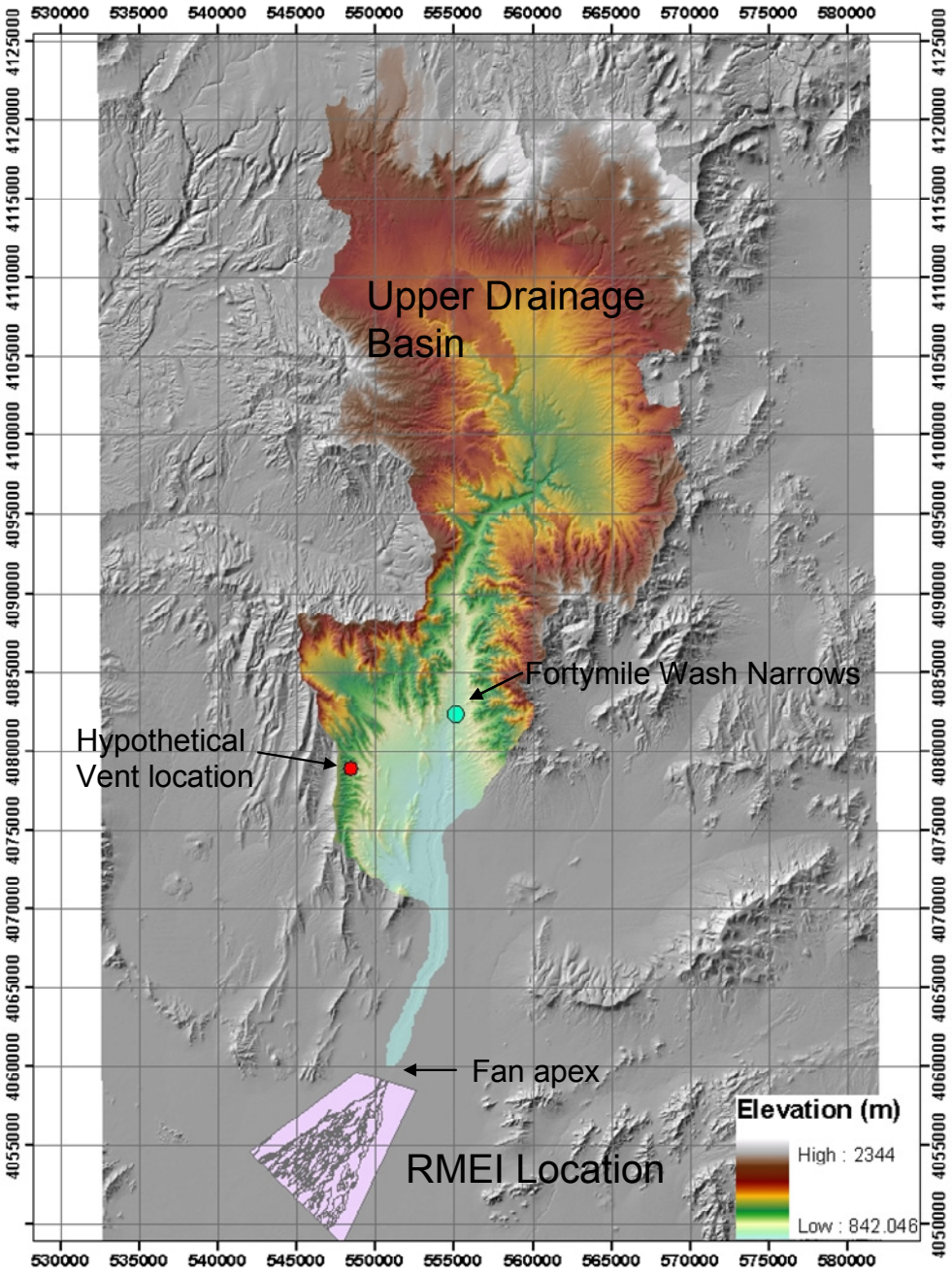

Sources: Digital elevation model (DEM) elevations in upper drainage basin from Output DTN: MO0605SPAFORTY.000. RMEI location map from Output DTN: SN0708GEOMOMAP.001.

NOTE: Elevations are not displayed outside the upper drainage basin area. Gray lines in RMEI location are geomorphic unit boundaries. See Appendix A for a detailed view of this area. Figure is for illustration purposes only.

Figure 1-2. Map Showing the Upper Drainage Basin Domain (colored by elevation), the RMEI Location (pink), and the Hypothetical Vent Location

1.1 SCOPE

This report describes the development of the FAR tephra redistribution model following the governing procedure SCI-PRO-006, *Models*, and the technical work plan (TWP) (SNL 2007 [DIRS 182219]) and develops model input data for use in TSPA compliance calculations. As such, this model development work is categorized as a Compliance Decision (CD) activity in the TWP, as defined by Section 2.0 of SCI-PRO-002, *Planning for Science Activities*.

The organization of the report follows the model documentation outline (SCI-PRO-006, Attachment 2). Section 1 provides an overview of the purpose, scope, and limitations of the model. Section 2 describes the applicability of the quality assurance program to this work and lists the procedures followed during model development and documentation. Section 3 identifies all controlled and baselined computer software that was used in the model development, performance, validation, and documentation process. Section 4 provides a complete listing of the direct inputs to the model and reference to all applicable requirements, criteria, codes, standards, and regulations. Section 5 lists assumptions used in the development of the model. Section 6 provides a detailed discussion of the model including a description of the conceptual and mathematical model, development of appropriate model input parameters and uncertainties, and a parameter sensitivity analysis. Section 7 documents activities used to validate the model during model development as well as post-development model validation. Section 8 summarizes the main conclusions of the model and provides a listing of all model output datasets. Section 9 provides a complete listing of references cited in the document. Appendix A provides additional details about the development of a geomorphic map of the Fortymile Wash alluvial fan. Appendix B describes how criteria from *Yucca Mountain Review Plan, Final Report* (YMRP) (NRC 2003 [DIRS 163274]) are covered in the documentation. Appendix C includes memos documenting independent critical reviews of model validation. Appendix D provides a listing of mathematical nomenclature used in the report. Appendix E provides verification of the analytic solution of the diffusion model described in Section 6.5.

1.2 MODEL LIMITATIONS

Given uncertainties, lack of data, and the desire to minimize mathematical complexity that does not provide value commensurate with the model purpose, there are recognized limitations in the capabilities of the FAR tephra redistribution model. Among the recognized limitations are:

- The model does not explicitly include the effects of future climate on model processes and parameters. Future climate is estimated to be wetter than present-day climate (see Section 5.1.1) and several model parameters may be affected by changes in climate. For example, the vertical migration rate of radionuclides into the soil at the RMEI location, which is controlled by diffusivity values, may increase with increasing precipitation due to higher net infiltration flux. Neglecting this feedback results in the model predicting a slower decrease in waste concentrations at the RMEI location than would result if this feedback were included. Such climate feedbacks are not considered by the model (see Section 5.1.1).

- The long-term geologic dynamics of fan interchannel divides and channel interactions are not represented. Alluvial fans are dynamic landforms that can evolve

topographically over both long and short time scales. Uncertainty in the fraction of the alluvial fan that is subject to active fluvial deposition is assumed to adequately account for future changes in the Fortymile Wash alluvial fan (see Section 5.1.2).

- The model is only applicable to channels without active floodplains. This limitation is inconsequential for the drainage networks in the Yucca Mountain region because these drainage networks have no significant active floodplains (see Section 5.1.3).

- Processes which may cause accumulation of contaminants within the soils at the RMEI location are not included in the model. Such processes are unlikely to occur in this environment (see Section 5.1.5).

- The model does not explicitly incorporate time in the remobilization calculations for the upper basin. Mobilization of the tephra in the upper domain is assumed to be instantaneous, as is movement of tephra through the lower domain; additionally, eventual removal of non-mobilized tephra is not considered (see Section 5.2.1).

- The model does not include the effects of eolian erosion or deposition. Eolian sediment transport is a significant geomorphic process in this environment. However, because of prevailing wind directions, eolian deposition and erosion will tend to further dilute contaminated tephra redistributed to the RMEI location by fluvial processes beyond that estimated by the model. Therefore, choosing not to simulate these effects explicitly in the model will tend to overestimate tephra and waste concentration at the RMEI location (see Section 5.2.2).

- The model assumes that channel geomorphology does not change over time. Following a volcanic eruption, it is expected that channel geomorphology would change in certain parts of the upper drainage basin, especially close to the vent. Such changes could result in changes in surface elevation and slope and associated changes in stream power and even drainage density and possibly affect the initial concentration at the RMEI location. None of these complex feedbacks are simulated by the model. It is assumed that the existing uncertainty considered in the input parameters accounts for the uncertainties in such possible changes (see Section 5.1.4).

- The model assumes that the contaminant and channel-bed material is transported primarily as bed-material load. The silt-sized fraction of the contaminated tephra will be transported as suspended load and will be transported past the RMEI location and into the Amargosa River valley. By treating this material as bedload, which can be deposited at the RMEI location, the model will tend to overestimate tephra and waste concentration at the RMEI location (see Section 5.2.3).

- The model assumes that the thickness and concentration of the contaminated tephra deposited in the RMEI area is the same as that calculated at the upper drainage basin fan apex. This approximation is justified because the contributing area (and by correlation, discharge and scour depth) does not increase significantly between the fan and fan apex. This assumption presumes that the drainage system is open, allowing some portion of the tephra and radionuclides initially mobilized in the upper drainage domain to flow

through and out of the lower drainage domain (the RMEI domain is not considered to be a perfect depozone) (see Section 5.2.4). This assumption is consistent with the observed lack of silt-sized sediment in the channel bed of Fortymile Wash.

- The model assumes that the concentration of waste associated with the ash in a particular location can be calculated after the ash has been re-distributed using the ratio of the total mass of waste and the total mass of ash mobilized in the upper drainage basin. This is a reasonable approximation because the redistribution process is likely to blend contaminated tephra from throughout the upper drainage basin (see Section 5.2.5).

- The model assumes that once the tephra and radionuclides are deposited at the RMEI location, redistribution of the radionuclides into the soil can be approximated by a diffusive process. Advection of the radionuclides is not included, nor is additional mixing of the contaminants in the channels included. This is considered a minor limitation because field observations over the past 50 years support the use of a diffusion model for representing radionuclide transport in the soil and any additional mixing that might occur would likely result in waste concentrations even lower than currently predicted by the model (see Sections 5.3.1, 5.3.2, and 5.3.3).

Each of these limitations is discussed within the context of model assumptions in Section 5.

There is one deviation from the TWP (SNL 2007 [DIRS 182219]). Section 2.6.5.2.3 of the TWP states: "The model will be considered valid if the independent critical reviewer concurs that the documentation of the tephra redistribution model report appropriately and adequately addresses [the] review criteria." Two independent experts each conducted an initial critical review of Draft A of this report using the review criteria presented in the TWP. One of these critical reviewers was not available to review the originator's responses to his review. Therefore, the other reviewer performed a final critical review of Draft D of this report, which included all of the changes made in response to both initial critical reviews.

2. QUALITY ASSURANCE

This report documents a conceptual and mathematical model for redistribution of tephra deposits by geomorphic processes and movement of radionuclides in soils by diffusion processes in the Fortymile Wash drainage and associated alluvial fan. The report contributes to the analysis and modeling of a process that could result in an increase in dose to the RMEI because of remobilization of contaminants in surficial materials. Hence, the process represents a potential disruption of the natural barrier system, which is classified in *Q-List* (BSC 2005 [DIRS 175539], Section 5) as "safety category" (SC) because of its importance to meeting the performance objectives of the Yucca Mountain disposal regulations (10 CFR 63.113 [DIRS 180319]).

Development of this report and the supporting activities has been determined to be subject to the Yucca Mountain Project (YMP) quality assurance program (DOE 2007 [DIRS 182051]; SNL 2007 [DIRS 182219], Section 8.1). The electronic management of data was accomplished in accordance with the controls specified in the TWP (SNL 2007 [DIRS 182219], Section 8.5) and the Lead Lab procedure IM-PRO-002, *Control of the Electronic Management of Information*. The TWP that controls the work described in this report was developed in accordance with SCI-PRO-002. This model report was developed in accordance with SCI-PRO-006.

This model report provides a description of the tephra redistribution model that is used by TSPA and develops input parameters for this model. The report contributes to the process models used to support performance assessment; the conclusions do not directly impact engineered features important to preclosure safety.

INTENTIONALLY LEFT BLANK

3. USE OF SOFTWARE

Section 3.1 discusses the qualified, controlled, and baselined software items that were used in this report. Section 3.2 discusses commercial, off-the-shelf software used in this report. Each software item is used within the range for which it was qualified. All software used for the work documented in this report was selected because it was appropriate for the intended use. No limitations on the use of selected software or on the use of outputs from selected software were identified for this work. All software was qualified before use except for FAR V.1.2, which was used prior to qualification. This use is allowed by, and consistent with, procedural requirements described in SCI-PRO-006, Section 6.2.1(L). FAR V.1.2 was subsequently qualified and the executable file did not change during the qualification process (documentation of this is included in the records associated with Output DTNs: SN0708DRAINDEN.001 and SN0708FARSENSS.001). Section 4 discusses the inputs used in this model for all software.

3.1 SOFTWARE TRACKED BY SOFTWARE CONFIGURATION MANAGEMENT

The qualified software used to develop the analyses described in this report includes ArcGIS Desktop V9.2, ASHPLUME_DLL_LA V2.1, FAR V.1.2, and MVIEW V4.0. The FAR V.1.2 tephra redistribution model is implemented as a dynamic link library (DLL) designed for use in GoldSim simulator, a commercial graphical, object-oriented, probabilistic computer modeling tool. GoldSim is a registered trademark of GoldSim Technology Group LLC. All qualified software items were obtained from Software Configuration Management, are appropriate for their intended applications, and are adequate for their intended uses as required by IM-PRO-003, *Software Management*. Table 3.1-1 lists these qualified, controlled, and baselined software items. ArcGIS Desktop was used to develop and analyze spatial data sets such as the digital elevation model for the Fortymile Wash upper drainage basin and the geomorphic map of the alluvial fan. ASHPLUME_DLL_LA (ASHPLUME) was used to generate the initial tephra deposit required to run FAR V.1.2. MVIEW was used to perform the stepwise linear regression analysis as part of the parameter sensitivity analysis. While MVIEW V.4.0 is qualified software, it is not used in this report as direct input.

Table 3.1-1. Qualified Software

Software Name	Version	STN	Baseline Date	Platform and Operating System	DIRS
ArcGIS	9.2	11205-9.2-00	Mar 12, 2007	PC, Windows XP	182849
ASHPLUME_DLL_LA	2.1	11117-2.1-00	Dec 19, 2006	PC, Windows 2000/2003 server	178870
FAR	1.2	11190-1.2-00	Sep 19, 2007	PC, Windows 2000/2003 server	182225
GoldSim	9.60.100	10344-9.60-01	Jul 10, 2007	PC, Windows 2000, 2003, XP	181903
MVIEW	4.0	10072-4.0-00	Jul 1, 2005	PC/Windows 2000	173438

NOTE: DIRS = Document Input Reference System; STN = software tracking number.

3.2 EXEMPT SOFTWARE

Commercial, off-the-shelf software (COTS) used in support of this model report is listed in Table 3.2-1. This software is exempt from the requirements of IM-PRO-003. Formulas, inputs, and outputs used in these software codes and other information required for a technically qualified person to reproduce or verify the work are documented in output data tracking numbers (DTNs) referenced in the report.

Standard spreadsheet software (MS Excel 2000 and 2003) was used for standard calculations supporting the development of input parameters and for visualization of data in this report. This software item is controlled as part of MS Office 2000 Professional SP-2 and MS Office 2003 Professional SP-2.

Mathcad V. 13.1 is a COTS controlled software item determined to be exempt in accordance with Section 2.0 of IM-PRO-003. It was used for standard post-processing calculations and plotting purposes.

Table 3.2-1. Exempt Software

Software Name and Version (V)	STN	Description	Platform and Operating System
Office 2000 Professional	610236-2000-00	The commercial software, Microsoft Excel 2000 was used for plotting graphs and statistical calculations. Only built-in standard functions in this software were used.	PC, Windows 2000/NT/XP
Office 2000 Professional SR1	610236-2000SR1-00	The commercial software, Microsoft Excel 2000 was used for plotting graphs and statistical calculations. Only built-in standard functions in this software were used.	PC, Windows 2000/NT/XP
Office 2000 Professional SR2	610236-2000SR2-00	The commercial software, Microsoft Excel 2000 was used for plotting graphs and statistical calculations. Only built-in standard functions in this software were used.	PC, Windows 2000/NT/XP
Office 2003 Professional	610236-2003-00	The commercial software, Microsoft Excel 2003 was used for plotting graphs and statistical calculations. Only built-in standard functions in this software were used.	PC, Windows 2000/NT/XP
Office 2003 SP1 and SP2	610236-2003SP1SP2-00	The commercial software, Microsoft Excel 2003 was used for plotting graphs and statistical calculations. Only built-in standard functions in this software were used.	PC, Windows 2000/NT/XP
Mathcad, v. 13.1	611161-13.1-00	This commercial software was used for post-processing FAR model results and generating plots of data.	PC, Windows XP

4. DIRECT INPUT

4.1 DATA, PARAMETERS, AND OTHER MODEL INPUTS

All direct data input used in the development and application of the tephra redistribution model for TSPA are listed in this section. These data consist of measurements and observations made by project scientists and recorded in scientific notebooks, topographic maps and aerial photography of the site, and other miscellaneous data described below. The data used to develop and apply the tephra redistribution model in TSPA are fully appropriate for their intended use. The qualification status of the input sources is provided in the Technical Data Management System and listed in the DIRS database. All direct inputs are qualified and no unqualified data from external sources were used in the development of the model. Data used to develop the model were not used to validate the model. Table 4.1-1 lists all the direct data sources and points to subsequent tables for specific data listings.

Table 4.1-1. Direct Input Data Sources

Input Data Description	Location in This Model Report	Source
3.75 minute digital orthophotos	Appendix A, Sections 6.5.3 and 6.5.4	DTN: SN0706DIGORTHO.001 [DIRS 182108]
USGS digital elevation model	Section 6.5.1	DTN: SN0707DEMSOURC.001 [DIRS 182111]
Scour depth, channel width, and drainage area at Fortymile Wash, Narrows streamgage	Section 6.5.6	DTN: SN0711SCOURCHM.002 [DIRS 183849]
Repository design layout	Section 6.5.7	SNL 2007 [DIRS 179466], Table 4-1, Parameter 01-02
Slope measurements and tephra mobilization observations from selected volcanic craters in Arizona	Section 6.5.2	DTN: MO0708SCSOC137.000 [DIRS 182344], Table 1
Permeable soil depth measurements	Section 6.5.5	DTN: MO0708SCSOC137.000 [DIRS 182344], Table 2
^{137}Cs measurements	Section 6.5.8	DTN: MO0708SCSOC137.000 [DIRS 182344], Table 3
Geomorphic field observations	Appendix A, Section 6.5.4	DTN: MO0708SCSOC137.000 [DIRS 182344], Table 4

NOTE: USGS = U.S. Geological Survey.

4.1.1 Repository Layout Data

The repository design layout of waste containers presented in *Total System Performance Assessment Data Input Package for Requirements Analysis for Subsurface Facilities* (SNL 2007 [DIRS 179466], Parameter 01-02) is used as direct input. These design data are appropriate for use to estimate the location of the volcanic vent because they define the extent and area in which waste will be placed in the repository. Because any vent location that intercepts the waste in the repository might lead to an eruptive release scenario, these data are qualified for their intended use.

4.1.2 Digital Orthophotos

Table 4.1-2 lists seven USGS digital orthophoto quarter quadrangles (DOQQs) that were used as direct input to this analysis. These data were used in the development of the Fortymile Wash alluvial fan geomorphic map, which is described in Appendix A, and associated model parameters. In addition these data were used to identify the locations of 34 channel heads along the eastern flank of Yucca Mountain for the purpose of estimating an appropriate range for the drainage density, which is described in Section 6.5.3. These data are qualified for their intended use.

Table 4.1-2. DOQQs Used in This Report

Filename	USGS Quadrangle	Quadrant	Source
36116F48.tif	Amargosa Valley	SW	SN0706DIGORTHO.001 [DIRS 182108]
36116F57.tif	Big Dune	SE	SN0706DIGORTHO.001 [DIRS 182108]
36116E45.tif	South of Amargosa Valley	NW	SN0706DIGORTHO.001 [DIRS 182108]
36116G45.tif	Busted Butte	NW	SN0706DIGORTHO.001 [DIRS 182108]
36116G46.tif	Busted Butte	NE	SN0706DIGORTHO.001 [DIRS 182108]
36116G48.tif	Busted Butte	SW	SN0706DIGORTHO.001 [DIRS 182108]
36116G47.tif	Busted Butte	SE	SN0706DIGORTHO.001 [DIRS 182108]

4.1.3 Critical Slope Data

Table 4.1-3 lists field measurements of land surface slope categorized according to the degree and nature of tephra erosion made in the Sunset Crater area near Flagstaff, Arizona. These data are used as the basis for estimating a critical slope parameter used by the FAR model (developed in Section 6.5.2) to predict whether tephra that initially falls on slopes will be mobilized and transported downstream. These data are qualified for their intended use.

Table 4.1-3. Critical Slope Measurements for Tephra Mobilization from Sunset Crater Area near Flagstaff, AZ

N [a]	E [a]	Geographic Description	Slope Magnitude (degrees)	Observations	Slope Type
469821	3898699	Rattlesnake Crater	12	Minor gully	Bedrock
469821	3898699	Rattlesnake Crater	15	Gullied	Bedrock
469821	3898699	Rattlesnake Crater	14	Gullied	Bedrock
469821	3898699	Rattlesnake Crater	17	Gullied	Bedrock
469821	3898699	Rattlesnake Crater	18	Gullied	Bedrock
469821	3898699	Rattlesnake Crater	10	Depositional	Alluvial deposit at base of slope
469821	3898699	Rattlesnake Crater	28	Dry slope processes, tephra ravel	Cinder cone
465320	3903732	Cochrane Hill	28	Dry slope processes	Cinder cone
465320	3903732	Cochrane Hill	28.5	Dry slope processes	Cinder cone

Table 4.1-3. Critical Slope Measurements for Tephra Mobilization from Sunset Crater Area, near Flagstaff, AZ (Continued)

N [a]	E [a]	Geographic Description	Slope Magnitude (degrees)	Observations	Slope Type
465320	3903732	Cochrane Hill	27	Dry slope processes	Cinder cone
465824	3903841	Cochrane Hill	26	Dry slope processes; ash moved without incision or channelization	Cinder cone
465824	3903841	Cochrane Hill	26	Dry slope processes; ash moved without incision or channelization	Cinder cone
464650	3911595	Moon Crater	19	Gullied	Ash and underlying slope material
464650	3911595	Moon Crater	19	Gullied	Ash and underlying slope material
464650	3911595	Moon Crater	19	Gullied	Ash and underlying slope material
464650	3911595	Moon Crater	18	Gullied	Ash and underlying slope material
465545 [b]	3911494 [b]	Moon Crater	20 to 21	Wind and dry slope processes dominant	Cinder cone
465545 [b]	3911494 [b]	Moon Crater	24	Wind and dry slope processes dominant	Cinder cone
465545 [b]	3911494 [b]	Moon Crater	28	Wind and dry slope processes dominant	Cinder cone
465292	3911144	Moon Crater	20	Stripped slope	Cinder cone
465292	3911144	Moon Crater	25	Ash transported by gullying	Cinder cone
465292	3911144	Moon Crater	20	Ash transported by gullying	Cinder cone
467647	3906916	Cinder cone	30	Dry slope processes, tephra ravel, creep	Cinder cone

Source: DTN: MO0708SCSOC137.000 [DIRS 182344], Table 1.
[a] Coordinates are in Universal Transverse Mercator (UTM) NAD83, Zone 11, meters.
[b] Coordinate north and east designators are reversed in Pelletier 2007 [DIRS 179612], pp. 58 to 59.

4.1.4 Permeable Depth Data

The FAR model uses measurements of the depth to Stage IV carbonate development to define the permeable depth model input for channels and interchannel divides at the RMEI location. Table 4.1-4 lists measurements of depth to Stage IV carbonate development made on interchannel divides of the Fortymile Wash alluvial fan. These data are used in Section 6.5.5 as the basis for estimating an appropriate range for this parameter. These data are qualified for their intended use.

Table 4.1-4. Summary of Permeable Depth Data

Station No.	Easting	Northing	Depth of Stage IV Carbonate Layer (cm)	Unit
93	549257	4054772	>96	Qa4
94	549301	4054754	102 to 130	Qa3
95	550086	4056809	>140	Qa4
96	550353	4056760	102 to 110	Qa3
249	546296	4051066	>110	Qa4
250	544116	4055019	>135	Qa4

Source: Coordinates (UTM NAD83, Zone 11, meters) and depth of Stage-IV carbonate layer: DTN: MO0708SCSOC137.000 [DIRS 182344], Table 2; geomorphology units determined by cross-referencing annotations in the field notes (shown in Table 4.1-6) with the geologic map unit nomenclature table in readme file for Output DTN: SN0708GEOMOMAP.001.

4.1.5 Cesium-137 Data

Table 4.1-5 lists measurements of bulk ^{137}Cs mass recovered from various soil depth intervals from samples collected in the vicinity of the Fortymile Wash alluvial fan. Only data from samples located on the alluvial fan are included in the analysis of diffusivity values presented in Section 6.5.8. These data are qualified for their intended use.

Table 4.1-5. Cesium-137 Measurements

Geographic Coordinates		Depth (cm)	Unit	Sample ID	Analysis Results (pCi/g)		
North	West				Value	Error [a]	MDC [b]
36°39'31.6"	116°28'15.9"	0 to 3	channel	Cs 071702-A1	0.259	0.045	0.016
36°39'31.6"	116°28'15.9"	3 to 6	channel	Cs 071702-A2	0.054	0.016	0.02
36°39"32.2"	116°28'17.2"	0 to 3	channel	Cs 071702-B1	0.146	0.03	0.025
36°39"32.2"	116°28'17.2"	3 to 6	channel	Cs 071702-B2	0.125	0.023	0.015
36°39'26.4"	116°28'12.8"	0 to 3	divide	Cs 071702-C1	0.209	0.036	0.013
36°39'26.4"	116°28'12.8"	3 to 6	divide	Cs 071702-C2	0.049	0.012	0.013
36°39'25.1"	116°27'47.2"	0 to 3	divide	Cs 071702-E1	0.159	0.03	0.021
36°39'25.1"	116°27'47.2"	3 to 6	divide	Cs 071702-E2	0.049	0.015	0.019
No coordinates. Sample collected 20 m east of Cs 071702-F1		0 to 3	divide	Cs 071702-G1	0.118	0.025	0.023
No coordinates. Sample collected 20 m east of Cs 071702-F1		3 to 6	divide	Cs 071702-G2	0 [c]	0.01	0.017
36°35'53.7"	116°28'22.2"	0 to 3	divide	Cs 071802-I1	0.374	0.065	0.023
36°35'53.7"	116°28'22.2"	3 to 6	divide	Cs 071802-I2	0.015 [c]	0.014	0.023
36°36'17.0"	116°28'59.1"	0 to 3	channel	Cs 071802-J1	0.099	0.022	0.021
36°36'17.0"	116°28'59.1"	3 to 6	channel	Cs 071802-J2	0.056	0.025	0.038
36°36'17.5"	116°29'00.3"	0 to 3	divide	Cs 071802-K1	0.325	0.055	0.016
36°36'17.5"	116°29'00.3"	3 to 6	divide	Cs 071802-K2	0.0145	0.0075	0.011
36°36'29.9"	116°29'13.8"	0 to 3	divide	Cs 071802-N1	0.198	0.037	0.022
36°36'29.9"	116°29'13.8"	3 to 6	divide	Cs 071802-N2	0.02	0.012	0.018
36°36'46.6"	116°29'36.0"	0 to 3	divide	Cs 071802-P1	0.231	0.04	0.015
36°36'46.6"	116°29'36.0"	3 to 6	divide	Cs 071802-P2	0.014 [c]	0.013	0.021
36°37'13.7"	116°30'09.8"	0 to 3	divide	Cs 071802-Q1	0.204	0.037	0.02
36°37'13.7"	116°30'09.8"	3 to 6	divide	Cs 071802-Q2	0.001 [c]	0.012	0.021
36°37'52.6"	116°30'23.2"	0 to 3	divide	Cs 071802-R1	0.227	0.042	0.021
36°37'52.6"	116°30'23.2"	3 to 6	divide	Cs 071802-R2	0.01 [c]	0.012	0.019
36°38'44.0"	116°30'23.1"	0 to 3	divide	Cs 071802-S1	0.251	0.043	0.017

Table 4.1-5. Cesium-137 Measurements (Continued)

Geographic Coordinates		Depth (cm)	Unit	Sample ID	Analysis Results (pCi/g)		
North	West				Value	Error [a]	MDC [b]
36°38'44.0"	116°30'23.1"	3 to 6	divide	Cs 071802-S2	0.034	0.01	0.013
36°39'15.8"	116°26'45.5"	0 to 3	divide	Cs 071802-BB1	0.255	0.045	0.018
36°39'15.8"	116°26'45.5"	3 to 6	divide	Cs 071802-BB2	0.066	0.015	0.016

Source: DTN: MO0708SCSOC137.000 [DIRS 182344], Table 3. Only stations located on the Fortymile Wash alluvial fan were selected.

[a] Total propagated uncertainty.

[b] Minimum detectable concentration.

[c] Reported result less than the minimum detectable concentration.

NOTES: West coordinates for samples Cs050902-D1, Cs050902-DII, and Cs050902-DIII are shown in Harrington 2003 [DIRS 164775] as 116°32'0.91". This value is apparently erroneous and should be 116°32'09.1."

Coordinates, sample depth, and associated unit from Harrington 2003 [DIRS 164775], pp. 16 to 53. Analytical results documented in Harrington 2003 [DIRS 164775], pp. 190a to 190e and 192a and 192b.

4.1.6 Geomorphic Field Observation Data

Table 4.1-6 lists geomorphic observations made during a number of field trips to the Fortymile Wash alluvial fan. These observations were used along with digital orthophoto data (Table 4.1-2) in the development of the geomorphic map of the Fortymile Wash alluvial fan, which is described in Appendix A. The orthophotos and these observations provide the direct inputs to the geomorphic map, which is used as the basis for the parameters describing the area of the fan and the fraction of that area that is active channels. The locations of the observations are shown on maps presented in Appendix A. These data are qualified for their intended use.

Table 4.1-6. Geomorphic Field Observations

Station #	Easting [m]	Northing [m]	Field Notes
1	547824[a]	4057482	This is the large alluvial surface that borders the 40 mi. fan on the west side. It appears extensive and uniform on the aerial photos. 80% pave sutured planar no bar/swale. Soil pit: 56cm A1, A2, A3; 65cm Bk; >85cm Btk or possibly stage III-IV. Petrocalcic "K" visible to east in wash at ~1.5m below surface of unit.
2	547908	4057415	60% pavement coverage, no suture, bar/swale preserved. Soil pit: 26 cm A (eolian sand with clasts); 26 to 45 cm Bk; sandy below 45cm
3	547947	4057392	rare bar/swale; 50% pavement coverage
4	548066	4057334	higher than station (3)~ 50 cm.; planar no bar/swale; 56 cm A-horizon
5	548084	4057327	bar/swale; 361-cm-thick A-horizon
6	548134	4057304	soil pit: 30-cm A-horizon; bar/swale topography present
7	548187	4057256	42-cm-thick A-horizon; bar/swale subdued bars by eolian input over time
8	548248	4057242	47-cm-thick A-horizon; rare bar
9	548353	4057211	45-cm-thick A-horizon; bars absent
10	549128	4056872	Moved E to Hwy 95; present development is very weak; ~40% clast coverage, subdued bar/swale; 16 cm A-horizon
11	548882	4056726	S. of Hwy. 95, W of Fortymile Wash; coppice dunes present here likely due to proximity to active channel; Soil pit: 57cm A-horizon, bar/swale present, pavement coverage ~70%, less eolian sand is present as move farther west
12	548538	4056615	moderate pavement development, bar/swale present but bars appear partially aggraded, could be one map unit all the way to Fortymile Channel
13	548460	4056682	23 cm A-horizon; moderate pavement
14	548440	4056682	Soil pit: 30cm A-horizon
15	548554	4056160	contact possible here, weak pavement with coppice dunes to E; moderate pavement to W
16	548692	4056313	continuation contact - station 15
17	548774	4056324	continuation contact - station 15
18	549228	4056185	Soil pit: 12 cm A-horizon; surface appears older on photos
19	547353	**4050195**[b]	moderate pavement, minor suturing, clast coverage is ~70%; A-horizon is 63 cm with two horizons; planar surface with no visible bar/swale
20	547208	4050317	Bar/swale topography present; 33-cm-horizon; Av-4 cm
21	547153	4050375	12-cm A-horizon; 4 cm Av
22	547093	4050386	pavement strongly developed; 4 cm Av, 65-cm A-horizon, no bar/swale
23	546925	4050525	Continuing transect across Racetrack Rd.; 17-cm A-horizon, Bar/swale present, coarse texture gravel Bk below A

Table 4.1-6. Geomorphic Field Observations (Continued)

Station #	Easting [m]	Northing [m]	Field Notes
24	546770	4050626	40% clast cover, pavement weak, A-horizon 17-cm then Bk gravel
25	546579	4050797	bar swale present; 19-cm A-horizon, 4 cm Av, gravelly Bk below
26	546550	4050857	40% clast coverage on surface, less pronounced bar/swale than station (25), 13-cm A-horizon
27	546490	4050927	stepped up 0.5m from station (26), 1m up from wash; 60-70% clast cover, no bar/swale, 42-cm A-horizon
28	546368	4051077	continued walking on planar surface, 60-70% clast coverage, no bar/swale, 42cm A-horizon
29	546290	4051147	active channel 1.5 m below oldest surface; to W step up .75 m to surface, 30% to 40% clast cover, 26 cm A-horizon
30	546228	4051425	60% to 70% clast cover - planar (no bar/swale); 42-cm A-horizon
31	546048	4051444	bar/swale present; 50% clast cover; 23-cm A1-horizon to 42-cm A2-horizon or sandy Bk
32	545998	4051467	8-cm A-horizon, ~30% clast coverage, young looking
33	545936	4051430	stepped up ~1m from station (32), 50% to 60% clast coverage; 60-cm-thick A-horizon
34	545905	4051474	Flood deposit – gravel- to boulder-size clasts up to 25cm, fining in downstream direction and with distance to channel. No eolian deposition indicates these deposits were very young. They sit ~75 cm above channel and ~ 20 to 30 cm above Holocene deposits
35	545878	4051497	A-horizon sandy with gravel, 58 cm; Surface coarse gravelly bar/swale; poor to no pavement
36	545859	4051523	30% paved clast coverage with some coppice dunes present; A-horizon ~20 cm thick
37	545808	4051621	50% pavement, bar/swale present; 19-cm-thick A-horizon
38	545728	4051710	~10m W of subtle riser; 40% to 50% pavement clasts, bars more subdued than unit to E; total surface <20 to 30 cm relief; 8-cm-thick A-horizon
39	545664	4051746	50% to 60% clast coverage - low relief surface; 16-cm-thick A-horizon
40	545602	4051825	1.0 m above wash, 40% clast coverage, minor bar/swale - gravelly, 20 cm A-horizon
41	545552	4051835	subdued bar/swale ~1.5 m above channel ~50% pavement, <20 cm overall relief, 57-cm thick A-horizon
42	549015	4056729	reoccupied soil pit /w CH
43	549116	4056191	Holocene surface with 20cm A-horizon
44	549230	4056139	same profile as west major terrace, A1 - 20cm, A2 - 65cm
45	547266	4057160	soil profile: 31-cm A1, 56-cm A2 sand/gravel, 82-cm (bottom of pit) argillic cemented gravel stage 1 carbonate, 7.5 YR soft subangular blocky peds
46	547228	4057176	Active Channel; 34 cm alluvium, below that paleosol argillic, gravelly stage 1 carbonate Btk to bottom of pit at 60cm.
47	547426	4056858	15-cm A-horizon, ~50 m to NW is an older surface with 52 cm A-horizon
48	545310	4052070	Small NW-SE road on middle portion of fan; 40% to 50% clast coverage, subdued bar/swale, 20 to 40 cm relief, 24 cm A1, 52 cm A2
49	545335	4052345	white on photos, fluvial silt laminated 1 mm. Local over deepening
50	545350	4052363	1.7 to 1.9 m above active channel, 40% pavement, bars present but very subdued. 38-cm-thick A-horizon
51	545188	4052456	Large continuous surface. Subdued bar/swale 40% to 50% clast coverage; A-horizon thin, ~ 10 cm

Table 4.1-6. Geomorphic Field Observations (Continued)

Station #	Easting [m]	Northing [m]	Field Notes
52	544921	4052456	Subplanar surface, subdued bar/swale. 30% to 40% clast coverage; 31 cm A-horizon
53	544752	4052909	Soil pit: A1 – 43 cm, A2 – 60 cm, Bk to bottom of pit at 1.1 m, minor bar/swale, widely spaced, subdued
54	544372	4053432	elevated spot ~.5m above surface, darker pavement, 50% clast coverage, landform ~50 m wide
55	544166	4053285	stepped up 30 to 40 cm, pavement coarsens, possible contact with older unit
56	547269	4057160	Drove up to Hwy. 95; Reoccupy CH cesium pit.
57	547233	4057176	Reoccupy CH cesium pit in active channel
58	547426	4056858	Surface here looks younger than unit N of channel ~30m. Subdued bar/swale, ~50% gravel pavement 15 cm A-horizon
59	547405	4056907	60% clast cover, very rare bars, subplanar; soil pit: 21 cm - A1, 52 cm - A2
60	547468	4056590	Station in active channel, oldest surface on both sides. Unit on N side pinches out in downstream direction and widens in upstream direction. Unit on S side fairly large, ~1.7-m relief above channel
61	547611	4056550	Gully in oldest unit
62	547687	4056514	>35-cm-thick A-horizon, 50% to 60% clast coverage. 1.5 to 1.8m above active channel
63	547482	4056366	Large bouldery flood deposit onlapped on U/S end of terrace at flow divergence. W channel incised 3 m
64	547547	4056248	Moving W-E, contact from second oldest to oldest surface
65	547748	4056093	<20-cm-thick A-horizon.
66	547835	4055929	Bouldery deposit on surface- possibly younger flood deposit or late Holocene 'channel fan'
67	547853	4055874	Bouldery deposit on surface- possibly younger flood deposit or late Holocene 'channel fan'
68	547721	4055673	Moving to W, stepped up to more well-developed pavement, 50% to 60%, and subplanar minor bar/swale. 61 cm A-horizon
69	548508	4056764	Starting short transect W of Fortymile Wash S of Hwy. Pronounced bar/swale topography with cobbles and boulders on surface. 53-cm-thick A-horizon. 50% gravel pavement, appears lower than adjacent surface.
70	548446	4056800	20-cm-thick A-horizon, pavement clast density is ~50%
71	548179	4056948	Well-developed pavement, no bars preserved
72	548540	4056751	Large unit, ~50-cm relief between bars and swales, bars are concentrations of boulders perched on surface, swales are fairly wide with moderate pavement development
73	548627	4056642	Moderate pavement development, no bars, subdued topography
74	547515	4052515	Possible contact between young unit to W and intermediate unit to E. Pavement density increases but relief change minimal
75	547532	4052525	Surface not quite planar, 50% pavement clast density, bars rare and subdued. 37-cm-thick A-horizon
76	547969	4052507	Subplanar, very subdued bars, moderate pavement 50% to 60% clast, soil pit: A 1 to 9-cm, A2 to 42cm
77	548332	4052505	Subplanar no visible bars within 50 m, 60% pavement clast covering; 27-cm-thick A1, A2 to 63 cm, should be same as large bounding units.
78	548218	4053283	Possible contact moving NW, young to old

Table 4.1-6. Geomorphic Field Observations (Continued)

Station #	Easting [m]	Northing [m]	Field Notes
79	547787	4053624	Low relief surface, BLM section corner monument here. Subtle, widely spaced bars, moderate pavement development, ~50% clast coverage. 22cm thick A-horizon,
80	547223	4053790	50- to 60-cm cutbank exposed bedded sand/ gravel covered by 25-cm coarse imbricated cobbles, flood deposit left channel and deposited ~30-m-wide lobe
81	546933	4053874	Very subtle E-W riser here, not apparent on photos
82	546890	4053993	Distinct coarse, well-varnished surface dissected by tributary streams, possibly fairly old
83	546915	4054045	Moving N, surface transitions to coarse bar and swale, no to very weak pavement development, bouldery
84	546858	4054128	Pronounced bar and swale with large and small bars ~20 m or less spacing
85	546753	4054147	Contact E-W younger to older, bar/swale to varnish pavement
86	546593	4053980	Good bar and swale, unit to W planar with good pavement
87	546346	4054039	Contact with younger bar and swale surface moving from E-W
88	546061	4054089	Maybe higher than surface across wash to E, subplanar - bar/swale, bars subdued and widely spaced
89	545570	4054341	Planar to subplanar varnished surface. Bars rare, very subdued, older surface?
90	545388	4054343	~20 m E of subtle scarp, higher on E, lower to W, but surface characteristics very similar - no bars, maybe slightly weaker pavement
91	545241	4054385	Moving from E-W, strong increase in bars and bar relief, pavement weakens. Surfaces have equal elevation so possibly unit to W in an onlapping overbank flood deposit
92	545148	4054428	No notes
93	549257	4054772	Soil pit dug by hand. Dug into unit Qy, a few km south at Hwy 95 on the E edge of fan. Soil pit revealed stage 1 to 2 carbonate to 95-cm depth; 96 cm and deeper stage 4 carbonate. Soil description included in Table 4.1-4.
94	549301	4054754	Soil pit dug by hand into Qo surface. Stage 1 carbonate common down to ~1 m; weak Bk horizon with incipient argillic development between 50 and 89 cm. Soil description included in Table 4.1-4.
95	550086	4056809	Continued to move up to N at Hwy 95. Soil pit dug into unit Qy, north of Hwy 95. Strongest soil development is a Bk horizon at 93 to 110 cm depth with stage 2 carbonate development. Soil description included in Table 4.1-4.
96	550353	4056760	Soil pit dug into surface at Qo. Btrk incipient argillic horizon at 54 to 88 cm. Sample taken at 54 to 62 cm for grain size analysis. Below 102 cm is stage 4 carbonate development. Soil description pasted into notebook. NOTE: summary from above four soil pits: Pits were dug to characterize permeable depth of alluvial surfaces. Qo surface has a well indurated impermeable stage 4 carbonate layer near 1m in depth; Qy surface is less clear. Probably the pit #93 is a paleosol and permeable depth is limited only by stage 1 and 2 carbonate and may be infinite for non-paleosol areas. Soil description included in Table 4.1-4.
97	548254	4057408	Moderate pavement development, low relief bars and weakly sutured (Qya4)
98	548299	4057607	Prominent bars with 30- to 50-cm clasts, swales have mod pavement, fairly dense clast packing, bars have some fine accumulation, bar stands 20- to 40-cm above swales (Qya5)
99	548696	4057450	Darker area on photo, surface is fairly planar, dense clast packing on pavement, some interlocking, on edges of unit some boulders are present, especially on fluvial scarp (Qya or Qo)
100	548637	4057324	Subdued bars, moderate pavement, low relief between bars and swales (Qya4)

Table 4.1-6. Geomorphic Field Observations (Continued)

Station #	Easting [m]	Northing [m]	Field Notes
101	548203	4057252	Sliver of Qya5 between older surfaces
102	548181	4057254	Reoccupy pit station 7. Pit is between two prominent bars. (Qa5)
103	549887	4057330	Near gravel pit, surface is bouldery bar swale, moderate pavement in swales, Unconformity in gravel pit; cut into finer, well cemented sandy gravel unit. Unconformity is 4 to 5 m thick
104	549516	4057693	Very subdued bar/swale, moderate pavement, subplanar. (Qya4)
105	549482	4057755	Moving NW, contact to coarse bar swale Qya5
106	549443	4057853	Moving NW - change to more closely spaced bars with poorly sorted pavement on surface
107	549424	4057914	Perhaps back onto the Qya5. More planar, bar swale
108	549309	4058034	Very prominent bars, 10s of meters long, 5 to15 m spacing, >1 m relief between bar swale (Qya6)
109	550198	4057810	Surface with moderate pavement, very low relief bars visible but mostly aggraded to same level as swales
110	550392	4056966	Tightly packed pavement generally finer than 5-cm clast size, very planar, some varnish darkens surface, no bars, stage 3 carbonate exposed in wash ~1.5 m below surface, continuous laminar cap appears ~4-cm-thick and laminated. (Qa3)
111	549955	4056852	Good bar/swale topography, bars 10 to 40 cm above swales, bars somewhat aggraded with fines, but less than Qa4. Pavement is moderate with variable clast size. (Qa5)
112	549776	4056977	Prominent coarse bar and swale, relief up to 50 cm between bar/swale. Bar clasts up to 50 cm. (Qa5)
113	549016	4056724	Reoccupied hole. Does not look like a Qa6, bar/swales fairly prominent, lots of sand on bars, bar relief indicates Qa5
114	548685	4056739	Subdued relief, subplanar, rare bars, pavement moderately well developed. (Qa4)
115	548572	4056849	Downstream end of huge bar. 40- to 50-cm clasts set above landscape, possible Qa6
116	548672	4057168	Very coarse bars, prominent features above landscape (Qa6?)
117	548802	4057143	Bars apparent, relief seems less than station (116). Relief ~50 cm. (Qa5?)
118	544236	4055275	Moved to power line road on W edge of map area. Contact with active deposition here, fresh fluvial silt approaching elevation of Qa3, silt widespread
119	544474	4055323	Planar, no bars, soil pit shows 1 m A-horizon consisting of fine/medium sand with floating gravel; good pavement development, no visible carbonate until bottom of soil pit.
120	544586	**4055246**[b]	Subplanar surface, bars very subdued, maximum size on bars is ~20 cm.
121	544755	4055108	Looks like Qa3, good pavement, no bars, but occasional swale
122	544740	4055033	Bars are subdued, 15- to 20-cm clasts (Qa4)
123	544733	4054971	Very planar, slightly higher than surrounding units. (Qa3)
124	549433	4055672	E side of alluvial fan, 2 to 3 miles S of highway. Bar/swale has 30 to 40 cm relief, bars are coarse and stand out above surface (Qa5)
125	549282	4055623	Good bar and swale topography here, 30 to 40 cm relief, boulders on surface not aggraded with eolian fines
126	549185	4055591	Subplanar surface, bars visible but no relief, pavement moderate not well sorted. (Qa4)
127	549343	4055493	Low relief with boulders. Appears dark in photos

Table 4.1-6. Geomorphic Field Observations (Continued)

Station #	Easting [m]	Northing [m]	Field Notes
128	549461	4055426	Possible contact from E to W (older to younger). E has darker pavement, is ~10 cm higher. No bars in either unit.
129	549403	4055471	Walked W across lower surface, W to E transition to darker, stronger pavement, possibly all Qa4.
130	549519	4055567	Qa4 rounded at edges, but stands ~50 cm above other surrounding surfaces, no bars.
131	546928	4050523	Moved on to Racetrack Road. Bar/swale 20 to 30 cm relief, bars fairly aggraded but appear younger than Qa4
132	546966	4050765	Low relief surface, aggraded bars with eolian fines
133	547045	4050810	Bar swale relief ~30 cm. Seems finer / lower relief than units farther up fan. Qa5
134	547149	4050888	Contact from W to E, bars subdued
135	547280	4050933	Contact from W to E clear ~40-cm riser up to well developed pavement, no bars.
136	547087	4051221	Subdued bar / swale, but light colored on photo. Surface appears to be a Qa4
137	547073	4051327	Bar and swale more prominent here, ~20 to 30 cm relief, Qa5?; Bar only subtly different than Qa4
138	547021	4051410	Edge of distributary looking feature on photo, could be Qa5 to Qa4 contact. Not necessarily a contact, though
139	546814	4051600	Very subtle bar / swale. Qa4
140	546678	4051648	Subdued bars Qa4 - subplanar
141	547310	4055710	Moved to middle of fan/map area. Moving to W, stepped up to Qa4 subplanar subdued bars
142	547375	4055516	Larger swales here (Qa4)
143	547464	4055344	No bars, good pavement development (Qa3)
144	547523	4055319	W to E contact, Qa3 to Qa4
145	547556	4055283	Moving SE, contact from Qa4 to a Qa5
146	547689	4055851	Qa4 on E side of channel
147	547772	4055096	Moving E, contact from Qa4 to Qa5. From subplanar to bar swale.
148	548685	4056027	Young-looking bar swale (Qa6)
149	548672	4055851	Area of finer material, low vegetation density, grassy (Qa6 or Qa5)
150	548620	4055845	Very high relief bar and swale with 30- to 50-cm clasts, bars not significantly buried by eolian fines, could be somewhat degradational (Qa6 or Qa5)
151	548480	4055879	Large swales bars have relief but are fairly well aggraded, Qa5 all the way to channel to W.
152	548403	4055967	Low relief bar and swale but tightly spaced. weak pavement, could be top of distributary Qa6 trending to the SW
153	548288	4056034	Bar and swale, bars have 30-cm relief over swales
154	548208	4055908	Qa5 here, to E is Qa6. Qa5 has bar/swale, Qa6 has finer, smaller bars
155	548137	4055874	Pinching out Qa5 by Qa6
156	549114	4055548	Extensive Qa4 surface here to E edge of fan. Subdued bars, low relief, subplanar
157	549000	4055687	Very young deposits, no obvious soil development, gravely bar and sandy swales, vegetation well established.
158	549047	4055829	Extremely young deposit, splayed over bank ~1 m to W.

Table 4.1-6. Geomorphic Field Observations (Continued)

Station #	Easting [m]	Northing [m]	Field Notes
159	549173	4055830	Contact moving from E-W, Qa4 to Qa3. Qa4 has visible bars with no relief; Qa3 has good pavement dominated by <5-cm clasts.
160	549804	4056039	Moving to W, stepped up to possible Qa5, bars visible, pavement weak
161	548783	4056083	Large Qa5 surface from here to W. sliver of younger (Qa6?) unit against channel to E. Lots of eolian input here.
162	548056	4055932	E to W contact. (Qa6 to Qa5)
163	548110	4055793	Bar and swale, young, bars closely spaced, braided. (Qa6)
164	548113	4055642	Stepped up onto older surface, subdued bar and swale, bars are fairly aggraded, moderate pavement (Qa5)
165	548144	4055576	Lens of Qa6
166	547721	4055673	No bars visible, possibly Qa3
167	547549	4055743	Subdued bars, subplanar (Qa4)
168	547446	4055711	Contact moving from E to W. Qa4 to Qa5. Qa4 has lower bars, less relief
169	547921	4055283	Good bars and swales (Qa5)
170	548246	4055260	E of channel (Qa4)
171	548350	4055239	Contact W to E. (Qa4 to Qa5)
172	548463	4055233	Contact up to subplanar surface, from W to E. (Qa5 to Qa4)
173	548597	4055199	Qa4 surface
174	548853	4055153	Qa5 here. Qa4 50 m E
175	549406	4055521	To E is obvious Qa4, to W is ambiguous, could be Qa4 or Qa5. Bar/swale possibly but could be a gully exposing coarse material.
176	549547	4055550	Subdued bars, subplanar, and pavement moderate. (Qa4)
177	549649	4055622	Bar swale more prominent here, bars above swales 20 to 30-cm, looks to be Qa5
178	549643	4055502	North edge Qa4. contact to E with Qa5
179	546455	4051752	Moved to SE part of map area for continued mapping. Subplanar, subdued visible bars
180	546332	4051606	Bar swale with 20- to 30-cm relief. Qa5
181	546575	4051616	Subplanar surface with very subtle bars (Qa4)
182	546711	4051797	Darker surface on photo, very subtle bars. (Qa4)
183	546812	4051846	Contact from W to E (Qa4 to Qa5)
184	546536	4051931	No bars or swales, pavement dominated by <5cm clasts, 40 cm A-horizon. (Qa3)
185	547983	4052087	Bar swale relief minor, well aggraded. (Qa4)
186	547802	4052048	Slightly more bars here, relief is ~ 20 cm for bars to swale, to E fewer bars. (Qa4 or Qa5)
187	548201	4051737	Moving W-E, either Qa3 or Qa4. Bars are absent, surface planar
188	548132	4051746	Contact possible (Qa3 to Qa4)
189	547818	4051741	Very subdued bars, subplanar surface (Qa4)
190	547690	4051779	Subdued bars, subplanar (Qa4)
191	547369	4051875	Still Qa4 moving to W
192	547067	4051966	Slightly more relief here-bar swale topography
193	547288	4051260	Difficult to distinguish between Qa4 and Qa5 in this area
194	546955	4052797	Riser here that goes up to the West but both surfaces are similar.
195	**546664**[a]	4052856	~1.5-m-thick flood deposit, fairly extensive next to active channel

Table 4.1-6. Geomorphic Field Observations (Continued)

Station #	Easting [m]	Northing [m]	Field Notes
196	**546484**[a]	4052844	Fewer bars here, possibly Qa4. Light on photos, possibly due to eolian input from channel to E Likely this is Qa5 with increased A-horizon development.
197	546172	4052873	Possible contact about 50 m to the E, from Qa5
198	545902	4052876	Older surfaces here are not set much higher than rest of landscape, bars not visible here, planar surface.
199	545365	4052309	Near contact of old to young. SE to NW, drops from subplanar unit of soil pit 48, possibly Qa4 or Qa5. This is edge of Qy6 unit showing densely packed bar swale. Relief between units is minimal but surface characteristics change noticeably.
200	545665	4052516	Prominent bar swale appears distributary in photos, bars closely spaced, ~3 to 4 m. (Qa6)
201	545742	4052617	Somewhat degraded by erosion but good pavement and rare bars (Qa4)
202	546019	4053004	Moving W to markedly increased bar swale contact. (Qa6 to Qa5)
203	545950	4053098	Moving W, contact from Qa6 to Qa5 is ~ 100 meters to E. Closely spaced bar and swale
204	545909	4053127	Contact moving W Qa6 to Qa5
205	545829	4053221	Contact E to W Qa5 to Qa4 or Qa3
206	545664	4053293	Moved W across channel- Qa6 flanked channel then up to Qa4 - subdued bars.
207	545241	4053226	Surface here has >45-cm A-horizon, but is cut by tributary network. (Qa4)
208	544960	4053377	Moving E to W, Rare bars, low relief probably Qa4
209	544749	4053460	Continuous Qa4 through here, some minor relief, occasional aggraded bars
210	544682	4053494	Contact moving W, Qa4 to Qa5. Qa5 here has slightly more bars, closely spaced.
211	544228	4053687	Possible ~75-m-wide Qa4 here.
212	544223	4053694	0.5- to 0.75-m riser from E-W ~30 m away.
213	544089	4054008	Slight riser ~25 m to SE going up to the west onto Qa3
214	544492	4052765	Same unit as soil pit # 53, likely Qa4
215	549073	4054755	Across wash E-W Stepped from Qa4 to a Qa5 with prominent bars.
216	549007	4054734	Riser E - W, contact Qa5 to Qa4
217	548909	4054716	Possible contact E -W Qa4 to Qa5
218	548620	4054712	Qa5 here
219	548541	4054718	Possible riser from E to W Qa5 to Qa4, to W subdued bars, but bars increase to W with 30 cm bar-to-swale relief, so possibly all is Qa5
220	548145	4054665	Slightly (0.5 m) above adjacent units; subplanar here with rare bars subdued. Qa4
221	548124	4054678	SE to NW down riser, Qa4 to Qa5
222	547947	4054695	Possibly on Qa4
223	547537	4054596	E to W contact, Qa5 to Qa4. Qa5 has prominent bar and swale with 30 cm relief. Qa4 has subplanar, subdued bars.
224	547267	4054455	Dropping down E-W from Qa4 to Qa5
225	547136	4054454	Closely spaced, poorly sorted bars, braided configuration, pavement weak, disorganized, microtopography much more pronounced than older units. (Qa6)
226	546936	4054452	Contact E to W of Qa6 to a Qa5, from dense bar/swale to 15-m- spaced bars.
227	546568	4054349	Bar and swale ~40-cm relief; Qa5 here. Qa4 across channel to WNW
228	546705	4054099	Contact W-E Qa4 to Qa6
229	546941	4053951	Contact W-E Qa6 to Qa5

Table 4.1-6. Geomorphic Field Observations (Continued)

Station #	Easting [m]	Northing [m]	Field Notes
230	547555	4053882	Surface has bars and swale topography Qa5
231	547963	4054090	Possibly Qa4. subdued bars, subplanar
232	550255	4058521	E edge of fan at power line Rd. E to W transect. Surface has prominent bar/swale topography, boulders/cobbles up to 30 to 40 cm, bars and swales up to 50-cm relief. Bars have signs of aggradation from eolian input.
233	550183	4058580	Continued on bar/swale surface but here is lower than previous station. Possible that this is Qa5 and previous station was Qa4
234	549929	4058323	W of Fortymile Wash, E of ab. Channel. Surface has wide clast size distribution, very disorganized bar development, weak pavement. Could be as young as Qa6 but sits fairly high in landscape
235	549802	4058312	Abandoned or flood channel with very young alluvium, bars approximately 20-m wide
236	549706	4058303	Bar swale surface here, up to 50-cm bar/swale relief, bars very coarse up to 60-cm clasts. Pavement moderate at best.
237	549632	4058296	Small planar surface here set above adjacent units, fairly well-developed pavement. No bars except on degraded edges (Qa4?)
238	549550	4058240	contact from E-W moving down ~0.5 m from generally planar surface to bar/swale
239	549354	4058310	W of active channel, fairly low-relief surface with very subdued bars, moderate pavement. (Qa4)
240	550280	4057495	New transect further S. Scarp here Qa3 edge contact to W with Qa4; subdued bars, good pavement
241	550080	4057493	W edge Qa4 surface, drops ~1m to W
242	550162	4057654	Moving N along contact relief difference still ~1m
243	550117	4057690	Qa4 here, gully or Qa5 inset between here and last station.
244	549987	4057752	Moving W, bar/swale relief, texture, has gradually increased, prominent bars spaced 30m, 0.5-1m relief close swales, Qa5
245	549831	4057813	Seems to be an N-S trending 0.5-1-m scarp here, higher to E. Could be E to W, Qa4 to Qa5. Unit here is ambiguous.
246	549656	4057831	Prominent Bar/Swale topography. bars are dense accumulation of 20- to 50-cm clasts
247	549556	4057859	W of large channel, stepped up ~2 m to subplanar surface with rare bars (Qa4)
248	549490	4057879	moving W, boulders increase, could be contact Qa4 to Qa5
249	546296	4051066	1.10-m soil pit dug - soil description pasted on pp. 54 to 55 of scientific notebook. Pit indicates no carbonate development more than stage I. 42 [cm] to 1.1 m is consistent Bk horizon; 24 to 42 cm A2; 0 to 24 cm A1. Soil description included in Table 4.1-4.
250	544116	4055019	Soil pit dug in planar, rare bar with cobble moderate pavement Qa4 surface. 135-cm deep. No obvious K-horizon, only a ~30- to 40-cm-thick Btk horizon. Above Btk horizon is either weak B horizon or new C horizon with unconformity. A-horizon is ~50-cm thick. Soil description included in Table 4.1-4.
251	544087	4054837	Intersection of Power line Rd and newly constructed road E.
252	544501	4054864	continuing on new road
253	545000	4054903	New road
254	545500	4054945	New road
255	546000	4054985	New road
256	546100	4054994	New road

Table 4.1-6. Geomorphic Field Observations (Continued)

Station #	Easting [m]	Northing [m]	Field Notes
257	550280	4057124	Qa4 contact to W at wash surface moderately well-developed, rare 40- to 50-cm coarse clasts, low relief
258	**550119**[a]	4057153	~50 m to E is apparent contact Qa4 to Qa5. Qa5 here. Bar/swale with 50-cm relief; clasts to 40 cm.
259	549935	4057225	Possible contact moving W Qa5 to Qa4
260	549905	4057364	Possible contact, moving NW, Qa4 to Qa5Qa5 has prominent boulders and bar/swale topography
261	549894	4057477	Qa5, prominent bar and swale topography
262	549918	4057639	Qa5 here, across channel to E is Qa4. Prominent Qa5 bar and swale here. East across channel is Qa4 with less bar and swale.
263	550136	4057649	Possible contact moving E Qa4 to Qa5
264	550225	4057628	Possible contact Qa5 to Qa4 to E. Bars decrease; planarity increases.
265	550297	4057595	Scarp between Qa4 and Qa3 here, Qa3 to E, 1 m higher, stronger pavement

Sources: DTN: MO0708SCSOC137.000 [DIRS 182344], Table 4.

[a] Easting coordinate value in source was in error. Value was corrected based on relative position of station to stations measured nearby, and verified once mapped.

[b] Northing coordinate value in source was in error. Value was corrected based on relative position of station to stations measured nearby, and verified once mapped.

NOTES: Coordinates are in UTM NAD83, Zone 11, meters; A-horizon refers to the top layer of the soil horizon dominated by eolian sand. This thickness is often correlated with the age of the underlying geomorphic unit. Map unit names and descriptions are those from Pelletier 2007 [DIRS 179612], pp. 94 and 95.

4.1.7 DEM and Watershed Boundary Grid

The FAR tephra redistribution model accepts a 30-m-resolution USGS digital elevation model (DEM) that covers the Fortymile Wash drainage basin down to the latitude of the Fortymile Wash fan apex. This DEM is input to the model as the file *farinputdem.txt*, which is developed from an acquired USGS DEM (DTN: SN0707DEMSOURC.001 [DIRS 182111]). The development of this DEM input file is described in Section 6.5.1 and in Output DTN: MO0605SPAFORTY.000. This grid also includes information on the boundary of the Fortymile Wash drainage basin: all grid cells within the Fortymile Wash watershed have values equal to the DEM elevation [m]; all grid cells outside the drainage basin have a value equal to "-9999.0."

4.1.8 Scour Depth Data

Scour depth measurements at the Narrows station on Fortymile Wash (six scour chains, A through F, as listed in Table 4.1-7) were used to calibrate a relationship between scour depth and contributing area in Section 6.5.6. These data are qualified for their intended use.

Table 4.1-7. Summary of Scour Depth Data

Measurement Description	(A)	(B)	(C)	(D)	(E)	(F)
7/12/1985						
Vertical length (ft) below LSD	4.9	5.7	5.3	5.5	4.9	4.7
Horizontal length (ft) above LSD (E in figure)	1.4	1.5	0.6	0.5	1.1	0.9
1/28/1992						
Horizontal length (ft) (E in figure)	1.27	1.6	0.68	0.49	1.12	0.85
11/16/1995						
Horizontal length (ft) (L in figure)	N/A	Pulled out w/ backhoe	1.64	2.28	3.7	2.6
Fill above chain	N/A	3.0 to 4.0	2.95	2.50	3.60	2.85

Source: DTN: SN0711SCOURCHM.002 [DIRS 183849].

4.2 CRITERIA

Yucca Mountain Review Plan, Final Report (YMRP) (NRC 2003 [DIRS 163274]) associates the integrated sub-issue of redistribution of radionuclides in soil with the requirements listed in 10 CFR 63.114(a) to (c) and (e) to (g) [DIRS 180319]. The YMRP (NRC 2003 [DIRS 163274], Section 2.2.1.3.13.3) describes the acceptance criteria that the U.S. Nuclear Regulatory Commission (NRC) will use to evaluate the adequacy of information addressing redistribution of radionuclides in soil in the license application. A listing of the acceptance criteria applicable to the tephra redistribution model along with information addressing how these acceptance criteria are met is presented in Appendix B.

4.3 CODES, STANDARDS, AND REGULATIONS

No codes, standards, or regulations, other than those identified above in Section 4.2, were used in this model report.

INTENTIONALLY LEFT BLANK

5. ASSUMPTIONS

The tephra redistribution model was designed to estimate the near-surface concentration of radionuclide materials at the compliance point, given a disruptive event where radioactive material is entrained into magma, which is then dispersed on the surrounding terrain. The model provides time dependent estimates of these near surface concentration profiles for elapsed time after the disruptive event.

A number of simplifying assumptions are made in the model. These assumptions are addressed in this section, including general assumptions of the model, assumptions in the initial mobilization and redistribution of the tephra and contaminant, and assumptions in the migration of the contaminant into the channels and divides of the RMEI location after its initial deposition or re-deposition.

5.1 GENERAL MODEL ASSUMPTIONS

5.1.1 Effects of Future Climate Changes

Assumption—Model processes and parameter values are assumed to be the same for modern and future climates.

Rationale—The model has been designed to calculate the redistribution of contaminated tephra after a single disruptive event (radioactive material in the repository is assumed to be entrained in the magma and dispersed on the surrounding terrain during this event). The time after closure of the repository for which this disruptive event occurs is unknown, and is treated as an uncertain parameter in the TSPA Monte Carlo analysis. The model processes and parameters are assumed to be the same for modern and future climates.

Future climates may be wetter than the modern climate (BSC 2004 [DIRS 170002]). Several tephra-redistribution model processes are controlled by precipitation and its resulting variables (i.e., flood discharges, infiltration rates, etc.), but these controls are very difficult to quantify. The simplifying assumption of a climate-independent model can be shown to be conservative with respect to the calculated concentrations, however. First, the volume of tephra mobilized from hillslopes will depend primarily on vegetation density. If the climate changes to a wetter (pluvial) period, this period is projected to have about 1-1/2 to 2 times the current annual precipitation (BSC 2004 [DIRS 170002), resulting in higher vegetation densities. Higher vegetation densities can be expected to result in a lower volume of remobilized tephra due to the increased anchoring of hillslope tephra and regolith by plant roots. Second, scour depth in channels increases proportionately with the square root of peak flood discharges. While mean precipitation in a pluvial climate would be greater than that of the modern climate, peak discharges may or may not increase. Any increases in peak discharges or storm intensities would result in increased scour depth, thereby lowering tephra concentrations in channel sediments due to increased mixing with uncontaminated sediments. Finally, a wetter climate would lead to increased infiltration rates, thereby increasing the radionuclide diffusivity in the soil profile. Higher diffusivity values would lower radionuclide concentrations in the critical near-surface layer that feeds the inhalation dose pathway. In summary, the effects of a wetter climate on

tephra redistribution are difficult to quantify but can reasonably be expected to result in lower waste concentrations at the RMEI location.

Confirmation Status—No testing or modeling activities are planned to provide further confirmation of this assumption.

Where Used—Section 6.

5.1.2 Spatial Distribution of Fluvial Activity across the Fortymile Wash Alluvial Fan

Assumption—It is assumed that the spatial distribution of past flooding and deposition, as constrained by surficial-geologic mapping and correlation with fan deposits of known ages, will be similar to that of future flooding.

Rationale—Alluvial fans are dynamic landforms that can evolve topographically over both long and short time scales. A distinction can be made, however, between the evolution of alluvial fans over time scales of millions of years and the evolution of "entrenched" or "segmented" alluvial fans over shorter time scales. In tectonically active areas and over time scales of millions of years, alluvial fans aggrade by sedimentation in channels and by channel shifting (avulsion). Over these long time scales, alluvial fans are best considered to be subject to fluvial deposition across the entire fan area. The Quaternary period, however, has caused cycles of channel aggradation and incision on alluvial fans in the western United States. As a result of these cycles, fluvial activity on many alluvial fans is confined to a small fraction of the fan area adjacent to the modern channels. Older terraces are commonly preserved from previous episodes of aggradation and incision, but these terraces are no longer subject to fluvial activity, even during extreme events (Bull 1991 [DIRS 102040]). Surficial characteristics observed in the field, including well-developed desert pavement and varnish, provide evidence for the stability of channels and the lack of significant, soil-disruptive flood events on interchannel divides.

Surficial characteristics were used to map the surficial geology of the Fortymile Wash alluvial fan (see Section 6.5.1). Surficial-geologic mapping is widely used as a technique, alone or in combination with hydraulic modeling, to constrain the future flood risk on alluvial fans (Pelletier et al. 2005 [DIRS 175659]). This approach assumes that past flooding activity is representative of future flooding activity. This assumption may not hold if major tectonic or climatic events lead to a large increase in sediment delivery to the fan. Such changes in sediment delivery would cause channel aggradation, avulsion, and an increase in the area of the fan subject to fluvial activity. If this occurred in the future, the effect would, however, lead to the same or lower surface concentrations for the fan as a whole compared with the spatial distribution of fluvial activity under modern conditions. If waste becomes partitioned over a larger fan area, channel concentrations would be proportionately lower.

Confirmation Status—No testing or modeling activities are planned to provide further confirmation of this assumption.

Where Used—Section 6.

5.1.3 Floodplain Sedimentation

Assumption—It is assumed that floodplain sedimentation and deposition will not affect tephra redistribution.

Rationale—This is not a significant limitation for drainage networks in the Yucca Mountain region, or, more generally, many regions in the western U.S. because these drainage networks have no active floodplains. Late Cenozoic climatic, tectonic, and internal drainage adjustments have created a series of nested alluvial terraces on many piedmonts and alluvial fans that rise like a flight of stairs from the active channel (Bull 1991 [102040]). Many alluvial channels in the Yucca Mountain region, therefore, are entrenched into and bounded by early Holocene and older deposits that have not been subject to fluvial erosion or deposition for at least several thousand years. This entrenchment often confines active fluvial erosion and deposition to relatively narrow, flat-bottomed channels that are entirely inundated from bank to bank during extreme flood events. In this report, the Fortymile Wash drainage basin is the primary study area. In that drainage basin, the main Fortymile Wash channel is incised up to 20 m into late Pleistocene terraces. Extreme flows in Fortymile Wash are approximately 1 m deep, so the active channel banks are about 20 times higher than the water depth. As such, overbank deposition will not occur. The 20-m incision depth gradually decreases downstream to approximately 2 m at the fan apex. However, even on the distributary Fortymile Wash fan where relief across the fan is relatively small, surficial geologic mapping indicates that active channels are entrenched into and bounded by mid-Holocene and older deposits (based on soil development and surficial characteristics diagnostic of age) with little to no evidence of overbank sedimentation (Pelletier et al. 2005 [DIRS 175800]). Therefore, overbank or floodplain deposition does not generally occur in the study area.

Confirmation Status—No testing or modeling activities are planned to provide further confirmation of this assumption.

Where Used—Section 6.

5.1.4 Channel Geomorphology

Assumption—It is assumed that the current channel geomorphology is an adequate representation of future channel morphology.

Rationale—It is recognized that some changes to the geomorphology may occur as a result of a future eruption or other changes in the environment, but it is assumed that these changes will have little effect on the overall geomorphology of the basin and its ability to redistribute contaminated tephra to the RMEI location. ASHPLUME is based on a model of Suzuki (1983 [DIRS 100489]) that Jarzemba et al. (1997 [DIRS 100987]) refined to represent violent Strombolian-type eruptions. A violent Strombolian eruption involves ejection of magma into the atmosphere as a ballistic fountain of up to cm-sized scoria fragments from which μm- and mm-size ash is elutriated in a rising convective plume above the fountain. Whereas the fountain deposits a cone of potentially contaminated scoria around the vent orifice, the convective plume provides a source for distal transport of potentially contaminated ash downwind over a wide area. Fallout of ash from the plume forms a ground layer that generally thins with distance from

the vent. The tephra deposited over the terrain after an eruption is unconsolidated, and the channel heads near the vent location may be impacted by the deposition of the thick tephra layer. However, as discussed in Section 5.1.3, the alluvial channels in the Yucca Mountain region are entrenched into and bounded by early Holocene and older deposits. While the channel heads near the vent may move, the overall channel geomorphology likely will not be impacted due to the deep entrenchment of the channels. Those channels further from the vent will be less impacted by the initial tephra deposition given the thinner tephra layer in these areas.

This assumption is bolstered by the Fortymile Wash flood potential analysis performed by Squires and Young (1984 [DIRS 180001]). The authors concluded that 100-year, 500-year, and even regional maximum floods would remain within the confines of Fortymile Wash Canyon. While unable to quantitatively determine the extent of erosion and sediment movement caused by flood flows in the ephemeral stream course meandering across the wash, they concluded that, qualitatively, erosion of or deposition in channels would probably be significant during the 100-year flood, and could be severe during the 500-year and regional maximum floods. They noted that excessive erosion and deposition was observed in places during field surveys. Thus, while the ephemeral-channel system will likely undergo significant changes in depth, width, and position within the main wash over time, it will stay within the walls of the wash.

Given that the deeply incised morphology confines the active fluvial erosion and deposition to the channels, and that extreme floods scour the channel bed during the waxing phase of the flow and redeposit sediments downstream during the waning phase of the flow, it is possible that the channel bed can be lowered or raised during flood events. Over significant time it is reasonable to assume that, in general, the streambed elevation will not change significantly. The units through which the channels are entrenched are over 10,000 years old. Given the relatively shallow channels developed on this time scale (on the order of one to 20 meters), the assumption is reasonable.

Confirmation Status—No testing or modeling activities are planned to provide further confirmation of this assumption.

Where Used—Section 6.

5.1.5 Concentrating Processes

Assumption—Physical, chemical, or biological processes that might concentrate radionuclides at the RMEI location are assumed to be negligible.

Rationale—Under most circumstances, the highest concentration of a contaminant will be the source of that contaminant, with concentrations becoming more dilute with distance from the source. However, there are some instances when accumulation of a contaminant will create a higher concentration of that contaminant at some distance from the source. Physical processes such as grain size or density sorting (e.g., winnowing and placering) can result in increasing concentrations of certain materials. Alluvial, eluvial, and eolian placers are formed by the deposition of dense particles at sites where velocities decrease to the point that the particles can no longer be entrained in the flow. To form a placer deposit, the particles must show a marked density contrast with the gangue material, which is able to be transported away from the trap site.

Typical locations for alluvial placer deposits are on the inside bends of rivers and creeks, in natural hollows, at the break of slope on a stream, the base of an escarpment, or other barrier, within sand dunes, or in gravel beds.

Chemical processes, such as preferential dissolution and/or precipitation, could also potentially cause increased concentrations of materials. Dissolution is very common in areas that have a great deal of evaporates and/or limestone, but is unlikely to play an important role in concentrating radionuclide concentrations at Yucca Mountain following a potential eruption scenario. Rather, dissolution of certain radionuclides into infiltrating waters will tend to reduce near-surface concentrations of these constituents, since they will be transported deeper into the soil. Therefore, it is reasonable to assume that chemical concentration processes are negligible and can be excluded from the model.

Biomagnification or bioaccumulation is another process which can cause increases in the concentration of a material. To the extent that bioaccumulation processes may have affected radionuclide concentrations, no specific mechanisms have been identified that cause bioaccumulation in the Yucca Mountain region soils or sediments, to the extent that they may affect radionuclide concentrations in the near surface layer they are implicitly included through the use of bulk soil concentration data from the Yucca Mountain region in the calibration of the diffusion model (Section 6.5.8). Possible bioaccumulation mechanisms within the biosphere exposure pathways are outside the scope of this model.

For the Fortymile Wash drainage basin, the most likely mechanism to accumulate contaminated material is placering. The ash redistribution model does not explicitly include the mechanical process of preferential concentration of sediment particles due to density contrasts. This process, which is a significant mechanism for concentrating pure mineral phases such as gold in placer deposits, will have a negligible effect on mean contaminant concentrations at the location of the RMEI. Uraninite placer deposits exist in the geologic record from early Precambrian metasedimentary rocks (older than approximately 2.3 billion years ago), but these deposits are interpreted as having formed in an atmosphere that was significantly less oxidizing than that of today (e.g., Canfield 2005 [DIRS 183192]). Uraninite is unstable in the present oxidizing atmosphere, and placer deposition is not a significant process for increasing the concentration of uranium-bearing minerals in the strongly oxidizing environment of an intermittent stream because the minerals themselves will not persist. Plutonium and other transuranic elements may form mineral phases that are stable in oxidizing environments and therefore may be transported with the bed-load sediment; however, the mass of these radionuclides that remains after uranium is leached from the spent fuel particles incorporated in the tephra is very small compared to the mass of the tephra particles themselves. Density contrasts within the sediment will be small compared to those that created the Precambrian uraninite deposits or modern gold placers. Preferential separation of contaminated particles due to density contrasts will therefore be a minor effect. In addition, should any preferential increase in the concentration of contaminants occur, it will be balanced by a comparable decrease in concentration at other locations: mass can reasonably (and conservatively) be assumed to be conserved in the sediment transport process. Because the overall performance assessment is probabilistic, mean concentrations of nuclides at the location of the RMEI and the mean annual radiation doses that form the regulatory basis of the compliance evaluation will be insensitive to small-scale local variations in radionuclide concentrations.

In the absence of site specific evidence which would indicate that any of these concentration processes may systematically occur within the Fortymile Wash area, these processes have not been included in the model.

Confirmation Status—No testing or modeling activities are planned to provide further confirmation of this assumption.

Where Used—Section 6.

5.2 ASSUMPTIONS IN THE INITIAL MOBILIZATION AND REDISTRIBUTION OF THE TEPHRA AND CONTAMINANT

5.2.1 Rate of Hillslope and Fluvial Redistribution to the RMEI Location

Assumption—Hillslope and fluvial redistribution to the RMEI location is not time dependent, but assumed to occur instantaneously following an eruption.

Rationale—Hillslope and fluvial redistribution occurs by a complex set of processes including mass movement, dry ravel, slope wash, rilling, and fluvial entrainment and mixing. Collectively these processes will remobilize tephra and waste rapidly at first, and then more slowly as a diminished tephra volume remains on the landscape and the landscape returns to a state similar to the pre-eruption conditions. Quantifying this transient response would be very difficult. The tephra redistribution model makes the assumption that hillslope and fluvial redistribution to the RMEI location takes place instantaneously following an eruption.

The hillslope component of the redistribution model redistributes tephra and waste if the hillslope gradient is greater than a threshold value. This model component represents landsliding of oversteepened slopes following the eruption, dry ravel, slope wash, and rilling. Landsliding of oversteepened slopes can be expected to occur during the eruption or within the first few years following the eruption, consistent with the assumption. Rates of dry ravel, slope wash, and rilling will vary from slope to slope depending on gradient, texture, slope aspect, morphology (i.e., converging versus diverging slopes) and other factors. In these cases instantaneous redistribution is not realistic but is considered to be an acceptable simplification because it puts waste at the RMEI location earlier than it might otherwise arrive there.

The fluvial component of the redistribution model integrates all of the tephra and waste remobilized from hillslopes and channels, mixes that volume with uncontaminated channel sediments in a scour-dilution-mixing process, and then deposits that mixture at the RMEI location. Graf's (1990 [DIRS 178705]) study of contaminant mixing with channel-bed sediments following the tailings-dam break on the Rio Puerco suggests that significant mixing can occur even during a single flood. Graf found that downstream radionuclide concentrations were inversely related to the duration of time that unit stream power exceeded the critical shear stress for entrainment. Flood duration may have been a controlling factor because longer flood durations result in more effective mixing during the early phase of contaminant introduction when mixing was incomplete. Based on this and other successful applications of the dilution-mixing model to cases of historical (i.e., decades-old) cases of contamination, the assumption of an effectively instantaneous scour dilution mixing model relative to a 10,000-year (or 1 million year) modeling period for calculating dose to the RMEI appears to be reasonable.

Thus, the hillslope component of the model mobilizes all tephra / contaminant instantaneously, and the fluvial component of the model mixes and deposits the material at the RMEI location instantaneously, capturing maximum concentrations. As the model does not calculate any further dilution due to mixing or transport of the material after its instantaneous re-deposition, these maximum concentrations are maintained for the entire period covered by the model results.

Confirmation Status—No testing or modeling activities are planned to provide further confirmation of this assumption.

Where Used—Section 6.

5.2.2 Eolian Redistribution to the RMEI Location

Assumption–Eolian transport of contaminated tephra to the RMEI location is assumed to be negligible compared with the direct deposition and fluvial redistribution.

Rationale–The exclusion of eolian transport processes in the tephra redistribution model is justified because eolian transport is expected to reduce the concentration of radionuclides at the RMEI area (by removal and dilution) and because the range of parameter values for the fluvial model accounts for the effect of migration of sediment from the channel onto divides. Wind directions in the region between Yucca Mountain and the RMEI location favor eolian transport from south to north. This is reflected in rose diagrams from regional weather stations (e.g., to the NW in SNL 2007 [DIRS 177431], Appendix D, and to the NNW in Pelletier and Cook 2005 [DIRS 175659]). These data indicate that while wind directions fluctuate by approximately 180 degrees over the year, the highest wind speeds occur when the wind is blowing generally toward the north and northeast and it is the highest wind speeds that influence eolian deposition and erosion. Because wind directions favor eolian transport at Yucca Mountain away from the RMEI location, eolian processes will generally tend to further dilute surface concentrations and may even lead to the erosion and transport of the initial tephra deposit at the RMEI location, further reducing the concentrations of waste in this area.

In addition to transport of contaminated tephra following an eruption, dust deposition from "clean" sources is an active process in this region. Neglecting this dust deposition in the model will tend to overestimate surface concentrations because the addition of clean material onto the divides and resulting burial (or erosion) of the primary tephra deposit is not included in the model. Modern dust mass deposition rates in southern Nevada and southeastern California have been measured since 1985 and range from 2 to 20 $g/m^2/yr$ (Reheis 2006 [DIRS 180898]), which, assuming a reasonable bulk density of 1 g/cm^3 results in a deposition rate of 2 to 20 cm/10,000 years. Dust deposition rates have varied significantly in the past, with rates during the late Pleistocene being considerably lower than modern rates, and rates in the early Holocene near pluvial lakes being much higher than modern rates (Reheis et al. 1995 [DIRS 106658]). Dust sources in this region are from both alluvial fans and playas located as far as 20 km upwind of the deposit location, and hydrologic conditions at these source regions (e.g., annual precipitation) have been correlated to local deposition rates (Reheis 2006 [DIRS 180898], p. 490).

Consider the potential transport pathways from the location of primary fallout to the RMEI area. These are:

1. Primary fallout at the RMEI location on the Fortymile Wash alluvial fan; eolian redistribution at the site of primary fallout; inhalation by the RMEI.

2. Primary fallout in the Fortymile Wash drainage basin; eolian entrainment from the site of primary fallout; deposition at the RMEI location; dose to the RMEI by inhalation and other pathways.

3. Primary fallout in the Fortymile Wash drainage basin; fluvial redistribution to the channels of the RMEI location; eolian transport from the channels to the divides of the RMEI location; dose to the RMEI by inhalation and other processes.

4. Fine particles transported from the Fortymile Wash drainage basin as suspended load during large floods and deposited south of the RMEI location in Franklin Lake Playa and then eolian transport of this material to the RMEI location; dose to the RMEI by inhalation and other pathways.

The first of these four pathways is included in the biosphere model (SNL 2007 [DIRS 177399]) and included in the TSPA. Additional explicit modeling of eolian transport at the RMEI location would result in a lower dose, as primary fallout tephra would be removed from the RMEI area (and hence waste concentrations would be reduced).

The second transport pathway is considered to be negligible based on the prevailing direction of the highest velocity winds, which is generally from the south in the vicinity of Yucca Mountain (e.g., SNL 2007 [DIRS 177431], Appendix D; Pelletier and Cook 2005 [DIRS 175659]). This wind direction does not result in significant eolian transport from the upper drainage basin domain to the RMEI location.

The third transport pathway deals with eolian transport of sand-sized particles from the channels of Fortymile Wash to the divides. Transport of this type occurs in the present, but deposition is primarily localized within a narrow margin along the active channels, with minor amounts of deposition extending for several hundred meters downwind from the channel. Figure 5-1 is an orthophoto mosaic of the Fortymile Wash alluvial fan. The figure identifies the locations of several sand streaks originating in the channel and extending to the NNW, consistent with the prevailing wind direction. Sand streaks are created as sand is blown from the channel bed up onto divides. In the field, these sand streaks are composed of continuous sand (covered by sand ripples) within approximately 10 to 20 m of the active channel. The continuous sand cover transitions to disturbed desert pavement, and eventually to undisturbed desert pavement, with increasing distance from the channel. Eolian sand and silt is found within the top tens of centimeters on the older alluvial fan units (Qa4 and Qa3); however, these surfaces are significantly older than 10,000 years and deposition has occurred gradually over this time (Appendix A). The consequence of not directly including this localized redistribution within the RMEI domain is expected to be insignificant. To calculate the eruptive dose to the RMEI, the TSPA model essentially sums the waste concentrations from active channels and interchannel divides weighted by the fraction of the fan composed of active channels (F) and divides ($1 - F$),

respectively. This approach is equivalent to assuming that the RMEI is exposed to radionuclides from the channels and divides proportional to their area. Since most scenarios result in greater concentrations within the channel sediments (due to prevailing wind direction being opposite to the direction of fluvial transport), the effect of redistributing tephra from the channels to the divides in the RMEI location can be approximated by increasing the fraction of area comprised of active channels, *F,* which is sampled from a uniform distribution between 0.09 and 0.52. The current active channel (Qa7) covers less than 5% of the fan area. The effect of this transport pathway is implicitly accounted for in the model by the very large range in the *F* parameter being used.

The forth transport pathway deals with the possibility that fine-grained waste-contaminated tephra may be blown to the RMEI from the south. In this scenario, silt- and clay-sized particles are carried as suspended load during large floods from the Fortymile Wash drainage basin into the Amargosa River. The primary depozone for silt and clay from Fortymile Wash is Franklin Lake Playa, which is about 30 km south of the RMEI location. Given the observed lack of silt sized particles in the channels of Fortymile Wash, and the prevailing wind direction, the predominant source of wind blown silt-sized particles to the RMEI location, therefore, is Franklin Lake Playa. Pelletier and Cook (2005 [DIRS 175659]) found that silt accumulation rates proximal to Franklin Lake Playa decrease very rapidly with distance from playa sources. The thickness of eolian deposits on divides 1 to 2 km downwind of Franklin Lake Playa were found to be 0.5 to 3.0 cm on early Holocene to late Pleistocene surfaces. These rates ($\approx$1 cm / 10,000 years) are considered to be maximum values for eolian deposition from a localized source in this region because (1) Franklin Lake Playa is one of the most emissive playas in the western U.S. (owing to a fine-grained porous surface) and (2) the divide locations studied by Pelletier and Cook were within 1 to 2 km of Franklin Lake Playa. In the event of a volcanic eruption at Yucca Mountain, fines redistributed from Franklin Lake Playa will require longer transport distances of approximately 20 km or greater to reach the RMEI location, and will entrain clean material along the way, resulting in an overall dilution effect of material deposited at the RMEI location.

Confirmation Status—Confirmation of the entrainment of primary fallout component is provided in the biosphere model report. Treatments of the remaining pathways are based on field observations. No additional testing or modeling activities are planned to provide further confirmation of this assumption.

Where Used—Section 6.

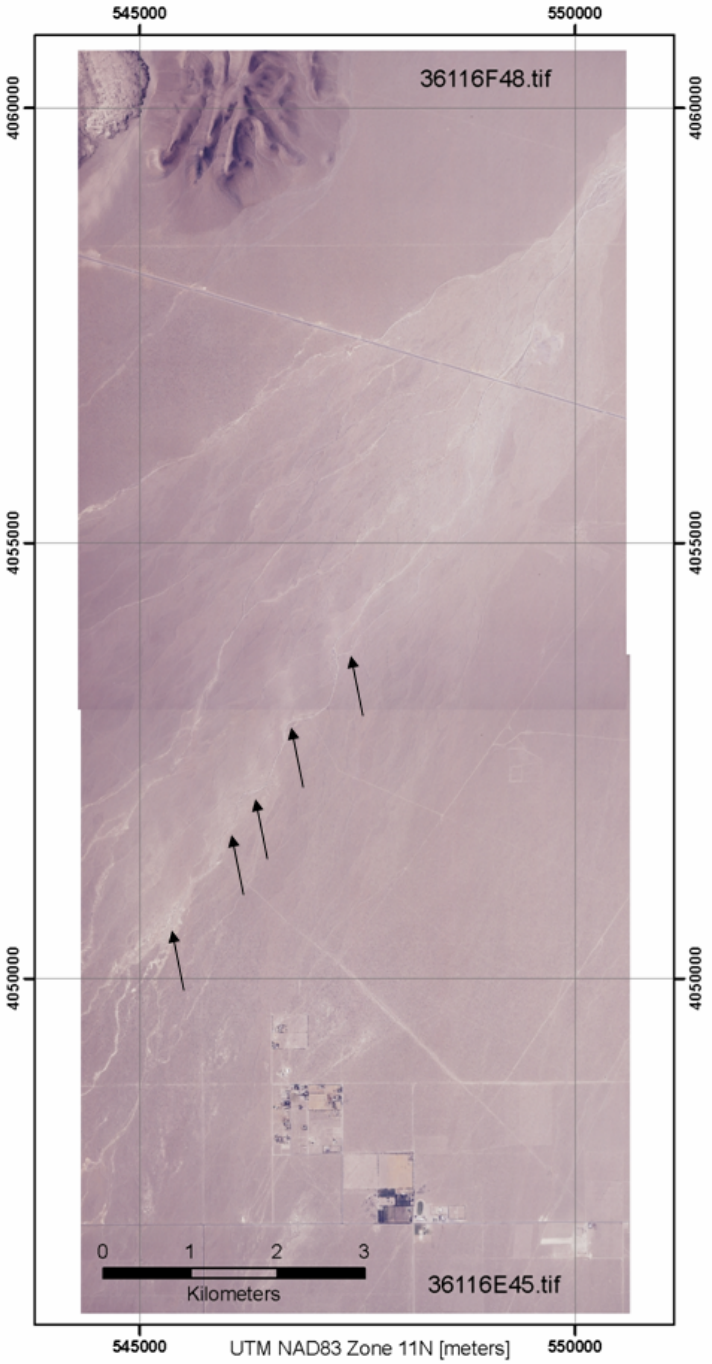

Source: DTN: SN0706DIGORTHO.001 [DIRS 182108].

NOTE: Arrow tips point to the origins of selected sand streaks that are parallel to the arrow directions. Mosaic includes SW quarter of "Amargosa Valley" quadrangle and NW quarter of "South of Amargosa Valley" quadrangle.

Figure 5-1. USGS Orthophoto Mosaic of the Fortymile Wash Alluvial Fan

5.2.3 Mode of Sediment Transport

Assumption—For the purpose of modeling transport of contaminants to the RMEI location, it is assumed that all sediment transport can be represented as bed-load transport.

Rationale—There are two general modes of sediment transport in channels: bed load and suspended load (wash load is a third type but can also be considered part of suspended load). Sediment that is coarser than a threshold grain size will move primarily as bed load; finer material will move predominantly as suspended load.

Material transported as suspended load will be carried high in the water column and will be transported past the RMEI location and into the Amargosa River more readily than coarse material. Silt-sized material is often transported as wash load, meaning that it will be transported in the water column until the flood waters infiltrate completely. While some floods will infiltrate completely before they reach the RMEI location or the Amargosa River downstream, the flood hydrology of large drainage basins in the western U.S. is dominated by frontal storms and tropical storms of significant duration (~ 1 to 3 days) that saturate channel sediments and result in continuous flood events throughout drainage basins of regional extent. The channels of Fortymile Wash fan are almost completely devoid of silt, indicating that this drainage basin is, indeed, dominated by these types of storms. It is noted that Franklin Lake Playa is the primary depozone for silt-sized particles in the area.

Material transported as bed material will be mixed with the channel bed sediment, as floods scour the channel bed during the waxing phase of channel flow, and then be redeposited downstream during the waning phase of the flow.

The adequacy of the bed-material-load assumption depends on the relative texture of the contaminant and channel-bed material. Measured grain size distributions from analogue explosive cinder-cone eruptions of the magnitude expected at Yucca Mountain result in a range of tephra particle sizes from 0.01 mm (silt) to 1.0 mm (coarse sand) with a median value of approximately 0.1 mm (fine sand) (DTN: LA0612DK831811.001 [DIRS 179987]). Channel sediments in the Fortymile Wash system are dominated by medium sand but also incorporate significant amounts of fine sand (Pelletier et al. 2005 [DIRS 175800]), indicating that sediments of fine-sand size and greater are transported as bed-material load, while finer size fractions (e.g., silt) may travel in suspension. The similar texture of tephra particles relative to channel bed sediments indicates that most of the tephra fallout will also be transported as bed material load in the channels of the Yucca Mountain region. On the alluvial fan, sediment transport as the result of sheetwash on low-slope inter-channel divides is not included in the model because there was no significant evidence of this process observed in the field.

By treating all of the tephra from the eruption as coarse-grained sediment for the purposes of fluvial transport, the model errs on the side of conservatism. Fine-grained sediments that are transported as suspended load will be transported past the RMEI location and into the Amargosa River (based on the lack of silt currently stored in channel bed material). By considering all of the tephra as bed load, the model predicts that contaminants will persist longer in the system, resulting in higher concentrations in the RMEI channels. The assumption that contaminants are only transported by bed load means that leaching of radionuclides dissolved into infiltration

water is also ignored. For certain radionuclides, including uranium, iodine, and technetium, this is most likely a conservative assumption, since these elements would be highly soluble in this environment. However, other radionuclides such as plutonium, thorium, and neptunium would likely be stable and persist with the tephra in the channels during fluvial transport.

Confirmation Status—No testing or modeling activities are planned to provide further confirmation of this assumption.

Where Used—Section 6.

5.2.4 RMEI Domain Is Not a Perfect Depozone

Assumption—The model is not a closed system, as it assumes that the tephra and contaminant can be transported through the RMEI domain.

Rationale—Flow at the Fortymile Wash fan apex (labeled in Figure 1-2) splits into roughly six separate channels distributed across the alluvial fan. During large floods, the flow velocity in these channels is somewhat less than in the main channel upstream, due to increased bed friction resulting from the channel splitting, but is still high enough that all but the largest particles remain entrained. This rationale is discussed in greater detail in Section 7.

Since the FAR model mobilizes and deposits tephra at the RMEI location instantaneously following the eruption (Section 5.2.1), contaminated material contributes immediately to the concentrations predicted at the RMEI location. Because the model does not allow further dilution of the contaminants after the initial redistribution, contaminated material remains in the RMEI at all times after the eruptive event. Therefore, the fact that the RMEI location is not a perfect depozone does not mean that radionuclide concentrations are underestimated.

Confirmation Status—No testing or modeling activities are planned to provide further confirmation of this assumption.

Where Used—Section 6.

5.2.5 Mass of Radionuclide Contaminant Is Directly Proportional to the Mass of Tephra Initially Deposited

Assumption—It is assumed that the concentration of fuel associated with the ash in a particular location can be calculated after the ash has been re-distributed using the ratio of the total mass of waste to the total mass of ash mobilized in the upper drainage basin.

Rationale—Both ash and fuel concentrations are currently calculated in ASHPLUME (SNL 2007 [DIRS 177431]). The ASHPLUME code determines the fuel fraction (ratio of fuel mass to ash mass) as a function of the particle sizes of the two constituents, where waste particles can only be incorporated into ash particles which are of equal size or larger. ASHPLUME does not adjust the ash / fuel particle size (the total mass of volcanic ash erupted will be much greater than the total mass of fuel available for incorporation, so the introduction of a relatively small amount of fuel mass into the ash mass is unlikely to alter the size distribution of the ash). The density of the combined ash-waste particles is adjusted to account for the presence of the

high-density waste. The mass of fuel deposited at a particular location is calculated using the fuel fraction term, particle size, and eruption column height. Both the fuel and the ash concentration distributions are used as input to FAR. In the divides of the RMEI location, the waste concentration calculated by ASHPLUME for this location is used directly by the FAR model. In the channels of the RMEI location, waste concentration is calculated as the sum of the concentration provided by ASHPLUME (the material initially deposited and distributed in the scour zone) and the average concentration in all of the mobilized tephra (the ash and fuel redistributed from the upper drainage domain) (see Section 6.3.3). This simplified approach is warranted because the tephra redistribution process mixes tephra and waste during transport, and the waste deposited in channels at the RMEI location is the result of mixing in a large area of the upper drainage basin.

Confirmation Status—No testing or modeling activities are planned to provide further confirmation of this assumption.

Where Used—Section 6.

5.3 POST-REDEPOSITION DIFFUSIVE TRANSPORT IN THE RMEI DOMAIN

Redistribution of radionuclides into the soil, once they have been deposited in the RMEI domain, occurs primarily through suspension and redeposition of fine particles by infiltration, and physical mixing of soil particles by freeze-thaw cycles and bioturbation. FAR models this movement of the contaminant into the soil as a diffusive process.

5.3.1 No Advection

Assumption—For the purpose of modeling radionuclide transport to the RMEI location, it is assumed that there will be no advective movement of the radionuclide material once it is deposited at the RMEI location.

Rationale—It is recognized that, in general, both advection and diffusion will occur. However, available data from anthropogenic radionuclide depositions is insufficient to determine the advection velocity, as the maximum concentration of radionuclides in all of the published literature considered was at the surface (consistent with zero advection). The modeling assumption of zero advection velocity is appropriate because it will tend to overestimate radionuclide concentrations near the surface.

Confirmation Status—No testing or modeling activities are planned to provide further confirmation of this assumption.

Where Used—Section 6.

5.3.2 No Further Mixing or Transport Occurs after Initial Deposition

Assumption—For the purpose of modeling radionuclide transport to the RMEI location, it is assumed that once the contaminated tephra has been re-distributed in the RMEI domain channels, no further fluvial mixing occurs.

Rationale—Tephra and waste redistributed from the Upper Fortymile Wash drainage domain are deposited only in the active channels of the alluvial fan. The depth of the contaminated tephra, and its associated radionuclide concentration, is taken to be the same as the scour depth near the fan apex. Vertical redistribution of radionuclides within the active channels is then modeled as a one-dimensional diffusion process in a finite soil layer. It is the diffusion of the radionuclides into the clean soil beneath the contaminated tephra layer that provides the time-dependent concentration profiles used in TSPA. The same diffusion process is used to predict concentration profiles on the inter-channel divides, with the only difference being the initial thickness and concentration.

The assumption of no additional fluvial mixing in the channel subdomain results in surface concentrations that are higher than at depth because the surface is furthest from the lower diffusion boundary (initially zero concentration). Subsequent fluvial mixing would therefore tend to homogenize the concentration profile and result in a net increase in the downward movement of radionuclides.

The assumption of no additional fluvial transport of the contaminant in the channel subdomain results in both a greater mass of contaminant in the channel bed and higher concentrations. Large floods will continue to transport material through the RMEI location over time, eventually cleaning the RMEI location channels. Disallowing this cleansing process is conservative.

Confirmation Status—No testing or modeling activities are planned to provide further confirmation of this assumption.

Where Used—Section 6.

5.3.3 Migration of Different Radionuclide Species in the Soil Profile at the RMEI Location

Assumption—It is assumed that all radionuclide species migrate into the subsurface at approximately the same rate.

Rationale—This assumption is appropriate because the dominant process of vertical migration of radionuclides into the soil is physical, rather than chemical in nature, despite the fact that it is generally represented with a diffusion model. Research following the Chernobyl accident indicates that different radionuclides migrated into the subsurface with similar rates. Results from Anspaugh et al. (2002 [DIRS 169793]) for ^{129}I, ^{137}Cs, ^{239}Pu, and ^{240}Pu indicate that all of these radionuclides move into the soil at the same rate and that their distributions in the soil were essentially identical. The authors conclude that the process of radionuclide migration into soil is essentially a physical rather than chemical process. Although data are limited on other radionuclides, the ^{235}U data from the Nevada Test Site (Gilbert and Eberhardt 1976 [DIRS 169808]) seem to follow similar migration rates.

Radionuclides will migrate into the subsurface through bulk mixing processes such as freeze/thaw, wetting/drying, and bioturbation, as well as by suspension in infiltrating flow. The species dependence of each of these processes is difficult to quantify. ^{137}Cs profiles measured at the RMEI location are used for model calibration, and it is assumed that other radionuclide

species migrate with the same range of diffusivity values. The range of values used in the model likely encompasses some of the species-dependent variation in diffusivity values.

Confirmation Status—No testing or modeling activities are planned to provide further confirmation of this assumption.

Where Used—Section 6.

INTENTIONALLY LEFT BLANK

6. MODEL DEVELOPMENT

This section provides a discussion of the tephra redistribution model used by total system performance assessment (TSPA).

- Section 6.1 lists the applicable and relevant features, events, and processes (FEPs).
- Section 6.2 describes the conceptual model.
- Section 6.3 provides a description of the mathematical model.
- Section 6.4 provides a description of the implementation of the model within TSPA.
- Section 6.5 discusses the development of the input parameters required to run the model.
- Section 6.6 presents the results of a parameter sensitivity study.

6.1 FEATURES, EVENTS, AND PROCESSES

This report documents a model that addresses FEP 1.2.04.07.0C, *Ash redistribution via soil and sediment transport* (DTN: MO0706SPAFEPLA.001 [DIRS 181613]).

6.2 CONCEPTUAL MODEL DESCRIPTION

This model report documents the development and validation of the Fortymile Wash ash redistribution (FAR) model (V.1.2), a conceptual, mathematical, and numerical model intended to estimate the redistribution (mobilization, transport, dilution, deposition, and diffusion) of waste-contaminated tephra deposited on the landscape surrounding Yucca Mountain, Nevada, following a potential volcanic eruption through the repository. Specifically, the FAR tephra redistribution model is intended to provide an estimate, including quantification of uncertainties, of the waste concentration as a function of time since an eruption at a compliance point located approximately 18 km south of the repository on the Fortymile Wash alluvial fan (Figure 1-1). This location represents where a hypothetical person called the reasonably maximally exposed individual (RMEI) lives. The radiological dose to this hypothetical person is calculated within the TSPA model. The TSPA model combines both the probability of future events and the resulting consequences of these events to evaluate the performance of the Yucca Mountain repository system. TSPA estimates the consequences of a potential volcanic eruption through the repository by integrating estimates, including uncertainties, of (1) the areal distribution of contaminated tephra with the ASHPLUME model (SNL 2007 [DIRS 177431]), (2) the hillslope and fluvial redistribution and transport of this material to the RMEI location with the FAR model, and (3) the dose to the RMEI with the biosphere model (SNL 2007 [DIRS 177399]).

The description of the FAR conceptual model begins with an overview in Section 6.2.1 of the important physical processes that will likely control the redistribution of contaminated tephra in this environment. Section 6.2.2 provides a conceptual description of how these processes are represented and simplified in the FAR model. This discussion provides a conceptual introduction to the mathematical model description in Section 6.3.

6.2.1 Physical Process Description of Tephra Redistribution

Tephra is defined as pyroclastic material, regardless of size or shape, ejected during an explosive volcanic eruption. The term “ash” refers to the subset of tephra that is smaller than 2 mm in

diameter. For the purposes of the model developed in this report, the term "tephra" redistribution is used because the developed model simulates the redistribution of contaminated pyroclastic material that includes and exceeds the ash size fraction. Waste is assumed to form a well-mixed suspension in the erupting magma (SNL 2007 [DIRS 177431], Section 5.1.3). Immediately prior to eruption, the magma-waste mixture fragments into particles that contain various proportions of silicate melt droplets, crystals, lithic fragments, and waste fragments (SNL 2007 [DIRS 177431], Section 5.1.4). Therefore, the waste, present as fine-grained "xenoliths" within particles of host tephra, will be largely mobilized, transported, and redeposited in similar fashion as uncontaminated tephra. The initial distribution of contaminated tephra after an eruptive event will depend on characteristics of the event (the type, magnitude, and duration of eruption), climatic conditions (wind direction, wind speed, etc.), tephra particle size/density, and terrain features. Eruption characteristics are developed and justified in the ASHPLUME report (SNL 2007 [DIRS 177431]). While the overall plume deposition will vary, there are a number of generalities that can be made given the proposed location of the repository. The repository is located in the lower third, and on the far west side, of the upper drainage basin (Figure 6.2-1). Thus, unless the prevailing wind at the time of eruption is from the east, the thickest tephra depositions will be in the upper drainage basin. While nearly all scenarios will result in some tephra being deposited in the upper drainage basin, scenarios in which the prevailing wind is out of the south will result in the greatest percentage of the total tephra being deposited in the basin. Conversely, scenarios where the prevailing wind is out of the north will result in the greatest percentage of tephra being directly deposited in the lower drainage basin (RMEI area).

Once deposited, the material will begin to be redistributed. Initially, the redistribution will be dominated by hillslope mobilization and fluvial entrainment. The hillslope component includes mass movement (landsliding of oversteepened slopes following the eruption), dry ravel, slope wash, and rilling. Landsliding of oversteepened slopes can be expected to occur during the eruption or within the first few years following the eruption. Rates of dry ravel, slope wash, and rilling will vary from slope to slope depending on gradient, texture, slope aspect, morphology (i.e., converging versus diverging slopes), and other factors.

Fluvial entrainment of both the material initially deposited in the regional channels and the material moved to the channels by hillslope mobilization will transport the contaminated tephra downstream. The transport mode will depend on the hydraulic characteristics of the contaminated tephra versus that of the local sediment. If the hydraulic characteristics of the two materials are similar, the contaminant and channel-bed material is transported primarily as bed-load material. The deeply incised morphology of the main channel in the upper basin confines the active fluvial erosion and deposition to the channels, where floods scour the channel bed during the waxing phase of the flow and redeposit the reworked sediments downstream during the waning phase of the flow.

Conversely, if the hydraulic characteristics of the two materials are not similar, then either:

1. the contaminated tephra will be transported primarily as suspended load (in instances where the contaminant particle size is considerably smaller than the channel bed sediment). Contaminated material will be entrained during floods and be transported

downstream without significant mixing with channel-bed material, and will be transported down the channel more quickly and much further than entrained material. Or

2. the contaminated tephra will preferentially migrate to the bottom of the channel bed material (in instances where the contaminant particle size is considerably larger than the channel bed sediment). Contaminated material will be transported downstream at a slower rate than the native channel bed.

The time required to move the contaminated material down the channel beds to the RMEI area will be a function of the frequency, magnitude, and duration of flood events, in addition to the initial distribution of the tephra deposit. The upper drainage domain is the major drainage basin in the western part of the Nevada Test Site. This drainage basin that feeds Fortymile Wash is bordered by Yucca Mountain on the southwest, Timber Mountain on the northwest, and Jackass Flats on the southeast. The channel of Fortymile Wash is well defined and is incised to a depth ranging from 50 to 70 ft (15 to 21 m); the bed of the wash is 1,000 to 1,500 ft (305 to 457 m) wide (Squires and Young 1984 [DIRS 180001], p. 3). An ephemeral stream course meanders across the main channel between the walls of the wash carrying runoff from small flood events. The mean annual precipitation in the area is only about 4 to 5 inches (Squires and Young 1984 [DIRS 180001], p. 6). Despite this low precipitation, flooding can be severe. The most significant flood events for sediment transport are typically caused by longer duration frontal and tropical storms. Geomorphic studies on the Nevada Test Site have indicated that some of the alluvial surfaces along Fortymile Wash are thousands of years old (Appendix A). While such ages might imply that the surfaces have not been flooded since their formation, Squires and Young (1984 [DIRS 180001, p. 12]) cite examples where distinct, unmistakable high-water marks were observed along Fortymile Wash, indicating that the alluvial surfaces along Fortymile Wash were inundated in the past. Squires and Young (1984 [DIRS 180001]) performed an analysis of the Flood Potential of Fortymile Wash. They concluded that 100-year, 500-year, and even regional maximum floods would fill the entire channel while remaining within the confines of the incised Fortymile Wash Canyon. While unable to quantitatively determine the extent of erosion and sediment movement caused by floodflows in the ephemeral stream course meandering across the wash, they concluded that, qualitatively, erosion of or deposition in channels would probably be significant during the 100-year flood, and could be severe during the 500-year and regional maximum floods. They noted that excessive erosion and deposition was observed in places during field surveys. Thus, while the ephemeral-channel system will likely undergo significant changes in depth, width, and position within the main incised wash over time, flow will stay within the walls of the wash. Ephemeral channel migration within the confines of the wash will allow mixing of the contaminated tephra with channel bed sediment to occur over a significant portion of the wash over multiple flood events. In between flood events, some fraction of the contaminant will remain stored in the channel bed sediments.

Regardless of the contaminant particle size, the concentration of contaminated particles changes as the material moves downstream and tributaries merge with the main channel and supply clean sediment to the system. This is true until the contaminants enter the narrow section of the wash that divides the upper and lower drainage domains (Figure 6.2-1). For this stretch of wash, and within the entire RMEI domain, there are no additional tributaries. The concentration of the radionuclides will depend on the overall ability of the material to mix within the bed sediment. The magnitude of the radionuclide concentration in this area can be thought of in terms of the

overall process discussed above. The collective hillslope processes will mobilize tephra and waste rapidly at first, and then more slowly as the contaminated tephra volume, which can be easily mobilized, is diminished. Mobilized material is moved into local channels, where fluvial transport moves the material downstream during flood pulses separated by periods of less significant or no flow. The time frame of these pulses is determined by the occurrence and characteristics of flood events. The contaminants from some areas in the upper drainage basin may never reach the main Fortymile Wash channel. Depending on the terrain, flatter areas may provide local deposition zones where the contaminants will simply be deposited on local, small-scale alluvial fans.

Contaminant concentrations in the channels of the RMEI area may gradually increase with time since the eruption as contaminated tephra is transported by the fluvial processes discussed above. However, because mixing and associated dilution is an integral part of the fluvial transport process, such an increase in concentration is not guaranteed and may not occur at all, depending on the nature of the eruptive event. In the event that redistribution increases the contaminant concentration in the RMEI area channels, peak concentrations will be reached during the period when the easily mobilized tephra is being moved via fluvial transport through the area. After this peak is reached, the concentration in the RMEI location will slowly decrease as cleaner material from upstream continuously dilutes the contaminated channel bed material.

During the time between fluvial transport pulses, eolian transport may move smaller particles of contaminants at the surface of the channels onto the divides if a significant amount of the contaminated tephra is transported as suspended load in the channels, since this material would not be as well mixed with the bed load. However, the importance and rate of eolian transport will be influenced by the wind speed and direction, channel morphology, and particle size. In any case, deposited radionuclides will also migrate deeper into the soil, through suspension and redeposition of fine particles by infiltration, and physical mixing of soil particles by freeze-thaw cycles and bioturbation. The rate of migration is highly dependent on site-specific parameters (such as climate and terrain).

6.2.2 FAR Conceptual Model Description

The conceptual tephra redistribution model divides the Fortymile Wash drainage area into two distinct modeling domains (Figure 6.2-1): (1) the upper portion of the drainage basin, which includes the repository location, and (2) the alluvial fan, which is assumed to represent the RMEI location. These two domains are connected at the fan apex, a narrow stretch of the Fortymile Wash channel that is the outlet of the upper basin. The source of the contaminated tephra is the volcanic vent location, which is located approximately at the center of the repository footprint. The model considers that any tephra deposited outside of the drainage basin and not directly deposited on the RMEI area has a negligible effect on concentration at the RMEI location.

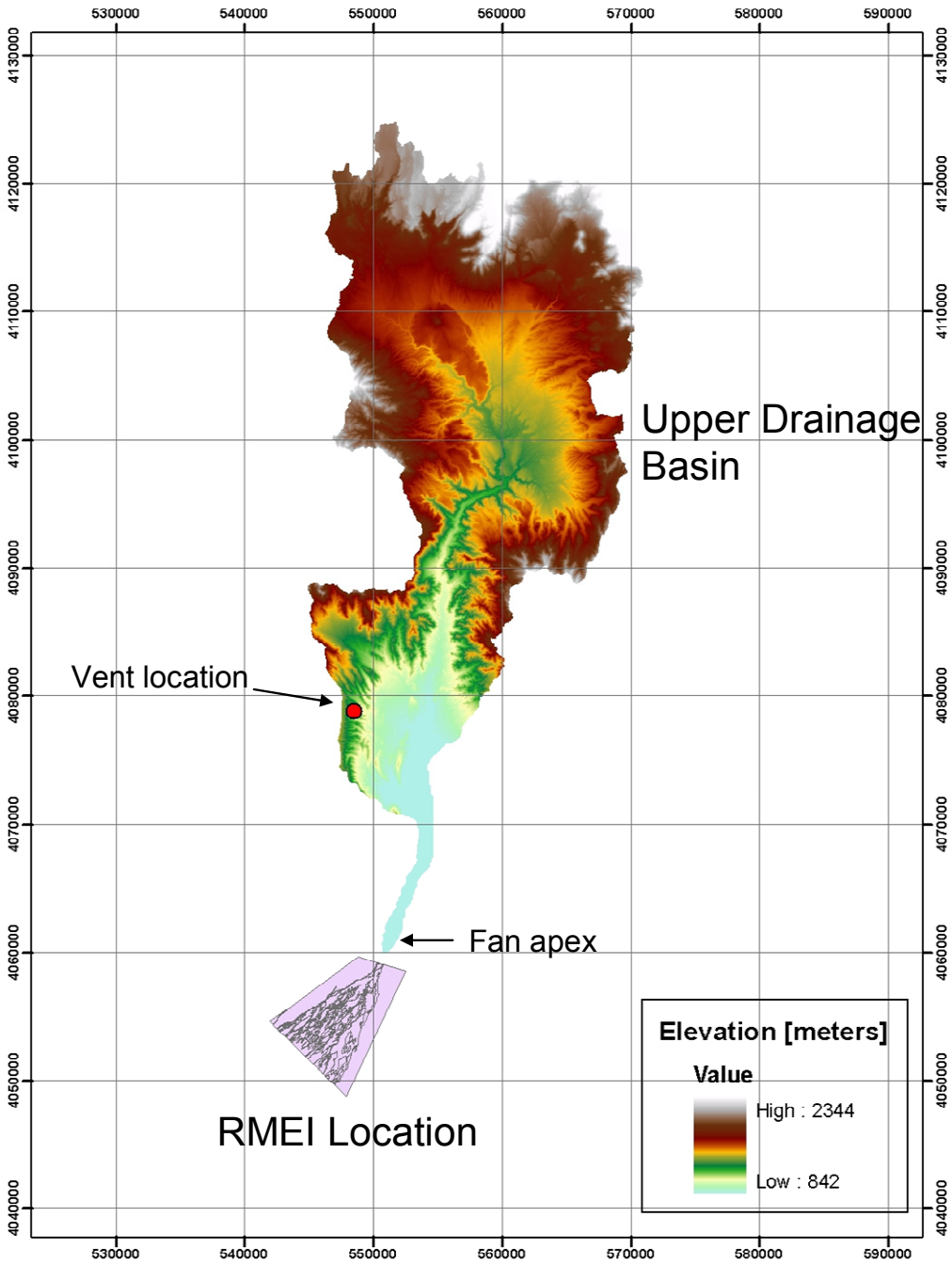

Source: Elevations from Output DTN: MO0605SPAFORTY.000, vent location developed in Section 6.5.7.1, RMEI domain map from Output DTN: SN0708GEOMOMAP.001.

NOTE: Coordinates in UTM NAD27, Zone 11.

Figure 6.2-1. Schematic Diagram of Tephra Redistribution Model

The FAR model was designed to estimate the effect of the key tephra redistribution processes described in Section 6.2.1 (mobilization, transport, dilution, deposition, and diffusion). The model significantly simplifies each of these steps, and can be thought of as a lumped parameter model, which aims to represent the result of the processes in a simplified manner. As such, this modeling approach must be calibrated to available field observations. Simplifications were made such that the overall results would be reasonable and perhaps conservative with respect to the calculated concentrations at the RMEI location. Additionally, the model simplifications reflect the uncertainties associated with the amount and type of available input data. Data are necessarily limited due to the large spatial coverage of the model, the limited amount of measured, site-specific data, and the influence of climatic conditions on both the parameters and processes. These limitations preclude the expectation of certainty in predictions at specific locations for specific events. Despite these limitations, the FAR model is able to provide radionuclide time-dependent concentration profiles at the RMEI location that are appropriate for use in TSPA Mont Carlo analyses that consider these uncertainties.

As a lumped parameter model, one of the key model elements is calculating domain averaged parameters based on cell specific input. The FAR model uses a 30-m resolution U.S. Geological Survey (USGS) Digital Elevation Model (DEM) as the grid of the upper drainage domain. This domain contains more than 2 million grid cells, each characterized by an elevation. Elevations from the grid are used to calculate the slope between individual cells, to determine if cells are channels, and if cells are channels to calculate the scour depth of the cell. The initial mass of tephra distributed on each cell, and the cell area (900 m^2 for the 30-m DEM) are also retained as cell specific data. The cell specific values are then used to calculate domain averaged parameters for each cell—in essence parameters that define how a cell behaves based on where it is within the domain. For example, a combination of elevation, cell area, and slope between neighboring cells is used to determine the contributing area for each cell, which is the total area of the upstream domain that will contribute flow to the cell. Domain averaged parameters include contributing area, averaged scour depth, stream power, and total mass of tephra deposited. While calculations of domain averaged parameters are completed for each grid cell, it is only the outlet grid cell (a single grid cell in the lower Fortymile Wash channel representing the transition between the upper and lower drainage domains) which is used in determining the concentration and thickness of contaminated tephra that is passed into the channel portion of the lower drainage domain (RMEI location).

The initial tephra deposit (mass of tephra per area) is simulated by the ASHPLUME model (SNL 2007 [DIRS 177431]) and provided to the tephra redistribution model as input. Assumptions associated with the ASHPLUME model are, in general, not discussed here, but can be found in the referenced report. It is assumed that the tephra can be represented with a homogeneous bulk density value and therefore tephra mass per unit area can be converted to tephra thickness.

Initial mobilization in the upper drainage domain by hillslope processes

The amount of tephra mobilized in the upper drainage basin by hillslope processes is calculated for each grid cell. The model assumes that primary fallout is mobilized and transported downstream if it falls on steep slopes or on active channels (except for the coarse material that would be deposited very close to the vent forming a cinder cone). The model performs a spatial

analysis of the slopes and contributing areas (a proxy for stream power) for the entire basin using the input DEM. These values are then compared to input values of critical slope (S) and drainage density (X), on a pixel-by-pixel basis, to integrate the total mass of tephra and waste mobilized from the upper basin. If a given pixel has a slope greater than the critical slope (S) or an inferred stream power greater than the reciprocal of drainage density ($1/X$), the tephra and waste in that pixel is considered to be mobilized. Mobilized tephra is transported downstream but may be deposited locally in the upper drainage basin when the channel enters a local area of very low slope and stream power falls below the threshold value used to define channels ($1/X$). Appropriate values for critical slope are discussed in Section 6.5.2. Drainage density values are discussed in Section 6.5.3.

The model assumes that the initial mobilization will occur in a reasonably short period of time as compared to the overall period of time encompassed by the model results. Section 5.2.1 provides the rational for this assumption.

Initial transport of mobilized tephra through the upper drainage domain channels

The transport and mixing of mobilized tephra and waste through the channel system of the upper drainage basin is represented by a conceptual model referred to as the "scour-dilution-mixing model." The model assumes that the hydraulic properties of the tephra are reasonably similar to those of the channel bed, and the contaminated tephra will be transported primarily as bed-material load (see Section 5.2.3). Mixing occurs during flood events as sediment and tephra are entrained from the bed, mixed by turbulent flow, transported downstream, and redeposited on the bed. In addition, clean sediment transported from catchments with no initial tephra deposition is added to the channel.

Given the arid climate, mixing and transport will take place over multiple flood events. These events (i.e., 100-year, 500-year, or regional maximal floods), are expected to remain within the overall defined wash (but will overflow the ephemeral stream course which meanders across the channel between the walls of the wash). The depth to which tephra and channel sediment are mixed is the scour depth. The dilution factor at each point (i.e., the fraction of channel sediment composed of tephra in each channel pixel) is calculated using the local thickness of mobilized tephra and the local scour depth, calculated from the contributing area at each point. Contributing area is estimated using a divergent flow (Freeman 1991 [DIRS 174195]) (bifurcation routing) algorithm that partitions the area of each upstream cell to each of the neighboring downstream cells in proportion to the local downstream slope between these cells. This same algorithm is used to route tephra thickness and scour depth downstream. The ratio of the routed tephra thickness to the routed scour depth at the fan apex, which is just upstream from the RMEI area, is used to calculate the fuel concentration for the channels at the RMEI location. The scour-dilution-mixing approach to modeling dilution is similar to earlier models widely used in the mineral exploration and contaminant-transport literature (Hawkes 1976 [DIRS 174136]; Helgen and Moore 1996 [DIRS 174138]). In these models, the contaminant concentration at a point downstream is a function of source and non-source concentrations weighted by the relative basin areas upstream of the point. These models do not make it clear whether mixing/dilution takes place by mixing with uncontaminated channel-bed sediments (in which case mixing could take place very rapidly) or by mixing due to transport of sediments from upstream. The scour-dilution-mixing approach improves on the earlier models by making the

channel mixing / dilution more process-based. A volumetric approach is taken, by allowing the contaminant concentration at each point to be equal to the ratio of the total contaminant volume from upstream to the total volume of the upstream scour zone (all transported sediment).

Storage of mobilized material in channels

Not all mobilized tephra is considered available for transport to the RMEI location. In cases when tephra initially falls on channel cells and is thicker than the local scour depth, only the tephra within the scour zone is considered to be mobile. Tephra below the scour zone does not contribute to the concentration at the fan apex. In addition, depending on the value of the drainage density parameter, certain channels will not be continuously linked with the main Fortymile Wash channel, and thus material in these unconnected channels will not contribute to the concentration at the outlet. Only that tephra mobilized and transported into channels connected to the main wash influences tephra concentration in the channels of the RMEI location.

Transfer of tephra from the upper basin to the RMEI location

Mapping of the RMEI area has indicated that relief above active channels is typically on the order of 0.5 to 1.5 m (Appendix A). The small elevation changes in this domain are of the same magnitude as the accuracy of the DEM (e.g., ~3 m for National Elevation Dataset (Smith and Sandwell [DIRS 177358])), and therefore the spatial analysis performed in the upper domain could not be applied to this area. Instead, the RMEI area is represented in the tephra redistribution model as two homogeneous subdomains representing active channel areas and inter-channel divides on the alluvial fan surface. In each of these subdomains, the waste concentration at the land surface and within a depth interval extending from the surface to a specified biosphere depth (B) is simulated. In TSPA calculations, the biosphere model specifies an appropriate depth (B) depending on the dose pathway considered and uses the resulting concentration profiles to calculate a dose to the RMEI via the volcanic ash exposure scenario (SNL 2007 [DIRS 177399], Section 6.3.2).

The inactive portion of the alluvial fan domain (interchannel divides) receives contaminated tephra only through primary deposition from the eruption. This assumes that eolian transport of contaminated tephra from the channels to the divides is insignificant. This assumption is discussed in Section 5.2.2. Therefore, the initial tephra thickness and waste concentration in this domain is provided by the ASHPLUME model.

In the active channel subdomain, the thickness of the contaminated tephra is set to the value of scour depth at the fan apex (an input parameter). The scour depth at this location is a conservative approximation of the scour depth within the active channels of the alluvial fan, as it represents a maximum depth for a particular case (and thus a larger total mass of contaminant is applied to the RMEI channels). This is discussed in greater detail in Section 7. The waste concentration in the active channels of the fan is represented as the sum of the waste deposited directly from the tephrafall and the waste delivered and diluted by the channel at the fan apex.

Time-dependent migration of radionuclide material in the lower drainage basin (RMEI location)

The contaminated tephra in each of these subdomains (defined by the thickness and concentration in each subdomain) is allowed to diffuse downward into the soil column over time.

The spatially distributed model of tephra and waste transported from the upper basin channel network supplies contaminated tephra to the RMEI location on the upper Fortymile Wash alluvial fan. Once the contaminated tephra has been emplaced in the RMEI domain, the model treats the migration of radionuclides within the soil as a diffusion process. Redistribution occurs primarily through suspension and redeposition of fine particles by infiltration, and physical mixing of soil particles by freeze-thaw cycles and bioturbation. This complex redistribution process is simplified by simulating it as one-dimensional diffusion into the soil, using a diffusivity value to adjust the diffusion rate. Such a lumped diffusion process is assumed to occur within a finite thickness corresponding to the distance from the surface to a zone of reduced permeability at the base of the active zone (with different thickness for the divides and channels). Soils in arid environments generally develop a petrocalcic horizon by solution and reprecipitation of calcium carbonate over time scales of tens to hundreds of thousands of years (Machette 1985 [DIRS 104660]). Deposition of calcium carbonate at depth in the soil locally decreases permeability.

In the natural system, the fan is composed of a complex suite of "terraces" that result from episodes of aggradation, incision, and lateral channel migration. Soil-geomorphic mapping has been performed on the modern fan surface to group these terraces into two types: inter-channel divides, that have not been subject to fluvial erosion and deposition for approximately the last 10,000 years or longer (broadly classified as "Pleistocene-age" terraces in this report), and channels that have been subject to erosion and deposition over the last 10,000 yrs (including both active channels and Holocene-age terraces that may be reoccupied over a 10,000-year time scale). Thus, "channels" in the RMEI area are not necessarily current active channels, but rather younger surfaces that have been reworked in the last 10,000 years. The results of soil-geomorphic mapping are described in Appendix A.

At the RMEI location, the model represents each of these subdomains by a one-dimensional diffusion calculation. These calculations require as input the thickness of the contaminated tephra layer, the waste concentration in that layer, and the diffusivity value. The diffusivity values vary between the divides and channels and are based on fitting near-surface ^{137}Cs profiles measured on the alluvial fan with a one-dimensional diffusion equation. Diffusion within the channels is likely to occur faster because of the higher permeability of channel-bed sediments (which increases the rate of fine-particle transport by suspension and redeposition). On interchannel divides, contaminated tephra is deposited only from primary fallout, which is calculated directly by the ASHPLUME model (SNL 2007 [DIRS 177431]). Tephra and waste redistributed from the Fortymile Wash drainage basin cannot be deposited on divides because divides, by definition, are not subject to fluvial erosion or deposition. In channels, the initial waste concentration includes the primary fallout as well as the waste redistributed from the Fortymile Wash drainage basin.

6.3 MATHEMATICAL MODEL DESCRIPTION

6.3.1 Nomenclature

All parameters and variables used in the text are defined where they are first used. In addition, parameters and variables used in multiple report sections are listed in Appendix D.

6.3.2 Initial Conditions and Input Parameters

The initial conditions for the tephra redistribution model correspond directly with the input data. These are:

- The tephra redistribution model implemented in the FAR.DLL software program accepts grids of tephra and waste areal concentration in g/cm^2 from ASHPLUME via the text file *ashplume.out*. ASHPLUME partitions waste to tephra particles according to particle size, and therefore the waste concentration in tephra varies with location (dependent on distance and direction from vent). FAR is capable of accepting grids in either Cartesian or polar coordinates, but only polar grids are used for the TSPA FAR calculation because of their greater efficiency. The ASHPLUME grid parameters used for TSPA calculations are documented and justified in the ASHPLUME model report (SNL 2007 [DIRS 177431], Table 8-2) and are listed below. In the input polar grid (i.e., a function of radius r and azimuth θ from the vent location), radial distance increases as a power of *rfactor*, which is set to a value of 1.2. The number of angular intervals, N_θ, is set to 36, which corresponds to $\Delta\theta = 10°$. The smallest radius (closest to the vent) is set to 0.2 km and the number of radial intervals is set to 31. The radius of each successive grid cell away from the vent increases with a factor equal to *rfactor* (e.g., 0.2 km, 0.24 km, 0.29 km, 0.36 km, …, 47.5 km).

- Values for the tephra and waste concentration (g/cm^2) at the RMEI location (about 18 km south of the repository) computed by ASHPLUME.

- A 30-m-resolution DEM that covers the Fortymile Wash drainage basin down to the latitude of the Fortymile Wash fan apex. This grid also includes information on the drainage-basin boundaries. Each grid cell within the drainage basin has a value equal to the DEM elevation (m). Each grid cell outside the drainage basin has a value of "-9999" (Section 6.5.1, Step 9).

- Values for model parameters, including the critical slope S, drainage density X, scour depth at fan apex H, RMEI fan area A, fraction of RMEI fan area comprised of channels F, the permeable soil depth in channels L_c, the permeable soil depth on divides L_d, the vertical diffusivity of radionuclides in channels D_c, the vertical diffusivity of radionuclides on divides D_d, and the biosphere depth B. The biosphere depth is defined depending on the dose pathway being considered by TSPA (either tillage depth or depth of resuspendible soil layer). Both of these parameter distributions are developed in the biosphere model (SNL 2007 [DIRS 177399], Table 6.6-3).

6.3.3 Algorithm Description

The mathematical model is described below as a series of six main steps.

STEP 1: Perform bilinear interpolation on input ASHPLUME tephra and waste concentration grids and rectify to DEM

The FAR tephra redistribution model uses input grids of tephra and waste concentration computed by ASHPLUME in either Cartesian or polar coordinates. ASHPLUME grids are computed at a relatively coarse resolution (~500 m) while FAR V.1.2 performs its calculations at the much finer resolution (30 m) in the Cartesian coordinate system only. For this reason, it is necessary to interpolate the ASHPLUME results to the same scale and coordinate system as the DEM. To do this, a bilinear interpolation procedure is used. Bilinear interpolation assumes that the tephra and waste concentrations vary linearly between ASHPLUME grid points in both grid-axis directions. For ASHPLUME results using a Cartesian grid, the areal concentration C (g/cm^2 of tephra or waste) at a DEM point (x, y), given concentration values at $C_{i,j}$, $C_{i+1,j}$, $C_{i,j+1}$, and $C_{i+1,j+1}$ at the surrounding ASHPLUME grid point locations (x_i, y_j), (x_{i+1} ,y_j), (x_i, y_{j+1}), (x_{i+1}, y_{j+1}), respectively, is given by Press et al. (2002 [DIRS 174134], p. 123) as:

$$C(x,y) = (1-u)(1-v)C_{i,j} + u(1-v)C_{i+1,j} + uvC_{i+1,j+1} + (1-u)vC_{i,j+1}, \quad \text{(Eq. 6.3-1)}$$

where

$$u = \frac{x - x_i}{x_{i+1} - x_i}, \quad v = \frac{y - y_j}{y_{j+1} - y_j} \quad \text{(Eq. 6.3-2)}$$

and i and j are the row and column indices (origin at the NW corner of the grid) of the grid cell containing the point (x, y).

Similarly, with a polar ASHPLUME input grid, the concentration C at a DEM point (x,y) is computed with Equation 6.3-1 from ASHPLUME concentration values $C_{i,j}$, $C_{i+1,j}$, $C_{i,j+1}$, and $C_{i+1,j+1}$ assigned values from the surrounding ASHPLUME grid point locations (r_m,θ_n), (r_{m+1},θ_n), (r_m,θ_{n+1}), and (r_{m+1},θ_{n+1}), respectively, where m and n are the radial and angular indices of the ASHPLUME grid cell containing the point (x,y). Figure 6.3.3-1 shows the layout and relationship of these points in space.

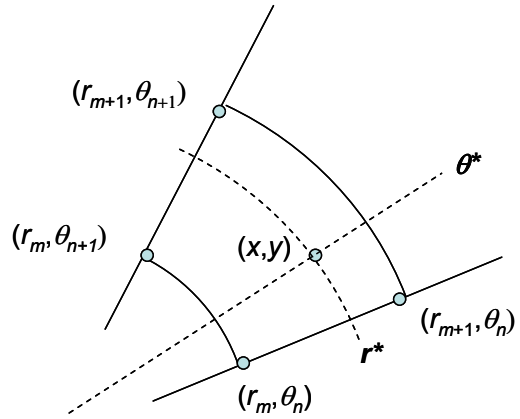

Figure 6.3.3-1. Geometry Conventions Used for Polar Coordinate Bilinear Interpolation

For the polar grid, u and v in Equation 6.3-1 are defined as:

$$u = \frac{r^* - r_m}{r_{m+1} - r_m}, \quad v = \frac{\theta^* - \theta_n}{\theta_{n+1} - \theta_n} \qquad \text{(Eq. 6.3-3)}$$

where (r^*,θ^*) is the point (x,y) in polar coordinates (Equation 6.3-4), with the origin of the ASHPLUME grid located at the vent location, which is assumed to be at the center of the repository.

$$r^* = \sqrt{x^2 + y^2}, \quad \theta^* = \tan^{-1}\left(\frac{y}{x}\right) \qquad \text{(Eq. 6.3-4)}$$

For the TSPA calculations, the ASHPLUME output grid is given in polar coordinates as shown in Figure 6.3.3-2.

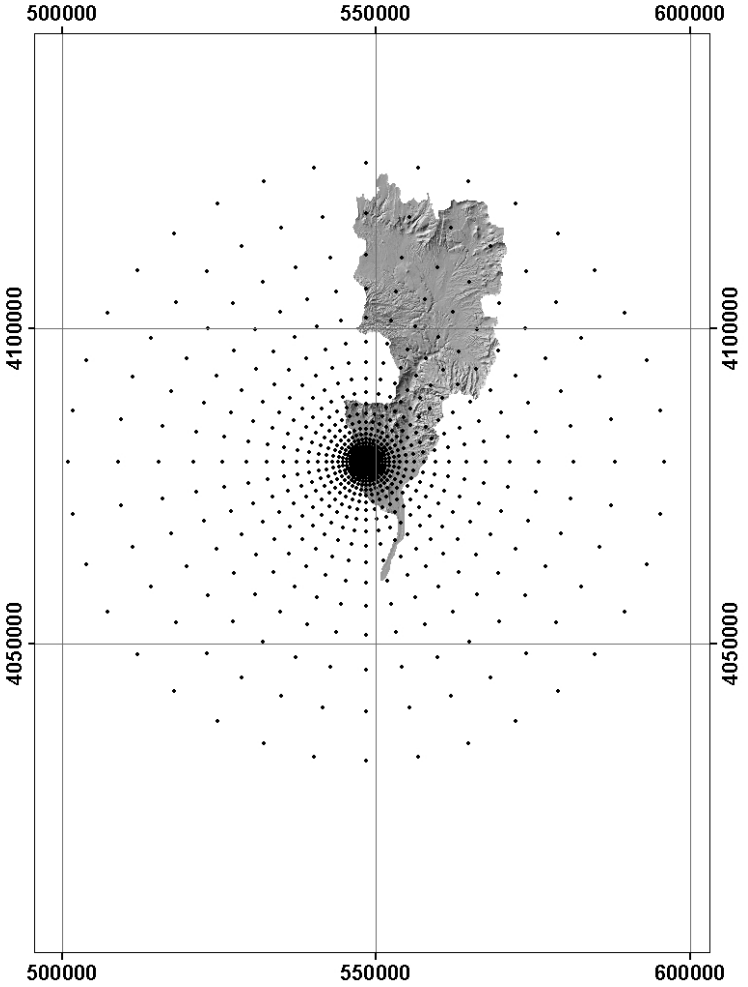

NOTE: In this example, the ASHPLUME grid has 31 radial and 36 angular increments, a minimum radial distance of 0.2 km, and a radial multiplier of 1.2. Figure is for illustration purposes.

Figure 6.3.3-2. Rectified ASHPLUME Output Grid Displayed over the Upper Drainage Basin Domain and Centered at the Vent Location

Alternative interpolation schemes are available (e.g., bicubic interpolation), but these methods can lead to errors when interpolating functions with steep gradients. Bilinear interpolation is the most robust interpolation method for two-dimensional functions and is adequate for its intended purpose in TSPA.

Following the bilinear interpolation procedure, the interpolated tephra and waste concentration grids are rectified to the DEM. This is done by shifting the grids so that the origin (vent location) of the interpolated grids corresponds to the vent location in the DEM grid. The Universal Transverse Mercator (UTM) coordinates of the vent location are computed as the center of the grid cell located at the center of the bounding box surrounding the waste emplacement area. Section 6.5.7 describes the calculation of these coordinates and provides the values to be used by TSPA. The interpolated grid of tephra concentration (g/cm^2) is converted to

tephra thickness (cm) by dividing tephra concentration by tephra density (g/cm^3) (*ashsettleddensity,* ρ in Table 6.4-1). Both the interpolated tephra thickness and waste concentration grids are used later in STEP 4 to calculate the total mass of tephra and waste mobilized from the upper drainage basin within the main Fortymile Wash channel system. These masses are also used to determine the concentration of waste in the channels at the RMEI location in STEP 5.

STEP 2: Fill pits and flats in the input DEM

The FAR V.1.2 software requires that each pixel in the DEM have a well-defined drainage direction to route contributing area, tephra, waste, and scour depth. Due to imperfections in DEMs, however, "pits" and "flats" may occur where the downstream direction is not well defined. While generating the input DEM for the Fortymile Wash drainage basin (Output DTN: MO0605SPAFORTY.000), pits have been removed (see Section 6.5.1); however, flats may still be present. The software forces each pixel to drain by using a recursive algorithm that searches the grid for "pits" and "flats". If a "pit" or "flat" is found, the elevation is raised slightly (1 cm). The raising of one pixel may cause neighboring points to become "pits" or "flats", so the model searches all of the neighboring areas recursively, filling any artificial "holes" in the topography. This algorithm was proposed and tested by Martz and Garbrecht (1999 [DIRS 175455]), who first lowered elevations in a few cells to simulate outlet breaching, and then when closed depressions remained, raised the elevations to fill them using the method described here.

STEP 3: Compute slope, contributing area, and scour depth grids

The local DEM slope is used to determine the mass of tephra mobilized from steep hillslopes throughout the drainage basin. In the model, the locations of steep hillslopes are determined by mapping the slope throughout the drainage basin and comparing each value to a critical slope *S*. All of the tephra, at distances greater than *rvent* from the vent location, that falls on grid cells with slopes greater than or equal to *S* is assumed to be mobilized and transported into the channels by mass wasting, overland flow, and/or rilling processes.

Mathematically, the local slope $|\nabla h|$ is defined as:

$$|\nabla h| = \sqrt{\left(\frac{\partial h}{\partial x}\right)^2 + \left(\frac{\partial h}{\partial y}\right)^2} \qquad \text{(Eq. 6.3-5)}$$

where $\frac{\partial h}{\partial x}$ and $\frac{\partial h}{\partial y}$ are the local elevation gradients in the *x* and *y* directions, respectively. The model implements Equation 6.3-5 using centered derivatives:

$$|\nabla h| = \sqrt{\left(\frac{h_{i+1} - h_{i-1}}{2\Delta x}\right)^2 + \left(\frac{h_{j+1} - h_{j-1}}{2\Delta x}\right)^2} \; . \qquad \text{(Eq. 6.3-6)}$$

Equation 6.3-6 assumes that the DEM grid cell resolution is the same in the x and y directions ($\Delta x = \Delta y$). Other techniques are available for computing the local DEM slope. For example, the slope can be computed as the rise-over-run between each pixel and its neighboring pixel along the direction of steepest descent. The method represented by Equation 6.3-6 was chosen for the model because it has been found to be the most accurate method based on comparisons with synthetic grids using mathematical functions (Jones 1998 [DIRS 174197]). Figure 6.3.3-3 shows the slope values calculated for the upper drainage basin DEM.

The variable *rvent* is included in FAR V.1.2 to represent limited mobilization of tephra close to the vent (on the tephra cone). To include all erupted tephra in the redistribution calculation, *rvent* should be set to zero. However, tephra in the immediate vicinity of the vent (i.e., within several hundred meters) may be too coarse for transport. Alternatively, ASHPLUME may overestimate tephra thickness close to the vent. In either of these cases, a finite value of *rvent* could be used to account for these variations.

The stream power is used to determine the mass of tephra and waste mobilized from active channels throughout the drainage basin. Stream power at grid cell (i,j) is defined as the product of the slope and the square root of contributing area:

$$power(i,j) = slopeavg(i,j) * contribarea(i,j)^{0.5} \quad \text{(Eq. 6.3-7)}$$

where *slopeavg (i,j)* is the 5 × 5 grid-cell average of the local slope calculated in Equation 6.3-6 and *contribarea(i,j)* is the contributing area (km^2).

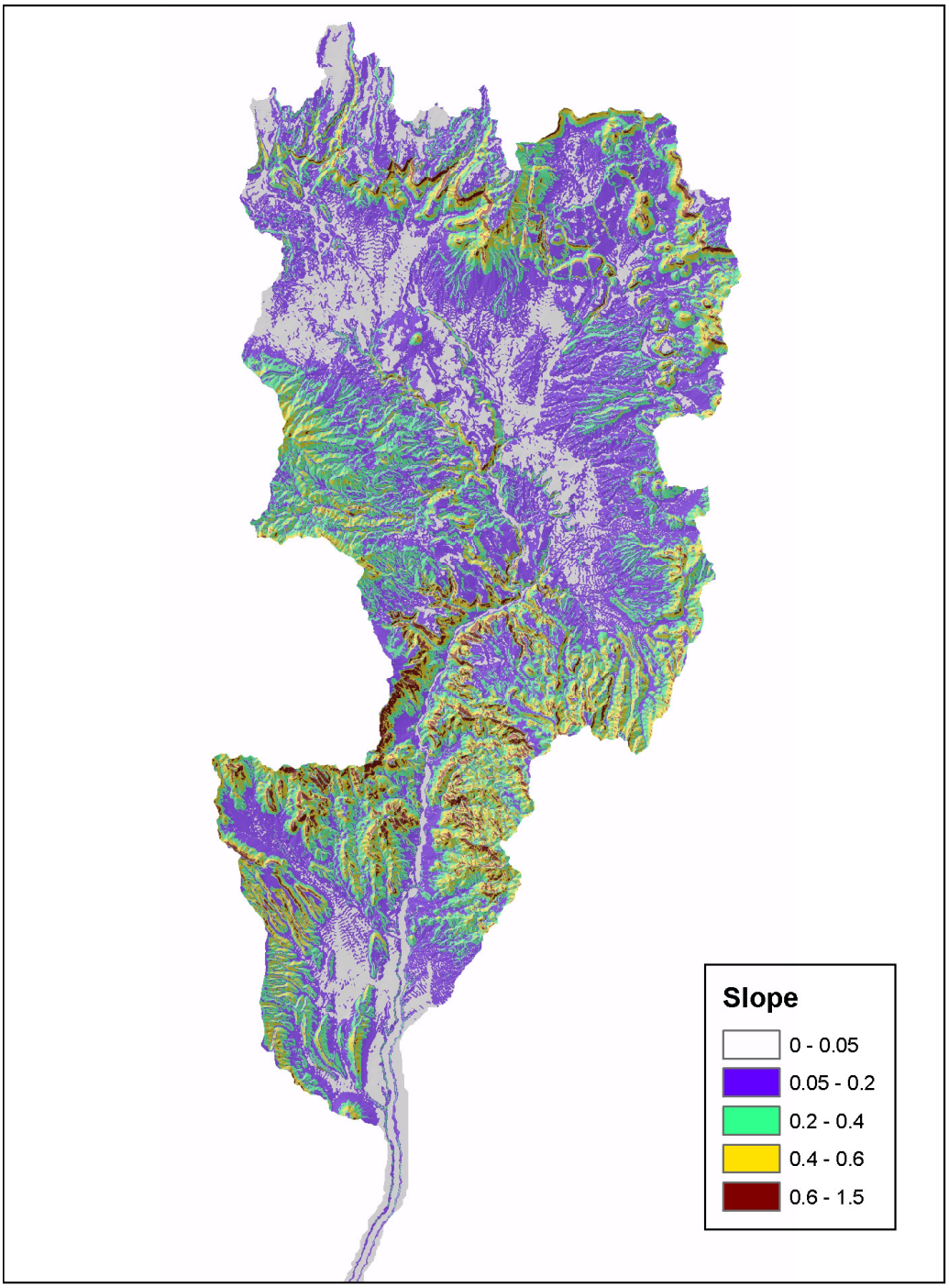

NOTE: Figure is for illustration purposes.

Figure 6.3.3-3. Local Slope Calculated in the Upper Drainage Basin Domain

In the model, grid cells are considered to be active channels when the stream power exceeds a critical threshold value, which is defined by the reciprocal of drainage density ($1/X$), where X is the drainage density (km^{-1}). The model uses a 5×5 grid-cell average of slope (Figure 6.3.3-4) instead of the local values to ensure that streams are able to flow through areas with low slopes.

Small imperfections in the DEM can result in artificially low slopes one or two pixels wide. By using a 5 × 5 moving average, FAR ensures that the stream power decreases (leading to tephra deposition locally) only when a true low-gradient area occurs. The drainage density is the ratio of the total length of all channels within a drainage basin to the area of that basin. This criterion is consistent with the fact that channels in nature occur when runoff or stream power is greater than or equal to a threshold value. Flows above this threshold are sufficient to entrain bed material and maintain an incised channel despite the tendency of hillslope processes to fill channel heads (Montgomery and Dietrich 1988 [DIRS 175760]).

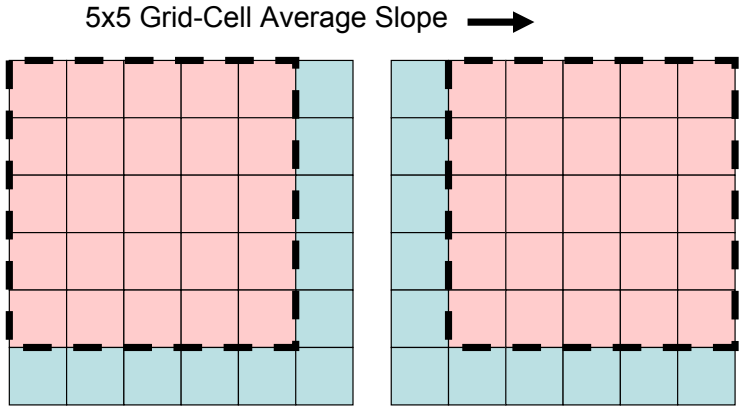

Figure 6.3.3-4. Illustration of the Moving Window Used to Calculate the 5 × 5 Grid-cell Average Slope

The simplest method for computing the contributing area on a grid is to assume that all of the flow entering a grid cell is routed along the direction of steepest descent. This method enforces a tributary drainage structure even in areas with distributary flow. This method was used to delineate the drainage basin defined in the DEM input file (Section 6.5.1). However, for estimating local values of contributing area in wide channels and low-relief areas, such as the lower parts of the Fortymile Wash drainage basin, the steepest descent method performs poorly. Therefore, the FAR model uses an alternative method developed by Freeman (1991 [DIRS 174195]) called the divergent flow method or "bifurcation routing" in this report. In this method, all incoming flow to a grid cell is partitioned between each of the downslope grid cells, weighted by a slope factor.

To use this method to calculate contributing area, each DEM grid cell is assigned an initial value of contributing area equal to Δx^2 (the area represented by the grid cell, which is 900 m^2 for a 30-m DEM). Contributing area values are then routed as "flow" through the basin from highest to lowest elevation, following the same paths that runoff would take downslope and summing along the way. To move from highest to lowest elevation, the model creates an elevation index list that ranks the DEM pixels by elevation. This ranked list is computed very efficiently within the model using the Quicksort algorithm (Press et al. 1992 [DIRS 174134], pp. 338 to 340). Following the construction of the index list, the model begins the bifurcation routing algorithm by calculating the contributing area at the highest pixel in the DEM not bordered by a cell outside the boundary. In the implementation of the method in FAR, all boundary grid cells within the drainage basin are assumed not to contribute to the routing. This pixel has no upstream tributaries, so its contributing area is equal to its initial value (Δx^2). This contributing area is then routed downslope by partitioning it between each of its downstream neighbors on

the grid (including diagonals). For a given cell with n downslope neighbors, each with a slope equal to s_k, where k = 1, 2, …n, the fraction of the upstream area routed to each neighbor, f_k, is defined as:

$$f_k = \frac{s_k^p}{\sum_{m=1}^{n} s_m^p} \quad \text{(Eq. 6.3-8)}$$

where p is power of the weighting factor. The FAR model assumes that the flow routing partitioning is linear with slope and therefore p is set to 1. Each downstream neighbor has its initial contributing area (i.e., Δx^2), to which is added a fraction (f_k) of the contributing area of the upstream neighbor. The model then proceeds to the next lowest grid cell, routing ever-increasing values of contributing area downstream while allowing this area to diverge and "flow" across the landscape. Figure 6.3.3-5 shows the contributing area calculated for the upper drainage basin DEM using the bifurcation routing method. By moving through the grid in order of descending elevation, the method ensures that all of the contributing area has been accumulated before routing the values downslope because all incoming flow must come from higher elevations. The primary importance of the bifurcation routing method for the model is that it provides an accurate method for mapping the entire channel area in a DEM, even if channels vary in width in a complex manner. In the bifurcation routing method, flow expands to accommodate the entire channel between opposite banks. In contrast, the steepest-descent method would force all flow into the lowest point in the channel. As such, it can provide an accurate measure of channel length, but channel width cannot be determined. This difference is important for enabling the model to integrate all of the tephra that falls on active channels. Pelletier (2004 [DIRS 174135]) compared results of steepest-descent and bifurcation routing applied to 30-m USGS DEMs to demonstrate the more realistic results obtained with the bifurcation routing method.

To calculate the grid of scour depth, the model uses several steps to relate the contributing area to scour depth. First, contributing area is related to discharge on a grid cell-by-grid cell basis using the regional "flood envelope'' curve of Squires and Young (1984 [DIRS 180001], p. 16). These authors found the maximum discharge (of 100- and 500-year floods) to be proportional to contributing area raised to the 0.57 power:

$$Q \propto contribarea^{0.57}, \quad \text{(Eq. 6.3-9)}$$

where Q is the maximum discharge (volume/time). Maximum discharge is used because it is the largest floods that control the long-term scour/mixing depth. Second, unit discharge (equal to $Q/\Delta w$, where Δw is the width of the channel) is related to scour depth using the square-root dependence identified by Leopold et al. (1966 [DIRS 175456], pp. 215 to 218):

$$scourdepth \propto \left(\frac{Q}{\Delta w}\right)^{0.5} \quad \text{(Eq. 6.3-10)}$$

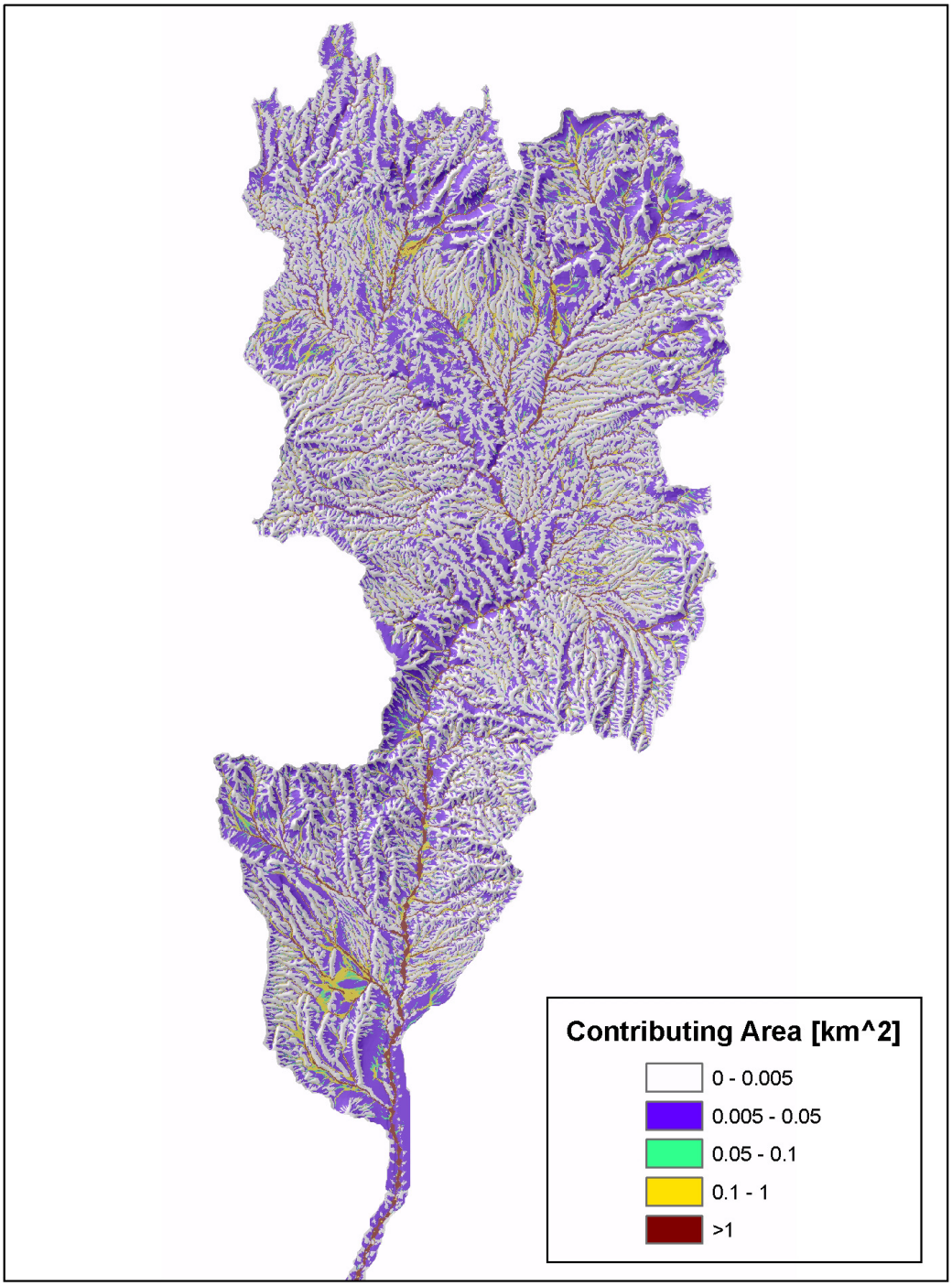

NOTE: Figure is for illustration purposes.

Figure 6.3.3-5. Map of Contributing Area for the Upper Drainage Basin Domain Calculated Using the Bifurcation Routing Method

Substituting the right hand side of Equation 6.3-9 into the numerator of Equation 6.3-10 leads to the product of scour depth and the square root of channel width being proportional to contributing area raised to the product of the exponents from each relationship, 0.29 power:

$$scourdepth * \Delta w^{0.5} \quad \propto \quad contribarea^{0.29} \qquad \text{(Eq. 6.3-11)}$$

or as an equality, after solving for scour depth:

$$scourdepth = p \frac{contribarea^{0.29}}{\Delta w^{0.5}} \qquad \text{(Eq. 6.3-12)}$$

where p is the proportionality constant (expressed in units of cm when Δw is given in meters, *contribarea* is in km^2, and *scourdepth* is in units of cm).

To apply Equation 6.3-12 to a DEM grid, and solve for scour depth at any location it is necessary: (1) to have measurements of scour depth, channel width, and contributing area at a single location following a representative large flood event (in order to solve for p); (2) to assume that the proportionality constant is invariant in space and time (i.e., p is constant for all channels in the domain for the maximum flood event); and (3) to know the full channel width and full contributing area for all channels in the domain. Measurements of scour depth, channel width, and contributing area for a representative large flood event are available from the USGS Narrows streamgage following the flood of March 11, 1995. However, the FAR model uses the bifurcation routing algorithm, which allows channels to extend beyond a single grid cell in width, and therefore information on full channel width and full contributing area is not calculated by the model. For this reason, Equation 6.3-12 could not be used directly. Instead, an alternate approximation was used that assumes that full channel width and full contributing area can be partitioned between the multiple grid cells that make up the channel. Thus, grid cell width, Δx, and contributing area from the divergent flow algorithm are used in place of full channel width and full contributing area, respectively. Combining this assumption with the assumption that p is constant, and using the direct observations from the Narrows streamgage station, means that scour depth at any grid cell location (i,j) can be calculated as the ratio of the scour depth at the Narrows:

$$\frac{scourdepth(i,j)}{scourdepth_{narrows}} = \frac{p * contribarea(i,j)^{0.29} / \Delta x^{0.5}}{p * contribarea_{narrows}{}^{0.29} / \Delta w_{narrows}^{0.5}}$$

$$scourdepth(i,j) = scourdepth_{narrows} \left(\frac{contribarea(i,j)}{contribarea_{narrows}} \right)^{0.29} \left(\frac{\Delta w_{narrows}}{\Delta x} \right)^{0.5} \qquad \text{(Eq. 6.3-13)}$$

Assuming that channel width and contributing area can be partitioned between more than one grid cell does not strictly honor the flood envelope curve of Squires and Young (1984 [DIRS 180001], p. 16), since contributing area is not linearly related to total discharge. For example, dividing the total contributing area among several grid cells across the channel width and summing the resulting discharges results in a higher total discharge than would be calculated if the channel was not subdivided. This problem is evident in Equation 6.3-13 because the scour

depth calculated varies depending on the value of Δx, which means DEM resolution will affect the final estimated scour depth. To remove this dependence, the second term was raised to the 0.57 power, yielding the following approximation that is implemented in FAR V.1.2:

$$scourdepth(i,j) = scourdepth_{narrows}\left(\left(\frac{contribarea(i,j)}{contribarea_{narrows}}\right)\left(\frac{\Delta w_{narrows}}{\Delta x}\right)\right)^{0.29} \quad \text{(Eq. 6.3-14)}$$

The scour depth in the equation is a maximum value from many large floods that will occur during the period of time when easily mobilized tephra is being transported toward the RMEI (note that the model assumes that this time is short when compared to the overall model duration, and occurs "instantaneously"). Direct measurements of this value are unavailable (both because of the recurrence interval for a 100- or 500-year flood, and because the scour measurements are labor intensive and not often made). Scour depths measured at the USGS Narrows gaging station on Fortymile Wash after a single flood on March 11, 1995 (described in Section 6.5.6), were used as input to Equation 6.3-14. The Narrows is located approximately 20 km upstream of the fan apex (see Figure 7.1.3-2) and downstream of the largest tributaries, making it an acceptable location for model calibration.

As described above, Equation 6.3-14 is not rigorously derived from Equations 6.3-11 and 6.3-12. The deviations occur as the result of the assumption that channel width and contributing area can be divided among multiple channel cells representing a single channel cross-section and the mathematical manipulation required to remove the dependence on grid resolution. In light of these changes, the approximation represented by Equation 6.3-14 needs to be validated. This validation is described in Section 7.2.3.

As an example of the model results, Figure 6.3.3-6 shows the scour depth calculated for the upper drainage basin DEM using Equation 6.3-14 with $scourdepth_{narrows}$ = 97.5 cm (equal to the mean of the scour depth distribution defined in Section 6.5.6). In the FAR V.1.2 code, the parameter *scourdepthoutlet* is used in place of $scourdepth_{narrows}$.

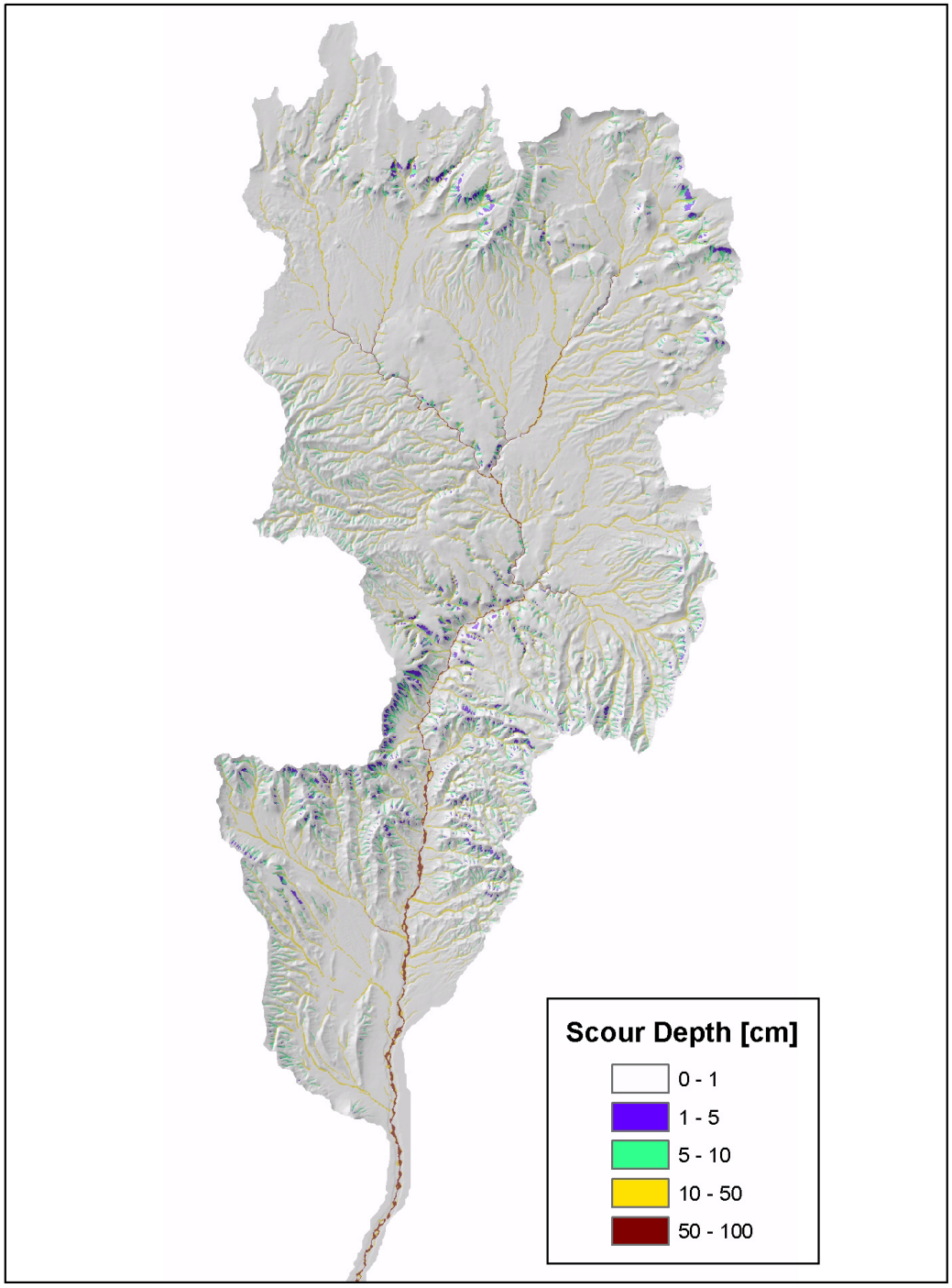

NOTE: Figure is for illustration purposes.

Figure 6.3.3-6. Scour Depth Predicted by the FAR for the Upper Drainage Basin Domain

STEP 4: Calculate dilution factor and total mass of mobilized tephra and waste

The dilution factor [dimensionless] represents the volume fraction of tephra within the scour zone and is calculated for each grid cell in the DEM domain. To calculate this factor, the

following substeps are followed: (1) identify grid cells where tephra is mobilized, (2) route mobilized tephra thickness using the bifurcation routing algorithm, (3) route scour depth using the bifurcation routing algorithm, and (4) calculate dilution as routed tephra thickness divided by routed scour depth.

To understand how the model mobilizes tephra it is helpful to introduce the tephra classification scheme used by the FAR model. Thresholds of slope and stream power are used to classify tephra and define whether and how it is mobilized. By combining these two parameter thresholds, four distinct and nonoverlapping regions can be defined (Figure 6.3.3-7): "Steep Channels" (*power(i,j)* ≥ 1/*X AND slope* ≥ S), "Gradual Channels" (*power(i,j)* ≥ 1/*X AND slope* < S), "Steep Hillslopes" (*power(i,j)* < 1/*X AND slope* ≥ S), and "Gradual Hillslopes" (*power(i,j)* < 1/*X AND slope* < S). The total tephra is equal to the sum of tephra that is in each of these regions.

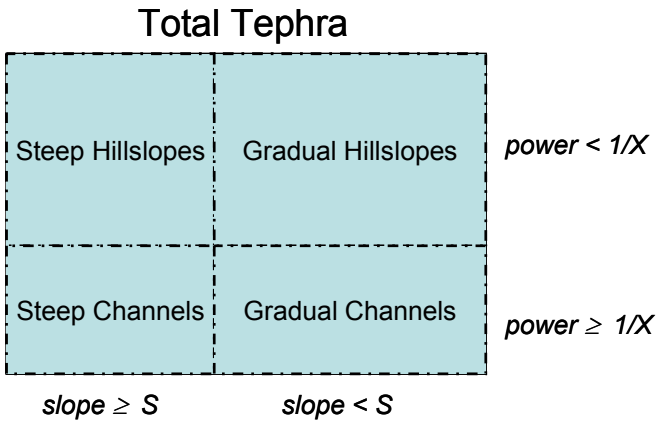

Figure 6.3.3-7. Tephra Classification Scheme Based on Slope and Stream Power

The model routes tephra thickness and scour depth in four computational substeps.

A. Mobilized tephra thickness in all channel cells (*power(i,j)* ≥ 1/*X*) is determined as the minimum of the initial tephra thickness from STEP 1 and the local scour depth. Thus, any tephra that falls on channel cells that is deeper than the local scour depth is assumed to be immobile.

B. Tephra thickness from Steep Hillslope cells is routed downstream using the bifurcation routing algorithm until all the routed tephra reaches channel-head grid cells, where it is temporarily stored. Next, the mobilized tephra thickness from channel cells calculated in step A above is then added to the routed tephra thickness from Steep Hillslopes. At this point in the calculation, all mobilized tephra is temporarily stored in the channel grid cells. Immobile tephra is stored in the Gradual Hillslope region and in channel cells (both Steep and Gradual) below the scour depth where the initial tephra thickness exceeds the scour depth.

C. Scour depth is routed downstream using the divergent (bifurcation) flow algorithm. Mathematically, *routedscour(i,j)* is: $\left(\sum_{up} scourdepth(l,m)\right) + scourdepth(i,j)$, where the first term is the sum of scour depth for upstream cells *(l,m)* using the bifurcation routing algorithm and the second term is the local scour depth.

D. Mobilized tephra in all channel grid cells (*power(i,j)* ≥ 1/*X*), including the temporary deposits from Steep Hillslopes, is routed downstream using the bifurcation routing algorithm. The result of this second routing is referred to as the "routed tephra thickness", (*routedash(i,j)*). Mathematically, *routedash(i,j)* is: $\min\left\{\left(\sum_{up} ashthickness(l,m)\right) + ashthickness(i,j), routedscour(i,j)\right\}$, where the term $\sum_{up} ashthickness(l,m)$ is the sum of tephra thickness for upstream cells *(l,m)* using the bifurcation routing algorithm and *ashthickness(i,j)* is the local tephra thickness at *i,j*, which includes tephra deposited by ASHPLUME within the scour zone and any tephra initially routed from Steep Hillslopes to a channel-head grid cell. The sum of these two terms is constrained to be less than the value of *routedscour(i,j)*.

To calculate the contributing area in STEP 3, each grid cell was initially given a value equal to its local area, and those values were "routed" downstream, adding up contributions (weighted by slope) from each upstream grid cell along the way. The same procedure is used to route tephra thickness and scour depth, except for two differences: (1) the starting grids are different and (2) the criteria used to determine if routing is performed for a cell is different. For example, in step B, the starting grid is tephra thickness on Steep Hillslopes (tephra thickness in channels is set to 0 during the routing) and the criterion used to determine if routing is performed is if *power(i,j) < 1/X*. This criterion ensures that the tephra is only routed to the first channel-head cell it encounters. For step C, the starting grid is local scour depth and the criterion used to determine if routing is performed is if *power(i,j) ≥ 1/X*. For the routing of tephra thickness (step D), the initial grid is equal to the thickness of tephra mobilized from Steep Hillslopes and deposited in active channel heads, plus the thickness of tephra (within the scour zone) that was deposited directly on the active channels as fallout and the criterion used to determine if routing is performed is if *power(i,j) ≥ 1/X*.

It should be noted that the routing of both scour depth and tephra thickness results in local deposits of material that never reaches the main Fortymile Wash channel. This is because channels (defined where *power(i,j)* ≥ 1/*X*) can terminate in areas of locally low slopes before connecting to the main Fortymile Wash channel. In this case, the material routed along these paths never reaches the main channel and is therefore not included in the dilution calculation at the outlet. These channel ends can be thought of as local depozones where tephra is deposited within the upper basin (in the channel). Figure 7.2.4-1 and accompanying text illustrates how bounding values of drainage density affect the connectedness of channel networks near the repository.

The dilution factor is calculated next as:

$$dilution(i,j) = \frac{\min\left[routedash(i,j), routedscour(i,j)\right]}{routedscour(i,j)} \qquad \text{(Eq. 6.3-15)}$$

Equation 6.3-15 is limited to values between 0 and 1.

The value of the dilution factor at the fan apex, *dilutionfactoroutlet*, is the value used in STEP 5 to calculate the tephra concentration in channels at the RMEI location. The values of the dilution factor at all other cells are not used by the model but are reported to enable examination of the algorithm behavior. Figure 6.3.3-8 shows the result of Equation 6.3-15 for all grid cells in the upper basin domain. The extent and thickness of the initial tephra deposit (thickness > 0.1 cm) is also shown for reference. Figure 6.3.3-9 shows a series of example results from STEPs 1 to 4.

The total masses of mobilized tephra (*ashmobilized*) and waste (*fuelmobilized*) influencing the concentration at the outlet are calculated by summing up tephra and waste mass for each grid cell starting at the outlet location and moving upstream along channel cells. These masses are less than the total masses of mobilized tephra and waste represented in Figure 6.3.3-7 because they only include material in channels that are connected to the main channel at the outlet location. These values are reported in the text output file from the FAR V.1.2 software. Section 7.2.8 provides a number of mass calculations that illustrate the relative magnitudes of mobilized tephra for a set of representative model simulations.

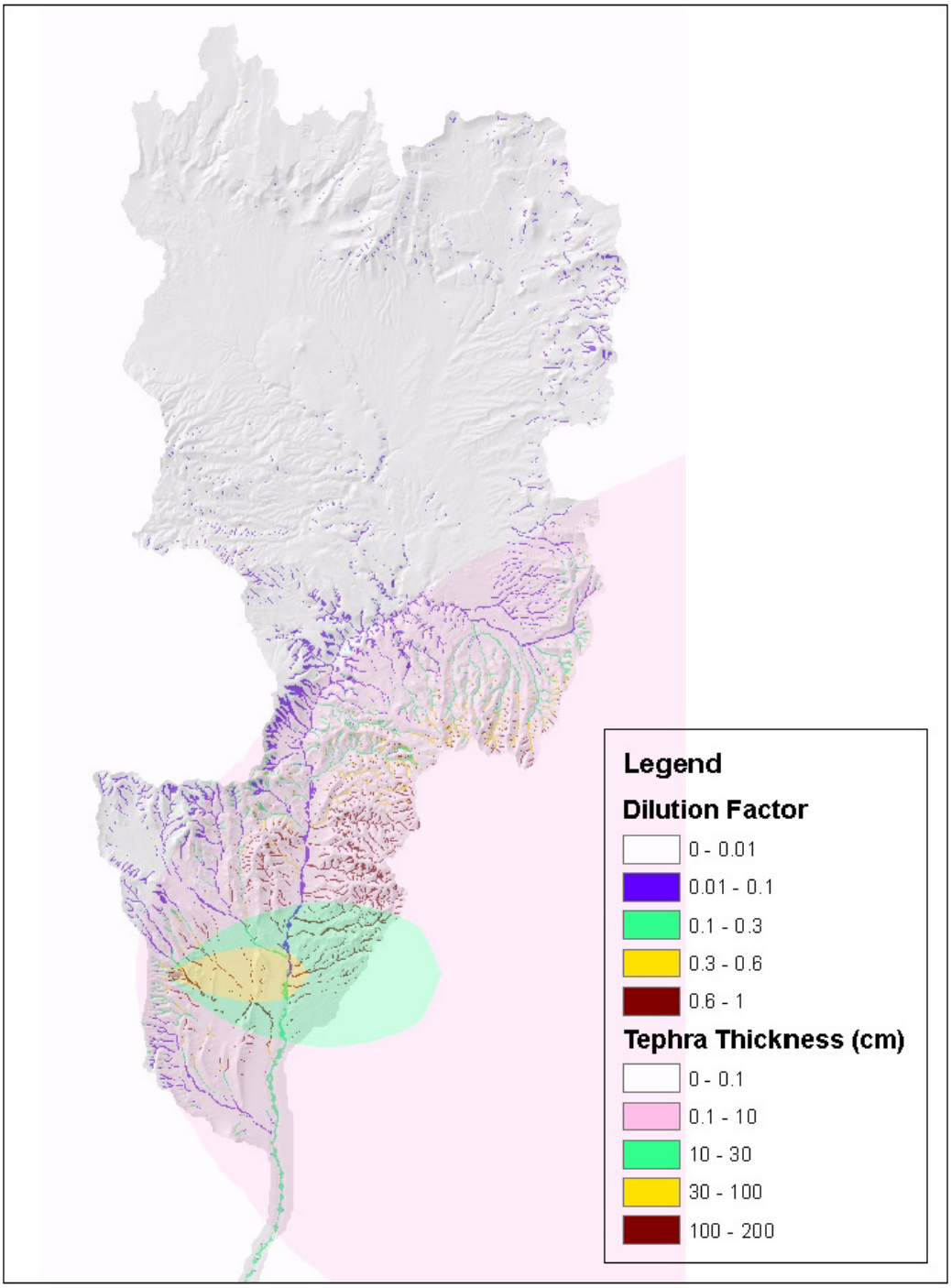

NOTE: The extent of the tephrafall deposit (>0.1 cm thickness) (westerly winds) is shown for reference. Figure is for illustrative purposes.

Figure 6.3.3-8. Dilution Factor Calculated within the Channel Network for an Example Run of the FAR Model

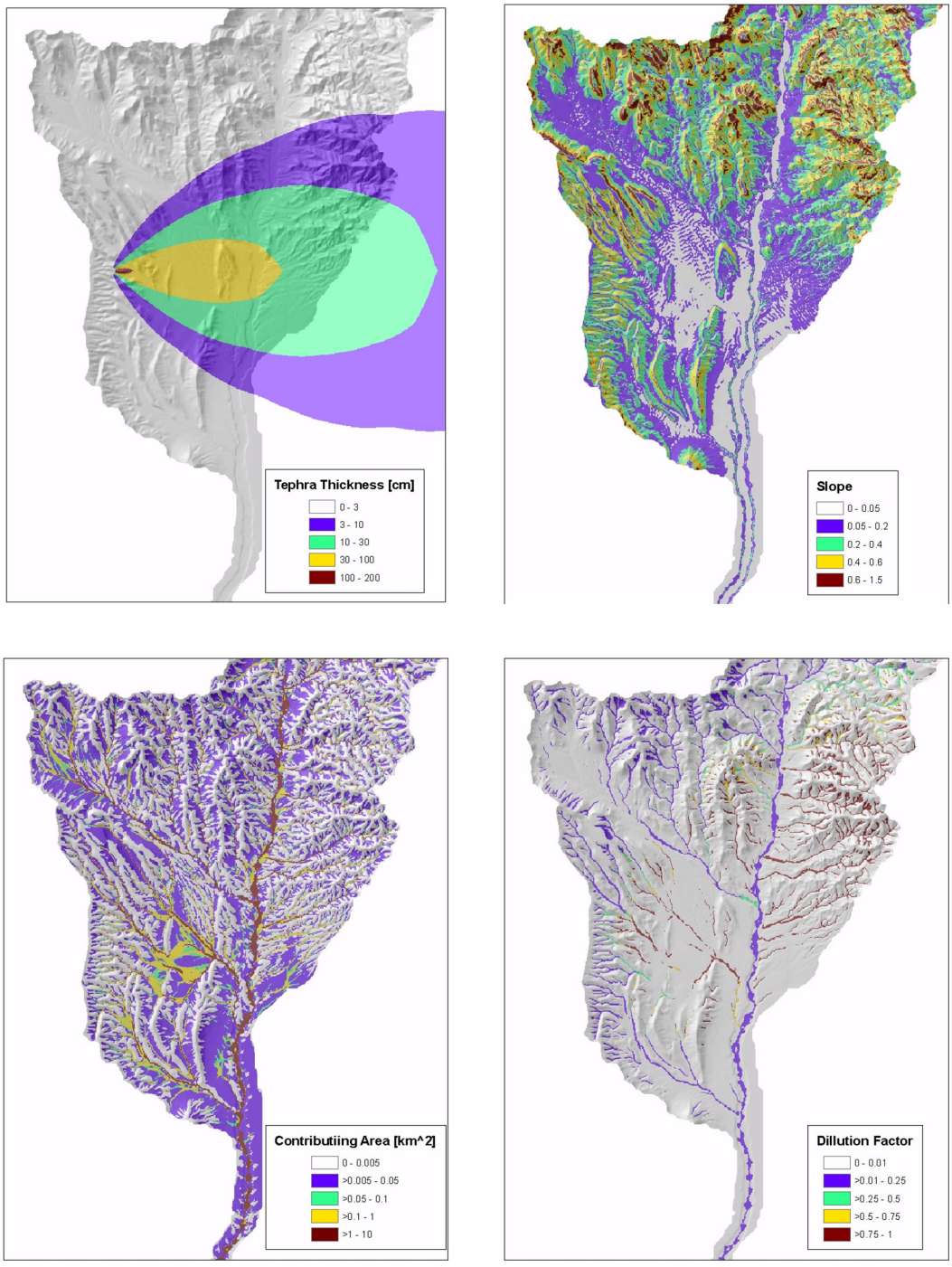

NOTE: Figure is for illustration purposes.

Figure 6.3.3-9. Example Model Output for Southern Part of Drainage Basin

STEP 5: Determine initial concentration and thickness of contaminated tephra on inter-channel divides and in channels at the RMEI location

This step transfers contaminated tephra from the upper basin to the RMEI location, which is represented as two distinct one-dimensional subdomains (inter-channel divides and channels).

On inter-channel divides, the thickness of tephra and concentration of waste is determined solely from the primary fallout deposited directly on the RMEI location and is therefore not influenced by the transport and dilution processes represented in the upper basin. This is consistent with the assumption that inter-channel divides are not subject to fluvial activity (erosion and deposition) over the model duration. The concentration of waste on inter-channel divides at the RMEI location, expressed as an areal density in the model (g/cm^2), is a direct input from the ASHPLUME model (SNL 2007 [DIRS 177431]). The thickness of the tephra layer is determined by dividing the tephra concentration (g/cm^2) by the tephra density, ρ (g/cm^3), to obtain a tephra thickness in centimeters. Mathematically, the tephra thickness on divides at the RMEI location (*primaryashthickness*) is given by:

$$primaryashthickness = ashdepositionRMEI/\rho. \quad \text{(Eq. 6.3-16)}$$

where *ashdepositionRMEI* (g/cm^2) is output from the ASHPLUME model. Because tephra and waste are represented separately by ASHPLUME, this estimate of thickness assumes that the volume fraction of the contaminated tephra that is waste is very small. This tephra thickness is used to calculate the initial waste concentration on divides, *fueldivideinit* (g/cm^3) (note that *fuel* in the following parameter names means *waste*). Mathematically, this is given by:

$$fueldivideinit = fueldepositionRMEI/primaryashthickness, \quad \text{(Eq. 6.3-17)}$$

where *fueldepositionRMEI* (g/cm^2) is output from the ASHPLUME model. In channels, the mass of waste is the sum of the waste deposited on the landscape directly from the tephrafall and the waste transported from the upper basin by fluvial processes. The scour-dilution-mixing model predicts the tephra concentration and depth of contaminated sediments within the scour zone at the fan apex. The waste concentration is calculated as the average waste concentration of all the mobilized tephra. FAR V.1.2 uses those values to compute the thickness and waste concentration of contaminated tephra in the channels of the RMEI location. The depth of contaminated tephra in channels (cm) is defined as:

$$depthfuelchannel = scourdepthoutlet \quad \text{(Eq. 6.3-18)}$$

This scour depth is the depth measured at the Narrows station and is a good estimation of the scour depth in the channels at the RMEI location for reasons discussed in Sections 6.5.6 and 7.2.3. The initial waste concentration within that layer, *fuelchannelinit* (g/cm^3), is computed as the sum of two terms.

$$fuelchannelinit = (fueldepositionRMEI / scourdepthoutlet) + \quad \text{(Eq. 6.3-19)}$$

$$(\rho * dillutionfactoroutlet * fuelmobilized / ashmobilized)$$

The first term on the right-hand side represents the primary tephra and waste deposited on the landscape by the tephrafall. The second term on the right-hand side represents the average waste concentration computed by the scour-dilution-mixing model. That model actually computes the tephra concentration in channels of the RMEI location, which is given by ρ * *dilutionfactoroutlet*. The concentration of waste, then, is simply given by the product of ρ **dilutionfactoroutlet* and the ratio of the mass of waste and tephra mobilized from upstream (*fuelmobilized / ashmobilized*). The use of this average waste concentration from upstream assumes complete mixing of tephra and waste during transport.

STEP 6: Compute diffusion of radionuclides in soil profiles on divides and in channels

The model quantifies the redistribution of radionuclides within the soil as a diffusion process. The model considers diffusion of radionuclides within a finite depth range representing the permeable soil. Divide surfaces accumulate pedogenic calcium carbonate and clay at depth, decreasing the soil permeability over time. Pleistocene-age surfaces can be considered relatively impermeable compared with channel sands. Field work was performed to measure the permeable soil thickness on divide surfaces. The measured values are used to prescribe a range of values for permeable depth of soil on divides (L_d) at the RMEI location. Soil horizons do not form in channel sediments because they are continually reworked by floods. The permeable depth of soil is greater in channels than on divides, but the thickness might be limited by the occurrence of paleosols at depth. Field work was performed to establish a minimum permeable depth in channels (L_c) (discussed in Section 6.5.5). That minimum permeable depth or range of depths is used for the value of L_c in the model. The radionuclide diffusivities are obtained by fitting post-bomb ^{137}Cs fallout profiles in the soil (discussed in Section 6.5.8).

The equation describing the evolution of waste concentration $C(z,t)$ (g/cm^3) at depth z (cm) and at time t (years), undergoing diffusion in a finite layer from $z = 0$ to $z = L$ (cm) with no-flux boundary conditions and an initial waste distribution $f(z)$, is given by (Carslaw and Jaeger 1959 [DIRS 100968], Section 3.4, Equation 6):

$$C(z,t) = \frac{1}{L}\int_0^L f(z)dz + \frac{2}{L}\sum_{n=1}^{\infty} e^{-n^2\pi^2 Dt/L^2} \cos\left(\frac{n\pi z}{L}\right)\int_0^L f(z)\cos\left(\frac{n\pi z}{L}\right)dz \quad \text{(Eq. 6.3-20)}$$

where n is the component of the Fourier series and D is the diffusivity constant (cm^2/yr).

Equation 6.3-20 is applied to both channels and divides within the model but with different values for L, D, and the initial contaminant-layer thickness. On both divides and channels, the initial condition is a layer of uniform concentration between $z = 0$ and some finite depth. On divides, that depth is equal to the thickness of primary tephra fallout denoted by the variable *primaryashthickness* within the model (the variable d_{df} is used to represent *primaryashthickness* in the equations of this section). In channels, the primary fallout and the tephra redistributed from upstream are added together and uniformly mixed from the surface to a depth equal to that of the Fortymile Wash fan apex (*scourdepthoutlet*), with concentration equal to *dilutionfactoroutlet* calculated in STEP 4 (in the model this depth is denoted by *depthfuelchannel*; in the equations of this section, it is denoted by d_{cf}).

Therefore, in the case of divides, the initial condition (concentration, f (g/cm^3), as a function of depth, z) for the diffusion model is given by:

$$f(z) = \begin{Bmatrix} C_{d0} & \text{if} \quad z \le d_{df} \\ 0 & \text{if} \quad z > d_{df} \end{Bmatrix} \qquad \text{(Eq. 6.3-21)}$$

where C_{d0} is the waste concentration within the primary fallout layer, *fueldivideinit* (g/cm^3) from Equation 6.3-17. Substituting Equation 6.3-21 into Equation 6.3-20 with C=C_d (g/cm^3), L=L_d, and D=D_d results in:

$$\begin{aligned} C_d(z,t) &= \frac{C_{do} \bullet d_{df}}{L_d} + \frac{2}{L_d}\sum_{n=1}^{\infty} e^{-n^2\pi^2 D_d t / L_d^2} \sin\left(\frac{n\pi d_{df}}{L_d}\right)\cos\left(\frac{n\pi z}{L_d}\right)\left(\frac{C_{do}L_d}{n\pi}\right) \\ &= C_{d0}\left(\frac{d_{df}}{L_d} + \frac{2}{\pi}\sum_{n=1}^{\infty} \mathrm{e}^{-n^2\pi^2 D_d t/L_d^2}\ \frac{1}{n}\sin\left(\frac{n\pi d_{df}}{L_d}\right)\cos\left(\frac{n\pi z}{L_d}\right)\right) \end{aligned} \qquad \text{(Eq. 6.3-22)}$$

The concentration at the surface (g/cm^3) at time t (yr) following deposition (*fuelsurfacedivide*) is given by evaluating Equation 6.3-22 at z = 0:

$$C_d(0,t) = C_{d0}\left(\frac{d_{df}}{L_d} + \frac{2}{\pi}\sum_{n=1}^{\infty} \mathrm{e}^{-n^2\pi^2 D_d t/L_d^2}\ \frac{1}{n}\sin\left(\frac{n\pi d_{df}}{L_d}\right)\right) \qquad \text{(Eq. 6.3-23)}$$

In the case of channels, the initial condition for the diffusion model is given by:

$$f(z) = \begin{Bmatrix} C_{c0} & \text{if} \quad z \le d_{cf} \\ 0 & \text{if} \quad z > d_{cf} \end{Bmatrix} \qquad \text{(Eq. 6.3-24)}$$

where C_{c0} is the waste concentration within the scour depth interval, *fuelchannelinit* (g/cm^3) from Equation 6.3-19. Substituting Equation 6.3-24 into Equation 6.3-20 with C=C_c, L=L_c, and D=D_c results in:

$$\begin{aligned} C_c(z,t) &= \frac{C_{co} \bullet d_{cf}}{L_c} + \frac{2}{L_c}\sum_{n=1}^{\infty} e^{-n^2\pi^2 D_c t / L_c^2} \sin\left(\frac{n\pi d_{cf}}{L_c}\right)\cos\left(\frac{n\pi z}{L_c}\right)\left(\frac{C_{co}L_c}{n\pi}\right) \\ &= C_{c0}\left(\frac{d_{cf}}{L_c} + \frac{2}{\pi}\sum_{n=1}^{\infty} \mathrm{e}^{-n^2\pi^2 D_c t/L_c^2}\ \frac{1}{n}\sin\left(\frac{n\pi d_{cf}}{L_c}\right)\cos\left(\frac{n\pi z}{L_c}\right)\right) \end{aligned} \qquad \text{(Eq. 6.3-25)}$$

The concentration at the surface (g/cm^3) at time t (yr) following deposition (*fuelsurfacechannel*) is given by evaluating Equation 6.3-25 at z = 0:

$$C_c(0,t) = C_{c0}\left(\frac{d_{cf}}{L_c} + \frac{2}{\pi}\sum_{n=1}^{\infty} \mathrm{e}^{-n^2\pi^2 D_c t/L_c^2}\ \frac{1}{n}\sin\left(\frac{n\pi d_{cf}}{L_c}\right)\right) \qquad \text{(Eq. 6.3-26)}$$

Figure 6.3.3-10 illustrates the behavior of the diffusion model in channels for hypothetical model parameters.

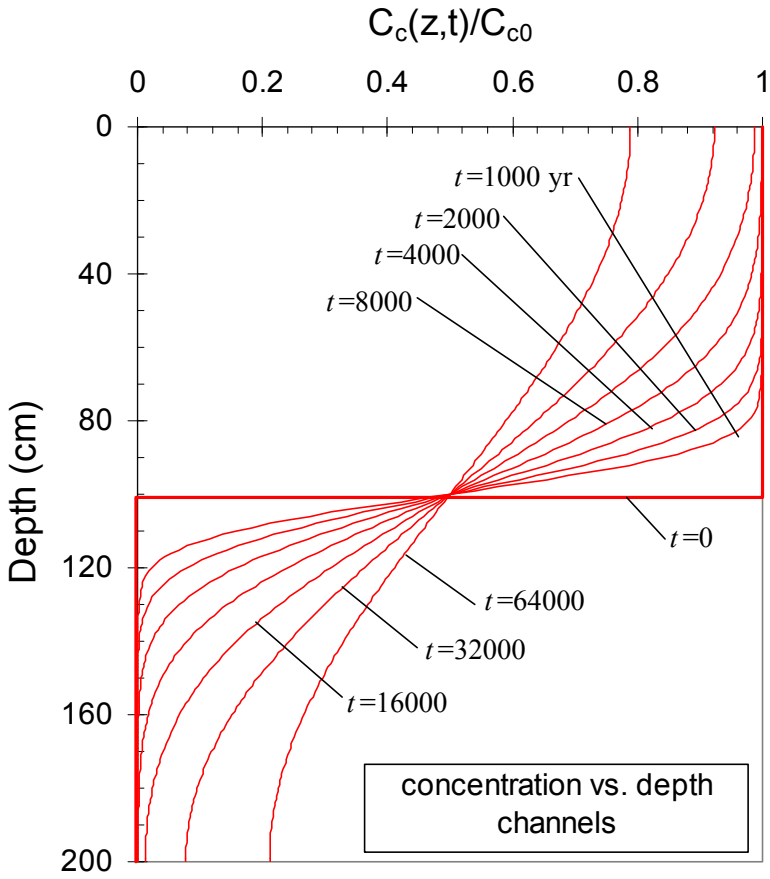

Source: Output DTN: SN0708DIFFEXMP.001.

NOTE: Plotted using a permeable channel depth of 200 cm, scour depth of 100 cm, and channel diffusivity of 0.05 cm^2/yr.

Figure 6.3.3-10. Plot of Normalized Concentration versus Depth in the Channels for a Range of Times Following an Eruption

The biosphere model within TSPA requires the average concentration within a finite surface layer of depth *B*. The thickness of that layer depends on the dose pathway being considered. The tillage depth is required for the ingestion and external exposure pathways, and a thin layer (1 to 3 mm) of resuspendible material at the surface is required for the inhalation pathway. To provide the depth-averaged concentration to TSPA, the FAR V.1.2 software accepts as input a parameter representing the biosphere depth *B*, and computes the average concentration from the surface to that depth for each model time step on divides and in channels. Within the TSPA implementation, FAR is executed twice, once with the parameter *B* set to the tillage depth and once with the parameter *B* set to the resuspendible depth. The values for each depth are provided by the biosphere model and are treated as uncertain parameters within the TSPA model.

The depth-averaged concentration on divides and in channels is calculated by integrating Equations 6.3-22 and 6.3-25 from $z = 0$ to $z = B$. On divides the depth-integrated concentration (g/cm^2) at time t (yr) following deposition (*fueldepthBdivide*) is:

$$\int_0^B C_d(z,t)dz = C_{d0}\left(\frac{Bd_{df}}{L_d} + \frac{2L_d}{\pi^2}\sum_{n=1}^{\infty}\frac{1}{n^2}\sin\left(\frac{n\pi B}{L_d}\right)\sin\left(\frac{n\pi d_{df}}{L_d}\right)e^{-n^2\pi^2 D_d t/L_d^2}\right) \quad \text{(Eq. 6.3-27)}$$

In channels, the depth-integrated concentration (g/cm^2) at time t (yr) following deposition (*fueldepthBchannel*) is:

$$\int_0^B C_c(z,t)dz = C_{c0}\left(\frac{Bd_{cf}}{L_c} + \frac{2L_c}{\pi^2}\sum_{n=1}^{\infty}\frac{1}{n^2}\sin\left(\frac{n\pi B}{L_c}\right)\sin\left(\frac{n\pi d_{cf}}{L_c}\right)e^{-n^2\pi^2 D_c t/L_c^2}\right) \quad \text{(Eq. 6.3-28)}$$

The depth-integrated concentration time series defined by equations 6.3-27 and 6.3-28 are the primary outputs from the FAR software to TSPA. The surface concentration time series defined by Equations 6.3-23 and 6.3-26 are also output by the software, but those two time series are not used by TSPA.

Figure 6.3.3-11 shows a flow chart that summarizes the steps described in this section.

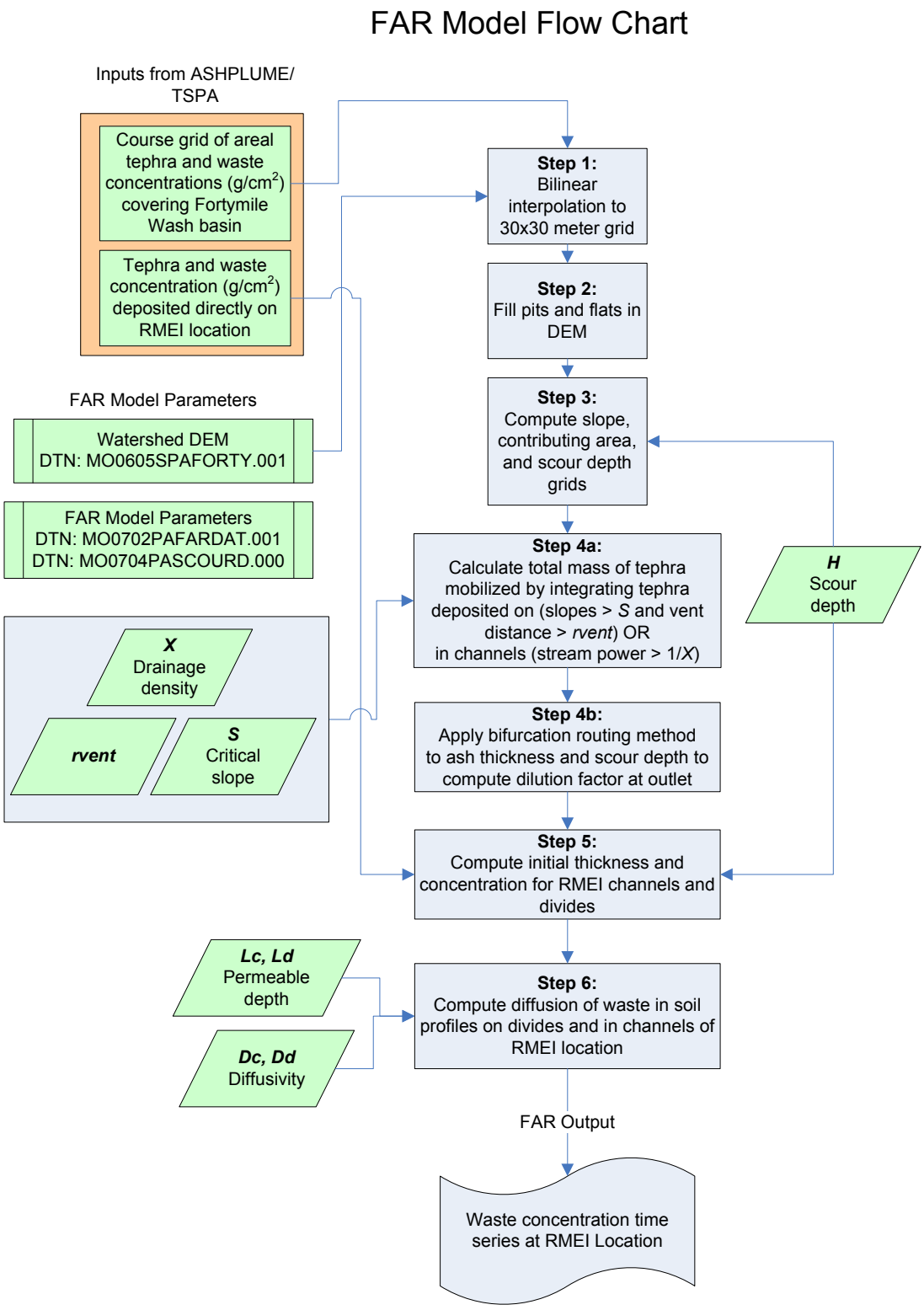

Figure 6.3.3-11. Flow Chart for Tephra Redistribution Model

6.4 MODEL IMPLEMENTATION IN FAR V.1.2

The tephra redistribution mathematical model is implemented as a computer code using the standard C++ language. For use in the TSPA, the FAR V.1.2 code (see Section 3) is implemented directly within the GoldSim software as a DLL. All model inputs are entered in GoldSim templates and passed directly to the FAR.DLL. Within the TSPA, the redistribution of tephra and waste implemented in the FAR V.1.2 code is used to predict the depth-integrated concentrations of waste after a violent Strombolian eruption that intersects the repository using output from the ASHPLUME model (SNL 2007 [DIRS 177431]). The waste concentration is converted to activities and then combined with biosphere dose conversion factors (SNL 2007 [DIRS 177399], Section 6.12.3) in the TSPA model to calculate an annual dose to the RMEI. FAR V.1.2 model results are produced at run time within the TSPA model. The FAR V.1.2 model inputs, developed in Section 6.5 and listed in Table 6.4-1, are provided as inputs to the TSPA model as GoldSim variables. These variables are passed to the FAR V.1.2 module at run time, along with ASHPLUME results of initial tephra and waste concentrations (in g/cm^2). The TSPA model evaluates uncertainty by sampling certain parameters from probability distributions. The results from multiple sampling realizations of input parameters are used to quantify the uncertainty in the results that can be attributed to uncertainty in the input parameters. The waste concentration values from each model realization are passed back to the GoldSim model in the form of one-dimensional table elements.

Table 6.4-1. Input Parameters for the FAR V.1.2 Tephra Redistribution Model

Parameter Name (symbol)	Description	Units	Where Developed
criticalslope (S) [a]	Critical slope for tephra mobilization from hillslopes	dimensionless	Section 6.5.2
drainagedensityupperbasin (X) [a]	Average drainage density (the ratio of the total length of channels in a drainage basin to the basin area) in the Fortymile Wash drainage basin (km^{-1})	km^{-1}	Section 6.5.3
scourdepthoutlet (H) [a]	Depth of scour in Fortymile Wash at the fan apex	cm	Section 6.5.6
RMElarea (A)	Area of the Fortymile Wash alluvial fan (the RMEI location) potentially subject to redistributed tephra deposition	km^2	Section 6.5.4
fractionchannel (F) [a]	Decimal fraction of the area of the Fortymile Wash alluvial fan subject to fluvial activity (channels)	dimensionless	Section 6.5.4
Ldivide (L_d) [a]*, Lchannel (L_c)*	Depth of permeable soil (interchannel divides or channels) at the RMEI location	cm	Section 6.5.5
Ddivide (D_d) [a], *Dchannel (D_c)* [a]	Diffusivity of waste in soil (interchannel divides or channels) at the RMEI location	cm^2/yr	Section 6.5.8
ashsettleddensity (ρ) [a]	Tephra settled bulk density	g/cm^3	DTN: LA0612DK831811.001 [DIRS 179987]
xvent, yvent	The easting and northing coordinate location of the vent in UTM NAD27, Zone 11	m	Section 6.5.7
gridflag	This variable indicates whether a Cartesian or a polar grid is input from ASHPLUME. If *gridflag* = 0, a Cartesian grid is used. If *gridflag* = 1, a polar grid is used.	dimensionless	ASHPLUME [b]

Table 6.4-1. Input Parameters for the FAR V.1.2 Tephra Redistribution Model (Continued)

Parameter Name (symbol)	Description	Units	Where Developed
minx, maxx, miny, maxy	The distance between the western, eastern, southern, and northern boundaries, respectively, of the input ASHPLUME grid and the vent location. Used only if *gridflag* = 0.	km	ASHPLUME [b]
lattice_size_x, lattice_size_y	Number of columns and rows in the ASHPLUME grid. Used only if *gridflag* = 0.	dimensionless	ASHPLUME [b]
minrad	Minimum ASHPLUME grid radius. Used only if *gridflag* = 1.	m	ASHPLUME [b]
rfactor	Factor by which grid radius increases away from the vent. Used only if *gridflag* = 1.	dimensionless	ASHPLUME [b]
lattice_size_r	Number of radial increments in the ASHPLUME grid. Used only if *gridflag* = 1.	dimensionless	ASHPLUME [b]
rvent	The radius inside which no tephra is mobilized	m	Section 6.5.7.2
Lattice_size_theta	Number of angular increments in the ASHPLUME grid. Used only if *gridflag* = 1.	dimensionless	ASHPLUME [b]
Timestep (Δt)	The output time step	yr	Section 6.5.9
Simulationlength (T)	The model duration	yr	Section 6.5.9
Bdepth (B) [b]	The biosphere depth. FAR V.1.2 outputs the areal (depth-integrated) radionuclide concentration between the surface and depth *B*, which represents a critical depth in the biosphere model (e.g., tillage depth or depth of resuspendible soil layer).	cm	BIOSPHERE [c]
oflag	The output grids flag. This variable indicates whether spatial grids (slope, contributing area, and preprocessed tephra and waste grids) should be output. This flag can be set to 1 for testing (send grids to output file), or 0 for use within TSPA (do not send grids to output file).	dimensionless	Section 6.5.9
ashdepositionRMEI	The tephra concentration at the RMEI location output by ASHPLUME	g/cm^2	ASHPLUME [b]
fueldepositionRMEI	The waste concentration at the RMEI location output by ASHPLUME	g/cm^2	ASHPLUME [b]

[a] Parameter sampled from probability distribution in TSPA.
[b] Parameter developed in SNL 2007 [DIRS 177431].
[c] Parameter developed in SNL 2007 [DIRS 177399].

Grids of selected model output are saved when the *oflag* parameter is set to a value of 1. In this case, the following grids are produced: (1) local slope, (2) contributing area, (3) interpolated tephra thickness prior to redistribution, (4) dilution factor, (5) scour depth, and (6) intermediate output from a small test grid used for software validation activities. These grids are used in later sections of the report to plot maps showing example model results. Other intermediate outputs are presented in the report for the sole purpose of illustrating how the FAR model algorithm functions and for comparing intermediate model results to alternative methods for model corroboration. These plots are for illustrative purposes. Data for these plots was generated by adding code to the FAR V.1.2 program in order to save additional intermediate results that are

not saved by the qualified version of the software. These plots are for illustrative purposes only and are not used to generate any qualified product output or results for TSPA.

6.5 DEVELOPMENT OF MODEL INPUTS FOR TSPA

6.5.1 Digital Elevation Model of the Fortymile Wash Drainage Basin

The tephra redistribution model requires a 30 by 30-m input grid of elevation values for the upper Fortymile Wash drainage basin. This data is supplied to the model via an ASCII input file (*farinputdem.txt*). This input file was developed from data obtained from the USGS National Elevation Dataset (DTN: SN0707DEMSOURC.001 [DIRS 182111]). This data was input to a set of processing steps that were performed to delineate the boundaries of the ~828 km^2 drainage basin that supplies water and sediment to the Fortymile Wash alluvial fan. This work, along with the associated computer files, is documented and archived in Output DTN: MO0605SPAFORTY.000. A summary of this work is presented below.

The development of the watershed ASCII input file was done in ten sequential phases, each of which required a set of software steps. The details of each of these steps are included as part of the documentation for Output DTN: MO0605SPAFORTY.000. The ten phases are summarized below.

1. **Create a mosaic raster from the four source raster datasets from source DTN: SN0707DEMSOURC.001 [DIRS 182111].** The input data were supplied in four separate raster datasets in Arc GRID format. These datasets were combined into a single raster using the ArcGIS tool: *Mosaic to New Raster*.

2. **Project DEM to UTM, NAD27, Zone 11 coordinate system.** The input data were supplied in geographic coordinates, NAD83 (latitude, longitude) in 1/3 arc second intervals (~10 m). In this phase, the data were projected into the UTM, NAD27, Zone 11 coordinate system and resampled into a 30 by 30-m grid resolution using bilinear interpolation. The phase was performed using the ArcGIS tool: *Project Raster*.

3. **Clip the UTM DEM.** The raster resulting from the previous phase was then clipped to an area surrounding the upper drainage basin. This was done using the ArcGIS tool: *Clip*.

4. **Fill sinks in clipped DEM.** The first step for defining the watershed boundaries is to fill any local depressions in the grid to ensure that all areas within the watershed drain to the lowest point (pour point). This was done using the ArcGIS (Spatial Analyst) tool: *Fill*.

5. **Calculate flow directions.** The second step for defining the watershed boundaries is to calculate direction of steepest descent vector. This was done using the ArcGIS (Spatial Analyst) tool: *Flow Direction*.

6. **Calculate flow accumulation.** The third step for defining the watershed boundaries is to calculate flow accumulation. Flow accumulation uses the flow direction raster

calculated above to sum up the number of upstream grid cells for each cell of the grid. This was done using the ArcGIS (Spatial Analyst) tool: *Flow Accumulation*.

7. **Define pour point for watershed.** The forth step for defining the watershed boundaries is to identify the outlet or pour point of the watershed. This is the grid cell that has the highest value of flow accumulation. This was done by displaying the flow accumulation raster in ArcMap and placing a point feature within the grid cell with the highest value of flow accumulation.

8. **Delineate watershed.** Using the flow accumulation raster and the pour point location, the watershed can be defined. The ArcGIS (Spatial Analyst) tool, *Watershed*, defines a watershed starting at the pour point and working upstream along all flow channels until the flow accumulation is equal to zero, which corresponds to the drainage divide. This tool assigns all cells inside the watershed with a constant value.

9. **Fill watershed with elevations.** The next step was to map all grid cells inside the watershed with the DEM elevations from the raster output of phase 4 (*Fill*). All grid cells outside the watershed were given a value of "-9999", which is required by the FAR software.

10. **Export watershed to ASCII file for use with FAR.** The final step was to export the raster file into an ASCII file. This was done using the ArcGIS tool, *Raster to ASCII*. Finally, the text header (the first six text lines) was removed from the text file so FAR was able to read the file. It should be noted that deleting the header resulted in a slight shift in the position of the resulting grid when it is read into the FAR model (~15 m to the west and ~10 m to the south). This occurs because when the FAR model reads in the grid input file, it assumes that the upper left corner of the input DEM is located at (542500, 4126000) (UTM, NAD27, Zone 11). This detail is not considered to be significant because it involves sub-grid-scale variations that are beyond the potential accuracy of the model. This detail is mentioned only to increase transparency.

6.5.2 Critical Slope

The critical slope parameter used by the model is a fraction of the vertical change over the horizontal change ($\Delta z/\Delta x$). It represents the steepest stable slope for tephra-blanketed hillslopes. Slope angle measurements, in degrees from horizontal, were collected at Rattlesnake Crater, Cochrane Hill Cinder Cone, and Moon Crater in the San Francisco Peaks volcanic field outside of Flagstaff, AZ (Table 4.1-3). Tephra that erupted from Sunset Crater blankets the hillslopes at these study sites. To determine the hillslope angle, a Brunton compass and two Jacob staffs were used. The slope was measured by placing one Jacob staff with a Brunton compass on top of it near the top of the hillslope, above the location of the incipient incision. The other Jacob staff was positioned directly downslope. Both staffs were held vertically (checked with a level) and the angle between the tops of the two Jacob Staffs was recorded. Measurements were made incrementally, directly down the steepest descent of the hillslope. After a measurement was made, the up-slope Jacob staff was moved to the location of the down-slope Jacob staff, and the down-slope staff was moved further downslope. The process was repeated until the entire slope was measured (to a location below the debris lobe). The hillslopes were measured at their

steepest stable angles, based on observed indicators for tephra mobilization such as incipient rilling and debris lobes. Data are presented in Table 6.5.2-1. The final slope fractions (i.e., $\Delta z/\Delta x$) were determined by taking the tangent of the measured slope angles (shown in Table 6.5.2-1).

Field observations indicate that slope values less than or equal to 0.18 (10°) were areas of deposition. Slopes between 0.21 (12°) and 0.34 (19°) were stable, with some gullies in the tephra. Slopes between 0.36 (20°) and 0.47 (25°) were transitional, being stable in some areas but stripped of tephra in others. Areas with slopes greater than or equal to 0.49 (26°) were stripped of tephra. Based on these data, the range for critical slope was taken to be a uniform distribution between 0.21 and 0.47.

Table 6.5.2-1. Critical Slope Measurements from Sunset Crater Area near Flagstaff, AZ

N	E	Geographic Description	Slope Magnitude (degrees)	Observations	Slope Type	Slope Fractions
469821	3898699	Rattlesnake Crater	12	Minor gully	Bedrock	0.21
469821	3898699	Rattlesnake Crater	15	Gullied	Bedrock	0.27
469821	3898699	Rattlesnake Crater	14	Gullied	Bedrock	0.25
469821	3898699	Rattlesnake Crater	17	Gullied	Bedrock	0.31
469821	3898699	Rattlesnake Crater	18	Gullied	Bedrock	0.32
469821	3898699	Rattlesnake Crater	10	Depositional	Alluvial deposit at base of slope	0.18
469821	3898699	Rattlesnake Crater	28	Dry slope processes, tephra ravel, creep	Cinder cone	0.53
465320	3903732	Cochrane Hill	28	Dry slope processes, tephra ravel, creep	Cinder cone	0.53
465320	3903732	Cochrane Hill	28.5	Dry slope processes, tephra ravel, creep	Cinder cone	0.54
465320	3903732	Cochrane Hill	27	Dry slope processes, tephra ravel, creep	Cinder cone	0.51
465824	3903841	Cochrane Hill	26	Dry slope processes, tephra ravel, creep	Cinder cone	0.49
465824	3903841	Cochrane Hill	26	Dry slope processes, tephra ravel, creep	Cinder cone	0.49
464650	3911595	Moon Crater	19	Gullied	Bedrock	0.34
464650	3911595	Moon Crater	19	Gullied	Bedrock	0.34
464650	3911595	Moon Crater	19	Gullied	Bedrock	0.34
464650	3911595	Moon Crater	18	Gullied	Bedrock	0.32
465545	3911494	Moon Crater	20 - 21	Dry slope processes, tephra ravel, creep	Cinder cone	0.37
465545	3911494	Moon Crater	24	Dry slope processes, tephra ravel, creep	Cinder cone	0.45
465545	3911494	Moon Crater	28	Dry slope processes, tephra ravel, creep	Cinder cone	0.53

Table 6.5.2-1. Critical Slope Measurements from Sunset Crater Area near Flagstaff, AZ (Continued)

N	E	Geographic Description	Slope Magnitude (degrees)	Observations	Slope Type	Slope Fractions
465292	3911144	Moon Crater	20	Dry slope processes, tephra ravel, creep	Cinder cone	0.36
465292	3911144	Moon Crater	25	Gullied	Cinder cone	0.47
465292	3911144	Moon Crater	20	Gullied	Cinder cone	0.36
467647	3906916	Cinder cone	30	Dry slope processes, tephra ravel, creep	Cinder cone	0.58

Source: DTN: MO0708SCSOC137.000 [DIRS 182344], Table 1; slope fraction is calculated as the tangent of the slope magnitude.

NOTES: Coordinates are in UTM NAD83, Zone 11 meters.

For a given value of critical slope, a certain percentage of the upper drainage basin domain is subject to tephra transport. Within the range of critical slope values developed above, between about 6% (S = 0.47) and 21% (S = 0.21) of the domain exceeds the critical slope. Figure 6.5.2-1 shows the distribution of slope values within the watershed domain. Figure 6.5.2-2 displays maps showing the location of these areas for the two end-member slope values.

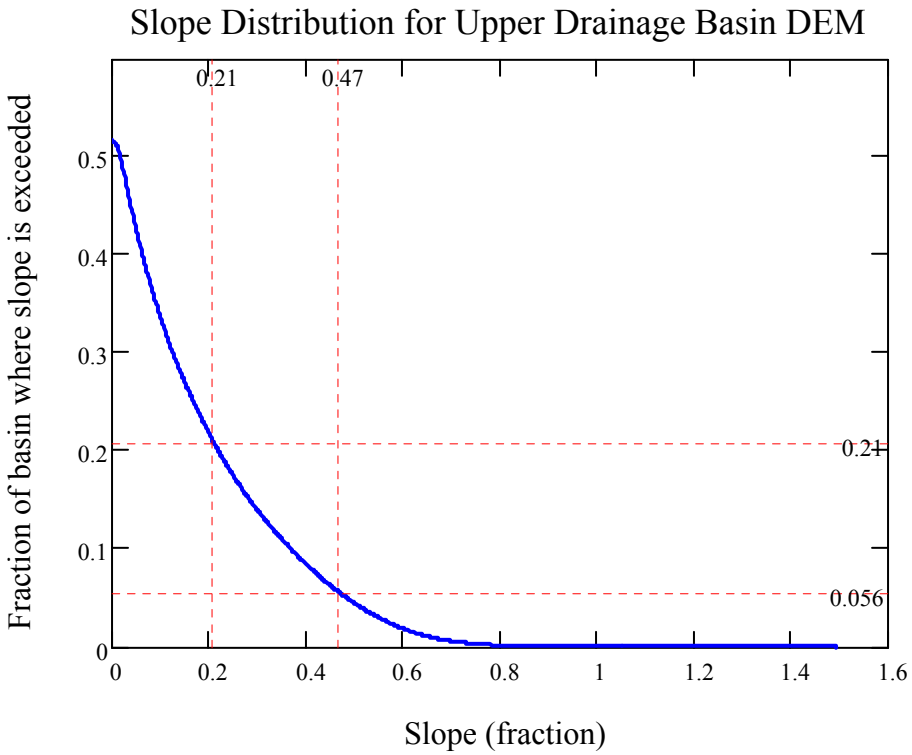

NOTE: Figure was generated from sample model output and is for illustrative purposes only.

Figure 6.5.2-1. Distribution Curve for Grid Cell Slope Values within the Watershed of the Upper Drainage Basin Domain

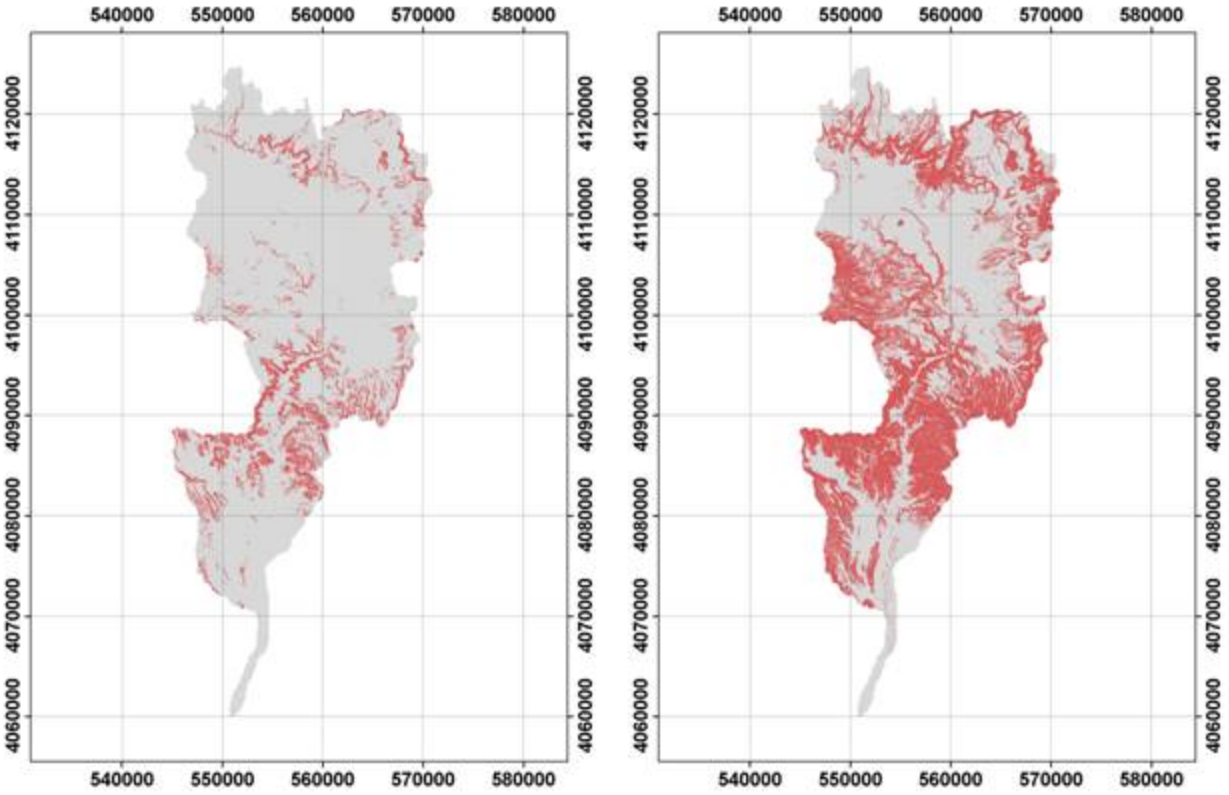

NOTE: From left, the critical slope values are 0.47 and 0.21, respectively. Coordinates are in UTM, NAD 27, Zone 11, meters. Figure was generated from sample model output and is for illustrative purposes only.

Figure 6.5.2-2. Maps Showing Areas (red) Where the Local Slope Exceeds a Critical Slope Value for the Upper Drainage Basin Domain

6.5.3 Drainage Density

The drainage density parameter (X) is used to define the channel system in the Fortymile Wash drainage basin as described in STEP 3 of Section 6.3.3. Drainage density is defined as the total length of channels in a drainage basin divided by the area of the basin and is in units of km^{-1}. Grid cells in the model domain are considered channels if the calculated stream power is greater than a threshold value equal to the inverse of the drainage density. Stream power is defined mathematically in Equation 6.3-7.

Because the drainage density parameter influences the amount of tephra that may be mobilized, it is important to define this parameter in a way that adequately addresses the uncertainty in the extent of channels and their ability to redistribute and transport tephra. To define an appropriate range of drainage density, a series of calibration model simulations using the FAR V.1.2 software were run with identical inputs except for the drainage density parameter value. As drainage density is increased (and stream power threshold is decreased), the predicted channel network begins closer to the watershed divides. To choose an appropriate drainage density range, the ground positions of 34 selected channel heads on the eastern slope of Yucca Mountain were located on digital orthophoto quarter quadrangles (DOQQs)

(DTN: SN0706DIGORTHO.001 [DIRS 182108]; Figures 6.5.3-1 and 6.5.3-2). These positions were then compared with the corresponding locations of these same channel heads predicted by the FAR model for each calibration model simulation. The horizontal distance between each observed and predicted channel head was calculated for each of the calibration model simulations. Table 6.5.3-1 lists these distances for each model simulation and shows the average distance. Figure 6.5.3-3 shows a plot of the average distance for each stream power threshold value that was run. The value of the drainage density that yields the lowest value for the average distance between the observed and predicted channel heads is considered the optimal value for the drainage density input into the tephra redistribution model. This analysis was performed using ArcGIS V.9.2 and is documented in Output DTN: SN0708DRAINDEN.001. The decision to use only channel locations on the eastern slope of Yucca Mountain is reasonable because this drainage sub-area is the closest to the vent location and therefore would have the thickest tephra deposit.

Table 6.5.3-1 shows that the best fit was obtained for the stream power value of 0.04 (drainage density value of $X = 25\ km^{-1}$), but the average distance for the two stream power thresholds bounding this best fit are only slightly larger and therefore represent an appropriate range for this parameter. Because of this, any drainage density value between $20\ km^{-1}$ and $33\ km^{-1}$ is considered to adequately match the observed channel heads. Therefore, a uniform range of values from $20\ km^{-1}$ to $33\ km^{-1}$ should be used by TSPA. There are variations in the best fit value for each of the individual channel heads used in this calibration. For example, channel head 16 is best matched with a stream power threshold value of 0.02. For this analysis, the minimum average distance is considered to be an adequate metric for estimating drainage density for the domain as a whole.

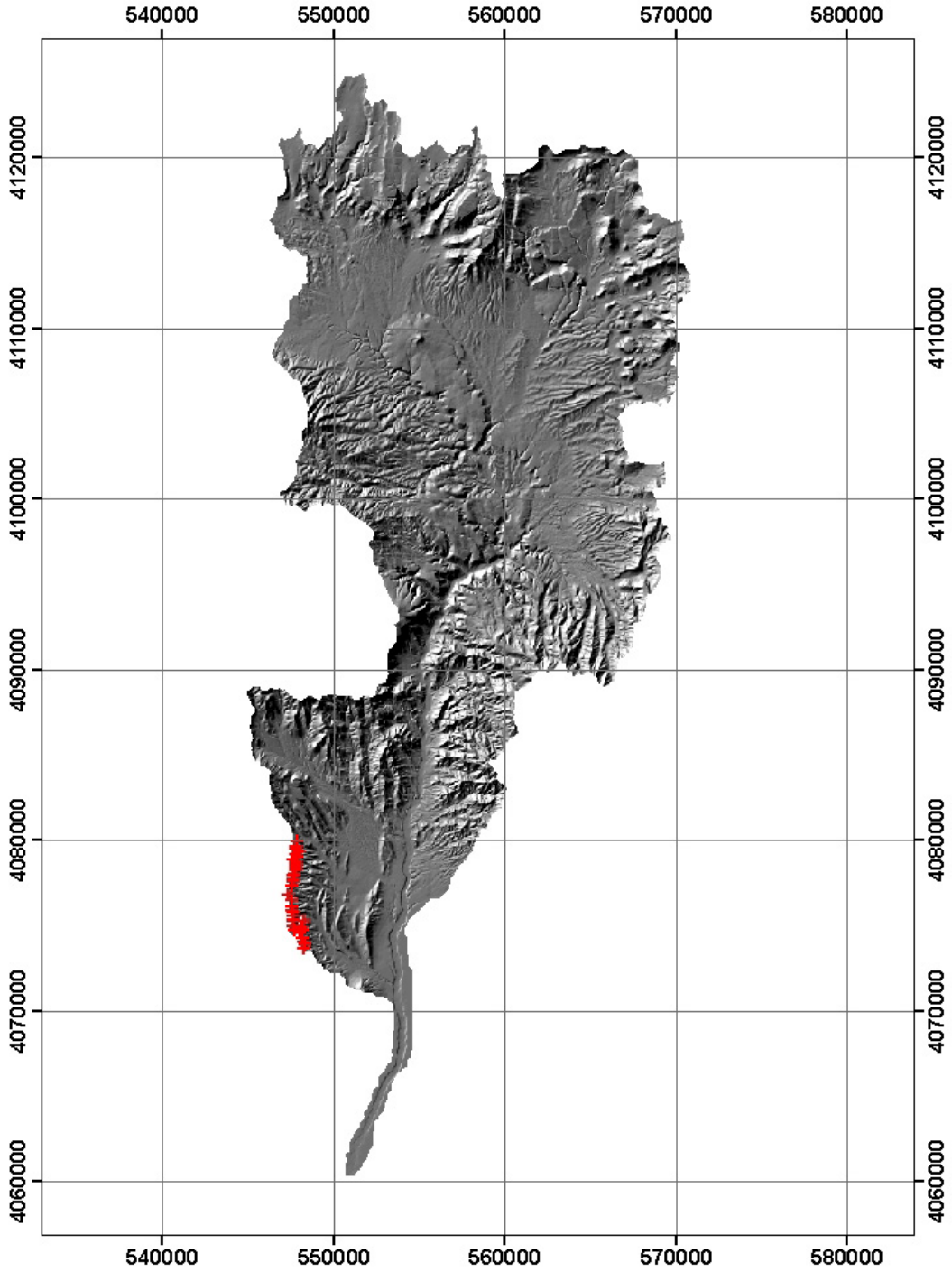

Source: Output DTN: SN0708DRAINDEN.001.

Figure 6.5.3-1. Upper Fortymile Drainage Basin Shaded Relief Map Showing the Location of the 34 Selected Channel Heads near the Top of Yucca Mountain

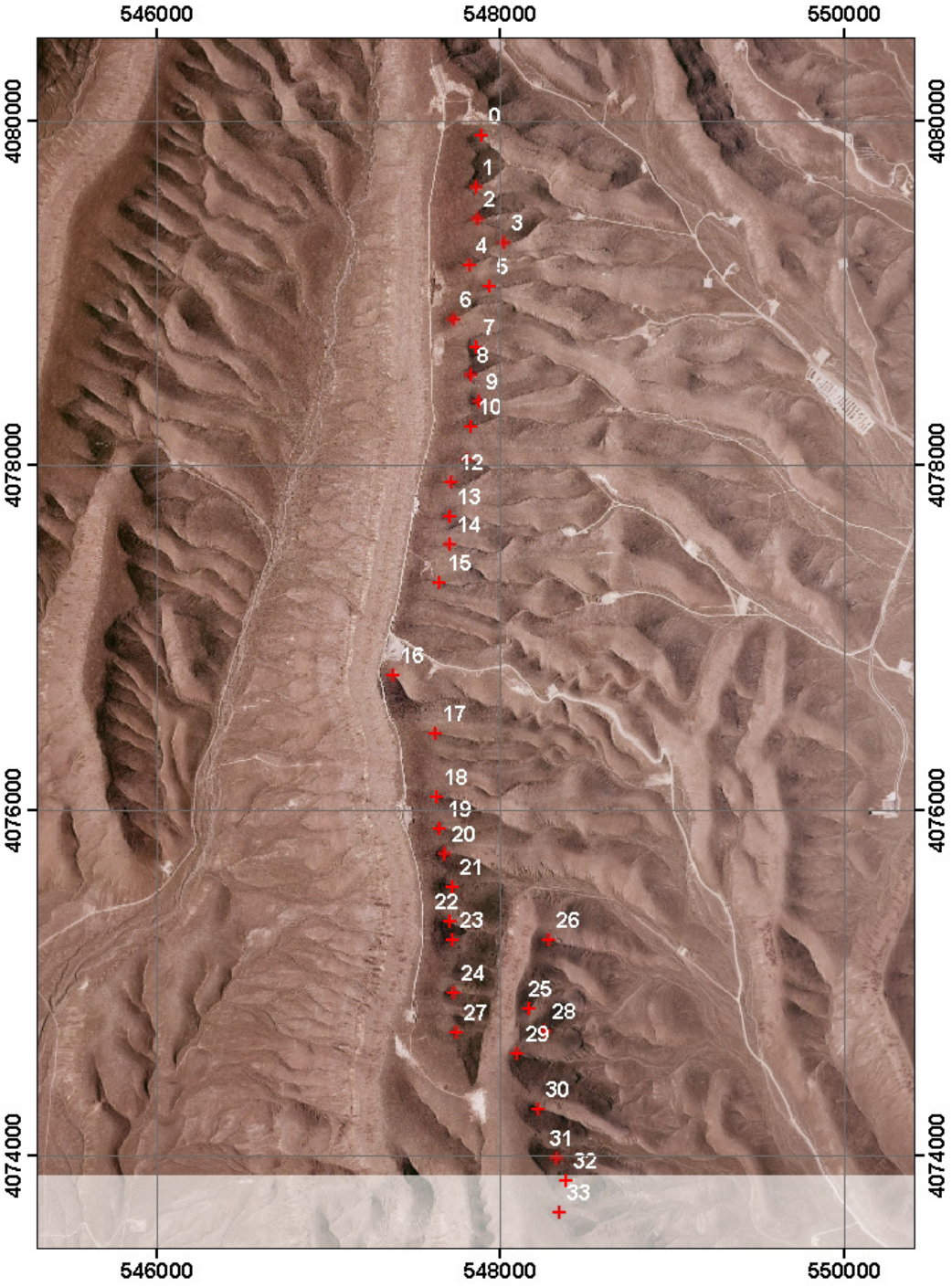

Source Output DTN: SN0708DRAINDEN.001.

Figure 6.5.3-2. Close-up View of the Top of Yucca Mountain Showing the Location of 34 Channel Heads Identified on the DOQQ Imagery

Table 6.5.3-1. Distances between Observed and Predicted Channel Heads for 34 Selected Channels on the East Slope of Yucca Mountain

Stream Power Threshold	0.02	0.03	0.04	0.05	0.06	0.07
Channel Head ID	Distance [m] between Predicted and Observed Channel Head					
0	111	75	60	58	40	40
1	98	68	39	16	16	16
2	75	45	14	50	52	81
3	51	41	70	108	175	259
4	90	32	18	36	65	107
5	54	5	66	156	187	217
6	5	48	116	113	138	182
7	134	104	74	45	17	16
8	66	37	4	60	64	129
9	122	90	29	6	4	214
10	101	66	37	5	57	61
11	74	50	16	18	54	52
12	53	18	16	40	73	107
13	67	35	22	56	59	90
14	66	11	26	122	151	181
15	68	28	60	85	85	118
16	6	42	68	107	174	174
17	22	58	120	146	177	235
18	78	49	21	20	44	139
19	71	9	22	52	147	263
20	76	64	37	15	30	61
21	122	85	48	19	19	11
22	70	67	40	38	44	111
23	92	62	44	15	42	57
24	119	62	34	21	38	68
25	41	19	24	51	91	111
26	88	48	27	31	84	176
27	133	104	74	41	31	46
28	82	62	20	41	73	318
29	59	56	32	57	76	99
30	98	75	38	5	24	63
31	180	151	122	87	95	64
32	116	84	53	22	46	105
33	76	74	44	13	15	57
average	***81***	***57***	***45***	***52***	***73***	***118***

Output DTN: SN0708DRAINDEN.001, file: *ChannelHead_Distance.xls*.

NOTE Average distance values in Output DTN: SN0708DRAINDEN.001 do not include distances from channel head ID 33. This minor error has been corrected in the above table.

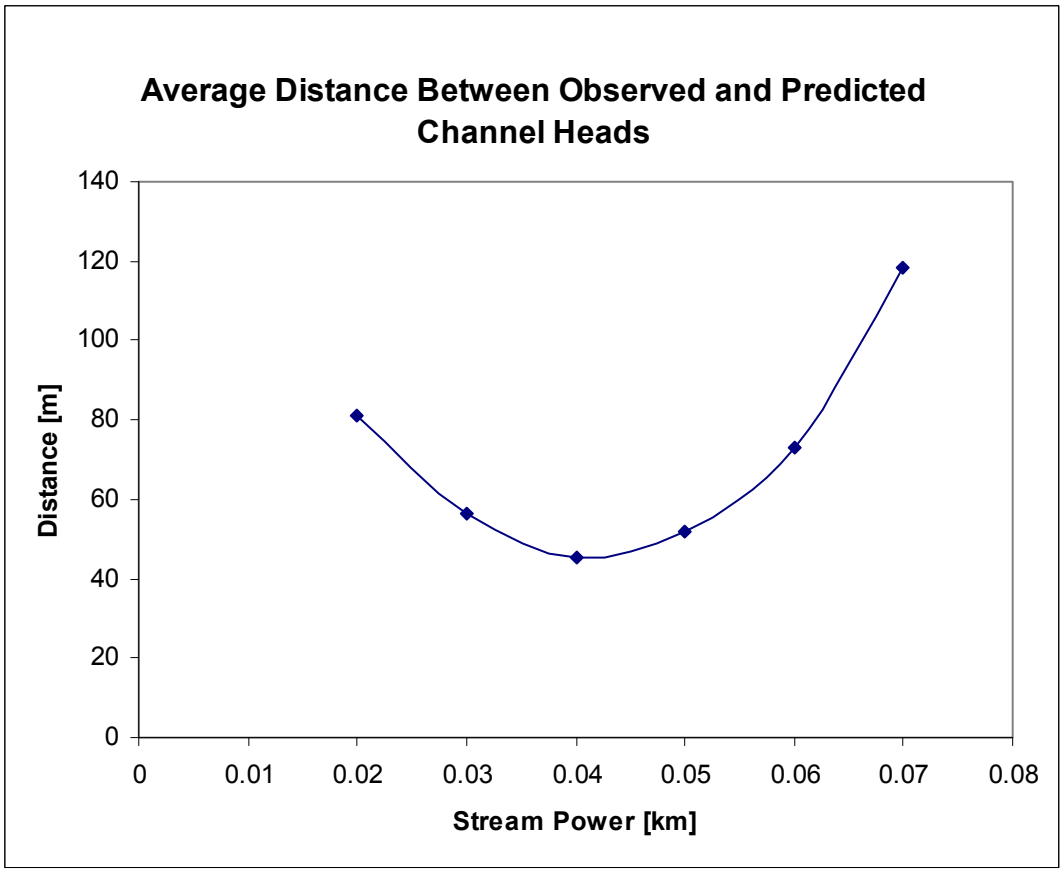

Source: Output DTN: SN0708DRAINDEN.001, file: *ChannelHead_Distance.xls*.

NOTE: Each point represents the FAR model results run with the noted stream power value. Average distance values in Output DTN: SN0708DRAINDEN.001 do not include distances from channel head ID 33. This minor error has been corrected in the figure above.

Figure 6.5.3-3. Plot Showing the Average Distance between Observed and Predicted Channel Heads for Various Values of Stream Power for 34 Selected Channels on the East Slope of Yucca Mountain

6.5.4 Area of Fortymile Wash Alluvial Fan and Channel Fraction Area

The depositional area (km^2) of the upper Fortymile Wash alluvial fan is used to calculate the fraction of the fan area covered by active depositional channels. The fan area (A) and fraction of active channels (F) are required as input to the FAR code. However, neither of these inputs is used directly for the calculation of tephra redistribution in the FAR model. The fraction, F, is used by TSPA in the calculations of dose to the RMEI as described in *Biosphere Model Report* (SNL 2007 [DIRS 177399], Section 6.12.3).

Soil-geomorphic mapping of the alluvial fan surface provides a basis for mapping the area of the alluvial fan and the fraction of the fan area that is active channels for input to the tephra redistribution model. The soil-geomorphic mapping activity used field observations of elevation above active channels, terrace dip, depth of dissection, degree of planarity, drainage pattern (tributary versus distributary), and the development of pavement, varnish, and calcic soils as relative-age indicators (Bull 1991 [DIRS 102040]). It also used digital orthophotos from

DTN: SN0706DIGORTHO.001 [DIRS 182108]. A total of five distinct units were mapped, ranging in ages from the oldest unit, Qa3 (middle-to-late Pleistocene), to the active channels (Qa7) that are recently formed. Holocene and Pleistocene units were readily distinguishable using pavement and varnish development, as is the case elsewhere in Amargosa Valley (Keefer et al. 2004 [DIRS 173899173899]). The degree of planarity was particularly useful for distinguishing between middle-to-late Pleistocene (Qa3) and late Pleistocene (Qa4) units on the Fortymile Wash fan. Drainage patterns were particularly useful for distinguishing between Qa4 (tributary drainage) and late Pleistocene to early Holocene (Qa5) surfaces (distributary drainage). The mapping of the alluvial fan is described in Appendix A and Output DTN: SN0708GEOMOMAP.001.

6.5.4.1 Area of Fortymile Wash, *A*

The depositional area (km^2) of the upper Fortymile Wash alluvial fan represents the area bounded by the large Qa3 (mid- to late-Pleistocene) terraces on either side of the active fan. The steps taken to determine the area, *A*, are documented in Appendix A, Section A4.1. The value of *A* was determined to be 33 km^2.

6.5.4.2 Channel Fraction Area, *F*

The fraction (dimensionless) of the Fortymile Wash alluvial fan area (*A*) is estimated by measuring the fractional area of the current fan that has been active over the past 10,000 years. Since accurate surface age dating is not available on the alluvial fan, an estimate of this areal fraction is bounded by calculating the areal fraction of the fan units deposited during the Holocene. However, the unit Qa5 spans the Pleistocene–Holocene boundary, and therefore including this unit in the areal fraction represents an upper bound on the value of *F*. Excluding Qa5 from the areal fraction represents the lower bound on the value of *F*.

The steps taken to determine this fraction, *F*, are documented in Appendix A, Section A4.1. The value of *F* was determined to range from 0.09 to 0.54.

For model durations significantly greater than 10,000 years, it is possible that the drainage system across the fan could be significantly altered. However, eruptive events may occur at any future time within the TSPA conceptual model, and it is assumed that the fraction of active channels calculated from data within the last 10,000 years will be applicable to any future event.

6.5.5 Permeable Depth on Divides and in Channels

6.5.5.1 Permeable Depth on Divides

Values of the permeable depth of the divides and channels were measured in the RMEI domain (DTN: MO0708SCSOC137.000 [DIRS 182344], Table 2). A total of six soil pits were dug with shovels and picks and each soil horizon was described (Table 4.1-4). The depth to the low permeability, petrocalcic horizon was measured at each soil pit, and a range of depths was recorded. The impermeable depth was assumed to coincide with Stage-IV carbonate development in the soil pit. Stage-IV carbonate provides a natural low permeability barrier in gravelly parent material because it has a platy, continuous laminar cap and carbonate

matrix that cements the gravel. Table 6.5.5-1 summarizes the measured depths to the Stage-IV carbonate layer.

Table 6.5.5-1. Summary of Permeable Depth Data

Station No.	Easting	Northing	Depth of Stage-IV Carbonate Layer (cm)	Unit
93	549257	4054772	>96	Qa4
94	549301	4054754	102 to 130	Qa3
95	550086	4056809	>140	Qa4
96	550353	4056760	102 to 110	Qa3
249	546296	4051066	>110	Qa4
250	544116	4055019	>135	Qa4

Source: Coordinates (UTM NAD83, Zone 11, meters) and depth of Stage-IV carbonate layer: DTN: MO0708SCSOC137.000 [DIRS 182344], Table 2; geomorphology units determined by cross-referencing annotations in the field notes (shown in Table 4.1-6) with the geologic map unit nomenclature table in the readme file for Output DTN: SN0708GEOMOMAP.001.

On the oldest (Qa3) surfaces, Stage-IV carbonate was encountered at a consistent depth. Both stations 94 and 96 show the Stage-IV carbonate layer starting at a depth of 102 cm (Table 6.5.5-1). Data for the Qa4 unit were collected at stations 93, 95, 249, and 250. No Stage-IV carbonate layer was seen in any of these pits. The pits ranged from 96 to 140 cm in depth. As no primary soil carbonate development was encountered at these locations, the maximum permeable depth is likely to be greater than the maximum depth at the sample sites (140 cm). Qa5 is considered to be a part of the inter-channel divide for the minimum area fraction case. Because soil-carbonate development is widely accepted to occur as a function of time, there was not any reason to determine the permeable depth on the Qa5 unit or any younger units because these units would be expected to have permeable depths greater than that determined for Qa4 and no direct measurements of this depth were available. Therefore, a permeable depth equal to that of Qa4 (>140 cm) was used to represent the upper bound on the permeable depth on divides. Based on these data, it was determined that the field data for L_d supported a uniform distribution between 102 and 140 cm.

6.5.5.2 Permeable Depth in Channels

The permeable depth of the channels or terraces younger than 10,000 years were not explicitly measured. Appropriate values of L_c are inferred from the data (Table 6.5.5-1). Soil pits on the Qa4 surface showed minimal carbonate development (Stage II was the maximum observed soil-carbonate development) to a depth of 140 cm. Additionally, USGS scour chain data has been measured to a depth of >120 cm (DTN: SN0711SCOURCHM.002 [DIRS 183849]). These data indicate that the permeable depth is at least 140 cm but could be much larger. While a finite permeable depth was not quantified in the field, it is appropriate to choose some finite value because buried soils could provide low permeability barriers at depths greater than 140 cm. If any low permeability boundaries exist on these surfaces, they are likely to be spatially discontinuous, in the form of buried paleosols. The Fortymile Wash alluvial fan is an aggrading landform, so it is likely that any paleosols exist well beneath a depth of 200 cm and are likely

much deeper. Further evidence that may support this depth is suggested by the incised younger surface. At several locations on the fan, though rare, active channels on historical timescales cut Holocene "active" surfaces by >1 m with no low permeability surfaces outcropping (i.e., station 60, Table 4.1-6). Based on these findings, L_c should be set to a constant value of 200 cm for TSPA.

6.5.6 Scour Depth at the Fortymile Wash Fan Apex

Equation 6.3-14 relates the scour depth throughout the upper drainage basin on a pixel-by-pixel basis to the contributing area of the pixel and the measured scour depth and drainage area of a known point. The Narrows in Fortymile Wash was chosen as this point because it is, as its name implies, the point in the wash having the narrowest flow width. This provides the most accurate flow measurements (as it provides the best defined flow area), and ensures that the scour depths recorded at this point are a function of bank-to-bank flow for large floods. In addition, there are few additional tributaries feeding Fortymile Wash below the Narrows, and therefore the overall contributing area does not increase significantly below this point.

Scour chains are vertically oriented lengths of chain buried in a row across a streambed with a short horizontal section, which lies on the bed at the surface. Their condition/orientation following a runoff event indicates the extent of scour (downward movement) and fill (upward movement) of the streambed during the event (Figure 6.5.6-1).

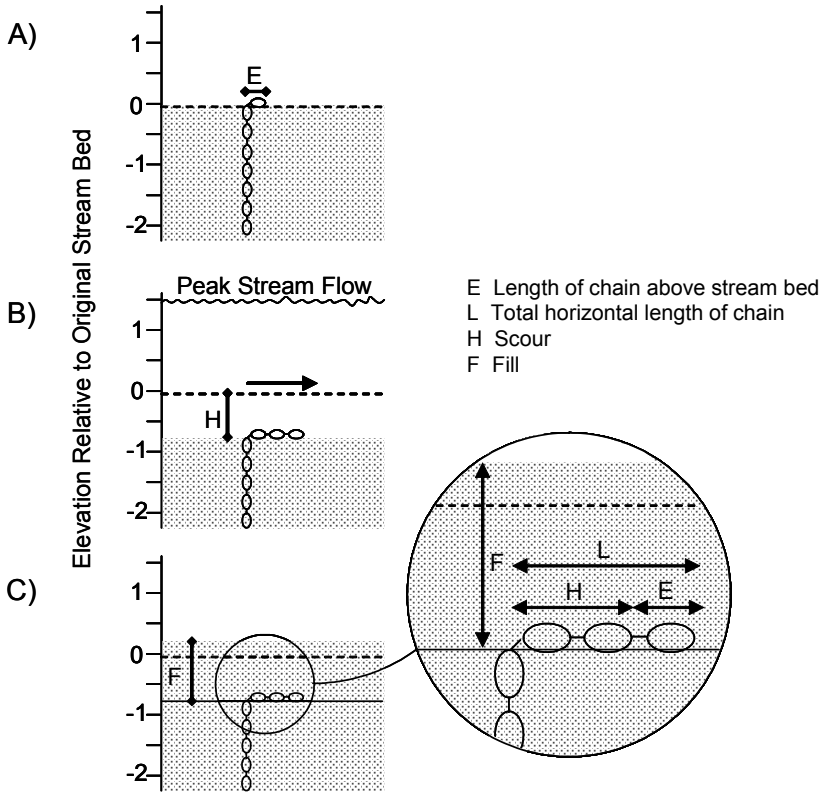

Source: DTN: SN0711SCOURCHM.002 [DIRS 183849].

Figure 6.5.6-1. Scour Measurements a) Pre-flood Emplacement, b) Maximum Scour in the Channel (H), and c) Post-flood Fill Emplacement

Six scour chains were installed in the Narrows of Fortymile Wash on July 11, 1985. Chains were evenly spaced across the channel at the gage station. The horizontal length of chain exposed at the surface was recorded periodically. During the flood of March 11, 1995, the scour chains were completely buried. They were excavated in November of that same year. Measurements of burial depth and horizontal lengths were obtained from four of the six scour chains. One of the chains was inadvertently pulled out by a backhoe during excavation and another chain could not be found and is presumed to have washed away. Measured data are found in DTN: SN0711SCOURCHM.002 [DIRS 183849], and are partially reproduced in Table 6.5.6-1. For the four chains for which measurements were made, scour depth is calculated by subtracting the length of the exposed chain recorded prior to the flood from the measured total horizontal length (from point of deflection) after the flood (Table 6.5.6-1). Chain A (closest to the left bank) had been washed out during the flood, indicating a scour depth close to the overall burial depth of about 5 ft (152 cm) (the chain was about 6.3 ft (192 cm) long; subtracting the pre-flood measurement of 1.27 ft (39 cm) provides an approximate scour depth of about 5 ft (~152 cm)). Chain B was inadvertently pulled out with the backhoe during excavation and therefore it is impossible to calculate scour depth at this location. Chains C, D, E, and F measured scours of 0.96, 1.79, 2.58, and 1.75 ft (29, 55, 79, and 53 cm), respectively. The average scour depth across the channel was 2.4 ft (73 cm). The scour depth used in the tephra redistribution model represents an average or effective scour depth associated with many large floods over hundreds or even thousands of years. While the flood of March 11, 1995, was a significant event, larger floods would be expected on a longer time scale. Such floods would create deeper scour. Thus, the average measured value from the data, 73 cm, was chosen as a lower bound. An upper bound of 152 cm, the maximum scour recorded at the site, was chosen as the upper bound. Maintaining an upper bound consistent with that measured is considered conservative as scour depth and concentration of the radionuclides are inversely proportional to one another (the deeper the scour, the greater the dilution) in the upper drainage basin (see Section 6.6). The range of scour depth is taken to be a uniform distribution between 73 and 152 cm.

The output from this model provided to TSPA (Output DTN: MO0704PASCOURD.000) uses an upper bound of 122 cm instead of 152 cm. This is considered acceptable because it will tend to overestimate concentration in the channels at the RMEI location.

Table 6.5.6-1. Summary of Scour Depth Data

	Chain Designator (chain A being closest to the left bank)					
	(A)	(B)	(C)	(D)	(E)	(F)
Horizontal length (ft) measured 1/28/92 (E in Figure 6.5.6-1)	1.27	1.60	0.68	0.49	1.12	0.85
Horizontal length (ft) measured 11/16/95 (L in Figure 6.5.6-1)	N/A	Pulled out w/ backhoe	1.64	2.28	3.7	2.6
Depth (ft) to chain measured 11/16/95 (F in Figure 6.5.6-1)	N/A	3.0 to 4.0	2.95	2.5	3.6	2.85
Estimated Scour Depth (ft) (H in Figure 6.5.6-1)	~5[a]	N/A	0.96[b]	1.79[b]	2.58[b]	1.75[b]

Source: Measured Data from DTN: SN0711SCOURCHM.002 [DIRS 183849].

[a] Scour depth estimated as original chain length (6.3 ft from DTN: SN0711SCOURCHM.002 [DIRS 183849]) minus the horizontal length prior to flood, 1.27 ft (E in Figure 6.5.6-1). Since chain washed out, this estimate is only approximate.

[b] Scour depth calculated by subtracting the horizontal length of chain measured before the flood (E in Figure 6.5.6-1) from the length of chain deflected during the flood (L in Figure 6.5.6-1). Scour depth for chain (A) is taken as 4 ft (the chain was completely washed away). Scour depth for chain (B) is taken as 3.5 ft (the chain was inadvertently pulled from the soil during excavation – field notes estimate a depth of 3.5 ft).

6.5.7 Volcanic Vent Parameters

6.5.7.1 Vent Location

As part of STEP 1 described in Section 6.3.3, the ASHPLUME waste and tephra concentration grids are resampled using bilinear interpolation so that the resulting grid size is the same as that of the DEM (30 m) and then rectified so that the origin of the ASHPLUME grid (vent location) is coincident with the center of the repository footprint. The center of the repository footprint is considered an appropriate position to assume for the location of the volcanic vent for TSPA calculations. However, in reality, any vent location within the waste emplacement area may intersect waste packages and result in an eruptive release scenario. Thus, both the center of the waste emplacement area and the bounds of this area are developed here.

To perform the rectification step, it is necessary to identify the location (easting and northing) of the vent location (assumed here to be the DEM grid cell that contains the center of the waste emplacement area within the repository footprint). Within the FAR software, these coordinates are converted to row and column indices (*ivent*, *jvent*) referenced to the input DEM file as follows:

$$ivent = [xvent - 542500)] / 30$$

$$jvent = [4126000 - yvent] / 30$$

where *xvent* and *yvent* are the X and Y coordinates of the vent, 542500 m is the minimum easting coordinate of the DEM input file, and 4126000 m is the maximum northing coordinate of the

DEM input file. Coordinates are UTM, Zone 11, NAD-27, meters, unless otherwise noted. These values are hardwired in the FAR software.

The inputs used for this calculation include repository parameter 01-02 referenced in *Total System Performance Assessment Data Input Package for Requirements Analysis for Subsurface* Facilities (SNL 2007 [DIRS 179466]). This drawing includes tables that list the waste package endpoint locations of each of the drifts. The waste package endpoints are slightly different than the drift endpoints.

The center of the waste emplacement area is estimated as the center of the bounding box surrounding the waste emplacement area. This is an approximation that is sufficient for its intended purpose in TSPA. The bounding box is defined by finding the minimum and maximum values of the easting and northing coordinates of the drift endpoints. Table 6.5.7-1 provides these coordinates from the drawing.

Table 6.5.7-1. Bounding Box Corner Coordinates for Waste Emplacement Area (State Plane)

Bounding Box Corner	Drift Name	Drift Side	Coordinate [m]
Min Easting	4-20	West Side	170085
Max Easting	3-4E	East Side	172309
Min Northing	2-27	East Side	231089
Max Northing	3-1W	East Side	236237

Source: SNL 2007 [DIRS 179466].

NOTE: Coordinates are in the Nevada State Plane Coordinate System, Central Zone, NAD 27, meters.

Since the DEM grid is in the UTM, Zone 11, NAD27, meters coordinate system, it is necessary to convert the State Plane coordinates listed in Table 6.5.7-1 to the UTM coordinate system. This was done using qualified ArcGIS 9.2 software. The corner coordinates listed in Table 6.5.7-1 were imported from an Excel file into an ArcMap project using *Tools – Add XY Data*. Note that ArcGIS defaults to units of feet when Nevada State Plane coordinates are selected. The user must manually select meters as the units of the imported coordinates. The coordinates were converted to UTM, Zone 11, NAD27, meters using: Arc Toolbox: *Data Management Tools – Projections and Transformations – Feature – Project*. Next, the UTM coordinates were added to the attribute table using Arc Toolbox: *Data Management Tools – Features – Add XY Coordinates*. The resulting coordinates are shown in Table 6.5.7-2.

Table 6.5.7-2. Bounding Box Coordinates for Waste Emplacement Area (UTM)

Bounding Box Corner	Drift Name	Drift Side	Coordinate [m]
Min Easting	4-20	West Side	547404
Max Easting	3-4E	East Side	549609
Min Northing	2-27	East Side	4076256
Max Northing	3-1W	East Side	4081410

NOTE: Coordinates are in the UTM, Zone 11, NAD27, rounded to the nearest meter.

The center of the bounding box is calculated as the mean of the minimum and maximum easting and northing components from Table 6.5.7-2 rounded to the nearest meter:

Easting coordinate: (547404 + 549609) / 2 = 548507 m
Northing coordinate: (4076256 + 4081410) / 2 = 4078833 m.

Because the FAR software converts this coordinate to (*ivent*, *jvent*), it is necessary to identify the position of the DEM grid cell inside which this position lies. The input DEM file has 1,037 rows and 2,200 columns. The upper left (NE) corner of the DEM grid is at (542500, 4126000) and the lower left (SW) corner of the DEM grid is at (573610, 4060000). The grid cell location of the repository center is:

DEM grid column: (4126000 – 4078833) / 30 = 1,572
DEM grid row: (548507 – 542500) / 30 = 200.

The values of *xvent* and *yvent* that correspond to the approximate center of the waste emplacement area are calculated as:

xvent = 542500 + (200 × 30) = 548500 m
yvent = 4126000 – (1,572 × 30) = 4078840 m.

It is suggested that TSPA use a constant value of 548500 m for *xvent* and a constant value of 4078840 m for *yvent*. It should be noted that a volcanic eruption anywhere within the waste emplacement area can be considered to result in an eruptive release. For this reason, alternative values of *xvent* and *yvent* are acceptable as long as they fall inside the waste emplacement area (SNL 2007 [DIRS 179466]), which is approximated by the bounding box coordinates given in Table 6.5.7-2.

6.5.7.2 Vent Radius

This parameter is used to eliminate the remobilization of the tephra and waste deposited within a distance less than *rvent* (meters) from the vent, since the volcanic cone will remain on the landscape. A value of 200 m is recommended for use in the FAR user's manual. However, for TSPA, it is suggested that *rvent* = 0. Setting this parameter to equal zero maximizes the amount of contaminated tephra that can be mobilized by the model.

6.5.8 Diffusivity of Radionuclides on Divides and in Channels

The FAR tephra redistribution model estimates vertical migration of radionuclides into the soil at the RMEI location using a one-dimensional diffusion model applied separately to the channel and interchannel divide subdomains at the RMEI location. The use of a diffusion model is justified because this model has been shown to match the shape of the concentration profile with depth following the deposition of radioactive material at the surface. However, chemical diffusion is not the dominant transport process; rather it is believed that physical mechanisms such as suspension and redeposition of fine particles by infiltration, and physical mixing of soil particles by freeze-thaw cycles and bioturbation control the radionuclide transport (e.g., Anspaugh et al. 2002 [DIRS 169793]; He and Walling 1997 [DIRS 178707]). For this reason, the diffusivities required to estimate this migration are not chemical diffusion constants.

Because the diffusivities used in this model are calculated from measured ^{137}Cs profiles, they represent the in situ transport rates and need not be adjusted for soil conditions and porosity.

For a large contaminant source, the diffusion process will be planar. The equation for one-dimensional transient diffusion in a semi-infinite medium is described by Fick's Second Law:

$$\frac{\partial C(z,t)}{\partial t} = D\frac{\partial^2 C(z,t)}{\partial z^2}; z \geq 0, \quad t \geq 0 \qquad \text{(Eq. 6.5-1)}$$

where:

C = concentration (g/cm^3)
t = time (yrs)
D = effective diffusivity constant of the contaminant through soil pores (cm^2/yr)
z = distance from the bottom of the source boundary (cm).

If there is no flux at the top boundary, that is $\frac{\partial C(z,t)}{\partial z} = 0$, z = 0, $t \geq 0$, and an initial contaminant fallout mass per unit area $C_0 d_w$ (g/cm^2) input at $z = 0$ at $t = 0$ (where C_0 is the initial concentration (g/cm^3) within a surface layer of thickness d_w (cm)), the solution of Equation 6.5-1 becomes (after Carslaw and Jaeger 1959 [DIRS 100968], Chapter 14, verified in Appendix E):

$$\frac{C(z,t)}{C_0 d_w} = \frac{1}{\sqrt{\pi D t}}\exp(-z^2/4Dt), z \geq 0, t \geq 0 \qquad \text{(Eq. 6.5-2)}$$

Field measurements of radionuclide materials are typically taken as the concentration within a defined depth interval. Because these measurements are bulk rather than point concentrations, Equation 6.5-2 must be integrated before field data can be used to determine the soil diffusivity. Integrating from the surface to a depth z, Equation 6.5-2 becomes:

$$\begin{aligned}\int_0^z \frac{C(\zeta,t)d\zeta}{C_0 d_w} &= \int_0^z \frac{1}{\sqrt{\pi D t}}\exp\left(-\zeta^2/4Dt\right)d\zeta \\ &= \frac{2}{\sqrt{\pi}}\int_0^{z/\sqrt{4Dt}} \exp\left(-y^2\right)dy \\ &= \text{erf}\left(z/\sqrt{4Dt}\right)\end{aligned} \qquad \text{(Eq. 6.5-3)}$$

for $t \geq 0$, where "erf" is the error function and ζ is an integration variable for depth ($y = \zeta/\sqrt{4Dt}$). Because the error function goes to one as its argument goes to infinity, the total mass per unit area is always $C_0 d_w$. Also, initially $C(z,0)$ is zero for $z > 0$. Therefore, the initial condition is satisfied. This is an accurate approximation, even in a soil with a petrocalcic horizon at depth, because radionuclides do not penetrate far into the soil over time scales of several decades (the maximum time scale for anthropogenic radionuclides).

Fieldwork was completed to measure ^{137}Cs with depth at various points in the Fortymile Wash area (DTN: MO0708SCSOC137.000 [DIRS 182344], Table 3). This bomb-pulse radionuclide was first produced approximately 50 years ago with the advent of atmospheric testing of nuclear weapons. In the time since deposition, this radionuclide has migrated vertically in the soil as a result of physical, chemical, and biological processes (e.g., Anspaugh et al. 2002 [DIRS 169793]; He and Walling 1997 [DIRS 178707]). ^{137}Cs is an ideal analogue to track vertical migration of radionuclides into the soil. This is supported by studies following the Chernobyl accident that have shown that vertical profiles of ^{137}Cs are nearly identical to profiles of several other radionuclides near the accident site (Anspaugh et al. 2002 [DIRS 169793], p. 677). Soil samples of 100 to 250 g were collected over a nominally 3 cm interval at increasing depths. Stable geomorphic surfaces (surfaces not connected to the hillslope), were selected on the upper Fortymile Wash alluvial fan. These data were used, with Equation 6.5-3, to determine the diffusivity of the soil at the sample location. The locations where the profiles were measured were cross-referenced with the soil-geomorphic map (Appendix A) to identify those points inside the RMEI domain boundary. Only those data inside the domain boundary were used in the calculations. Also excluded were scoping data (data whose sample ID includes either 050702 or 050902) and surface samples.

6.5.8.1 Diffusivity of Radionuclides on Divides

The diffusivity of radionuclides on the interchannel divides (D_d) of the RMEI location were calculated using measured ^{137}Cs profiles (DTN: MO0708SCSOC137.000 [DIRS 182344], Table 3) on interchannel divides of the upper Fortymile Wash alluvial fan. Data from terraces older than 10,000 years (units Qa3, Qa4, and Qa5) were used, as these locations correspond to interchannel divides for the minimum channel fraction case.

The radionuclide diffusivity was determined by first computing the fraction of total activity at 3 cm by dividing the activity from 0 to 3 cm by the total activity from 0 to 6 cm. Equation 6.5-3 was then used to calculate the value of the error function argument, equal to $z/\sqrt{4Dt}$, corresponding to the fraction of activity at 3 cm after 50 years of diffusion (based on the time elapsed since nuclear testing). Analyses were performed in an Excel workbook, using the error function (*erf*) and the Excel *solver* tool (Output DTN: SN0708DIFFRNGS.001, file: *radionuclide diffusion Fortymile Wash.xls*). Results are shown in Table 6.5.8-1. It is noted that some of the bulk activity values for the 3- to 6-cm interval were reported despite being less than the minimum detectable limit (see footnote c for Table 4.1-5). It is acceptable to use these small values because the measurement error is included in the determination of the final range. The base values of D_d varied from 0.004 to 0.064 cm^2/yr. Considering the full range of errors associated with the measurements, the range increases to 0.001 to 0.095 cm^2/yr. Therefore, a uniform distribution from 0.001 to 0.095 cm^2/yr was used in the tephra redistribution model.

Table 6.5.8-1. Calculated Values for D_d

Sample ID	Bulk Activity for 0 to 3 cm Depth		Bulk Activity for 3 to 6 cm Depth		Total Activity (pCi/g)	Fraction of Total Activity to Depth of 3 cm	Calculated Diffusivity, D (cm^2/yr)
	pCi/g	Error	pCi/g	Error			
Cs-071702-C	0.209	0.036	0.049	0.012	0.210 to 0.306	0.739 to 0.869	0.040 to 0.071
Cs-071702-E	0.159	0.030	0.049	0.015	0.163 to 0.253	0.668 to 0.848	0.044 to 0.095
Cs-071702-G	0.118	0.025	0.000	0.010	0.093 to 0.153	0.903 to 1.000	0.004 to 0.033
Cs-071802-I	0.374	0.065	0.015	0.014	0.310 to 0.468	0.914 to 0.998	0.010 to 0.030
Cs-071802-K	0.325	0.055	0.015	0.008	0.278 to 0.403	0.923 to 0.981	0.016 to 0.029
Cs-071802-N	0.198	0.037	0.020	0.012	0.169 to 0.267	0.834 to 0.967	0.020 to 0.047
Cs-071802-P	0.231	0.040	0.014	0.013	0.192 to 0.298	0.876 to 0.996	0.011 to 0.038
Cs-071802-Q	0.204	0.037	0.001	0.012	0.167 to 0.254	0.928 to 1.000	0.001 to 0.028
Cs-071802-R	0.227	0.042	0.010	0.012	0.185 to 0.291	0.894 to 1.000	0.001 to 0.035
Cs-071802-S	0.251	0.043	0.034	0.010	0.232 to 0.338	0.825 to 0.925	0.028 to 0.049
Cs-071802-BB	0.255	0.045	0.066	0.015	0.261 to 0.381	0.722 to 0.855	0.042 to 0.077

Source: Geomorphology unit from DTN: MO0708SCSOC137.000 [DIRS 182344], Table 3 (provided in Table 4.1-5). Bulk activity taken from DTN: LA0302CH831811.002 [DIRS 162863] (presented in Table 4.1-5). Calculations can be found in Output DTN: SN0708DIFFRNGS.001.

6.5.8.2 Diffusivity of Radionuclides in Channels

The diffusivity of radionuclides in the channels (D_c) of the RMEI location were calculated using measured ^{137}Cs profiles on channels and young terraces of the upper Fortymile Wash alluvial fan. Data identified as active channels (units Qa7 and Qa6) were used.

The radionuclide diffusivity was determined by first computing the fraction of total activity at 3 cm by dividing the activity from 0 to 3 cm by the total activity from 0 to 6 cm. Equation 6.5-3 was then used to calculate the value of the error function argument, equal to $z/\sqrt{4Dt}$, corresponding to the fraction of activity at 3 cm after 50 years of diffusion (based on the time elapsed since nuclear testing). Analyses were performed in an Excel workbook, using the *erf* function and the *solver* tool. Results are shown in Table 6.5.8-2. Base values for D_c range from 0.048 to 0.166 cm^2/yr. Considering the full range of errors associated with the measurements, the range increases to 0.035 to 0.266 cm^2/yr. Therefore, a uniform distribution from 0.035 to 0.266 cm^2/yr was used in the tephra redistribution model for D_c.

Table 6.5.8-2. Calculated Values for D_C

Sample ID	Bulk Activity for 0 to 3 cm Depth		Bulk Activity for 3 to 6 cm Depth		Total Activity (PCi/g)	Fraction of Total Activity to Depth of 3 cm	Calculated Diffusivity, D (cm^2/yr)
	PCi/g	Error	PCi/g	Error			
Cs-071702-A	0.259	0.045	0.054	0.016	0.252 to 0.374	0.754 to 0.889	0.035 to 0.067
Cs-071702-B	0.146	0.030	0.125	0.023	0.218 to 0.324	0.439 to 0.633	0.111 to 0.266
Cs-071802-J	0.099	0.022	0.056	0.025	0.108 to 0.202	0.487 to 0.796	0.056 to 0.210

Source: Geomorphology unit from DTN: MO0708SCSOC137.000 [DIRS 182344], Table 3 (provided in Table 4.1-5). Bulk activity taken from DTN: LA0302CH831811.002 [DIRS 162863] (presented in Table 4.1-5). Calculations can be found in Output DTN: SN0708DIFFRNGS.001.

6.5.9 Miscellaneous Input Parameters

6.5.9.1 The Output Time Step (Δt)

This parameter is the time interval for which FAR V.1.2 will provide concentrations in the output time series. The nominal value is 100 years, but any value may be used. The only restriction is that the ratio of the model duration T to the time step Δt cannot exceed 10,000.

6.5.9.2 Model Duration (T)

This parameter is the length of time for which FAR V.1.2 will provide concentrations in the output time series. The nominal value is 10,000 years, but any value may be used.

6.5.9.3 *oflag*

This variable is a toggle flag, used to determine whether spatial grids (elevation, slope, contributing area, and pre-processed tephra and waste grids) should be output. This flag can be set to 1 (send grids to output file) for detailed analysis of spatial results and/or testing, or 0 (grids not saved to output file) for use within TSPA (dimensionless).

6.5.10 Summary of Model Parameter Values for TSPA

Table 6.5.10-1 summarizes the FAR V.1.2 model input parameters developed in this model report. Table 6.4-1 lists model inputs developed in this and other model reports.

Table 6.5.10-1. Summary of Developed Parameter Values for the TSPA Tephra Redistribution Model

Parameter	Type	Units	Distribution	Values
criticalslope (S)	float	dimensionless	Uniform	[0.21 to 0.47]
drainagedensityupperbasin (X)	float	km^{-1}	Uniform	[20 to 33]
Scourdepthoutlet (H)	float	cm	Uniform	[73 to 122]
RMElarea (A)	float	km^2	Constant	33
Fractionchannel (F)	float	dimensionless	Uniform	0.09 to 0.54
Ldivide (L_d)	float	cm	Uniform	102 to 140
Lchannel (L_c)	float	cm	Constant	200
Ddivide (D_d)	float	cm^2/yr	Uniform	0.001 to 0.095
Dchannel (D_c)	float	cm^2/yr	Uniform	0.035 to 0.266
rvent	float	m	Constant	0
xvent	float	m	Constant	548500
yvent	float	m	Constant	4078840
oflag	integer	dimensionless	Constant	0

Source: Output DTNs: MO0702PAFARDAT.001, MO0704PASCOURD.000.

6.6 PARAMETER SENSITIVITY ANALYSIS

A sensitivity analysis examines how uncertainty in input parameters affects the uncertainty in model results. In addition, a sensitivity analysis can identify which input parameters have the greatest influence on model predictions, so that characterization efforts and studies can be focused to reduce the uncertainty in those parameters, and thus most efficiently reduce uncertainty in the model outputs.

In risk analysis, uncertainty is generally separated into two categories depending upon the source of the uncertainty. Epistemic uncertainty stems from a lack of knowledge about the system being considered. This type of uncertainty is characterized by assigning probability distributions to parameters that describe the properties of the system. Epistemic uncertainty can usually be reduced with more studies, experiments, and observations of the system. This uncertainty is also sometimes referred to as reducible or state-of-knowledge uncertainty. A second type of uncertainty is aleatory uncertainty, which refers to inherent and irreducible randomness, such as the uncertainty in weather and how much it will rain in the future. The distinguishing characteristic of aleatory uncertainty is that it is a property of the system and cannot be reduced by further study.

In the current analysis, any uncertainty associated with parameters describing the physical properties of the drainage system is considered to be epistemic uncertainty. Aleatory uncertainty is considered in TSPA in the timing and sequence of various event scenarios, such as volcanic eruptions and intrusions, seismic events, etc., which are combined along with their probability of occurrence to calculate dose as a function of time.

The sensitivity analysis here was structured in a way that acknowledges that certain parameters only affect certain parts of the model. For instance, the diffusivity (D_d and D_c) and permeable depth parameters (L_d and L_c) have no affect on the tephra redistribution from the upper drainage basin via hillslope and fluvial processes. Therefore, the sensitivity analysis of these parameters

was done separately from the analysis on the parameters affecting the processes in the upper drainage basin.

6.6.1 Parameter Sensitivity for the Hillslope and Fluvial Redistribution of Tephra in the Upper Drainage Basin

The uncertain parameters that affect the transport and dilution of waste from the upper drainage basin include the critical slope, scour depth at the fan apex, and the drainage density. To evaluate the relative sensitivity of model results to variations in these parameters, a Latin Hypercube Sample (LHS) was generated of 100 realizations that varied these three parameters. The FAR V.1.2 software was run using a single eruption scenario that remained constant for each realization. The model result used to test the parameter sensitivity was the initial waste concentration in the channels at the RMEI location (Equation 6.3-19). A stepwise regression analysis was performed with the qualified software MVIEW V.4.0. The model result was relatively insensitive to any of the parameters, varying by only a factor of 2.5 (from 8.82×10^{-9} g/cm^3 to 2.21×10^{-8} g/cm^3 with a mean of 1.43×10^{-8} g/cm^3). The results of the stepwise analysis indicate that the critical slope parameter (S) is the most important parameter, accounting for 47% of the variance in the results (standardized rank regression coefficient (SRRC) = −0.66). The next most influential parameter is the scour depth at the fan apex (*scourdepthoutlet* or H), accounting for an additional 39% of the variance in the results (SRRC = −0.59). The least influential parameter is the drainage density (X), accounting for an additional 10% of the variance (SRRC = 0.32). Together these parameters account for 96% of the variance in the model results. Figures 6.6.1-1 to 6.6.1-3 display scatter plots showing the model result plotted against each input parameter.

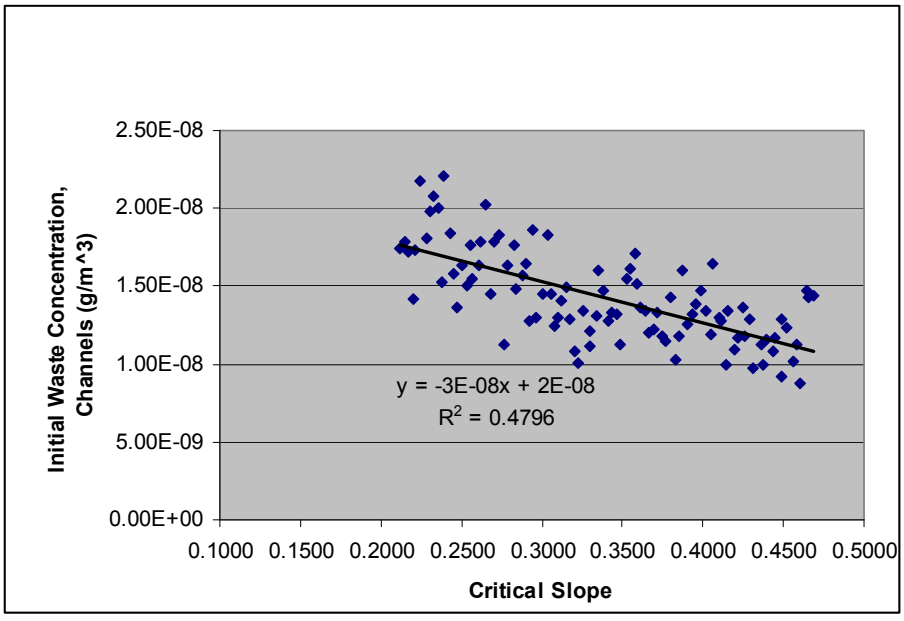

Source: Output DTN: SN0708FARSENSS.001.

Figure 6.6.1-1. Plot of 100 Realization LHS Results against Critical Slope Value

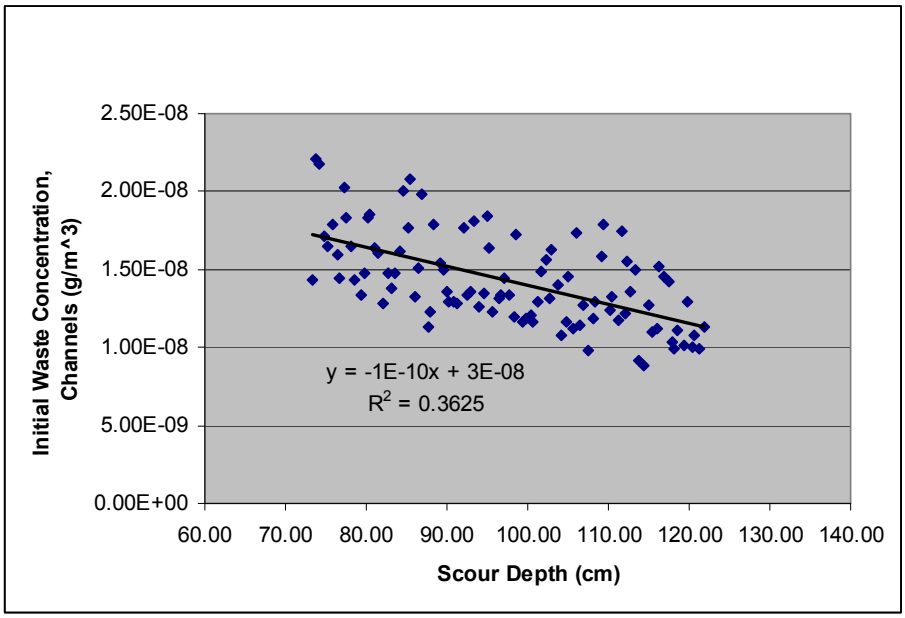

Source: Output DTN: SN0708FARSENSS.001.

Figure 6.6.1-2. Plot of 100 Realization LHS Results against Scour Depth Value

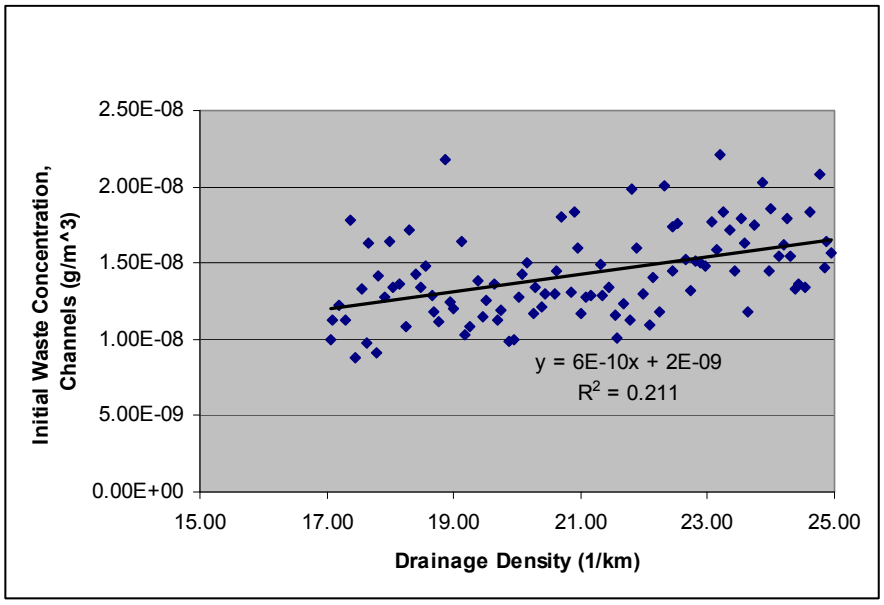

Source: Output DTN: SN07087FARSENSS.001.

Figure 6.6.1-3. Plot of 100 Realization LHS Results against Drainage Density Value

6.6.2 Parameter Sensitivity for the Diffusion of Radionuclides at the RMEI Location

The uncertain parameters that affect the diffusion of radionuclides into the soil at the RMEI location include the diffusivity (D_d and D_c) and permeable depth (L_d and L_c) parameters. The model results examined include the time-dependent surface concentration on divides and in channels and the integrated waste from the land surface to the biosphere depth B. A total of nine

FAR V.1.2 simulations were run. Table 6.6.2-1 lists the applicable parameter values for each of these runs.

Table 6.6.2-1. Diffusion Sensitivity Analysis FAR V.1.2 Simulations

Model File	D_d (cm^2/yr)	D_c (cm^2/yr)	L_d (cm)
D1_FAR.gsm	0.00100	0.03500	121.0
D2_FAR.gsm	0.02450	0.09275	121.0
D3_FAR.gsm	0.04800	0.15050	121.0
D4_FAR.gsm	0.07150	0.20825	121.0
D5_FAR.gsm	0.09500	0.26600	121.0
Ld1_FAR.gsm	0.04800	0.15050	102.0
Ld2_FAR.gsm	0.04800	0.15050	111.5
Ld4_FAR.gsm	0.04800	0.15050	130.5
Ld5_FAR.gsm	0.04800	0.15050	140.0

Source: Output DTN: SN0708FARSENSS.001.

The sensitivity of the results to each of the input parameters is illustrated graphically in Figures 6.6.2-1 to 6.6.2-6. From an examination of these figures, it is clear that the greater the diffusivity value the quicker the initial waste concentration declines to an equilibrium value. The sensitivity to permeable depth is not apparent until later times (~60,000 years), when larger permeable depths result in slightly lower final concentrations.

Because the diffusion process is fastest during the first 20,000 years, radionuclide concentrations are more sensitive to the diffusivity parameter than to the permeable depth parameter.

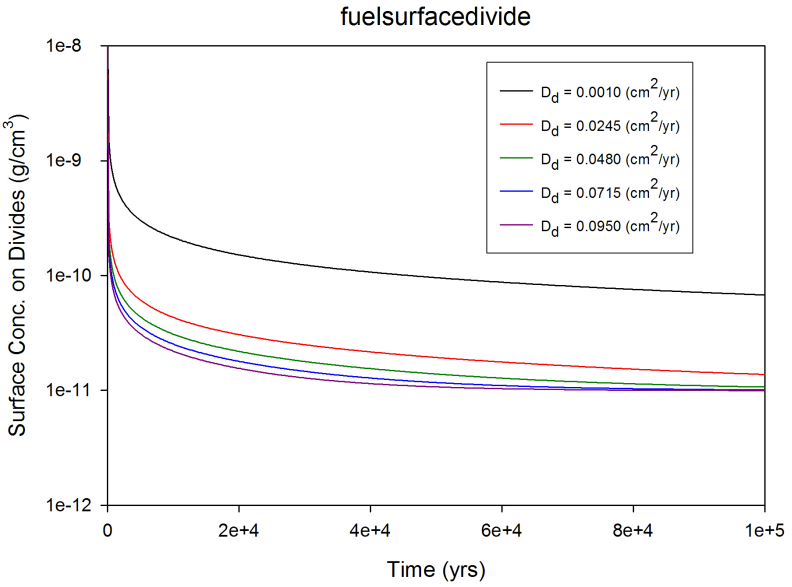

Source: Output DTN: SN0708FARSENSS.001.

Figure 6.6.2-1. Surface Concentration on Divides versus Time for Various Values of D_d

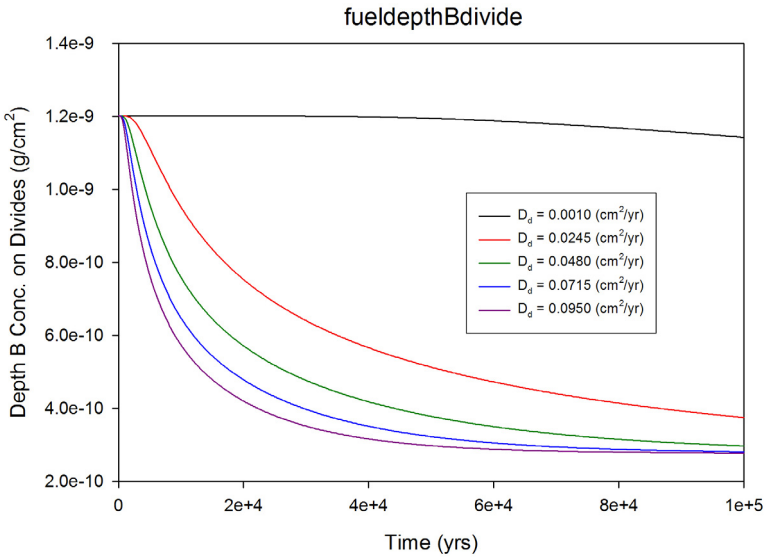

Source: Output DTN: SN0708FARSENSS.001.

Figure 6.6.2-2. Integrated Waste to the B Depth on Divides versus Time for Various Values of D_d

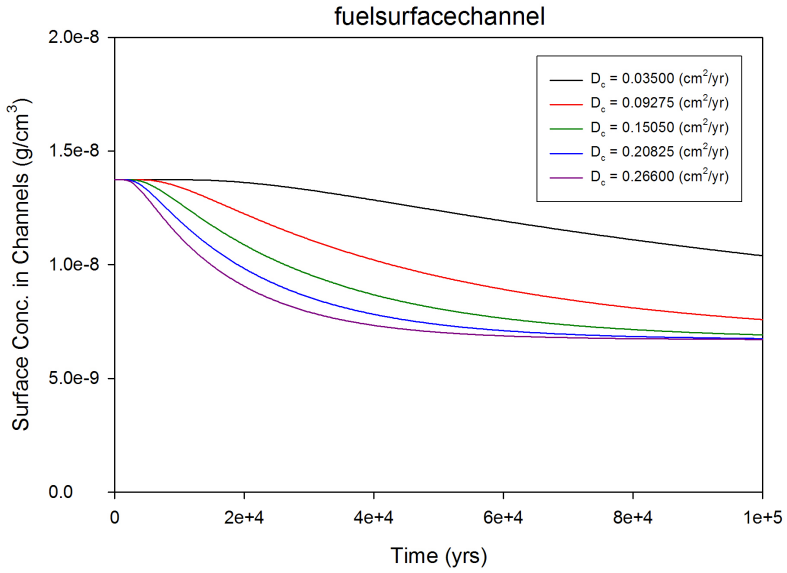

Source: Output DTN: SN0708FARSENSS.001.

Figure 6.6.2-3. Surface Concentration in Channels versus Time for Various Values of D_c

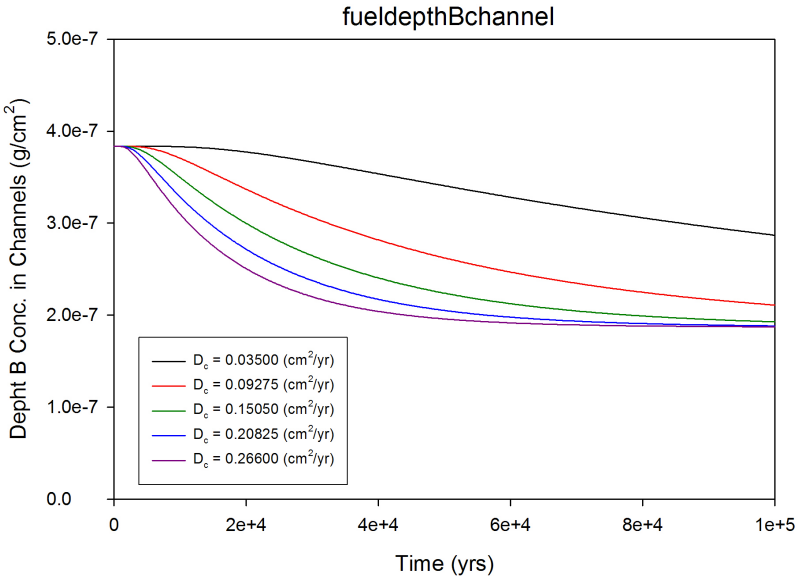

Source: Output DTN: SN0708FARSENSS.001.

Figure 6.6.2-4. Integrated Waste to the B Depth in Channels versus Time for Various Values of D_c

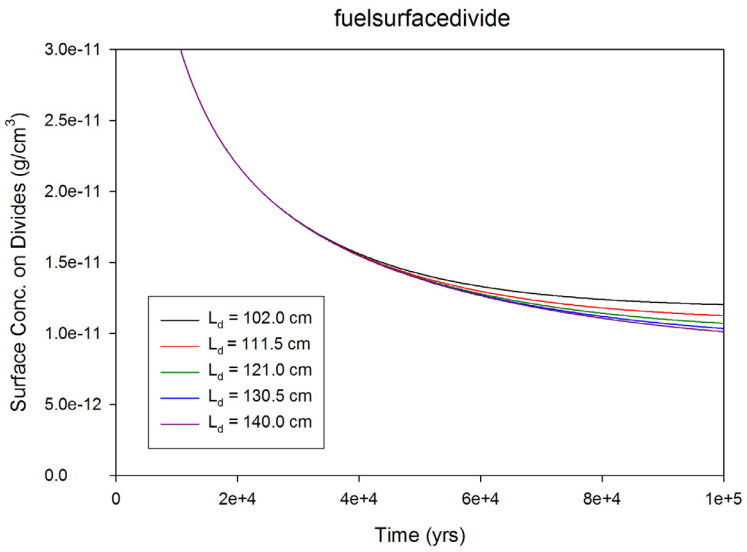

Source: Output DTN: SN0708FARSENSS.001

Figure 6.6.2-5. Surface Concentration on Divides versus Time for Various Values of L_d

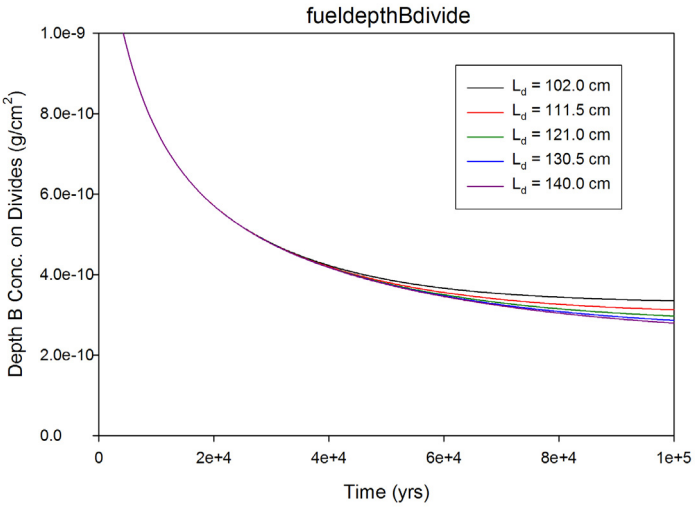

Source: Output DTN: SN0708FARSENSS.001.

Figure 6.6.2-6. Integrated Waste to the B Depth on Divides versus Time for Various values of L_d

6.6.3 Sensitivity Analysis Conclusions

In summary, the analysis presented in Section 6.6.1 determined that the variance in the initial waste concentration in the channels at the RMEI location was most sensitive to the value of the critical slope (*S*) (accounting for 47% of the variance in the results) and scour depth at the fan apex (*H*) (accounting for an additional 39% of the variance in the results). The drainage density (*X*) was the least sensitive parameter (accounting for only an additional 10% of the variance in the results). The analysis in Section 6.6.2 identified the general parameter sensitivity to the time-dependent diffusion process that is represented in the RMEI location. The results from these two analyses provide confidence that the model is functioning as expected (see Section 7.2.9).

7. MODEL VALIDATION

The level of confidence required for the tephra redistribution model has been determined to be Level II in accordance with the TWP (SNL 2007 [DIRS 182219], Table 2-3) and SCI-PRO-002, Attachment 3. Requirements of a Level II validation dictate that both confidence building during model development and post-model development validation activities are discussed. In addition, Level II validation requires that model predictions are reasonably corroborated by at least two post-model development model validations methods described in Step 6.3.2 of SCI-PRO-006. Section 7.1 discusses validation of model input. Section 7.2 discusses activities supporting validation during model development, including validation of sub-models using published data from other sites. Section 7.3 provides a discussion of the application of the two post-model development validation methods used: (1) corroboration of model results with relevant information published in refereed journals and (2) critical review conducted by a technical specialist. Appendix C provides copies of the memos written by two critical reviewers for model validation. Section 7.3.2 discusses relevant author responses to issues raised by the critical reviewers for model validation in Appendix C.

7.1 VALIDATION OF INPUT

Each input parameter was evaluated for its overall adequacy for the model. Reasonable ranges of values were determined based on available measured data and/or information in the literature.

7.1.1 Grids of Tephra Thickness and Waste Concentration

The ASHPLUME model (SNL 2007 [DIRS 177431]) provides the input grid of tephra concentration and waste concentration for each eruption simulated with the FAR tephra redistribution model. These data feeds are justified within the ASHPLUME model report (SNL 2007 [DIRS 177431]) and are justified for their intended use in that report. The FAR tephra redistribution model performs a bilinear interpolation on the output of ASHPLUME to estimate the extent, thickness, and concentration of the tephra and waste at 30×30-m scale (Section 6.3.3, STEP 1).

7.1.2 DEMs and DOQQs

While an aerial photograph and an orthophoto or orthoimage may look alike, there are several important differences. A conventional perspective aerial photograph contains image distortions caused by the tilting of the camera and terrain relief (topography). It does not have a uniform scale and thus cannot be used to measure distances. A digital orthophoto quarter quadrangle (DOQQ) is a computer-generated image of an aerial photograph in which the image displacement caused by terrain relief and camera tilt has been removed, giving it a uniform scale. Since an orthophoto has a uniform scale, it is possible to measure distance directly on it like other maps. An orthophoto may serve as a base map onto which other map information may be overlaid, and thus the usage of such images is appropriate in this model. The DOQQs used in this work (DTN: SN0706DIGORTHO.001 [DIRS 182108]) have a 1-m ground resolution that is more than adequate for the 30-m grid resolution of the model.

A digital elevation model (DEM) is a digital file consisting of terrain elevations for ground positions at regularly spaced horizontal intervals. The USGS produces five different digital elevation products. Although all are identical in the manner the data are structured, each varies in sampling interval, geographic reference system, areas of coverage, and accuracy, with the primary differing characteristic being the spacing, or sampling interval, of the data. For the model, a National Elevation Dataset DEM having 30 × 30-m grid spacing was used (Output DTN: MO0605SPAFORTY.000). The ability of grid resolution to adequately resolve hillslope morphology is site specific. In very rugged terrain characterized by high drainage density, individual pixels can be larger than the typical hillslope area above channel heads. In such cases, pixels in the DEM will combine both hillslope and channel components, leading to an underestimation of slope values on hillslopes (because channels have lower slope values). Given the drainage density in the Fortymile Wash drainage basin, a typical hillslope contains approximately 30 pixels above each channel head. As such, hillslopes are well resolved in the 30 m/pixel DEM. Therefore this DEM resolution is sufficient to resolve important features such as channels and divides within the upper drainage basin domain.

Over the years, the USGS has collected digital elevation data using a number of production strategies including manual profiling from photogrammetric stereomodels; stereomodel digitizing of contours; digitizing topographic map contour plates; converting hypsographic and hydrographic tagged vector files; and performing autocorrelation via automated photogrammetric systems. Of these techniques, the derivation of DEMs from vector hypsographic and hydrographic data produces the most accurate model and was used on the source DEM for this model (DTN: SN0707DEMSOURC.001 [DIRS 182111]). DEMs are commonly used in the generation of three-dimensional graphics displaying terrain slope, aspect (direction of slope), and terrain profiles between selected points, and thus are adequate for their usage in this model. Elevation errors are typically less than about 3 m on average (Smith and Sandwell 2003 [DIRS 177358]).

7.1.3 Field Data

***Area of Alluvial Fan and Fraction of Active Channels*:** To create a map of surface depositional units across the Fortymile Wash alluvial fan (RMEI location), geomorphic field observations were made (DTN: MO0708SCSOC137.000 [DIRS 182344], Table 4). These data were collected incrementally with preliminary mapping of data performed between field trips, which were used to guide where additional data should be collected. The primary goal of the mapping was to provide information for two model input parameters:

1. Area of the Fortymile Wash alluvial fan representing the RMEI environment (A).

2. Fraction of that area subject to active fluvial deposition (F), assumed to be equal to the fraction of the fan area active within the last 10,000 years.

Both of these input parameters require that the area of the soil units comprising the RMEI domain be known. More specifically, they require that both the total area, as well as the areas of soil units older than approximately 10,000 years (units deposited before the Holocene), be known. Units Qa3 and Qa4 were deposited during the Pleistocene (prior to the Holocene). Unit Qa5 spans the Pleistocene-Holocene boundary, so it is used to bound the area calculations (lower

bound not including the unit, and an upper bound with the unit included). Units Qa6 and Qa7 were deposited most recently. Mapping results (Appendix A and Pelletier et al. 2005 [DIRS 175800]) showed that a large fraction of the alluvial fan was comprised of the oldest units. Almost 46% of the total area was made up of Qa3 and Qa4 units. The youngest units, Qa6 and Qa7, accounted for only a small fraction of the total area (just under 9%). The Qa5 unit was the single largest unit, making up 45% of the total area (Table A-3). Thus, calculating *F* as a range that encompasses the Qa5 unit expands the parameter range by a factor of 6, from 0.09 to 0.54. While *F* is not used directly in the FAR tephra redistribution model, it is used by TSPA to determine the overall dosage to the RMEI. The FAR model computes time-dependent waste concentration profiles in two RMEI subdomains: in the channels and on the divides. These profiles are different because the source concentration, thickness, and diffusivities vary between the two surfaces. The overall dose to the RMEI is then a function of the measured profiles in each of these domains and the relative amount of exposure the RMEI has to each of these domains, which is determined by the biosphere model (SNL 2007 [DIRS 177399]). The impact of *F* on the calculated dose depends on a number of factors, including biosphere parameters (such as biosphere depth) and assumptions (such as the length of time an individual would be exposed to the channels versus the divides). An absolute trend between *F* and the calculated dose is not clear. A broad range of *F*, as described above, ensures that the overall dose calculated in the RMEI location encompasses all reasonable scenarios. For example, the large uncertainty in *F* implicitly accounts for uncertainty introduced by the decision not to explicitly model eolian redistribution from channels (see Section 5.2.2).

***Permeable Soil Depths*:** Permeable soil depths were measured at several locations on the Fortymile Wash alluvial fan (DTN: MO0708SCSOC137.000 [DIRS 182344], Table 2). The model uses a different depth for each of the two subdomains in the RMEI location (channels and divides). The influence of the permeable depth on model results is determined by Equations 6.3-22 and 6.3-25 (Section 6.3.3). Boundary conditions used in developing the equations are both zero flux (no advection at the upper boundary and an impermeable layer for the bottom boundary). The radionuclide mass deposited (either directly or from mixing), will equilibrate within the boundaries—the defined permeable depth. The smaller the permeable depth, the higher the equilibrium concentration will be. Thus, capturing the lower bound for this parameter is important.

A range of values for the permeable depth on the divides was measured on older units on the alluvial fan (Qa3 and Qa4). A total of six soil pits were dug with shovels and picks in these units. The depth to the low permeability, petrocalcic horizon (assumed to coincide with Stage-IV carbonate development) was measured at each soil pit. Stage-IV carbonate provides a natural low permeability barrier in gravelly parent material because it has a platy, continuous laminar cap and carbonate matrix that cements the gravel. The minimum measured depth to the Stage-IV carbonate in the Qa3 units was 102 cm. No Stage-IV carbonate was seen in the four pits dug into the Qa4 unit, indicating that the layer was at least as deep as the deepest pit dug (140 cm). Because soil-carbonate development is widely accepted to occur as a function of time, the depth to the Stage-IV carbonate for the younger units will be at least as deep as that of the Qa4. Thus, for the units comprising the divides (Qa3, Qa4), the range of permeable depth was taken to be between 102 and 140 cm. This range captures the minimum depth observed and limits the upper bound to a reasonable value based on field observations.

The permeable depth in the channel subdomain was inferred from the measurements made on the divides. Soil pits on the older Qa4 surface showed minimal carbonate development (Stage II was the maximum observed soil-carbonate development) to a depth of 140 cm, indicating that the depth to a Stage-IV carbonate for the younger surfaces could be much larger—if one exits at all. For these younger surfaces, it is possible that a Stage-IV carbonate may not have had time to form. While a finite permeable depth was not quantified in the field, it is appropriate to choose some finite value because buried soils could provide low permeability barriers at depths greater than 140 cm. If any low permeability boundaries exist on these surfaces, they are likely to be spatially discontinuous, in the form of buried paleosols. The Fortymile Wash alluvial fan is an aggrading landform, so it is likely that any paleosols exist well beneath a depth of 200 cm and are likely much deeper. Further evidence that supports such depth is suggested by the incised younger surface. At several locations on the fan, though rare, active channels on historical timescales cut Holocene "active" surfaces by more than 1 m, with no impermeable surfaces outcropping. Based on these findings, a constant value of 200 cm was chosen. This minimum value ensures reasonable and somewhat conservative equilibrium concentrations are predicted in the RMEI domain.

***Scour Depth*:** The scour depth at the fan apex is directly proportional to the amount of dilution (and to initial waste concentration) predicted in the channel domain by the model. In the upper drainage domain, as the scour depth across the grid increases (e.g., due to larger flood events), the amount of dilution will increase and the waste concentration within the channels of the upper drainage basin domain will tend to decrease. The concentration calculated at the fan apex is applied (in addition to direct deposition) throughout the RMEI channel subdomain, so a decrease in concentration equates to both a lower surface concentration and a lower depth integrated concentration. Therefore, it is especially important to capture the lower end of the scour depth range.

Once the tephra has been redistributed to the RMEI domain, further dilution of the radionuclide material is modeled as a vertical diffusion process. The greater the scour depth, the greater the overall mass stored in the channels, and the higher the potential associated dose. Review of Equation 6.3-25 shows that as time goes to infinity the summation term approaches zero, and the normalized concentration approaches the ratio of the depth associated with the distributed tephra to the permeable depth of the channels:

$$C_c(z,t)/C_{c0} \rightarrow \frac{d_{cf}}{L_c} \qquad \text{(Eq. 7-1)}$$

In the model, a reasonable but conservative (with respect to the resulting concentration profiles) constant value for the permeable depth of the channels is used. Thus, as the scour depth increases, the normalized concentration increases. The overall impact on the concentration profile is not readily apparent, as there is a tradeoff between the initial source concentration, C_{c0} (which is inversely proportional to the scour depth—see Equation 6.3-19), and the calculated time- and depth-dependent concentration calculated for the RMEI location (which is directly proportional to the scour depth).

Equation 6.3-26 can be rewritten as:

$$\frac{C_c(0,t)}{p_c} = \frac{1}{d_{cf}}\left(\frac{d_{cf}}{L_c} + \frac{2}{\pi}\sum_{n=1}^{\infty} e^{-n^2\pi^2 D_c t/L_c^2}\,\frac{1}{n}\sin\left(\frac{n\pi d_{cf}}{L_c}\right)\right) \qquad \text{(Eq. 7-2)}$$

by defining a proportionality constant, p_c, for which $C_{c0} = p_c / d_{cf}$. Figure 7.1.3-1 demonstrates how scour depth impacts the calculated concentrations in the channels of the RMEI location. Deeper scour depth results in a lower initial concentration, and slower diffusion into the medium. At equilibrium conditions, the competing effects of scour depth on the lower and upper drainage basins cancel each other out, and the resulting concentration in the channel is independent of scour depth. Thus, scour depth only influences the concentration profiles for non-equilibrium times. A rough estimate of the time required for the system to equilibrate can be found by dividing the distance to the impermeable layer squared by the diffusivity ($t_{est\ eq.} = (L_c - d_{cf})^2 / D_c$). For the example depicted in Figure 7.1.3-1, the equilibrium time for the shallower scour depth (73 cm) would be on the order of 460,000 years, while for the deeper scour depth (107 cm), the time to equilibrate would be on the order of 250,000 years. Until the concentration equilibrates, the calculated concentrations in the channels will be higher for shallower scour depths, making it essential to capture the lower bound of scour depth range.

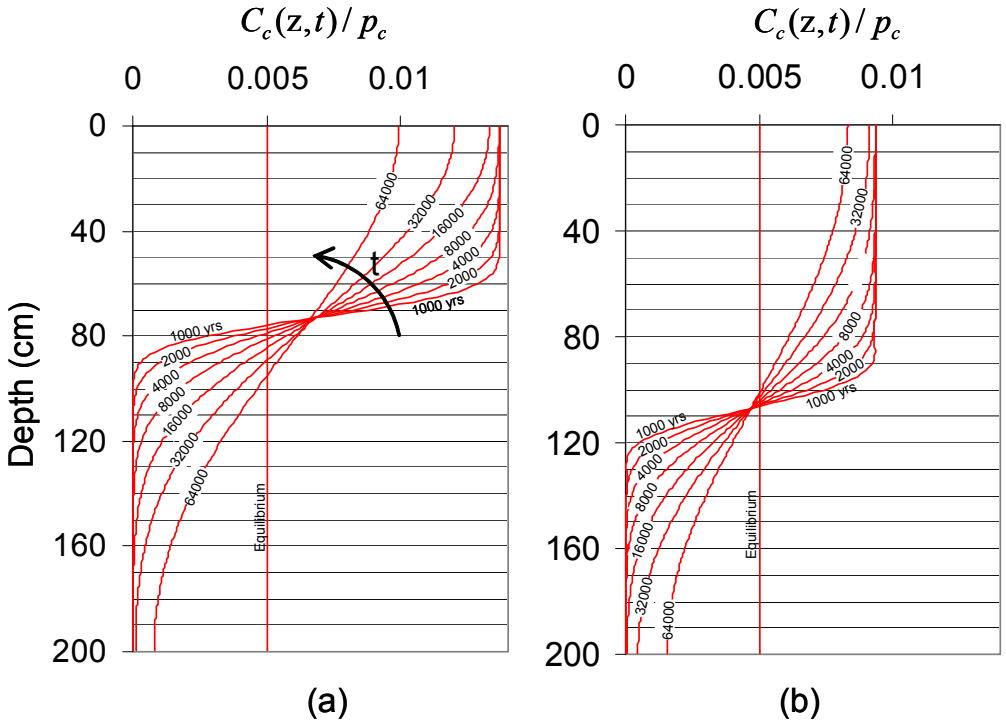

Source: Output DTN: SN0708DIFFEXMP.001.

NOTE: A permeable channel depth of 200 cm, a channel diffusivity of 0.035 cm^2/yr, and a scour depth of (a) 73 cm or (b) 107 cm were used.

Figure 7.1.3-1. Plot of Normalized Concentration versus Depth in the Channels for a Range of Times Following an Eruption

Little relevant data are available for estimating scour depth within either of the model domains, predominantly because of the timing associated with significant flood events. Data for one such flood at the Narrows are available and were used to estimate a range on the scour depth for a point in the upper drainage basin. These data were used to calibrate the scour depth equation (Equation 6.3-14). As described in Section 6.5.6, the range of scour depth at this location is taken to be a uniform distribution between 73 (the average scour depth for a significant flood event) and 122 cm (the maximum scour depth for a significant flood event) by TSPA.

While the 1995 flood event that was used to calibrate the scour depth range was significant, larger floods would be expected on a 10,000-year timescale. Squires and Young (1984 [DIRS 180001], p. 16) developed the following equations to estimate discharges for the 100- and 500- year floods in Fortymile Wash:

$$Q = 482A^{.565}; \text{ for a 100 yr flood}$$
$$Q = 2200A^{.571}; \text{ for a 500 yr flood} \quad \text{(Eq. 7-3)}$$

where the peak flow, Q, is in cubic feet per second, and the contributing area, A, is in square miles. For the upper drainage basin, the contributing area at the Narrows is 258 mi^2 (~670 km^2), and the resulting predicted discharges using Equation 7-3 are approximately 11,000 and 52,000 ft^3/s (~315 and ~1,500 m^3/s). As a comparison, the USGS estimated a peak discharge for the 1995 flood of 3,000 ft^3/s (85 m^3/s) (DTN: GS960908312121.001 [DIRS 107375]), which suggests that the 1995 flood was smaller than the expected 100-year flood. Because scour depth is proportional to the square root of discharge per unit width of channel (Section 6.3.3, Equation 6.3-10), the associated scour depths with the 100- and 500-year floods area are 1.4 and 3.1 m, respectively. Given these calculations, the chosen range for scour depth (73 to 122 cm) is reasonable and will result in a lower dilution factor (and thus higher concentration) at the outlet of the upper drainage basin (*dilutionfactoroutlet*).

These same data are used in the FAR model to set the scour depth of the lower drainage domain channels (Section 6.3, Step 5). The small elevation changes in this domain required that a different approach be used (rather than the spatial analysis of the upper domain) to determine the concentration and thickness of contaminated tephra redistributed to this area. In the active channel subdomain, the thickness of the contaminated tephra is set to the input value of scour depth at the Narrows location, which is the same value used to calibrate the scour depth for all channel cells in the upper drainage basin. Because the Narrows is a location where the channel width is constricted, scour depth measured at this location is expected to be somewhat greater than that on the alluvial fan, where channel width can adjust to larger flow events. Therefore, assigning the Narrows scour depth to the channels of the alluvial fan provides an upper bound approximation (and thus a larger total mass of contaminant is applied to the RMEI channels, as shown by Equation 7-1). The value is conservative in the context of transferring waste mass to the RMEI location because it is expected that the scour depth downstream from the Narrows will be smaller than at the Narrows. Equation 6.3-14 shows that scour depth is directly proportional to the ratio of the contributing area of a given pixel to that of the Narrows and inversely proportional to the ratio of the width of the stream flow at the Narrows and the width of the pixel (a constant value). The contributing area at the Narrows is 258 mi^2 (~670 km^2) and the width at the Narrows is approximately 52 m (slightly more than a single pixel width of 30 m). Because

there are only a few additional tributaries feeding Fortymile Wash below the Narrows, the overall contributing area for the wash does not increase significantly below this point. Given that Fortymile Wash widens downstream from the Narrows (by approximately an order of magnitude), and contributing area is calculated using the bifurcation routing technique which weights the area as a function of slope, the contributing area for a given channel pixel downstream from the Narrows will be lower than calculated for the single channel pixel at the Narrows. The resulting scour depths downstream from the Narrows will, in reality, be somewhat smaller than that at the Narrows. Figure 7.1.3-2 shows model results for the southern section of the Fortymile Wash channel between the Narrows and the channel outlet, demonstrating this difference. Given this, the chosen range for scour depth (73 to 122 cm) is reasonable and will result in greater mass of contaminated tephra being deposited in the RMEI channel subdomain.

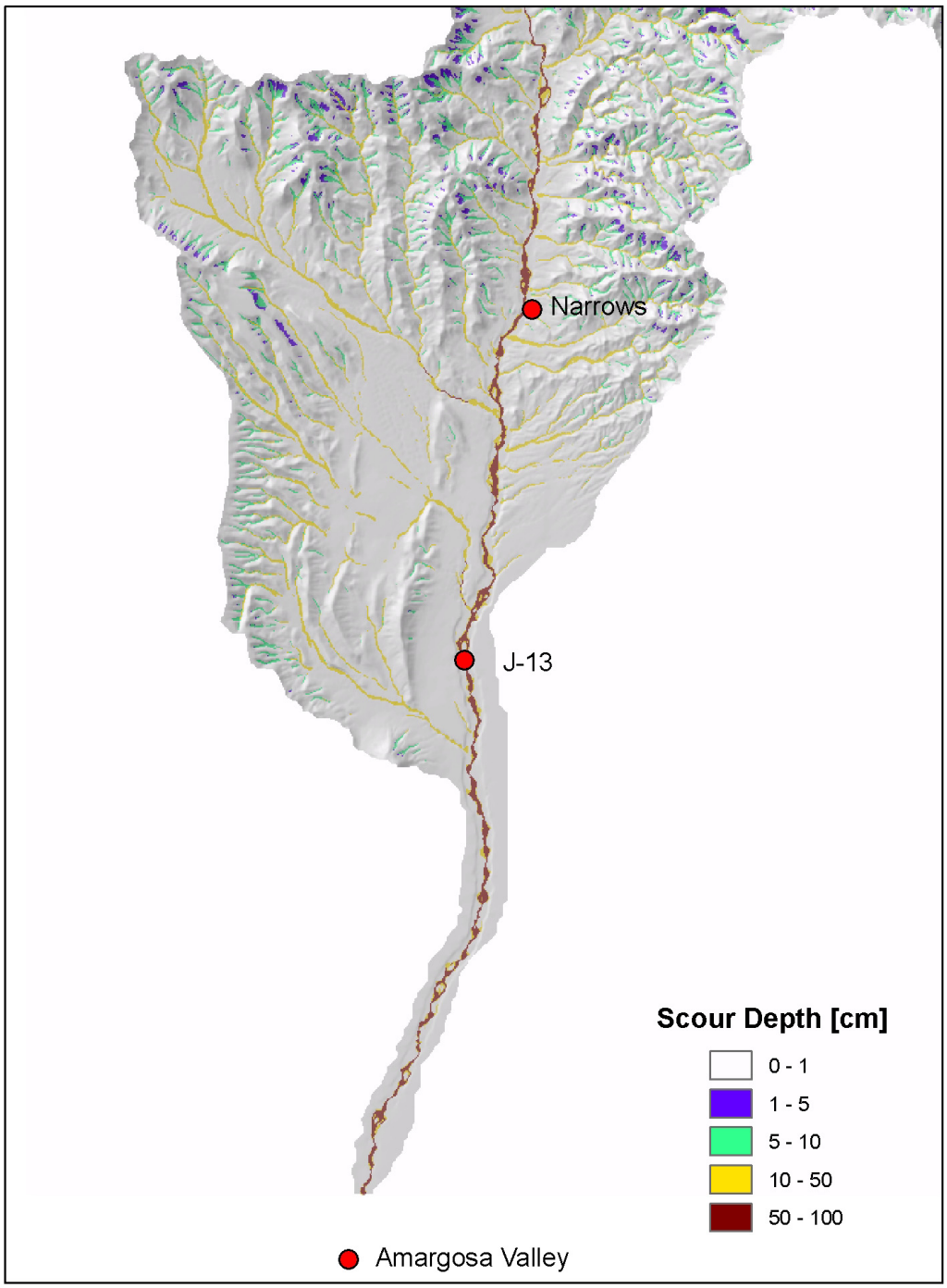

Sources: Station locations from DTN: GS960908312121.001 [DIRS 107375].

NOTE: Locations of USGS scour chain measurements shown as red circles. Note that only the southern portion of the upper watershed domain is shown. Figure is for illustrative purposes only.

Figure 7.1.3-2. Example Scour Depth Predicted by the FAR Model for Fortymile Wash between the Narrows and the Fan Apex

Critical Slope: To estimate a range on the critical slope required for tephra mobilization, field measurements and observations were made at the San Francisco Volcanic Field in northern Arizona (DTN: MO0708SCSOC137.000 [DIRS 182344], Table 1). This is an area of young volcanoes along the southern margin of the Colorado Plateau. During its 6-million-year history, this field has produced more than 600 volcanoes. Sunset Crater, the state's youngest volcano, erupted less than 1,000 years ago. Tephra erupted from this crater and blanketed the hillslopes at Rattlesnake Crater, Cochrane Hill Cinder Cone, and Moon Crater, the study sites for determining critical slope. The eruption type of Sunset Crater (violent Strombolian eruption) was consistent with that assumed in ASHPLUME (SNL 2007 [DIRS 177431]), the relatively young age of the crater allowed direct measurement of the mass of tephra easily mobilized, and the range of slopes at the site was broad enough to allow a distinct transition region to be determined. While both Flagstaff and Amargosa Valley are arid climates, Flagstaff has a higher yearly precipitation rate than Amargosa Valley, which might influence the stability of slopes (via vegetation anchoring), but such differences are not considered significant, especially given the wide uncertainty range in the critical slope parameter.

As the critical slope increases, the predicted mass of tephra/waste mobilized decreases. Capturing the lower bound of the critical slope is thus necessary to ensure reasonable and conservative results with respect to the final concentration profiles predicted by the model. Field data indicated that the transitional range (the range of slopes for which tephra was found to be stable in some areas but stripped in others) varied between 0.36 (20°) and 0.47 (25°) (Section 6.5.2). This range was expanded to include all slopes for which even marginal erosion was noted (0.21 (12°)), to ensure that the lower bound was encompassed. The final range for the critical slope parameter was determined to be between 0.21 and 0.47.

Diffusivity in Channels and on Divides: The diffusivity model is used to calculate the waste concentration profile over time in the RMEI domain. As the diffusivity parameter increases, the rate of diffusion into the soil increases, decreasing the near-surface contamination at a more rapid rate. Capturing the low end of the diffusivity range is thus critical to ensure reasonable and conservative surface concentrations and integrated concentrations to depth.

Bulk ^{137}Cs concentrations were measured at numerous locations on the Fortymile Wash alluvial fan. This bomb-pulse radionuclide was first produced approximately 50 years ago with the advent of atmospheric testing of nuclear weapons at the nearby Nevada Test Site and provides a radionuclide tracer at this location. Sample transects were established longitudinally along the length of the alluvial fan and laterally across the fan (DTN: MO0708SCSOC137.000 [DIRS 182344], Table 3). Samples of 100 to 250 g were collected over a nominally 2-ft^2 (0.2-m^2) area and a 3-cm thickness at increasing depths. Collected data were annotated as being either in the active channel system or on the divides.

Data were analyzed by gamma spectroscopy. The measured value, total propagated uncertainty, and minimum detect limits were reported (DTN: LA0302CH831811.002 [DIRS 162863]). An effective diffusion rate was calculated for each measurement (Section 6.5.8). A similar calculation using these data is documented by Pelletier et al. (2005 [DIRS 175800]). For the divides, the base values of D_d varied from 0.004 to 0.064 cm^2/yr. Considering the full range of errors associated with the measurements, the range increased to 0.001 to 0.095 cm^2/yr. Higher diffusivities were seen in the channels. Base values for D_c range from 0.048 to 0.166 cm^2/yr.

Considering the full range of errors associated with the measurements, the range increased to 0.035 to 0.266 cm^2/yr.

The diffusion calculations make two important assumptions. First, they assume that the analytical diffusion equation (Section 6.5.8, Equation 6.5-3) adequately represents the data. This is discussed in detail in Section 7.2.6. Second, they presume that the radionuclide profile extends to a minimum depth equal to the bottom of the upper sample zone (3 cm) and a maximum depth equal to the bottom of the deepest sample zone (6 cm). If the radionuclide profile does not extend to the bottom of the upper sample zone, the actual diffusivity is likely lower than the calculated diffusivity determined by Equation 6.5-3. If the radionuclide profile extends beyond the bottom of the lower measurement zone, the actual diffusivity is likely higher than the calculated diffusivity determined by Equation 6.5-3.

Review of the sample measurements for the divides shows that in all but one instance the radionuclide profile extends to at least the 3-cm depth. At this sample location, Cs-071702-G, the measured quantity of ^{137}Cs was 0, with an uncertainty of 0.01 pCi/g. The resulting diffusivity was 0.004 to 0.033 cm^2/yr. The lower end of this diffusivity range was not the lowest value and therefore did not define the lower bound of the divide diffusivity range. The lower bound was instead determined from sample Cs-071802-Q, which did have a small but non-zero bulk activity measurement for the lower sample. Further, the data show that the bulk of the radionuclide material for all of the samples was found in the upper measurement zone. The fraction of the total activity in this zone ranged from a low of 67% to 100% of the total. Figure 7.1.3-3 plots the normalized ^{137}Cs concentration versus depth for the sample having the greatest potential for radionuclide mass below the lowest measured zone (Cs-071702-E). As seen in the figure, even for this measurement point, only a small portion of the radionuclide would be below the lower sample zone (below 6 cm). Given that the error associated with this assumption results in a lower diffusivity value being calculated (and thus higher concentrations at the surface), the range of diffusivity values calculated for the divides is reasonable for the model.

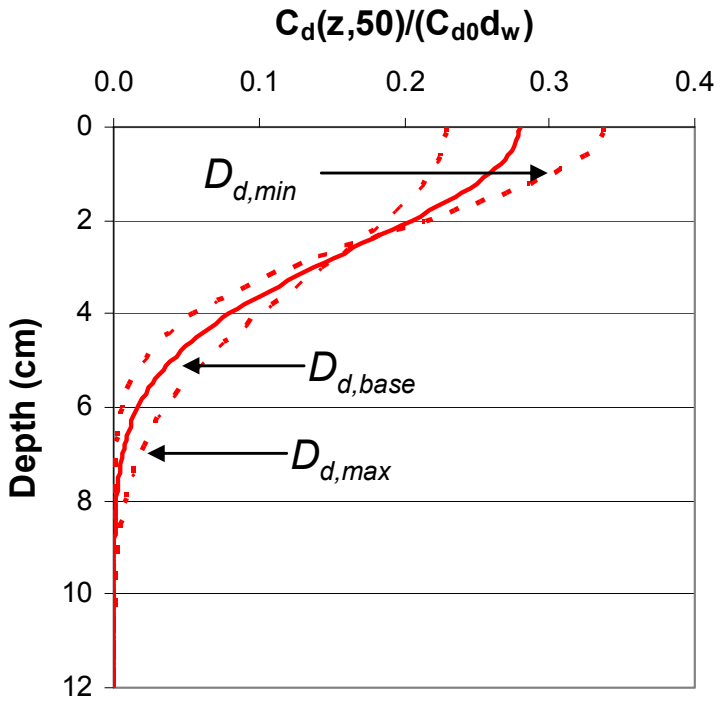

Source: Output DTN: SN0708DIFFRNGS.001.

Figure 7.1.3-3. Plot of Normalized Concentration versus Depth for the Divide Sample Point Cs-071702-E at a Time of 50 Years after Deposition of the Cesium and the Maximum Range of Calculated Diffusivities Based on Measurement Error

Review of the sample measurements for the channels show that each of the sample points measured significant bulk activity in the 3- to 6-cm sample zone, indicating that the radionuclide profile extends beyond the 3-cm depth. The lower bound of the calculated diffusivity range for channels is thus reasonable. The assumption of no radionuclide material below 6 cm is not supported by two of the three channel measurement points. Figure 7.1.3-4 plots the normalized concentration for one of these points (Cs-071702-B). As seen in the figure, the diffusion equation would predict considerable radionuclide mass below the 3- to 6-cm sample interval. The greater the radionuclide mass below 6 cm is, the higher the calculated diffusion rate. The magnitude of the overall error associated with this assumption can be estimated by calculating the diffusivity as a function of mass below the 6-cm zone (calculations were completed as described in Section 6.5.8). Figure 7.1.3-5 shows the results for a range of fraction of activity below 6 cm corresponding to a minimum value of zero to a maximum value of 0.30. This maximum value was chosen by assuming that the maximum bulk activity for a zone below the 3-to 6-cm zone would be 75% of the bulk activity for the 3- to 6-cm zone. This plot indicates that the upper bound of the channel diffusivity could be more than twice as high as the value reported in Section 6.5.8. As discussed in the *Permeable Soil Depths* section above, the radionuclides deposited in the channels will approach an equilibrium value over time. This value can be calculated using Equation 7-1. For the channels, the deposition depth will range from 73 to 122 cm (range of *scourdepthoutlet*, Table 6.5.10-1), while the permeable depth is a constant 200 cm (Table 6.5.10-1). Thus, the radionuclide concentration, at equilibrium conditions, will range from 36% to 61% of the initial concentration—a relatively insignificant change. The

diffusivity constant determines how quickly the concentration will equilibrate (see the *Scour Depth* section above). Increasing the diffusivity by a factor of two will decrease the time to equilibrate by roughly a factor of two; this can be seen graphically in Figure 6.6.2-4. Given the relatively small overall range of the channel concentrations, the insensitivity of the concentration profile to this parameter, and the fact that calculated concentrations are more conservative with lower diffusivity values, no change was made to the calculated channel diffusivity range of 0.035 to 0.266 cm^2/yr.

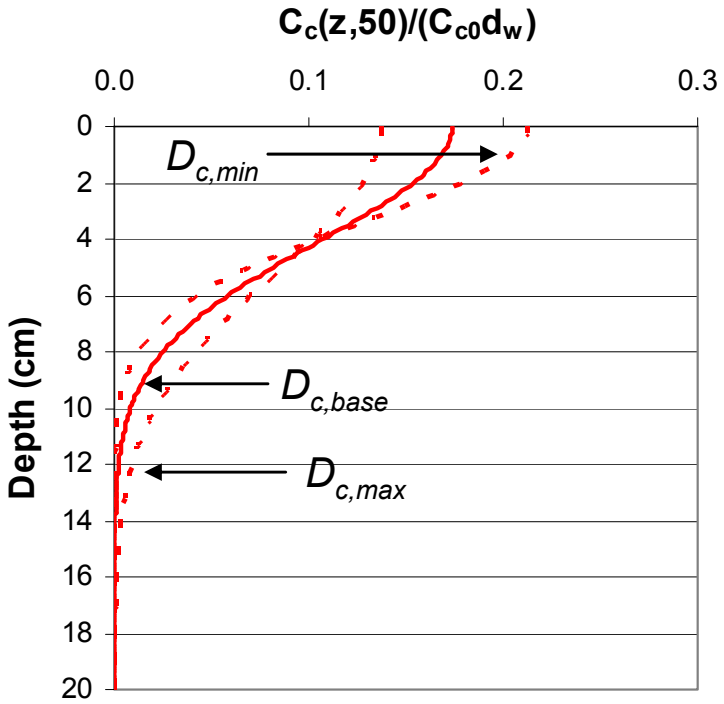

Source: Output DTN: SN0708DIFFRNGS.001.

Figure 7.1.3-4 Plot of Normalized Concentration versus Depth for the Channel Sample Point Cs-071702-B at a Time of 50 Years after Deposition of the Cesium and the Maximum Range of Calculated Diffusivities Based on Measurement Error

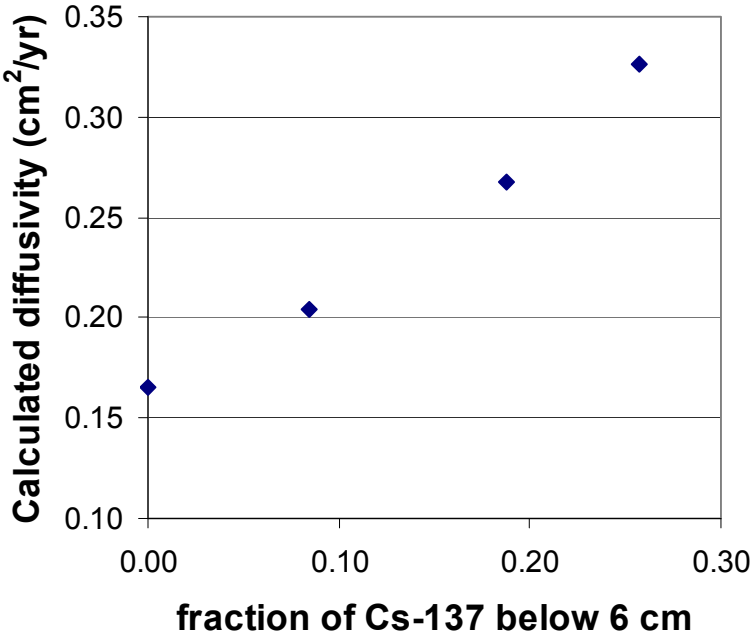

Source: Output DTN: SN0708DIFFRNGS.001.

NOTE: Base bulk diffusivities were used for the calculation.

Figure 7.1.3-5. Plot of Diffusivity versus an Assumed Fraction of ^{137}Cs below the Lower Sample Zones Maximum Depth of 6 cm for Sample Point Cs-071702-B

7.2 VALIDATION DURING MODEL DEVELOPMENT

A number of conceptual and computational approaches were considered for the various steps of the model during the model development process. Both of these methodologies, along with the reasoning used to choose those methodologies implemented in the FAR V.1.2 software, are discussed in Sections 7.2.1 through 7.2.6. After the FAR V.1.2 software was completed, the software was validated under Lead Laboratory procedure IM-PRO-004, *Qualification of Software*. A summary of the software validation test cases is presented in Section 7.2.7. These test cases and the acceptance criteria for V.1.2 are described in detail in *User Information Document for: FAR Version 1.2* (DOE 2007 [DIRS 183116]). The validation results for V.1.2 are included in *Software Validation Report for: FAR Version 1.2* (DOE 2007 [DIRS 183120]).

7.2.1 Bilinear Interpolation on Input ASHPLUME Tephra and Waste Concentration Grids and Rectification to DEM (Step 1)

The tephra redistribution model uses input grids of tephra and waste concentration computed by ASHPLUME. These grids are relatively coarse (on the order of 500-m grid spacing), while FAR V.1.2 performs the grid analysis at the much finer resolution of the DEM (30-m grid spacing). The ASHPLUME results were interpolated to the same scale as the DEM. Two different interpolation schemes were tested during model development. The bilinear interpolation provided correct values on a grid-cell scale, based on visual inspection of output results. A bicubic interpolation scheme was attempted to try to improve smoothness of the

plume shape. Results showed that this scheme actually led to negative concentrations in some areas because the concentrations changed so rapidly upwind from the vent. Therefore, a bilinear scheme was determined to be the best solution and was incorporated into the code.

In addition to developing an interpolation routine for Cartesian DEMs, a scheme for interpolating a polar grid was also developed (Section 6.3.3). For TSPA FAR calculations, ASHPLUME generates a grid in polar coordinates. For these calculations, FAR uses a routine designed to interpolate from a polar grid to a Cartesian grid. The routine calculates the values of tephra and waste concentrations by interpolating the input ASHPLUME grids. The tephra concentration grid is used to determine the thickness of tephra in each grid cell, and this thickness is mobilized from the slopes and active channels of the landscape by the FAR model. The waste concentration grid is used to integrate the total mass of waste mobilized and connected to the main Fortymile Wash channel. The Cartesian and polar grid routines were tested for different ASHPLUME grid sizes and dimensions to ensure that the code worked correctly for a range of input values.

Following the bilinear interpolation procedure, the grid is rectified to the DEM. This is done by shifting the grid so that the origin (center) of the interpolated grid (the vent location) corresponds to the center of the repository location in the DEM. The center of the repository emplacement area was found as the average of the maximum and minimum coordinates in the north/south and east/west directions of the waste emplacement area. Because the footprint of the emplacement area is non-rectangular, this calculation does not provide the actual center of the area. However, this approximation is sufficient for its intended use, since any eruption occurring within the emplacement area is relevant to the eruption scenario. The area of the repository (~11 km^2, calculated from bounding box defined in Table 6.5.7-2) is much smaller than the overall area of the upper drainage basin (~828 km^2, calculated from Output DTN: MO0605SPAFORTY.000 as the product of 900 m^2 and the number of grid cells in the basin (cells with an elevation not equal to "-9,999.0")). Moving the vent location to anywhere within the repository emplacement area will have little impact on the overall distribution of the tephra plume.

During FAR software validation, the interpolated and rectified ASHPLUME grid was verified using an independent calculation performed in an EXCEL workbook. The two results matched to within two decimal points of accuracy (DOE 2007 [DIRS 183120]).

Using an example ASHPLUME result, a comparison between tephra thickness (tephra concentration (g/cm^2) / tephra density (g/cm^3)) at each ASHPLUME grid point to the nearest interpolated tephra thickness within the watershed (obtained from the nearest 30 × 30 m grid cell) provides additional confidence that the interpolation scheme is working as designed. For this example, the mean difference in thickness for all the ASHPLUME grid points is approximately 0.2 cm with a standard deviation of 2.6 cm. These differences are shown graphically in Figure 7.2.1-1. The main deviations in the interpolation scheme appear to occur near the vent location where both the magnitude (> 50 cm) and gradient of tephra thickness is large.

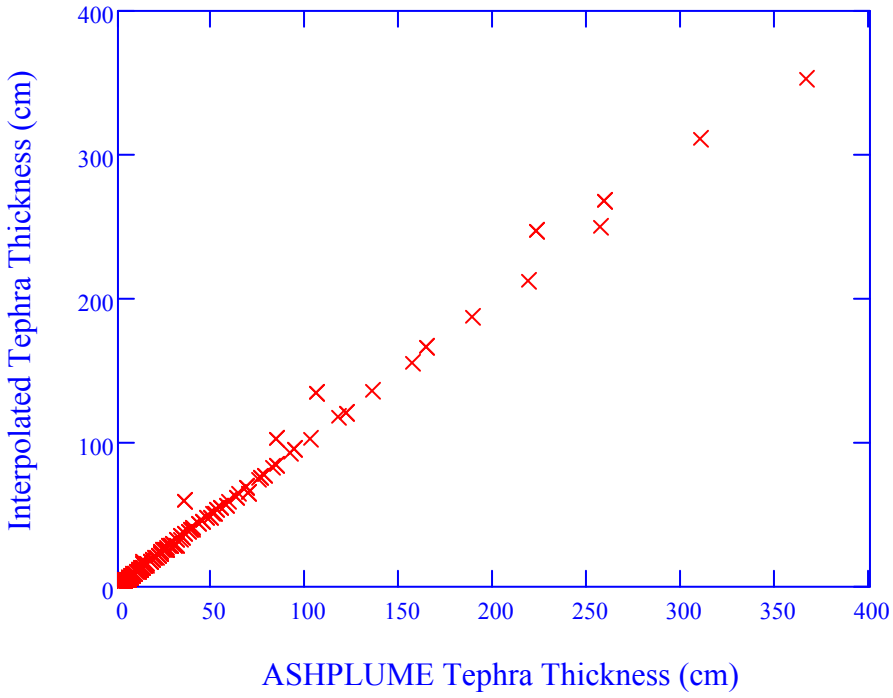

NOTE: Figure was generated from sample FAR and ASHPLUME model output and is for illustrative purposes only.

Figure 7.2.1-1. Comparison between ASHPLUME Tephra Thickness and Interpolated Tephra Thickness Values for an Example Eruption

7.2.2 Fill Pits and Flats in the Input DEM (Step 2)

All USGS DEMs are interpolated from contour maps. As a result, they often have artifacts of interpolation on low-relief surfaces. These artifacts, called "pits" and "flats," can make it difficult to route flow locally, which is required for calculating contributing area (and here to identify channels). Pits are defined as single grid cells which are lower in elevation than all of the eight surrounding grid cells (including diagonals). Flats are defined as areas where at least one grid cell is surrounded by eight grid cells that are at the same elevation. Lakes, when they exist, show up on the DEM as flats. Various algorithms have been developed for removing pits and flats from DEMs when they show up in error. One of the simplest is to use recursion to raise the level of every grid cell that does not have proper drainage. In the FAR model, any grid cell that does not have a neighbor with lower elevation is raised up in elevation by a small amount (1 cm). If raising that grid cell causes any of the neighboring grid cells to become pits or flats, those grid cells are, in turn, raised incrementally. In this way, the routine can "fill" any flats in the DEM until a gently sloping surface drains the area to the lowest "spill point." This routine is similar to, but simpler than, the published approach of Martz and Garbrecht (1999 [DIRS 175455]). To test this routine during model development, a synthetic DEM was created (30 × 30 grid cells). A pit, created as the product of two sine functions, was placed within the DEM. The synthetic DEM was run through the recursive routine. The routine successfully filled the pit to the level of the spill point, and every grid cell in the synthetic DEM drained to the spill point or to one of the border cells.

The result of this step is that a very small fraction of the DEM grid cells (0.25%) are raised in elevation to remove flats. Figure 7.2.2-1 shows the locations where elevations were raised. Most of the changes were concentrated in the northern part of the drainage basin far from the vent location. Figure 7.2.2-2 shows a histogram of the elevation changes that were made for these cells. The mean elevation change made for these cells was approximately 20 cm, with a standard deviation of about 40 cm.

NOTE: Figure was generated from intermediate results produced by an unqualified version of the FAR V.1.2 software that was modified to save additional output. It is for illustrative purposes only.

Figure 7.2.2-1. Map Showing the Location of Grid Cells Filled with the “Fill Pits and Flats” Routine

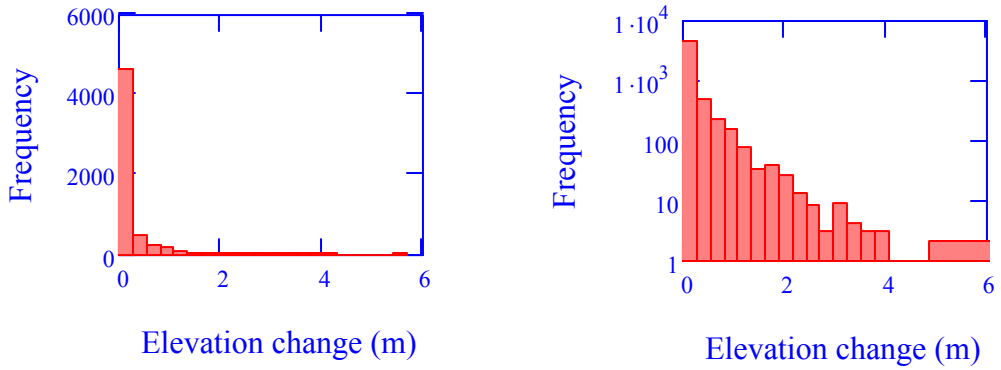

NOTE: Left plot shows frequency on a linear scale and the right plot uses a log scale. Figure was generated from intermediate results produced by an unqualified version of the FAR V.1.2 software that was modified to save additional output. It is for illustrative purposes only.

Figure 7.2.2-2. Histograms Showing the Frequency of Elevation Changes Made to Fill Pits and Flats

7.2.3 Compute Slope, Contributing Area, and Scour Depth Grids (Step 3)

FAR performs a GIS-type spatial analysis on the input DEM for the upper drainage basin. These analyses include mapping the DEM slope and contributing area for the drainage basin, and calculating scour depth for all channel cells.

A four-neighbor slope was implemented in the code. The code was tested by hand calculation on a small 5 × 5 subset of the grid. The hand calculations matched the code output. It is noted that there are other ways to calculate DEM slope, such as steepest descent. However, the four-neighbor slope was found to be more accurate based on comparisons with synthetic grids using mathematical functions (Jones 1998 [DIRS 174197]).

A comparison of local slopes was made using the upper Fortymile Wash drainage basin DEM calculated by the FAR modeling approach and calculated by the steepest descent method. The resulting difference in the slopes calculated with these two methods is quite small, as illustrated in Figure 7.2.3-1. The mean slope difference for all grid cells in the upper basin is approximately 4×10^{-3}, with a standard deviation equal to 0.02. This difference is very small when compared with the uncertainty in the critical slope parameter. Therefore, the method used by the FAR model is considered valid for its intended use.

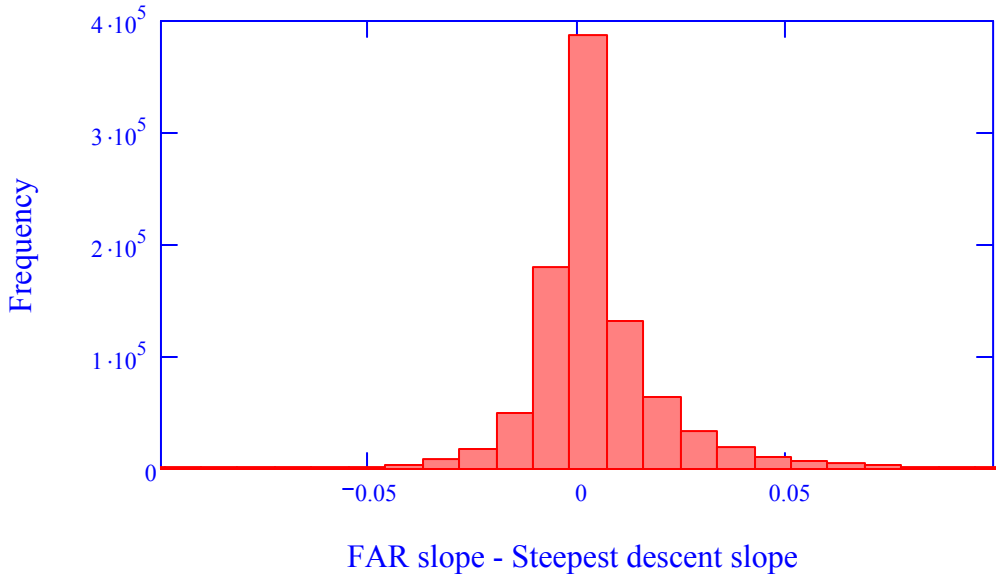

NOTE: FAR slopes are produced as output when *oflag* is set to equal 1. Steepest descent slopes were calculated using standard tools in ArcGIS V. 9.2. Figure for illustrative purposes only.

Figure 7.2.3-1. Histogram of the Difference in Cell Values of Slope Calculated Using the Four-Direction Method Used by FAR and the Steepest Descent Method Implemented Using ArcGIS Tools

The "fill in pits and flats" routine (Section 6.3.3) is significant for flow routing because the entire DEM must have well-defined drainage directions everywhere for the contributing area to be correctly calculated. While there are many different algorithms for performing flow routing calculations, a divergent flow routing or "bifurcation routing" method (Section 6.3.3) was chosen for this model. This routing method has been shown to work much better in distributary environments than the more simplistic "steepest-descent" method (Pelletier 2004 [DIRS 174135]).

In the bifurcation routing method, all incoming flow to a grid cell is partitioned between each of the downslope grid cells, weighted by slope. In an area with multiple downslope grid cells with equal slopes, contributing area is split evenly in each downslope direction. To use this method, each DEM grid cell is initially assigned a contributing area (the local area represented by the grid cell). Contributing area values are then routed as "flow" through the basin from highest to lowest elevation, following the same paths that runoff would take downslope. To move from highest to lowest elevation, the model creates an elevation index list that ranks the DEM grid cells by elevation. The model begins the bifurcation routing algorithm by calculating the contributing area at the highest grid cell in the DEM. This grid cell has no upstream contributors, so its contributing area is equal to its grid cell area. This contributing area is then routed downslope by partitioning it between each of its eight neighbors on the grid (including diagonals), weighted by slope. Cells outside the watershed boundary are excluded. Each of the neighbors at a lower elevation receives a fraction of the contributing area from the highest grid cell, which is added to their initial values. The model then proceeds to the next lowest grid cell, routing contributing area from the highest to lowest grid cells in the DEM. By moving through the grid in this order, the method ensures that all of the contributing area has been accumulated

before routing the values down slope because all incoming flow must come from higher elevations. The primary importance of the bifurcation routing method for the model is that it provides an accurate method for mapping the entire channel area in the DEM even if channels vary in width in a complex manner. The steepest-descent method would force all flow into the lowest point in the channel. As such, the steepest-descent method could provide an accurate measure of channel length, but channel width would not be determined. In the bifurcation routing method, flow expands to accommodate the entire channel between opposite banks. This difference is important for enabling the model to integrate all of the tephra that falls on active channels.

Implementation of the bifurcation routing method was tested by comparing the output of the model for a small 5 × 5 grid subset with calculations performed by hand in an Excel spreadsheet during software validation (DOE 2007 [DIRS 183120]). Results between the hand calculations and the code matched to the fifth significant figure.

To calculate the scour depth throughout the grid, the model uses an approximation (Equation 6.3-14) developed from two empirical proportionalities. First, contributing area is related to total maximum discharge on a grid-cell-by-grid-cell basis using the regional "flood envelope'' curve developed by Squires and Young (1984 [DIRS 180001], p. 16). These authors studied the flood potential of Fortymile Wash and found that, for this specific site, the maximum discharge (for 100-year and 500-year floods) is proportional to contributing area raised to the 0.57 power. Maximum discharge is used because it is the largest floods that control the long-term scour/mixing depth. Second, unit discharge is related to scour depth based on work by Leopold et al. (1966 [DIRS 175456], pp. 215 to 218), who found, generally, that the scour depth is proportional to the square root of total discharge divided by channel width (unit discharge). To combine these relationships, it was necessary (1) to assume that total channel width and total contributing area can be subdivided between multiple grid cells that represent wide channels defined by the divergent flow algorithm, and (2) to mathematically manipulate the ratio of observed channel width to DEM pixel size by raising it to the 0.57 power in order to ensure that DEM resolution does not influence the estimated scour depth. The validation of this approach is done in three steps. First, the square-root dependence of scour depth to unit discharge is validated using data from Powell et al. (2005 [DIRS 178706]). Second, the approximation used in the model (Equation 6.3-14) is validated by demonstrating that it will tend to slightly underestimate the integrated scour depth from the upper drainage basin, which according to the sensitivity analysis presented in Section 6.6 results in overestimating the initial waste concentration in the RMEI channels. Third, scour depth observations from a location different from the Narrows, but within the upper basin, are compared with scour calculated by the FAR model.

Data from Powell et al. (2005 [DIRS 178706]) were used to validate the square-root dependence between scour depth and unit discharge observed by Leopold et al. (1966 [DIRS 175456] pp. 215 to 218). Powell published measurements of scour and unit discharge in low-order stream channels at Walnut Gulch experimental watershed in Arizona. Data are presented in Table 7.2.3-1. Figure 7.2.3-1 shows the data with a trend line, indicating a power constant of 0.48, which is very close to a square root relationship. Thus, these data corroborate the relationship used in the FAR model.

Table 7.2.3-1. Data for Discharge and Scour Depth in Low-order Ephemeral Streams at Walnut Gulch Experimental Watershed

Measured Discharge Q (m^3/s)	Unit Discharge q ($m^3/s/m$)	Maximum Observed Scour (m)
0.21	0.06	0.08
0.33	0.11	0.08
0.46	0.15	0.1
0.46	0.14	0.16
0.48	0.15	0.06
0.71	0.23	0.12
1.45	0.47	0.24
3.85	1.24	0.28
4.55	1.47	0.3
11.4	3.68	0.48

Source: Powell et al. 2005 [DIRS 178706], Figure 4, for measured discharge and maximum observed scour; Table 1 for channel width.

NOTE: Channel width = 3.1 m. Unit discharge calculated as measured discharge divided by the channel width.

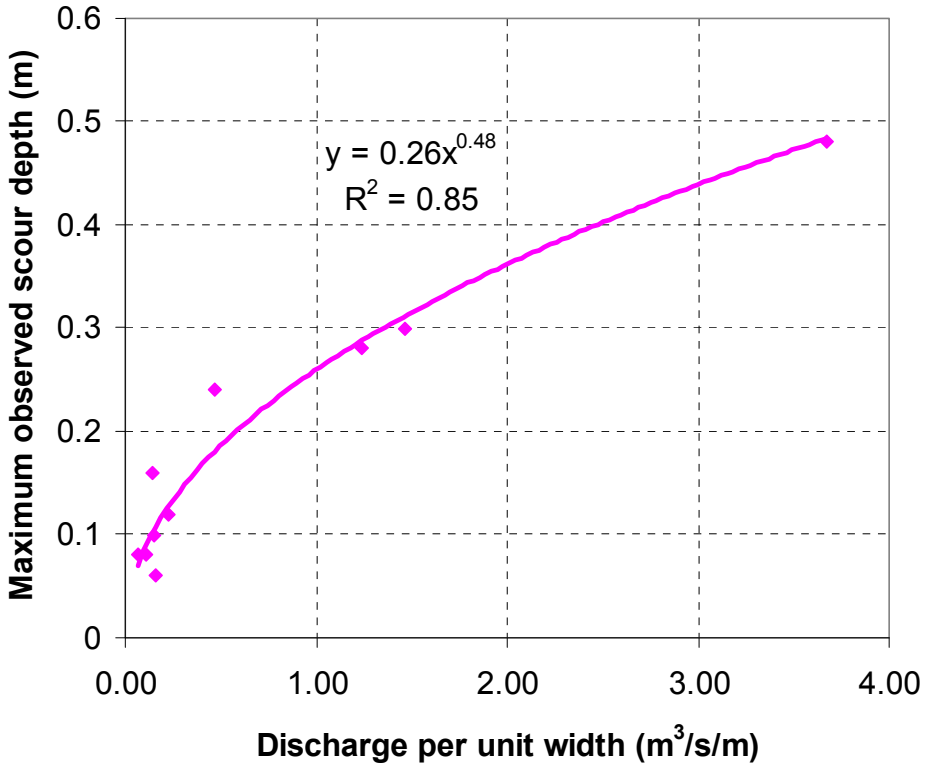

Source: Powell et al. 2005 [DIRS 178706]—presented in Table 7.2.3-1, plotted using Excel.

NOTE: Trend line added using standard Excel functions.

Figure 7.2.3-1 Plot of Observed Scour Depth versus Unit Discharge

As described in STEP 3 of Section 6.3.3, the equation used by the FAR model to estimate scour depth as a function of contributing area (Equation 6.3-14) is an approximation of the rigorously derived equation (Equation 6.3-12). The approximation was necessary in order to apply the equation to grid cells representing channels wider than individual grid cell dimensions, which are present in the basin and predicted with the divergent flow algorithm. To validate this approximation, it is compared with scour depth predicted using Equation 6.3-12 for a characteristic channel configuration. Because Equation 6.3-12 requires actual channel width as input, an accompanying calculation was performed to estimate the average channel width in the upper drainage basin for use in this comparison.

Average channel width is estimated by dividing channel area by the length of all channels. Channel area can be calculated from FAR model output counting the number of channel grid cells and multiplying by grid-cell area. Channel area is directly proportional to the drainage density input parameter. Channel length is calculated by counting channel cells identified using a steepest descent flow routing algorithm, which produces channels that are one grid-cell in width, and multiplying the number of channel cells by an effective grid-cell length. Channel cells are identified by evaluating the upstream contributing area of each grid cell and comparing this to a threshold area. Cells are defined as channels if the contributing area exceeds this threshold area. A number of methods are available to estimate an appropriate threshold area (e.g., Tarboton et al. 1991 [DIRS 183748]), but it is important that the resulting channel networks are consistent with field observations. In the present analysis, an appropriate threshold area of 40 grid cells was determined by adjusting this threshold until 34 field observations of channel head locations on the eastern slope of Yucca Mountain were best-fit by the predicted channel network.

Effective grid-cell length is taken as the mean of Δx and $\Delta x\sqrt{2}$, where $\Delta x = 30$ m. An effective length of Δx is appropriate if all flow is oriented with the grid (e.g., N, S, E, and W) while a value of $\Delta x\sqrt{2}$ is appropriate if all flow is oriented diagonally at 45 degrees to the grid (e.g., NE, SE, NW, and SW). The mean of these two values is appropriate for flow oriented in a variety of directions (e.g., Lin and Oguchi 2006 [DIRS 183770]). These calculations result in average channel width ranging from 27 to 57 m for drainage density values from 20 to 33.3 km^{-1}, respectively.

Using this range for the average channel width, the difference in predicted scour depth (Equation 6.3-14 minus Equation 6.3-12) is plotted as a function of contributing area in Figure 7.2.3-2. Equation 6.3-12 was solved by evaluating the proportionality constant, *p*, from the scour depth measurements at the Narrows station following the 1995 flood (contributing area = 258 mi^2, channel width = 52 m, and scour depth = 97.5 cm, which is the mean of the distribution for this parameter as described in Section 6.5.6). The fact that most of the area between the two bounding curves is characterized by a negative difference indicates that the FAR approximation tends to underestimate scour depth when compared with Equation 6.3-12.

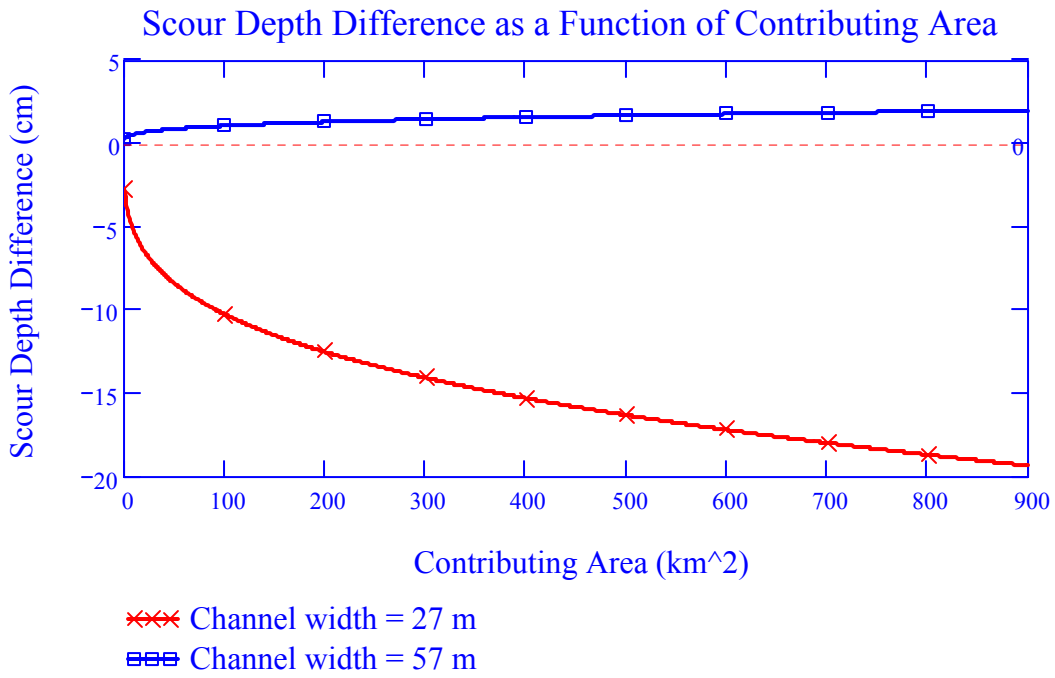

NOTE: Difference calculated as Equation 6.3-14 minus Equation 6.3-12.

Figure 7.2.3-2. Difference in Scour Depth Predicted by Equations 6.3-12 and 6.3-14 for Two Bounding Values of Average Channel Width

Sensitivity analyses presented in Section 6.6.1 indicate that initial tephra (and waste) concentration in the RMEI location channels is negatively correlated with scour depth. Therefore, the approximation used by the FAR model will tend to *overestimate* waste concentration when compared with the use of Equation 6.3-12, and therefore the FAR approximation is considered valid for its intended purpose.

An additional corroboration of the scour depth calculation was performed after the scour depth equation (Equation 6.3-14) was applied to the channels of Fortymile Wash using the scour depth range at the Narrows (Section 6.5.6). In addition to the scour chains installed at the Narrows, the USGS installed scour chains in at least two other locations in Fortymile Wash. Scour chains were emplaced in Fortymile Wash near well J-13, which is approximately 9 km south of the Narrows (Figure 7.1.3-2). Mean scour measured at this location was 37 cm with a maximum scour of 61 cm (DTN: GS960908312121.001 [DIRS 107375]). A comparison of scour predicted by Equation 6.3-14 using the range of scour depths for the Narrows (73 to 122 cm) in the channel cells within a radius of 60 m from the measurement location resulted in average scour depth ranging from 49 to 81 cm. This result indicates that the approach for estimating scour depth as a function of contributing area and a single calibration measurement at the Narrows appears to result in reasonable values when compared to other scour measurements. Another scour chain measurement was made by the USGS at the Amargosa Valley station, but is outside the upper drainage basin domain and therefore cannot be directly compared with modeled scour depth.

7.2.4 Calculate Total Mass of Mobilized Tephra/Dilution Factor (Step 4)

***Mobilization (Step 4)*:** During the initial development of the FAR model, the code determined the overall mobilization of tephra within the channels as a direct function of channel slope. Using this scheme, low-order streams with sufficient slope and high-order streams with sufficient contributing area were defined as channels. Initial review of this approach determined that this methodology mobilized too much tephra from the landscape as it did not allow any local storage of the material in alluvial flats, which are observed in the field. A new methodology was implemented that identifies channel grid cells with either a local slope greater than a critical slope or a stream power greater than a stream power threshold value (defined as $1/X$, where X is the drainage density). Stream power is calculated as:

$$\text{Power} = \text{slope}_{\text{avg}} \times A^{0.5} \qquad \text{(Eq. 7-4)}$$

where A is contributing area and $slope_{avg}$ is the moving average of the local slope on a 5×5 grid-cell area. USGS DEMs have small artifacts in them that can result in artificially low slopes one or two grid cells wide. By using a 5×5 grid-cell average, FAR ensures that the stream power decreases (leading to tephra deposition locally) only in true low-gradient areas.

Figure 7.2.4-1 shows channel maps calculated for bounding values of drainage density. Channels are identified as any grid cell for which a scour depth is greater than zero. Channels are divided into those that eventually connect to the main Fortymile Wash and those that are not connected. As the value of the drainage density increases, the number and length of channels reaching the main wash (Fortymile Wash) increases. Of particular importance is the area just east of Yucca Mountain, which is fairly flat and may provide a significant local depozone. The proximity of this area to the repository, and its location with respect to the prevailing winds at the site, make it potentially influential in determining the mass of tephra and waste that are mobilized to the RMEI location. At low drainage density values, channels originating on the Eastern slopes of Yucca Mountain do not connect with the main Fortymile Wash drainage system, resulting in local deposition of tephra in this area. As the drainage density increases, channel systems on the north and south of the repository area begin to connect with the main Fortymile Wash, providing a pathway for the potentially thick tephra deposits near the vent to reach the RMEI location. There is uncertainty in the appropriate extent of channels in this area, and therefore it is important that the range in the drainage density parameter span the range between values leading to local deposition and those leading to a connected channel network through the area. As seen in Figure 7.2.4-1, the drainage density range determined in Section 6.5.3 (20 to 33 km^{-1}) results in an appropriate range in the extent of the channel network.

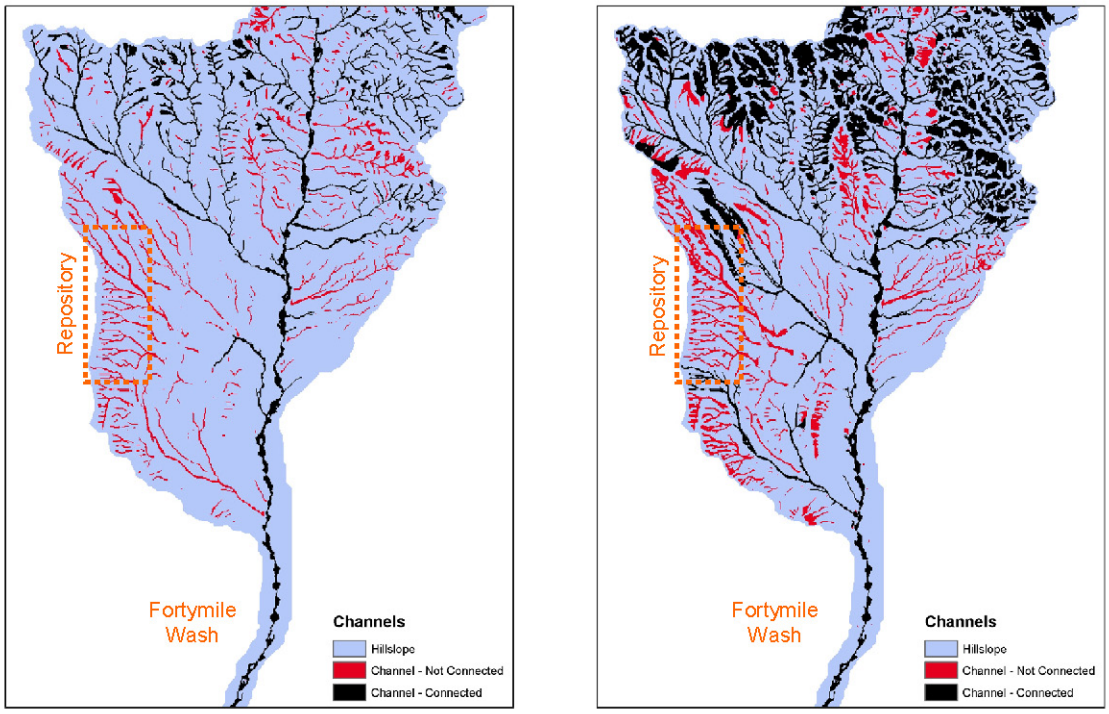

NOTE: Figure was generated using intermediate results produced by an unqualified version of the FAR V.1.2 software that was modified to save additional output. It is for illustrative purposes only.

Figure 7.2.4-1. Channel Maps for Two Values of Drainage Density: (a) 20 km^{-1}, (b) 33 km^{-1}

Implementation of this methodology impacted the use of *rvent*, the parameter used to define a distance from the vent below which tephra would not be mobilized. This parameter was initially used to ensure that the code would not grossly overestimate total tephra transport to the RMEI location. Using the stream-power methodology allows the FAR model to assume a conservative scenario (*rvent* = 0, thus maximizing the radionuclide mass mobilized), without grossly overestimating the amount of tephra reaching the RMEI location.

Another minor factor affecting the mobilization of tephra is how the model limits the mobilized tephra thickness to the local scour depth in channel grid cells. This limitation accounts for a very small percentage of the mobilized tephra as is illustrated by several examples presented later (in Section 7.2.8). Figure 7.2.4-2 shows a map of the distribution of tephra thickness stored under the scour zone for an example ASHPLUME eruption. This material rarely exceeds 1 m in thickness and is limited to the channel cells that lie directly in the path of the plume.

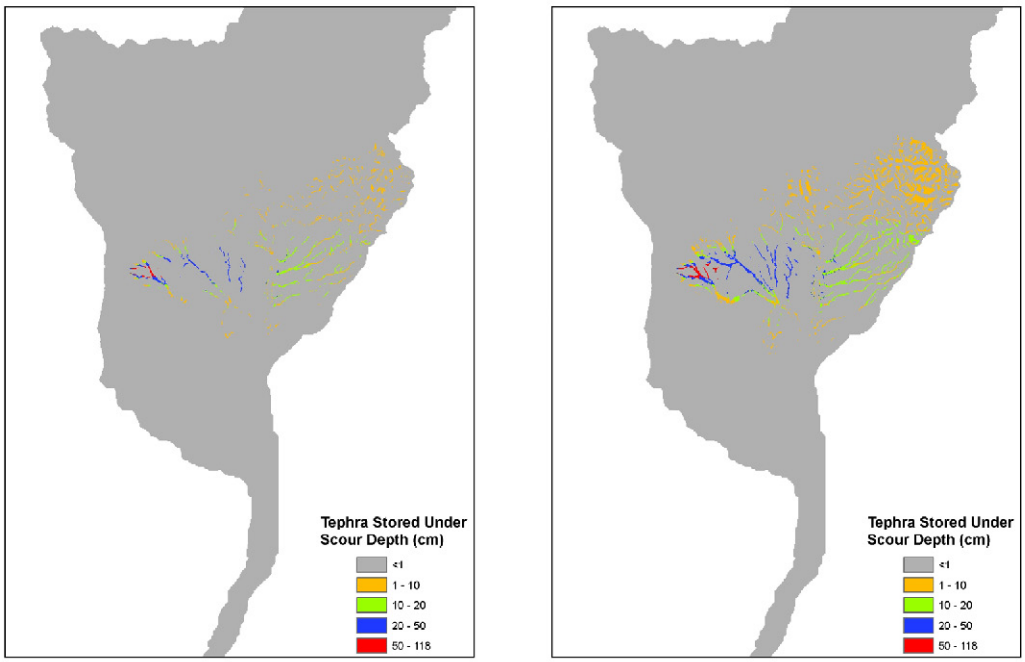

NOTE: Figure was generated using sample model results and is for illustrative purposes only.

Figure 7.2.4-2. Maps of Tephra Thickness Stored under Scour Depth for an Example ASHPLUME Result Shown with Two Values of Drainage Density: Left: 20 km^{-1} and Right: 33 km^{-1}

***Dilution Factor (Step 4)*:** Dilution modeling in FAR is based on the concept that tephra is vertically mixed with uncontaminated channel bed sediments by floods that scour the bed during the waxing phase of the flow and redeposit mixed sediment downstream during the waning phase of the flow. The cumulative effect of many large floods is to mix tephra and uncontaminated sediments both vertically and horizontally downstream.

Conceptually this model is somewhat different from the models used in the mining exploration and contamination literature. In those models, the contaminant concentration at a point downstream is a function of source and non-source concentrations weighted by the relative basin areas upstream of the point. Those models do not make it clear whether mixing/dilution takes place by mixing with uncontaminated channel-bed sediments (in which case mixing could take place very rapidly) or by mixing due to transport of sediments from upstream. The FAR model improves on the earlier models by making the channel mixing/dilution more process based. A volumetric approach is taken by allowing the contaminant concentration at each point to be equal to the ratio of the total contaminant volume from upstream to the total volume of the upstream scour zone (all transported sediment).

7.2.5 Transfer of Tephra from the Upper Basin to the RMEI Domain and the Calculation of Initial Radionuclide Concentrations on Divides and in Channels (Step 5)

Mapping of the RMEI area indicated that relief above active channels is typically on the order of 0.5 to 1.5 m (Appendix A). The small elevation changes in this domain are of the same order of accuracy of a standard USGS DEM (e.g., ~3 m for National Elevation Dataset (Smith and Sandwell [DIRS 177358])), and therefore the spatial analysis methods performed in the upper drainage basin domain could not be used. Another method for determining the thickness and concentration of tephra was necessary.

In earlier software versions, the FAR model conservatively assumed that all of the tephra mass mobilized in the upper drainage basin and transported to the RMEI location was deposited within the channels of the RMEI domain—treating the RMEI location as a perfect depozone. The concentration of that material was equal to the concentration calculated at the basin outlet by the dilution model. The calculated concentration and mass were used to determine a volume of contaminated sediments at the RMEI location. The total channel area at the RMEI location was then used to compute a depth that represented the thickness of surface contamination in the channels of the RMEI location.

While conservative (in that maximum concentrations would be calculated), this early approach was unrealistic. Hydrologic analyses of 100-year , 500-year, and regional maximum floods in Fortymile Wash suggest that mean flow velocities will range between 6 and 28 ft/s (1.8 to 8.5 m/s) (Squires and Young 1984 [DIRS 180001], p. 28). Figure 7.2.5-1 displays a "Hjulström Diagram" developed by Hjulström (1939 [DIRS 182545], Figure 1). This diagram defines whether sediment particles of a given diameter are eroded, transported, or deposited at a given flow velocity. Overlain on the diagram is the expected tephra particle size from measured grain size distributions from analogue explosive cinder-cone eruptions of the magnitude expected at Yucca Mountain (DTN: LA0612DK831811.001 [DIRS 179987]) and the mean flow velocities determined for the Fortymile Wash (Squires and Young 1984 [DIRS 180001], p. 28). The figure shows that for the anticipated flow velocities of major floods, the tephra particles will be eroded and transported downstream.

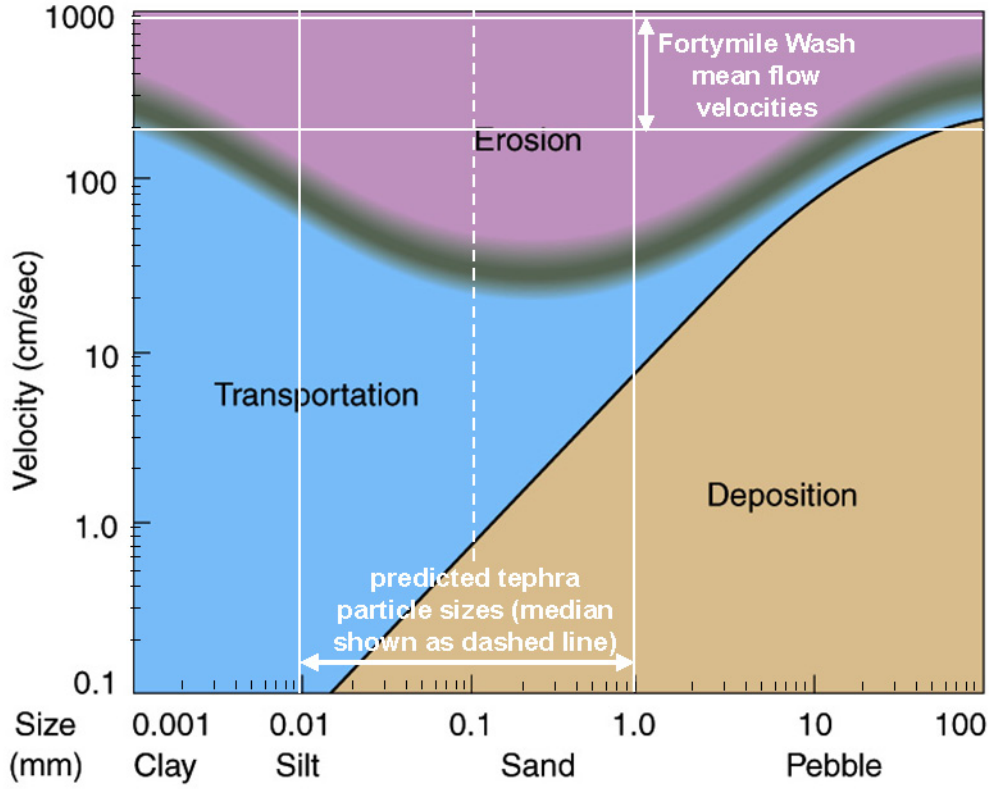

Sources: Adapted from Hjulström 1939 [DIRS 182545], Figure 1.
Expected tephra size range from DTN: LA0612DK831811.001 [DIRS 179987].
Mean flow velocity range from Squires and Young [DIRS 180001], p. 28.

Figure 7.2.5-1. Plot of Stream Flow Velocity versus Particle Size Suspended

At the fan apex, the single channel divides into several separate channels that flow out over the modern alluvial fan (Appendix A, Figures A-4 to A-7). An estimate of the total channel width on the fan is obtained by dividing the area of the active channels (Qa7 from Table A-3, ~1.48×10^6 m^2) with the axial length of the alluvial fan (measured from the map in Figure A-4 to be approximately 9.2 km). The resulting estimated channel width is ~160 m. This is approximately three times the width measured at the Narrows (170 ft or 52 m).

A first order estimate of the effect on flow velocity of increasing the channel width by a factor of 3 is made for the 100-year flood using the Manning Equation (Ritter et al. 1986 [DIRS 154124], p. 195), an empirical formula for open channel flow:

$$V = \frac{1.49}{n} R_h^{(2/3)} \cdot S^{(1/2)} \qquad \text{(Eq. 7-5)}$$

where V is the cross-sectional average velocity (ft/s), n is the Manning coefficient of roughness, R_h is the hydraulic radius (ft), and S is the slope (ft/ft). The hydraulic radius is defined as the cross-sectional area of flow, CA, divided by the wetted perimeter, P ($R_h=CA/P$). The slope is calculated by dividing the hydraulic head, hf, by the length of the channel, L ($S = hf/L$). The

Manning coefficient of roughness is an empirically derived coefficient. The units of (1.49/*n*) are $ft^{1/3}/s$. The 1.49 value is changed to 1, when metric units (m) are used (*n* is unchanged).

Squires and Young (1984 [DIRS 180001], p. 28) estimate water depths ranging from 3 to 8 ft in Fortymile Wash for the 100-year flood and flow velocities that range from 6 to 9 ft/s. If one assumes a rectangular channel with water depth = 5 ft, channel width = 170 ft, n = 0.03 (Squires and Young 1984 [DIRS 180001], p. 24), and adjust slope to equal 0.002, this results in a predicted flow velocity of ~6 ft/s (1.9 m/s), which is consistent with the flow velocity range given by Squires and Young (1984 [DIRS 180001], p. 28). An estimate of the change in velocity as the stream flows out of Fortymile Wash and across the RMEI location is made by adjusting the channel width. If the channel width is increased by a factor of 3, the channel height is adjusted to keep the cross-sectional area constant, and all other parameters are held constant, the flow velocity decreases by a factor of ~2, resulting in a flow velocity of ~3 ft/s (~1 m/s). Despite decreasing, this velocity will still result in significant sediment transport and allow a significant fraction of the mobilized tephra to be transported through and out of the alluvial fan. Therefore, it is reasonable to conclude that the alluvial fan is not a perfect depozone during flood events. Flows in excess of the 100-year flood will be even more likely to transport tephra across and out of the alluvial fan domain.

In the current version of the FAR model (V.1.2), the RMEI location is given as two homogeneous subdomains representing active channels and inter-channel divides, respectively. The inactive portion of the alluvial fan domain (inter-channel divides) receives contaminated tephra only through primary deposition from the eruption. Therefore, the thickness is equal to the erupted tephra-fall thickness at that location and the relative waste concentration is equal to 1 (undiluted). In the active channel subdomain, the thickness of the contaminated tephra is represented by the scour depth at the fan apex. The scour depth at this location is a reasonable but conservative approximation of the scour depth within the active channels of the alluvial fan (see Section 7.1.3, *Scour Depth*). The waste concentration in the active channels of the fan is represented as the sum of the waste deposited directly from the tephrafall and the waste delivered and diluted by the channel at the fan apex. Figure 7.2.5-2 shows a close-up view of example dilution factor results in the vicinity of the fan apex. The color legend has been compressed to illustrate the spatial pattern in the dilution factor in this region. It is clear from the figure that the dilution factor decreases with distance downstream, although the magnitude of the decrease in this region is very small. This figure also shows the location of the grid cell that is used by the model to assign the value: *dilutionfactoroutlet*. It is noted that very little contaminated tephra is actually transported through the RMEI area (examples are presented in Section 7.2.8).

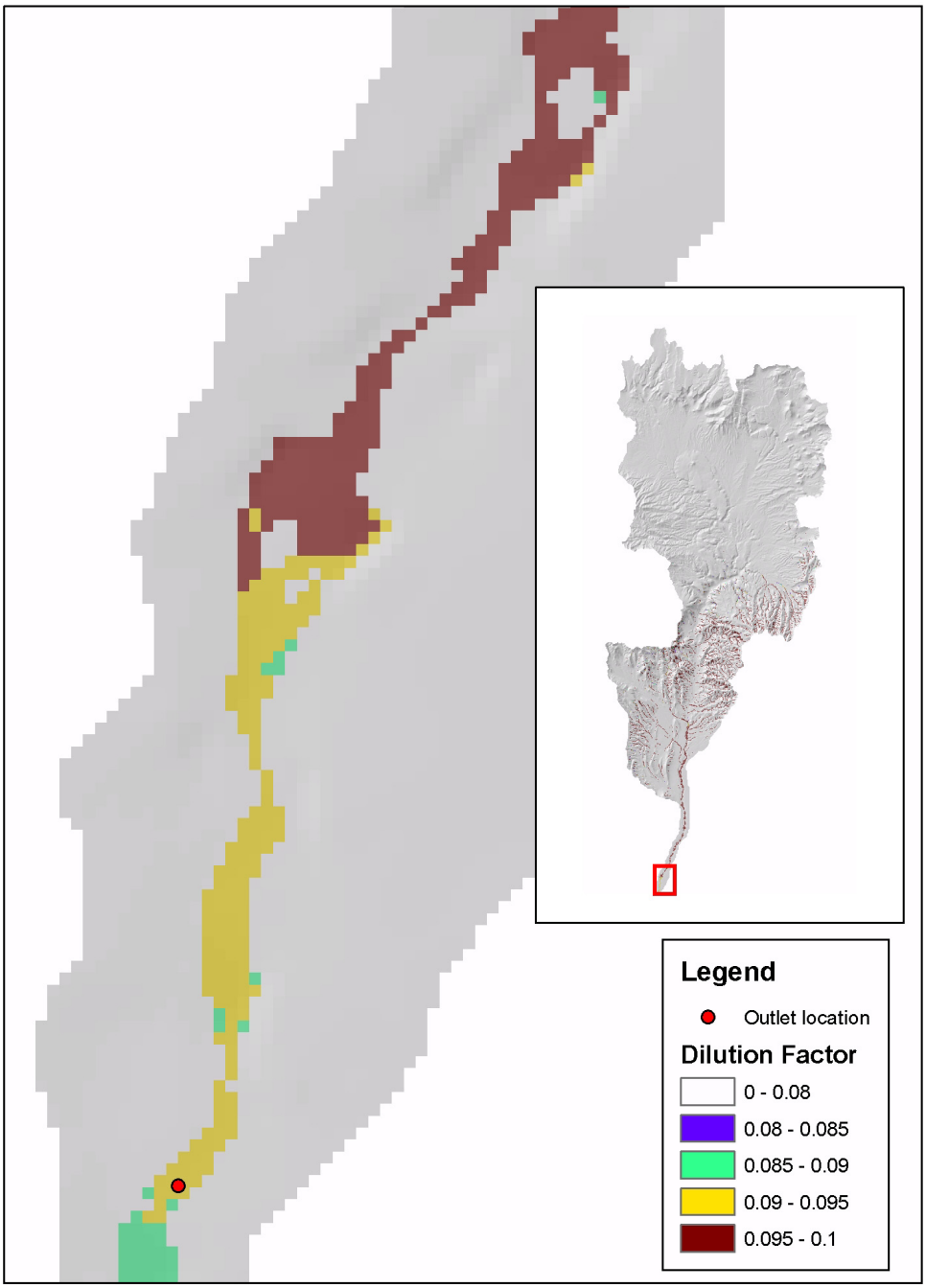

NOTE: Extent is shown with red rectangle in inset map. Figure was generated using sample model results and is for illustrative purposes only. Outlet location is hardwired in the FAR V.1.2 software.

Figure 7.2.5-2. Example Dilution Factor Results near Fan Apex

7.2.6 Compute Diffusion of Radionuclides into Soil (Step 6)

To validate the use of the diffusion equation in the FAR model, various data from the literature were reviewed. A number of vertical profiles of radionuclide concentrations in soil profiles following anthropogenic releases documented in the published literature were plotted. Two sources that provide an abundance of data include: the study by Likhtarev et al. (2002 [DIRS 169810]), who report ^{137}Cs abundance around Chernobyl, and the study by Gale et al. (1964 [DIRS 169807]), who report ^{137}Cs abundance fallout in anthropogenic release experiments done in the United Kingdom. Validation of the diffusion model was performed by fitting observed radionuclide concentrations from these authors to the diffusion model prediction using the methodology detailed in Section 6.5.8.

A nuclear power plant in Chernobyl, Ukraine, released radioactive material in 1986 during a well-publicized accident. Likhtarev et al. (2002 [DIRS 169810]) reported measured vertical profiles of ^{137}Cs activity as a function of distance from the power plant in a southern direction for two years, 1997 and 1999 (11 and 13 years after the event, respectively) (Tables 7.2.6-1 and 7.2.6-2). Diffusivity constants for the six locations varied considerably, from 0.44 to 1.73 cm^2/yr. Soil types associated with the measurements were not recorded but could account for this spread. An average of the mean diffusivity constants calculated for each location is 0.97 cm^2/yr. Four curves of total activity versus depth were generated using this value in Equation 6.5-3 (Section 6.5.8): one curve corresponding to each of the elapsed times from deposition corresponding to the data sets (11 and 13 years), and one curve for the maximum and minimum diffusivity constants calculated for the data set (at an average time from deposition of 12 years). Data are plotted in Figure 7.2.6-1, along with the fraction of total activity calculated from the measured data. The analysis verified that the diffusion model is an appropriate redistribution model.

Gale et al. (1964 [DIRS 169807]) reported ^{137}Cs abundance values from anthropogenic release experiments in the United Kingdom. The experiments were designed to measure the weathering effect over several years for ^{137}Cs deposited on a number of different soil types. Eighteen circular plots of soil, each 200 cm in diameter and 15 cm deep, were spaced 7 m apart in open grassland on the Harwell airfield. Three plots of each of the following soils from the airfield were used: (1) peaty soil, (2) sandy loam, (3) calcareous sandy loam, (4) clayey loam, and (5) calcareous loam. Activity profiles were measured 4.8 years from the initial deposition in the form of cumulative activity in 2-cm-thick layers. For peat, activity profiles obtained by both direct and indirect methods are given. For the calcareous loam from the airfield, activity profiles obtained in disturbed and undisturbed samples are provided. Data and calculation results are presented in Table 7.2.6-3. Diffusivity constants for the five soil types varied from 1.95 to 5.98 cm^2/yr. Modeled curves of total activity versus depth were generated for each soil type using the average diffusivity constant for each type in Equation 6.5-3 (Section 6.5.8). Data are plotted in Figure 7.2.6-2, along with the fraction of total activity calculated using the calculated diffusivity constant from the measured data. Agreement between the calculated curves using the diffusion model and the measured profiles is excellent, again verifying that diffusion is an appropriate and valid vertical redistribution model.

The significance of these analyses was to show that the diffusion model works well for predicting the vertical redistribution of radionuclides in a variety of environments. It is important to recognize that, in general, both advection and diffusion will occur. However, available data from anthropogenic radionuclide depositions is insufficient to determine the advection velocity, since the maximum concentration of radionuclides in all of the published literature considered was in the surface interval (consistent with zero advection). A conservative assumption of zero advection velocity was made for the FAR model (conservative because the radionuclide concentration remains higher at the surface).

It is noted that there are considerable differences in the climatic and geomorphic environments between the published data sets discussed above and the RMEI location. Therefore, while these data demonstrate the ability of the diffusion model to capture the migration of radionuclides into the subsurface, they do not provide a quantitative diffusivity constant that can be applied to the RMEI domain.

Table 7.2.6-1. ^{137}Cs Measurements as a Function of Depth near Chernobyl in 1997

Year of Measurement -->			1997								
Dist from Power Plant -->			30 to 50 km			150 to 240 km			40 to 220 km		
Depth Interval	Starting Depth (cm)	Ending Depth (cm)	Mean Activity	Fraction of Total Activity to Depth z	D (cm^2/yr)	Mean Activity	Fraction of Total Activity to Depth z	D (cm^2/yr)	Mean Activity	Fraction of Total Activity to Depth z	D (cm^2/yr)
1	0	2	70.2	0.70	0.17	34.9	0.35	0.89	27.0	0.27	1.53
2	2	4	15.5	0.85	0.34	27.3	0.62	0.94	34.6	0.62	0.96
3	4	6	6.6	0.92	0.53	16.7	0.79	1.05	19.0	0.81	0.97
4	6	8	3.5	0.96	0.72	9.3	0.88	1.19	9.7	0.90	1.06
5	8	10	2.1	0.98	0.89	5.6	0.94	1.31	5.1	0.95	1.14
6	10	12	1.4	0.99	0.99	3.6	0.97	1.32	2.8	0.98	1.17
7	12	14	1.0	1.00		2.6	1.00		1.8	1.00	
Total Activity			100.30			100.00			100.00		
Average Diffusivity					0.61			1.11			1.14

Sources: Output DTN: SN0708DIFFVALD.001; mean activity values are from Likhtarev et al. 2002 [DIRS 169810].

NOTE: Fraction of total activity to depth z is calculated by summing the mean activity to the desired depth and dividing by the total activity (calculated as the sum of the mean activity for all depth intervals). Diffusivity constants are calculated as described in Section 6.5.8.

Table 7.2.6-2. ^{137}Cs Measurements as a Function of Depth near Chernobyl in 1999

Year of Measurement -->			1999								
Dist from Power Plant -->			50 to 70 km			170 to 240 km			70 to 220 km		
Depth Interval	Starting Depth (cm)	Ending Depth (cm)	Mean Activity	Fraction of Total Activity to Depth z	D (cm^2/yr)	Mean Activity	Fraction of Total Activity to Depth z	D (cm^2/yr)	Mean Activity	Fraction of Total Activity to Depth z	D (cm^2/yr)
1	0	2	70.0	0.70	0.14	38.7	0.39	0.60	20.1	0.20	2.36
2	2	4	16.6	0.87	0.27	26.1	0.65	0.71	34.4	0.55	1.10
3	4	6	6.0	0.93	0.43	16.7	0.82	0.79	14.6	0.69	1.33
4	6	8	3.2	0.96	0.60	9.5	0.91	0.86	7.8	0.77	1.70
5	8	10	1.9	0.98	0.74	3.9	0.95	1.01	4.9	0.82	2.14
6	10	12	0.8	0.99	(1)	2.1	0.97	(1)	3.6	0.86	(1)
7	12	14	0.7	0.99	(1)	1.7	0.99	(1)	4.0	0.90	(1)
8	14	16	0.4	1.00	(1)	0.8	1.00	(1)	5.3	0.95	(1)
9	16	18	0.2	1.00	(1)	0.3	1.00	(1)	2.2	0.97	(1)
10	18	20	0.2	1.00	(1)	0.2	1.00	(1)	2.9	1.00	(1)
Total Activity				100.00			100.00			99.80	
Average Diffusivity					0.44			0.79			1.73

Sources: Output DTN: SN0708DIFFVALD.001; mean activity values are from Likhtarev et al. 2002 [DIRS 169810].

(1) Incremental fraction of total activity to depth z is so small that the calculated D approaches zero. Data were not used.

NOTE: Fraction of total activity to depth z is calculated by summing the mean activity to the desired depth and dividing by the total activity (calculated as the sum of the mean activity for all depth intervals). Diffusivity constants are calculated as described in Section 6.5.8.

Table 7.2.6-3. ^{137}Cs Measurements as a Function of Depth at Harwell Airfield, England

Start Depth (cm)	End Depth (cm)	Peat		Peat		Sandy Loam		Calcareous Sandy Loam		Clayey Loam		Air Field – Disturbed		Air Field – Undisturbed	
		% of Total Act. to Depth z	D cm^2/yr	% of Total Act. to Depth z	D cm^2/yr	% of Total Act. to Depth z	D cm^2/yr	% of Total Act. to Depth z	D cm^2/yr	% of Total Act. to Depth z	D cm^2/yr	% of Total Act. to Depth z	D cm^2/yr	% of Total Act. to Depth z	D cm^2/yr
0	2	0.22	5.34	0.47	1.06	0.21	5.88	0.37	1.80	0.32	2.45	0.31	2.62	0.28	3.24
0	4	0.41	5.74	0.72	1.43	0.41	5.74	0.66	1.83	0.55	2.92	0.58	2.56	0.54	3.05
0	6	0.57	6.02	0.85	1.81	0.60	5.29	0.82	2.09	0.70	3.49	0.76	2.72	0.76	2.72
0	8	0.70	6.21	0.92	2.18	0.76	4.83	0.90	2.46	0.81	3.88	0.87	2.91	0.89	2.61
0	10	0.80	6.34	0.96	2.47	0.86	4.78	0.95	2.71	0.88	4.31	0.93	3.17	0.95	2.71
0	12	0.88	6.21	0.98	2.77	0.93	4.57	0.97	3.19	0.92	4.89	0.96	3.56	0.98	2.77
0	14	0.94	5.77	0.99	3.08	0.97	4.34	0.99	3.08	0.96	4.84	0.98	3.77	0.99	3.08
0	20	1.00		1.00		1.00		1.00		1.00		1.00		1.00	
Avg. D (m^2/yr)			5.98		1.95		5.18		2.18		3.41		2.80		2.87

Sources: Fraction of total activity to depth z is from Gale 1964 [DIRS 169807]. Diffusivity constants are calculated as described in Section 6.5.8, Output DTN: SN0708DIFFVALD.001.

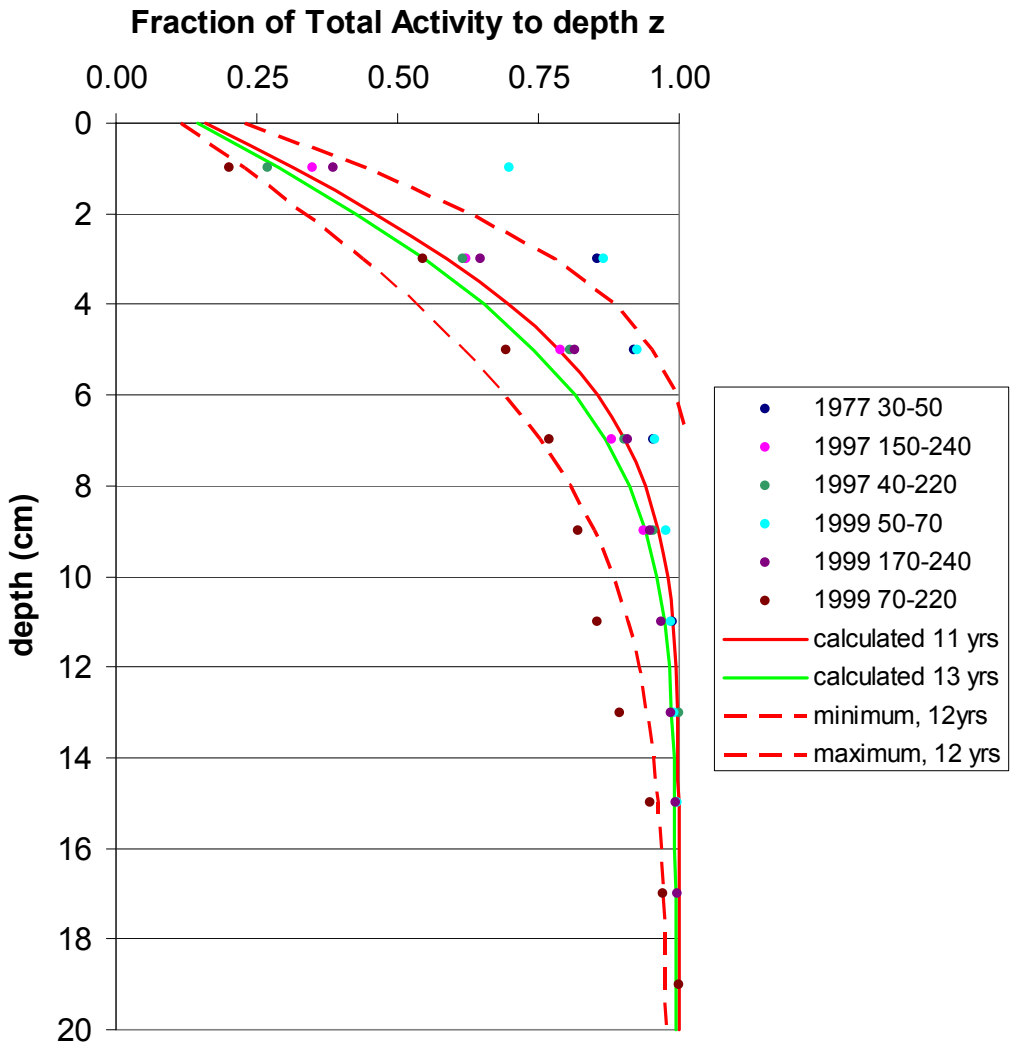

Source: Output DTN: SN0708DIFFVALD.001.

NOTE: Measured data are from Tables 7.2.6-1 and 7.2.6-2, and show the fraction of total activity to the specified depth for various ranges of distance from the power plant (in km). Calculated curves were generated using an average diffusivity value from all data for times corresponding to 11 and 13 years after deposition. Bounding curves (based on the maximum and minimum calculated diffusivity values from the data) are shown for an average time after deposition of 12 years.

Figure 7.2.6-1. Total Activity of ^{137}Cs as a Function of Depth for Chernobyl

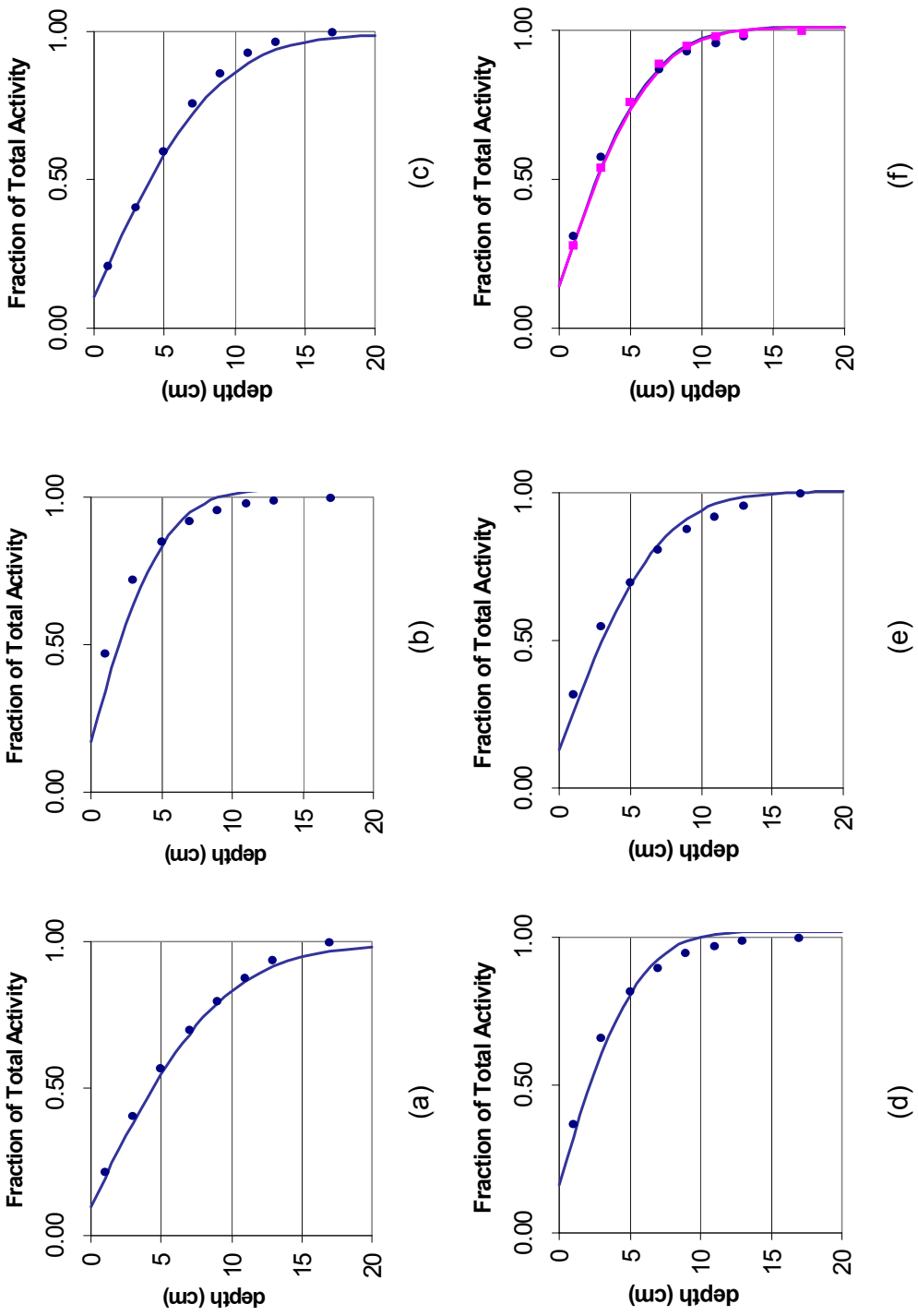

Source: Output DTN: SN0708DIFFVALD.001.

NOTES: (a) Peat-measured profile from observations of core samples; (b) peat-activity profile deduced with five-chamber "probe"; (c) sandy loam (combined profile); (d) calcareous sandy loam (combined profile); (e) clayey loam (combined profile); (f) calcareous loam from the airfield, both disturbed and undisturbed profiles.

Figure 7.2.6-2. Total Activity of ^{137}Cs as a Function of Depth for Harwell Airfield

7.2.7 Test Cases for the FAR Model

FAR V.1.2 was developed under IM-PRO-004, *Qualification of Software*. Two test cases were completed for the software validation report (DOE 2007 [DIRS 183120]). The first test case validated the model using Cartesian coordinates; the second validated the model using polar coordinates. Criteria associated with these test cases included validation that the:

1. Output elevations of the model were equal to the input values to within one decimal point.

2. Output slope calculations from the model were equal to values calculated using an Excel workbook (to within two decimal points of accuracy).

3. Value of the output contributing area from the model is equal to the value calculated using an Excel workbook (to within two decimal points of accuracy).

4. Output dilution factor from the model is equal to the value calculated using an Excel workbook (to within two decimal points of accuracy).

5. Output interpolated, rectified ASHPLUME grids are equal to the values calculated using an Excel workbook (to within two decimal points of accuracy).

6. Values of the mobilized tephra and fuel grids are equal to the values calculated by hand to within two decimal points of accuracy.

7. Values for *primaryashthickness*, *fuelsurfacedivide*, *fueldepthBdivide*, *depthfuelchannel*, *fuelsurfacechannel*, and *fueldepthBchannel* match the values calculated using an Excel workbook to within two significant figures.

8. Output time series for the concentration on inter-channel divides, depth-integrated concentration on divides, surface concentration in channels, and depth-integrated concentration in channels is equal to the values calculated in an Excel workbook for two time steps (100 and 1,000 years) to within two significant figures.

7.2.8 Distribution of Tephra Mass

Although the FAR model represents an open system in which redistributed tephra can leave the model domain at the outlet, it is possible to track tephra mass in the calculation to (1) demonstrate that all tephra in the system can be accounted for, and (2) provide a level of confidence that the model results are reasonable.

There are several mass balance equations that can be evaluated from the results provided by FAR V.1.2. The FAR output file provides a selection of summary results, including the total mass of tephra and waste that is initially deposited within the upper drainage basin. This tephra mass can be divided into the four classification regions (presented graphically in Figure 6.3.3-7) depending on local values of slope and stream power. FAR V.1.2 can output grid cell values for initial tephra thickness, local slope, contributing area, scour depth, and dilution factor. These cell-by-cell values can be used along with the summary output to illustrate the mass balance.

To demonstrate the calculation of the mass balance, a set of FAR simulations is used. These simulations are identical except for the values assigned to the following input variables: critical slope (*S*), drainage density (*X*), and scour depth (*H*). Table 7.2.8-1 lists the parameter values used for the simulations analyzed in this section.

Table 7.2.8-1. List of FAR V.1.2 Simulations Used in Mass Balance Calculations

Run Name	Critical Slope (*S*)	Drainage Density (*X*) (km^{-1})	Scour Depth at Outlet (*H*) (cm)
FAR01	0.34	33.33	97.5
FAR02	0.34	20	97.5
FAR03	0.34	33.33	73
FAR04	0.34	33.33	122
FAR05	0.21	20	73
FAR06	0.21	20	122

7.2.8.1 Topographic Classification of Tephra on Landscape

Total mass of tephra deposited in the upper drainage basin (*totalash*) (g) is provided in the FAR text output file. Tephra is considered mobilized according to grid-cell characteristics related to slope and stream power. Table 7.2.8-2 presents the percent of *totalash* that is present in each of the four classification regions (presented graphically in Figure 6.3.3-7) for each of the FAR runs listed in Table 7.2.8-1. In addition, the mass fraction in the channel regions has been divided into material present above the scour depth (mobile) and material below the scour depth (immobile).

Table 7.2.8-2. Summary of Tephra Mass Fraction Partitioning

Run Name	% Steep Channels (above scour) (below scour)	% Gradual Channels (above scour) (below scour)	% Steep Hillslopes	% Gradual Hillslopes
FAR01	(1.4) (0.4)	(4.9) (2.4)	5.4	85.4
FAR02	(0.4) (0.1)	(3.4) (1.0)	6.8	88.3
FAR03	(1.3) (0.6)	(4.3) (3.0)	5.4	85.4
FAR04	(1.5) (0.3)	(5.4) (1.9)	5.4	85.4
FAR05	(0.6) (0.2)	(2.8) (1.3)	14.1	81.0
FAR06	(0.7) (0.1)	(3.4) (0.7)	14.1	81.0

7.2.8.2 Calculation of Mobilized Tephra Mass

Tephra mobilization occurs in a number of calculation steps detailed in Section 6.3.3. Table 7.2.8-3 presents the calculated mass of mobilized tephra for each of the FAR runs listed in Table 7.2.8-1. The calculation of tephra mobilization is described below.

1. Total mass of tephra deposited in upper drainage basin (*totalash*) (g) is provided in FAR text output file.

2. The total mass of tephra that is mobilized in the upper basin (*totalmobilizedash*) (g) is not reported in the text output, but can be calculated from grid outputs of tephra thickness, slope, and scour depth. *totalmobilizedash* is the sum of tephra thickness in all grid cells (except those bordering the watershed) where slope ≥ S or scour depth > 0. If scour depth > 0 and tephra thickness > scour depth, the thickness of mobilized tephra from that grid cell is assumed to equal scour depth.

3. The total mass of tephra mobilized in the upper basin that enters channels that are **connected** to the basin outlet (*ashmobilized*) (g) is reported in the text output file.

Table 7.2.8-3. Summary of Mobilized Tephra Mass Balance Results

Run Name	*totalash* (g)	*totalmobilizedash* (g) {% *totalash*}	*ashmobilized* (g) {% *totalash*}	Percent of *totalmobilizedash* connected to main Fortymile Wash channel	*dilutionfactoroutlet*
FAR01	2.83×10^{13}	3.31×10^{12} {11.7}	2.09×10^{12} {7.4}	63.2	0.094
FAR02	2.83×10^{13}	3.00×10^{12} {10.6}	1.48×10^{12} {5.3}	49.6	0.090
FAR03	2.83×10^{13}	3.09×10^{12} {10.9}	1.97×10^{12} {6.9}	63.7	0.116
FAR04	2.83×10^{13}	3.47×10^{12} {12.3}	2.18×10^{12} {7.7}	62.6	0.079
FAR05	2.83×10^{13}	4.95×10^{12} {17.5}	2.18×10^{12} {7.7}	44.1	0.157
FAR06	2.83×10^{13}	5.14×10^{12} {18.1}	2.24×10^{12} {7.9}	43.7	0.103

7.2.8.3 Transfer of Tephra Mass to RMEI Location

Since the output of the FAR scour-dilution-mixing model is tephra concentration in the channels of the RMEI location, it is impossible to calculate a total mass of tephra (or waste) deposited at this location without assuming a total RMEI area and fraction of that area composed of active channels. These parameters are developed in this report despite the fact that TSPA only uses the value for the fraction of the RMEI area composed of active channels to calculate dose. If the RMEI area, A, and channel fraction, F, which were developed in Section 6.5.4, are used to characterize the RMEI location, it is then possible to calculate the fractions of *ashmobilized* that are deposited in the RMEI location, stored in the channels of the upper basin, and, potentially, the fraction that flows beyond the RMEI location into Amargosa Valley. The mass of this tephra deposited in the channels at the RMEI location is equal to the product of H, *dilutionfactoroutlet*, F, and A divided by the tephra density, ρ. The mass of this tephra assumed to be stored in the upper basin after redistribution is calculated as the integral of the product: dilution factor times scour depth for all channel cells in the upper basin that are connected to the outlet. Any mass that is left over when these two quantities are summed and subtracted from *ashmobilized* is assumed to have flowed out of the system. Table 7.2.8-4 lists these masses as percentages of *ashmobilized* for each run and bounding values of F. Looking at the results, it is obvious that the utility of this calculation is limited because in many cases (highlighted in the table) the total mass of tephra redistributed to the RMEI domain is larger than what is available, assuming a mass balance (the mass deposited in the RMEI is larger than *ashmobilized* – mass stored in the connected channels of the upper basin). This result is not surprising because the methodology used to transfer tephra and waste to the RMEI domain (Section 6.3.3, STEP 5) does not enforce a

mass balance. In any case, the results of this exercise do show that the concentrations predicted for the RMEI channels are reasonably consistent with the available information characteristics of the RMEI location, because mass balance inconsistencies are not more than a factor of two. Furthermore, when there is a mass-balance inconsistency, the model predicts a concentration in the channels that is greater than would be calculated if mass balance was enforced, and therefore the results are conservative with respect to initial channel concentration in these cases.

Table 7.2.8-4. Summary of Tephra Transfer to RMEI Location

Run Name	% *ashmobilized* deposited in RMEI channels	% *ashmobilized* stored in upper basin	% *ashmobilized* transported beyond RMEI location
FAR01 (F = 0.09)	13	82.2	4.8
FAR01 (F = 0.54)	*78.3*	*82.2*	*–60.4*
FAR02 (F = 0.09)	17.6	72.4	10.0
FAR02 (F = 0.54)	*105.6*	*72.4*	*–78*
FAR03 (F = 0.09)	12.7	76.1	11.2
FAR03 (F = 0.54)	*76.4*	*76.1*	*–52.5*
FAR04 (F = 0.09)	*13.2*	*87.2*	*–0.4*
FAR04 (F = 0.54)	*79.4*	*87.2*	*–66.6*
FAR05 (F = 0.09)	15.6	54.5	29.9
FAR05 (F = 0.54)	*93.6*	*54.5*	*–48.0*
FAR06 (F = 0.09)	16.6	64.7	18.8
FAR06 (F = 0.54)	*99.4*	*64.7*	*–64.1*

NOTE: Percentages in red italics indicate that the inferred mass of tephra deposited at the RMEI location exceeded the difference between the total mobilized tephra and amount of mobilized tephra stored in the upper basin following the redistribution process.

7.2.8.4 Summary of Tephra Mass Distribution

Overall, review of these model results indicates that, of the total mass of contaminated tephra deposited in the upper drainage domain (*totalash*), most will be stored on the relatively flat areas classified as gradual hillslopes. Of the total tephra mass transported to the channel system within the drainage domain (*totalmobilizedash*), approximately half of this material is available to channels that are connected to the main Fortymile Wash channel (*ashmobilized*). This tephra mass (*ashmobilized*) becomes diluted during transport to the outlet. The tephra concentration at the outlet (*dilutionfactoroutlet*) varies from about 0.1 to 0.16 in the runs presented.

7.2.9 Confidence Building from Sensitivity Studies

A parameter sensitivity study is documented in Section 6.6. The study was divided into two separate analyses. The first analysis examined the sensitivity of the scour-dilution-mixing model to three uncertain parameters: critical slope, drainage density, and scour depth at the Narrows. The results of this analysis build confidence that model is working as designed and giving reasonable results. By increasing critical slope, a greater proportion of the tephra deposit is mobilized and transported into channels. A portion of these channels are connected to the outlet, and thus, in general, tephra included in the dilution calculation at the outlet increases and

concentration increases. Scour depth and drainage density parameters are linked in a more complicated way. As scour depth increases, less tephra that initially fell in channels is stored beneath the scour zone (which would increase mobilized tephra), but more clean sediment is also included in the dilution calculation. For the eruption scenario used in the sensitivity study (east directed plume), the role of increased clean sediment outweighed the effect of adding more tephra, and therefore concentrations tend to decrease with increasing scour depth. Drainage density controls how much of the landscape is classified as channels, and therefore as it increases there is more of the basin that becomes connected to the outlet. Given the eruption scenario in this example, outlet concentration increases as drainage density increases.

The second analysis examined the effect that uncertainty in the inputs to the diffusion calculation had on the time-varying concentration at the RMEI location. These results build confidence that the diffusion submodel is behaving as designed; both surface and depth integrated concentrations decrease with increasing diffusivity values, the time to reach an equilibrium concentration decreases with increased diffusivity values, and equilibrium concentrations remain constant for all diffusivity values (all other parameters being constant).

7.3 POST-DEVELOPMENT MODEL VALIDATION

Level II validation requires that model predictions are reasonably corroborated by at least two post-model development validation methods described in Step 6.3.2 of SCI-PRO-006. This section provides a discussion of the application of the two post-model development validation methods used: (1) corroboration of model results with relevant information published in refereed journals and (2) critical review conducted by a technical specialist. Section 7.3.1 summarizes two refereed journal articles that describe the application of a mathematical model that is nearly identical to the qualified FAR V.1.2 software to an analogue site near Yucca Mountain and its corroboration by field data. Section 7.3.2 discusses issues raised by the critical reviewers for model validation and provides author responses to these issues. The memos written by the critical reviewers for model validation are included in Appendix C.

7.3.1 Corroboration of Model Results with Relevant Information Published in Refereed Journal

The qualified version of FAR V.1.2 contains a number of input parameters specific to the Fortymile Wash study area that are hard coded into the software (e.g., the coordinates, extent, and resolution of the DEM). As such, the qualified code cannot be used to model other sites. However, Pelletier et al. (2007 [DIRS 182110]) applied a model very similar to the qualified version of FAR V.1.2 to the Lathrop Wells volcanic area near Yucca Mountain, Nevada, and compared model results against measured field data. The following discussion summarizes this study published in a refereed journal article.

There are several differences between the modeling approach used for Yucca Mountain TSPA calculations and that used for the Lathrop Wells study. The essential steps of the Lathrop Wells model, including using the bifurcation routing methodology, were the same as those for the qualified FAR V.1.2 model described in this report. One significant difference is that the Lathrop Wells model did not include the critical slope threshold for tephra mobilization as is done with the FAR model. This is appropriate because the extent and thickness of the original

tephra sheet is unknown at Lathrop Wells because of its age, and therefore the measured tephra concentration and scour depth in channels were used to estimate the tephra source concentration and thickness. In addition, the time-dependent diffusion model is not implemented in the Lathrop Wells modeling study.

7.3.1.1 Lathrop Wells Site Description

At 77 ka in age (Heizler et al. 1999 [DIRS 107255]), the Lathrop Wells cinder cone is the youngest basaltic volcano in the Yucca Mountain region. It is the southern-most surface expression of the Plio-Pleistocene-age Crater Flat Volcanic Zone (CFVZ) (Crowe and Perry 1990 [DIRS 100973]). The tephra sheet surrounding the cinder cone was deposited during a single explosive eruption. Tephra from this eruption is unconsolidated and hence readily mobilized by hillslope and fluvial processes into downstream channels. The lava flows associated with Lathrop Wells have, in contrast, weathered very little since emplacement and hence contribute very little sediment to downstream channels. The relative youth and location of Lathrop Wells with respect to Yucca Mountain have made it a focus of intense study as a possible analogue for an eruption through the repository.

The Lathrop Wells volcanic center provides a concentrated source of tephra that is diluted by non-volcanic sediment within channels during transport downstream. The site is 18 km south of the Fortymile Wash Narrows (Figure 7.3.1-1). The scour-dilution-mixing model was applied to the site to predict the fraction of basaltic sediments in channels draining the Lathrop Wells tephra sheet. Lathrop Wells is the sole source of basaltic sediments in the surrounding drainage basin (Miocene-age welded tuff comprises the other rock type), so it acts as a well-defined and localized source of basaltic sediments to downstream channels. Basaltic and non-basaltic sediments in the basin are of similar grain size (medium sand to pebble), so the contaminant is well-mixed with and transported at rates similar to uncontaminated channel sediments.

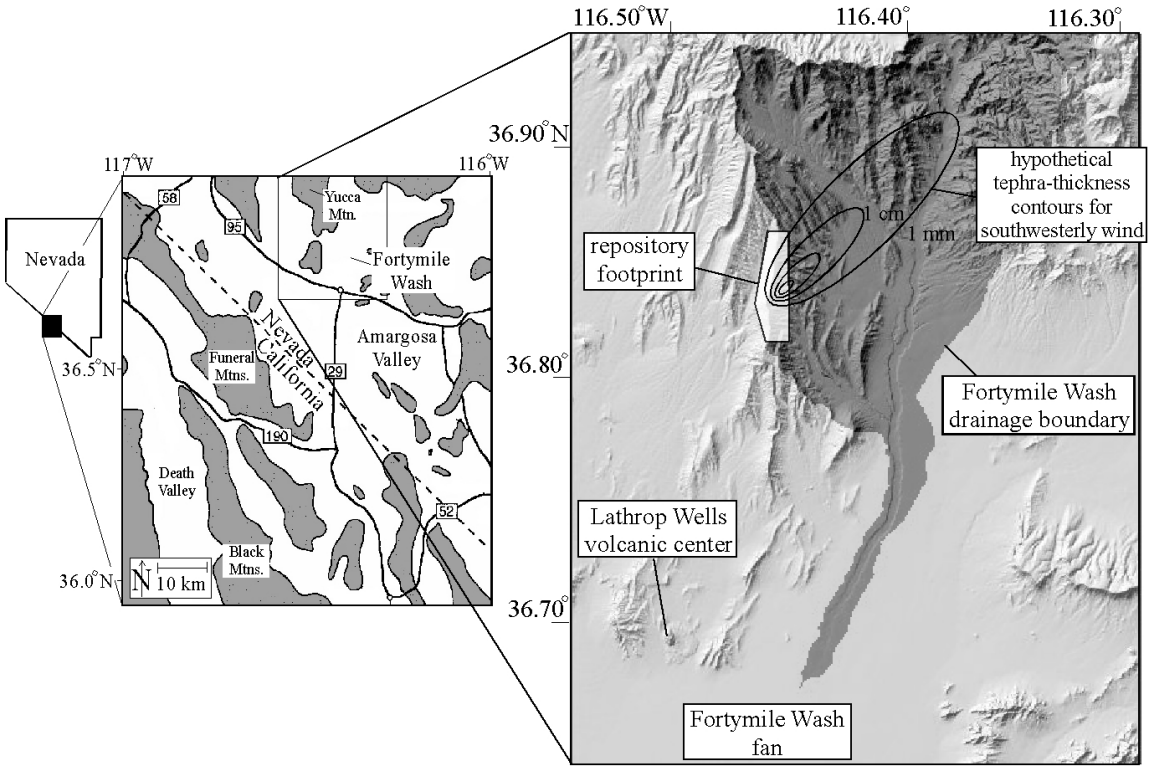

Source: Pelletier et al. 2007 [DIRS 182110], Figure 1.

NOTE: Shaded relief image includes Lathrop Wells volcanic center, the footprint of the repository at Yucca Mountain, and the southern portion of the Fortymile Wash drainage basin (i.e., the site of primary fallout for tephra with potential for redistribution to the Fortymile Wash fan where the nearest population resides).

Figure 7.3.1-1. Location Map of the Study Areas in Amargosa Valley, Nevada

7.3.1.2 Field Data

There are two principal drainages that transport tephra from Lathrop Wells (Figure 7.3.1-2). The western drainage system transports material from the exposed tephra sheet on the northwest side of Lathrop Wells cone west and south into Amargosa Valley. The eastern drainage system heads near the northern margin of the tephra sheet and transports material around the eastern side of the Lathrop Wells cone and adjacent lava flows. Twenty-five samples of channel-bed sediments were collected along these two channel systems to evaluate the significance of the dilution process and validate the scour-dilution-mixing model. In small channels on the tephra sheet, the bottom of the scour zone was clearly visible and ranged from 12 to 29 cm in depth in channel-bed-sediment sample pits. In larger channels downstream from the tephra sheet, the bottom of the scour zone was not visible within the sample pits (which were limited to 30 to 40 cm in depth). Samples were taken by uniformly sampling pit-wall material to a depth of 30 cm or to visible scour depth if less than 30 cm. Samples were sieved, and material larger than silt size was separated with a magnet into basaltic and non-basaltic fractions and visually checked for complete separation using a stereomicroscope. The basaltic material was strongly magnetic and total separation error was estimated to be less than 5% by mass. Non-basaltic material was comprised of Miocene welded tuff and eolian sand. The fraction of basaltic sediment by mass was calculated for each sample. This value was converted to a fraction by volume (for

comparison to the volumetric dilution-mixing model) using an average measured basalt density of 1.5 g/cm^3 (low due to its high vesicularity) and a tuff density of 2.7 g/cm^3.

Mixing occurs along both drainages according to the trend evident in the table of basaltic content in the sediment (Table 7.3.1-1) and in plots of basalt concentration as a function of distance from the channel head (Figure 7.3.1-2B). These data indicate that the concentration of basaltic tephra is reduced by more than 50% within 1 km from where each channel leaves the tephra sheet.

Table 7.3.1-1. Basaltic Sediment Percentages (by volume) of Channels Draining Lathrop Wells Tephra Sheet

Sample ID	UTM Northing, Easting	Distance from Channel Head (km)	Basaltic Sediment (%)	Scour Depth (cm)
West Channel Data				
SD091405.01	4061145, 543337	0.1	77.44	27
SD091405.02	4061073, 543384	0.3	74.66	22
SD091405.03	4060892, 543383	0.6	69.96	15
SD091405.04	4061117, 543057	N/A	37.49	N/A
SD091405.05	4061007, 543095	N/A	44.97	N/A
SD091405.06	4060872, 543167	N/A	11.11	N/A
SD091405.07	4060680, 543243	N/A	25.80	N/A
SD091405.08	4060618, 543290	0.9	76.31	29
SD091405.09	4060531, 543284	1.0	40.92	N/A
SD091405.10	4060341, 543288	1.3	47.04	N/A
SD091405.11	4060115, 543361	1.6	38.77	N/A
SD091405.12	4059904, 543473	1.9	36.20	N/A
East Channel Data				
SD091505.01	4061258, 543556	0.3	61.01	25
SD091505.02	4061272, 543520	0.2	83.14	12
SD091505.03	4061346, 543448	0.0	67.29	16
SD091505.04	4061193, 544413	1.5	36.84	N/A
SD091505.05	4061176, 544565	N/A	6.76	N/A
SD091505.06	4061189, 544811	2.2	10.96	N/A
SD091505.07	4060676, 544963	2.7	14.25	N/A
SD091505.08	4060779, 545172	N/A	2.98	N/A
SD091505.09	4059949, 545051	3.2	5.24	N/A
SD091505.10	4059467, 544883	3.7	7.16	N/A
SD091505.11	4059552, 544784	3.7	6.57	N/A
SD091505.12	4059244, 544557	4.2	5.17	N/A
SD091505.13	4059077, 544609	4.2	3.19	N/A

Source: Pelletier et al. 2007 [DIRS 182110], Table 1.

NOTE: Distances from channel heads are only listed for samples taken from the two channels. The samples with no distances listed (N/A) were taken to estimate background values. Scour depth could only be observed if it was less than about 0.5 m and if the basalt concentration was sufficiently high that changes could be observed at the base of the scour zone. N/A in this column means that scour depth could not be measured.

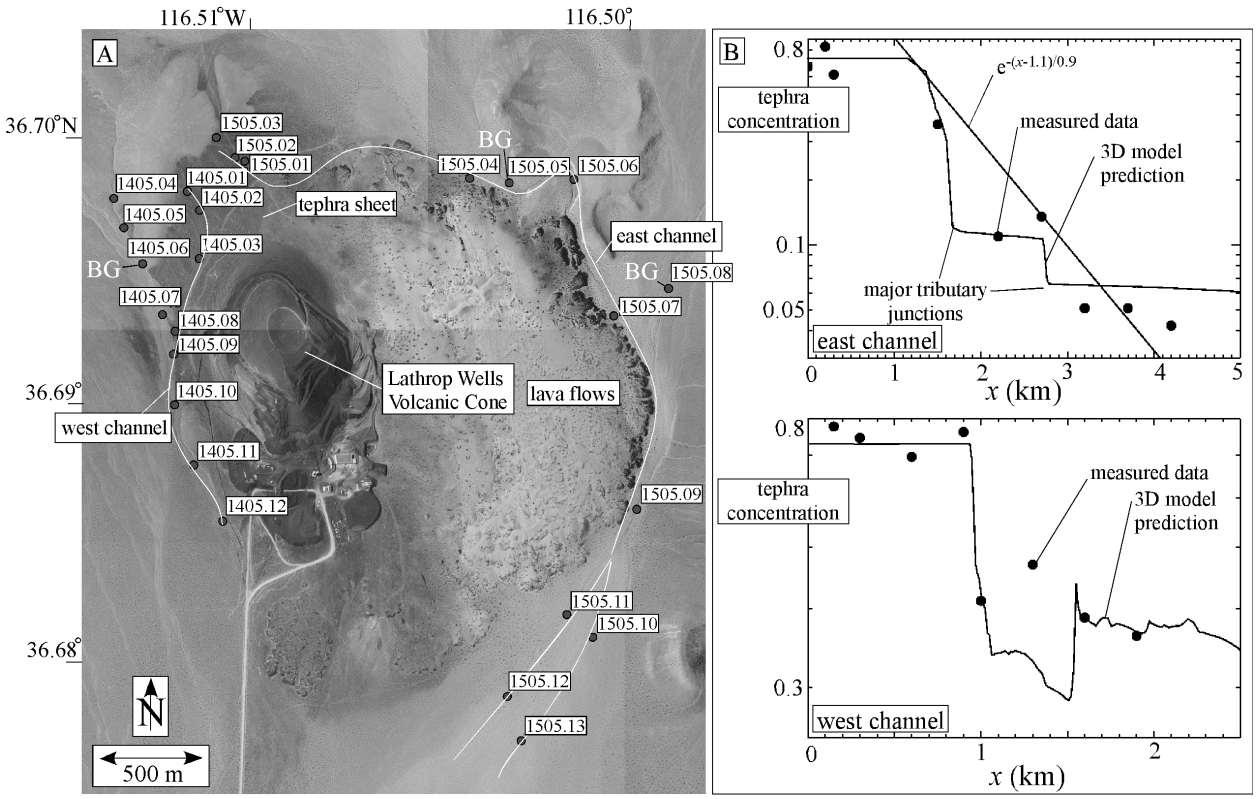

Source: Pelletier et al. 2007 [DIRS 182110], Figure 4.

NOTE: (A) Sample location map for tephra concentration in the east and west channels draining the Lathrop Wells tephra sheet (data in Table 1). The first four letters of each sample ID ("SD09") were left out because they are the same for each sample. (B) Comparison plots of measured and modeled predictions for tephra concentration as a function of distance along-channel (note logarithmic scale on vertical axis, needed to visualize data over 1 to 2 orders of magnitude). Also graphed is a best-fit exponential curve for the east channel.

Figure 7.3.1-2. Sample Location Map, Tephra Concentration, and Model Results for Lathrop Wells Site

Both the east and west drainage systems are discontinuous: incised channels head in the steep, northern end of the tephra sheet and give way to broad, unincised depositional "saddles" that become re-incised as they leave the tephra sheet. Field photographs illustrate the three-dimensional patterns of dilution in these channel systems (Figure 7.3.1-3). In the headwaters of the east and west channel systems, sediment-sample pits reveal a fluvially mixed scour zone with approximately 73% tephra ranging in depth from 12 to 29 cm, underlain by the primary tephra sheet characterized by nearly 100% tephra concentrations. In the middle portion of the tephra sheet (i.e., the depositional "saddle"), a shallow scour zone is underlain by debris-flow deposits composed primarily of Miocene welded tuff (Figure 7.3.1-3A). At the edge of the tephra sheet, channels become re-incised and a fluvially-mixed layer is underlain by pure tephra (Figure 7.3.1-3B). Channels on the tephra sheet are not pure tephra because the northern drainage divide is composed of Miocene welded tuff (and hence a small component of the tephra-sheet drainage basin has non-basaltic source rocks) and because eolian sand has been deposited in the basin. Off of the tephra sheet, the dilution effect downstream of tributary junctions is clearly visible in the field as small channels draining the tephra sheet join with larger channels of primarily non-basaltic sediments (Figure 7.3.1-3C).

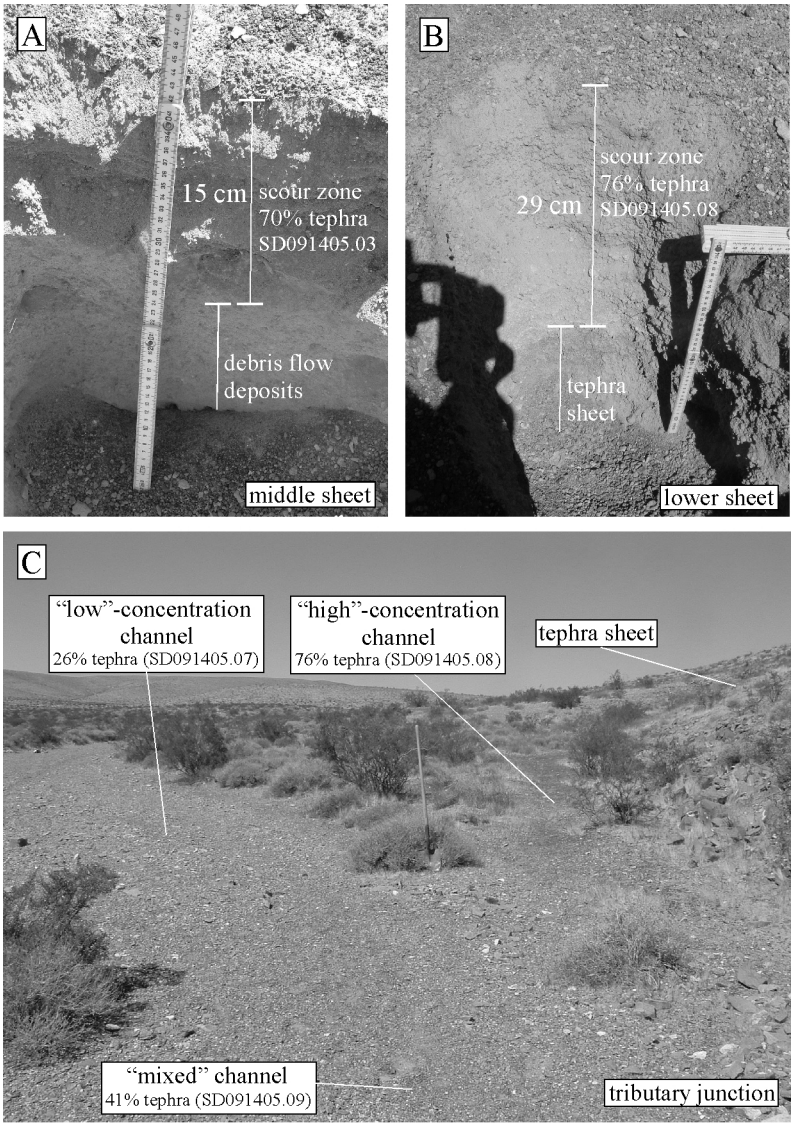

Source: Pelletier et al. 2007 [DIRS 182110], Figure 5.

NOTES: Channel pits on the tephra sheet ((A) and (B)) expose a fluvially mixed scour zone ranging from 12 to 29 cm in thickness. Two types of deposits occur beneath the scour zone: the tephra sheet itself (exposed on the upper and lower sheet) and debris-flow deposits comprised predominantly by Miocene volcanic tuff and eolian silt and sand transported from the upper tephra sheet. (C) The effects of dilution are visible as "high"-concentration channels draining the tephra sheet (channel at right, 76% tephra) join with "low"-concentration channels (at left, 26% tephra). Tephra concentration in these channels correlates with the darkness of the sediments, with the dark-colored channel at right joining with the (larger) light-colored channel at left to form a light-colored channel downstream.

Figure 7.3.1-3. Field Photos Illustrating the Three-dimensional Pattern of Contaminant Dilution near Lathrop Wells Tephra Sheet

It is noted that samples acquired from upstream along the tributary to the western channel have high concentration values. There are several small outcrops along this tributary to the western channel that are being actively eroded, primarily by bank retreat. These small sources locally enrich the channel along short (10- to 100-m) sections of incomplete mixing. Upstream and

downstream of these small outcrops the concentration values return to the background values within distances of 10 to 100 m from the sources.

7.3.1.3 Lathrop Wells Scour-Dilution-Mixing Model

A scour-dilution-mixing model, very similar to the qualified version of FAR V.1.2, was applied to the Lathrop Wells study site. DEM data acquired from the USGS was used to represent the drainage network at the site. In this framework, the contributing-area grid was first initialized with the value of grid cell area, Δx^2. Second, a bifurcation flow-routing algorithm was used to calculate the contributing area routed through each grid cell in the DEM. Third, a critical stream-power threshold was used to distinguish between hillslopes and channels in the DEM, where the stream power was defined as the product of the local slope S and the square root of the drainage area A. The critical stream power was related to the drainage density X through the relationship $1/X$. The value of the drainage density was estimated using digital map products. Grid cells with stream-power values less than $1/X$ were made zero in the grid, leaving finite values in the remaining grid cells. Fourth, the contributing-area grid was converted to a unit-discharge grid using empirical data (i.e., a "flood-envelope" curve), which, in turn, was converted to a scour/mixing-depth grid using the empirical square-root relationship documented by Leopold et al. (1966 [DIRS 175456], pp. 215 to 218) and corroborated by Gellis et al. (2005 [DIRS 178708]). Following this series of operations, the resulting grid represented the estimated scour depth in each channel grid cell. The model routed the tephra (expressed as an equivalent thickness for each grid cell) and the scour depth downstream using the same bifurcation flow-routing algorithm used for routing contributing area, calculating the ratio for each grid cell. That ratio was the tephra concentration.

The fundamental tool for the numerical scour-dilution-mixing model was the bifurcation-routing algorithm. In this algorithm, contributing area, tephra thickness, and scour depth were routed from each grid cell to its down-slope neighboring grid cells weighted by topographic slope. The bifurcation-routing method provides a more realistic method for mapping drainage on gentle slopes, wide channels, and distributary channel systems. This algorithm is implemented by initializing the grid with the area of a grid cell, Δx^2 (e.g., 100 m^2 for a 10-m resolution DEM). The algorithm then ranks all grid points in the basin from highest to lowest in elevation. Incoming flow to each grid cell is partitioned between all of the down-slope neighboring grid cells, weighted by slope. Routing is performed successively at grid points in rank order from highest to lowest, thereby ensuring that all incoming area has been accounted for before downstream routing is performed. The scour-dilution-mixing model of this journal article uses the bifurcation-routing algorithm three times, first to route contributing area and then to route the tephra thickness and scour depth to calculate tephra concentration as the ratio of the total tephra thickness to the total scour depth routed from upstream. While all flow-routing methods are approximations to the actual physical processes of hydraulic flow and sediment transport, the bifurcation method is more realistic because it depends on both drainage-network topology and basin shape (Pelletier 2004 [DIRS 174135]).

7.3.1.4 Lathrop Wells Input Data and Model Results

The Lathrop Wells tephra sheet was mapped by Valentine et al. (2005 [DIRS 177782]), providing a preliminary source map for input to the scour-dilution-mixing model for this application. The source map is complicated in this case by the fact that tephra from the 77 ka eruption dispersed tephra in all directions. Samples collected in the study reveal three separate "groups" of values. On the tephra sheet itself, basaltic sediment concentrations vary between 61% and 83% (Table 7.3.1-1), with an average value of 73%. Therefore, 73% was used as the value for the source concentration. Off the tephra sheet, "background" concentrations are relatively high to the north of the vent where most of the tephra was deposited (11.1% and 6.8% in samples SD091405.06 and SD091505.05, respectively) and lower to the south (3.0% in sample SD091505.08). These background samples were collected in large drainages to provide representative values over broad areas. To resolve the two "background" values in the model, a ternary "mask" (Figure 7.3.1.3-4A) with a source concentration of 73%, a "distal source" value of 9% (north of the primary tephra sheet), and background value of 3% (everywhere else) was used. The results of the model do not depend on the exact boundaries of the distal source region.

Additional inputs to the model are the threshold stream power and a 10-m-resolution USGS DEM (Figure 7.3.1.3-4A). The value for the stream-power threshold was chosen to be 0.015 km by forward modeling. In this forward-modeling procedure, a map of incised channels was made by comparing the stream power at each point in the grid to a threshold value. This threshold value was varied to produce different incised-channel maps. Maps were then overlain and visually compared with USGS orthophotographs to identify which value of the critical stream power produced the most accurate map.

In the first step of this model application, all grid cells of the contributing area grid were initialized as 10^{-4} km^2 (i.e., the grid cell area for a 10-m-resolution DEM). The bifurcation-routing algorithm was then used to calculate the contributing-area grid (Figure 7.3.1.3-4B). In the second step, the contributing-area grid was converted to a unit discharge map using the regional flood-envelope curve of Squires and Young (1984 [DIRS 180001], p. 16). These authors found the maximum discharge to be proportional to the contributing area to the 0.57 power using available stream gage data and paleoflood estimates from a range of basin sizes in the Yucca Mountain region. Maximum discharge is used because the largest floods control the long-term scour/mixing depth. The unit discharge map was then used to create a relative map of scour/mixing depth in channels using the square-root dependence of Leopold et al. (1966 [DIRS 175456], pp. 215 to 218) and a stream-power threshold of 0.015 km (Figure 7.3.1.3-4C). Only a relative grid of scour/mixing depth was needed in this case because the scour depths in the source area were used to calculate the effective volume of contaminant routed downstream, and the scour depths downstream of the source region were used to dilute that contaminant. Since the contaminant concentration is a ratio of these quantities, the concentration was unaffected by scaling the scour depth up or down by a constant factor. In all cases where the source is specified as a concentration (as opposed to an effective thickness), the absolute value of the scour depth is not needed to predict concentration values downstream; only relative values are needed. The model predicted tephra concentrations (expressed as a fraction; Figure 7.3.1.3-4D) in all channels draining the Lathrop Wells tephra sheet. This color map has a quadratic scale varying from < 0.01 (black) to 1.0 (white).

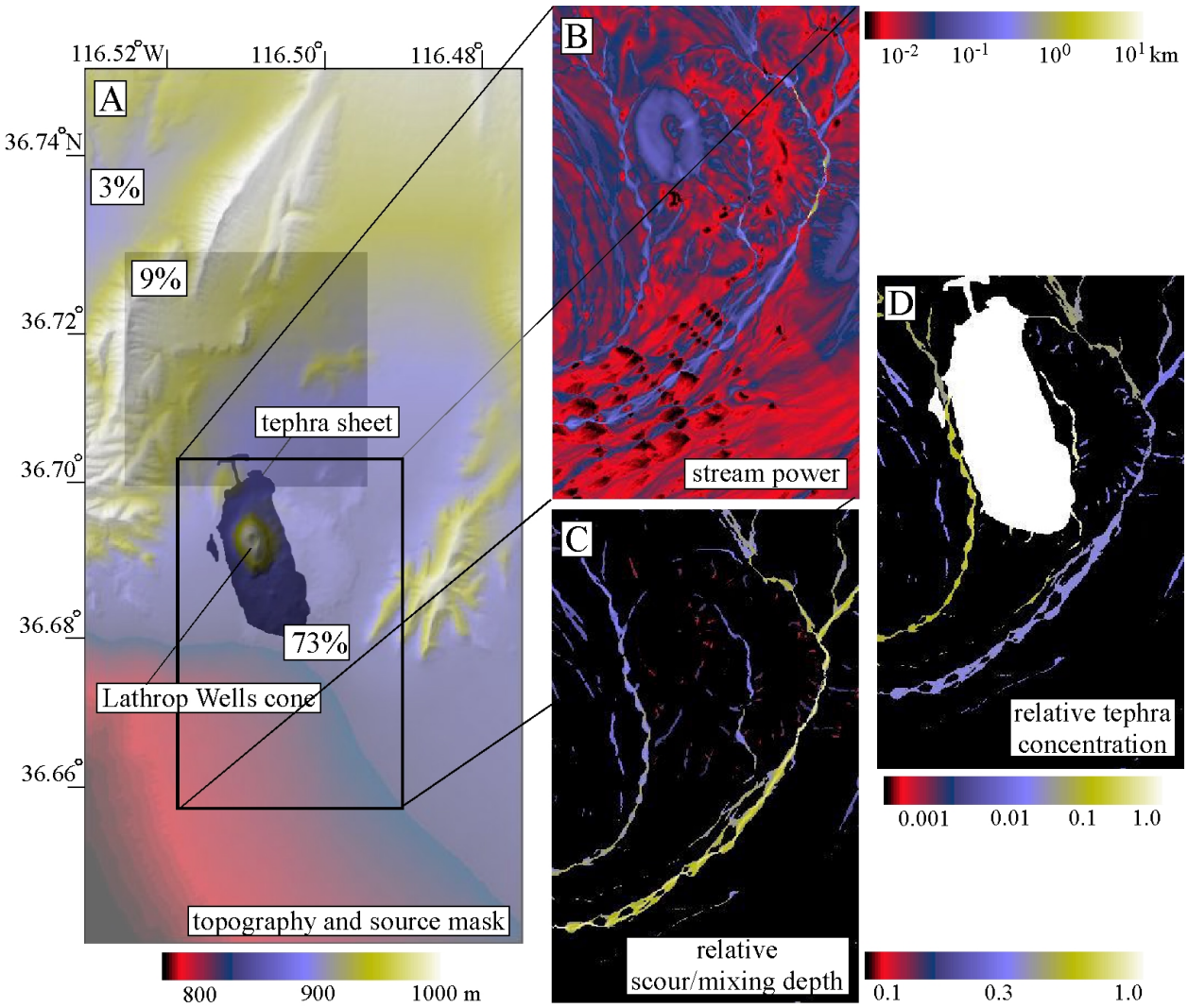

Source: Pelletier et al. (2007) [DIRS 182110], Figure 6.

NOTES: (A) Model inputs include a 10-m resolution USGS DEM of the region and a co-registered ternary grid indicating source (shown as black), distal source (gray), and background (white) regions with 73%, 9%, and 3% input concentrations, respectively. (B) Color map of stream power in the vicinity of the source region. Color scale is logarithmic, ranging from 10^{-2} to 10^{1} km. (C) Color map of scour/mixing depth (scale is quadratic, ranging from 10 cm to 1 m). (D) Color map of tephra concentration (scale is quadratic, ranging from 0.001 to 1).

Figure 7.3.1.3-4. Model Prediction for Tephra Concentration and Scour/mixing Depth Downstream from the Tephra Sheet of the Lathrop Wells Volcanic Center

The numerical model prediction was compared to the measured tephra concentrations by extracting tephra concentrations along channel profiles of the western and eastern channels. Along both channels, concentrations are near their maximum values for approximately the first 1.0 km downstream from the channel head. Along the eastern channel (Figure 7.3.1-2B, top graph), abrupt concentration declines are associated with major tributary junctions at 1.6 and 2.7 km from the channel head. The first major step down is associated with an increase in discharge and scour depth associated with a relatively uncontaminated tributary channel entering the channel from the northeast just upstream of the U-shaped channel bend. Another abrupt drop

in concentration occurs approximately 2.7 km from the channel head (just downstream of sample SD091515.07) where another large tributary enters. As the channel curves around the southeast corner of the Lathrop Wells lava field, it bifurcates into two distributary channels. Each pair of samples located at similar distances from the channel head was averaged to comprise the final two points on the curve (Figure 7.3.1-2B, top). The overall downstream-dilution pattern can be roughly approximated by an exponential function with a characteristic length of 0.9 km. This fit implies that for every 0.9 km downstream, the tephra concentration decreases by approximately a factor of 1/e. It should be noted that the model used to fit this data was not calibrated with this data.

Along the western channel, concentrations follow a similar pattern (Figure 7.3.1-2B, bottom). Note that this profile extends only about half as far from the channel head as the eastern channel due to the presence of the mine road, which disturbs the western channel about 2.5 km from the channel head. As the channel leaves the tephra sheet, the concentration decreases by about 50% (sample SD091415.09) resulting from the input of a large tributary from the northwest that adds significant quantities of clean sediment to the downstream channel. The channel quickly re-enters an area of exposed tephra, and this local source region has the effect of enriching the basaltic composition of channel sediments between 1.0 and 1.3 km from the channel head. The numerical model does not reproduce the pattern of tephra enrichment in this reach very accurately, perhaps because tephra is deposited in this reach primarily through bank retreat processes rather than channel-bed scour. These small sources locally enrich the channel along short (10- to 100-m) sections of incomplete mixing. Upstream and downstream of these small outcrops the concentration values return to the background values within distances of 10 to 100 m from the sources. Within this 300-m reach, the 10-m pixel size limited the ability of the model to capture the small side channels bringing tephra from the adjacent tephra sheet into the main channel.

The input DEM for this application exhibits the contour-line artifacts common to many USGS DEM areas in low-relief terrain. This example shows that despite clear limitations in the accuracy of the input DEM, meaningful results can be obtained from the scour-dilution-mixing model.

7.3.1.5 Summary of Lathrop Wells Corroboration

Pelletier et al. (2007 [DIRS 182110]) applied a scour-dilution-mixing model very similar to the qualified version of FAR V.1.2 to the Lathrop Wells volcanic area near Yucca Mountain, Nevada, and compared model results against measured tephra concentrations in channels downstream from the tephra sheet. This study was published in a peer-reviewed, refereed journal article. This study is an ideal opportunity to test important components of the conceptual and mathematical model implemented as FAR V.1.2. The published Lathrop Wells analysis demonstrates that the scour-dilution-mixing model adequately represents the redistribution of tephra by fluvial and hillslope processes in an environment very similar to what would be expected in the volcanic eruption scenario for Yucca Mountain. The model was able to accurately predict the correct value of the change in concentration associated with the tributary influxes along both the western and eastern channels. In the western channel, data followed two populations controlled by a single, large influx of nonbasaltic tributary sediments that leads to a single “step” change in concentration. The eastern channel includes several significant tributary

inflows along its course. The model predicted the same overall trend as the observed data in both channels studied as well as the magnitude and locations of the discrete "jumps" associated with tributary in fluxes. The relatively small study area of Lathrop Wells (compared to Fortymile Wash) provides a compelling demonstration of the fact that dilution is effective even at distances of only 1 to 2 km from the contaminant source. It is further noted that the input DEM for this application exhibits the contour-line artifacts common to many USGS DEM areas in low-relief terrain. This example shows that despite clear limitations in the accuracy of the input DEM, meaningful results can be obtained from the scour-dilution-mixing model.

This study provides confidence that the model implemented in the FAR V.1.2 software is adequate and valid for its intended use.

7.3.1.6 Publication of Diffusion Model for Radionuclide Migration into Soil

As part of post-development model validation activities described in the TWP, a peer-reviewed journal article was published describing the diffusion model for radionuclide transport into the soil (Pelletier et al. 2005 [DIRS 175800]). This paper describes and documents the application of the one-dimensional diffusion model that is used in the FAR model to ^{137}Cs measurements from the soil in the vicinity of the Nevada Test Site. The paper describes the conceptual and mathematical model, and presents a solution to the diffusion equation. The paper reviews previous work in this area, compares model results to other analogue datasets, and explains how this model is applicable for representing radionuclide transport in the soil following a potential volcanic eruption scenario at Yucca Mountain.

7.3.2 Critical Review

The second method of model validation used in this report is Critical Review as described in the TWP (SNL 2007 [DIRS 182219], Section 2.6.5.2). Dr. Larry Mayer and Dr. William Hackett were selected to review Draft A of the document and perform separate critical reviews. Both of these reviews were done independently on the same draft material and each reviewer was provided with the specific requirements and review criteria, which are duplicated in the bulleted list below.

- *Is the conceptual model for tephra redistribution reasonable and appropriate for its intended use?*
- *Are the mathematical relationships appropriate and representative of the scientific understanding of the geomorphic processes for the transport of sediment from the Fortymile drainage basin to the location of the RMEI on the Fortymile Wash alluvial fan?*
- *Are the outputs of the model reasonable and representative?*
- *Are there alternative models or approaches that should be considered?*
- *Are the limitations of the model adequately described?*

- *Are the model validation activities (in addition to validation by technical review) that have been planned in the TWP and reported in the model report appropriate and adequate, and adequately and correctly conducted and interpreted?*

As noted in Section 1.2, there is one deviation from the TWP (SNL 2007 [DIRS 182219]). Section 2.6.5.2.3 of the TWP states: "The model will be considered valid if the independent critical reviewer concurs that the documentation of the tephra redistribution model report appropriately and adequately addresses [the] review criteria." Two independent experts (Dr. Mayer and Dr. Hackett) each conducted an initial critical review of Draft A of this report using the review criteria presented in the TWP. One of these critical reviewers (Dr. Mayer) was not available to review the originator's responses to his review. Therefore, the other reviewer (Dr. Hackett) performed a final critical review of Draft D of this report, which included all of the changes made in response to both initial critical reviews.

The text of these reviews is reproduced in Appendix C and includes specific inline author responses, in the case of Dr. Mayer's review. More general originator responses to the principal technical concerns raised by Dr. Mayer are presented in the following section. Dr. Hackett's final review included consideration of all the responses to Dr. Mayer's review of Draft A.

7.3.2.1 Originator's General Response to Dr. Mayer's Critical Review

One of the critical reviewers (Dr. Larry Mayer) raised five principal technical concerns with the model. These are discussed separately below. In addition, this reviewer felt that the description of the conceptual model presented in Draft A was inadequate, and therefore this description has been rewritten and expanded in the subsequent draft. All other specific comments are addressed as in-line responses included in Appendix C, Section C1.

Technical Concerns Raised by Critical Reviewer

1. **The input DEM may not resolve important terrain features, or provide accurate slope values**

Originator Response:
The accuracy of any raster data set depends on the data resolution. All users of geospatial data should be keenly aware of limitations posed by data resolution. The redistribution model itself does not depend on any particular DEM. The FAR model has, however, been implemented in TSPA using a 30 m/pixel USGS DEM (the only available DEM at the time the work was performed). The best DEM to use for a particular application depends on the size of the study area. For relatively small study areas (i.e. < 100 km^2), LIDAR and photogrammetric DEMs are generally considered to be the best DEM data available. These products do have many technical issues that have not been fully resolved, however, such as how to filter out vegetation to represent "bare" ground. Given the size of the Fortymile Wash drainage basin, (828 km^2), USGS DEMs were the only practical solution. They are widely used for many types of geomorphic studies.

The key question, then, is whether a 30 m/pixel DEM resolves hillslope morphology for a particular application. The answer depends on the drainage density of the study area. In very

rugged terrain characterized by high drainage density, individual pixels can be larger than the typical hillslope area above channel heads. In such cases, pixels in the DEM will combine both hillslope and channel components, leading to an underestimation of slope values on hillslopes (because channels have lower slope values). Given the drainage density in the Fortymile Wash drainage basin, a typical hillslope contains approximately 30 pixels above each channel head. As such, hillslopes are well resolved in the 30 m/pixel DEM. The "jagged" landscape sketched by Dr. Mayer illustrates a theoretical example that is not representative of the actual terrain in the vicinity of Yucca Mountain

2. **The dilution model is inadequate or incorrect as applied**

Originator Response:
Dr. Mayer poses the extreme case where all the tephra falls on a single pixel near the outlet. He correctly states that the model predicts that mixing will dilute the concentration in this pixel. He states that this result "does not seem reasonable given the process of stream flow and sediment transport." No other information is given, however, making it difficult to respond to this comment (except to say that the case where all the tephra lands on a single, isolated pixel would not occur in nature). Dr. Mayer appears to be suggesting that a localized source of tephra will be mixed over some finite distance downstream. This is a legitimate point. Field observations at Lathrop Wells indicate that small outcrops of pure tephra can enrich adjacent channels over channel lengths up to 100 meters. In the theoretical example provided by Dr. Mayer, therefore, incomplete mixing over a distance of approximately three pixels could lead to slightly higher values locally than the dilution model predicts. A clarifying statement on this point is provided in Section 7.3.1.4.

In Figures 4 and 5 of Dr. Mayer's review (Appendix C), he correctly notes that the dilution model assumes that channels can not be scoured down to the base of tephra sheets when tephra thickness is greater than the scour depth. This was a point of consideration during model development. If the tephra initially distributed on channels that was thicker than the scour depth was allowed to be transported downstream (the model was allowed to "cut" the tephra down to the original elevation of the channel bed), the model results may be more realistic in cases of very thick tephra deposition. However, if the model did not allow the tephra to be cut, it would be inconsistent with the assumption that current channel geomorphology is an adequate representation of future channel morphology (Section 5.1.4). In the end, it was determined that the impact of either method would be relatively small with regard to the overall model results. As such, the decision was made to maintain the integrity of the assumption (Section 5.1.4) and not allow "cutting." The discussion of this particular aspect of the model has been improved in the new draft, including graphics showing the relatively minor general impact on the model results.

3. **Eolian redistribution should be represented in the model**

Originator Response:
Eolian transport includes two different types of transport. Silt and clay-sized particles are introduced into Amargosa Valley as "wash load" during large floods from the Fortymile Wash drainage basin. The primary depozone for silt from Fortymile Wash is Franklin Lake Playa. The predominant source of silt-sized particles redistributed to the RMEI location by eolian processes,

therefore, is located approximately 30 km south of the RMEI location. Eolian silt accumulation rates on terraces immediately adjacent to Franklin Lake playa (Pelletier and Cook 2005 [DIRS 175659]) indicate that silt accumulation rates decrease very rapidly with distance from playa sources, and suggest that silt accumulation on the terraces of Fortymile Wash fan will be limited to significantly less than 1 cm in 10,000 years.

Sand-sized particles transported in the RMEI environment by eolian processes are sourced from the active channels of Fortymile Wash. The report clearly acknowledges that there will be eolian redistribution of sand from channels to older terraces of the RMEI location. Indeed, soil-profile analysis provides evidence for ~10 to 50 cm of windblown sand on the oldest terrace of the Fortymile Wash fan. The recognition that sand is redistributed by eolian processes from channels to divides actually highlights the importance of fluvial transport and dilution in this model system, because it is that process that controls the radionuclide concentration of the eolian sediments. As described in Section 5.2.2, uncertainty in the fraction of the RMEI area that is active channels implicitly accounts for the uncertainty introduced by neglecting eolian redistribution from channels to divides in the RMEI location.

4. **The model does not accurately represent the transport and mixing of fine-grained tephra**

Originator Response:
Two types of sediment motion exist in channels: bed load and suspended load (wash load is a third type but can also be considered part of suspended load). Bed material that is coarser than a threshold grain size will move primarily as bed load; finer material will move predominantly as suspended load. The significance of this distinction is that material transported as suspended load will be carried high in the water column and will be transported past the RMEI location and into the Amargosa River more readily than coarse material. Silt-sized material is often transported as "wash load," meaning that it will be transported in the water column until the flood waters infiltrate completely. Franklin Lake Playa is the primary depozone for silt-sized particles in the area. The channels of the Fortymile Wash fan are almost completely devoid of silt. It is true that some floods will infiltrate completely before they reach the RMEI location or the Amargosa River downstream, but the flood hydrology of large drainage basins in the western U.S. is dominated by large floods from frontal and tropical storms of significant duration (~1 to 3 days). These longer storms saturate channel sediments and result in continuous flood events throughout drainage basins of regional extent.

An **ideal** model for tephra redistribution would explicitly include the role of grain size and would distinguish bed load and suspended-load types of transport and even include eolian transport. Such a model, however, is not needed for the purpose of this study and would require input data that is not available. Dr. Mayer includes a figure that suggests an alternative approach. Two points should be noted, however. The fact that sediments of Fortymile Wash do not contain significant silt undermines the rationale for modeling suspended-load transport (i.e. to provide input for an eolian transport model that moves silt from channels to terraces). By treating all of the tephra from the eruption as coarse-grained sediment for the purposes of fluvial transport, the model errs on the side of conservatism. Fine-grained sediments that are transported as suspended load will be transported past the RMEI location and into the Amargosa River (based on the lack of silt currently stored in channel bed material). This type of transport is difficult to

model because there are no readily available measurements that constrain this type of transport. In the case of bed-load transport and channel scour, however, scour depths can be measured directly during large flood events, as was done by the USGS in 1995. By considering all of the tephra as bed load, the model predicts that contaminants will persist longer in the system than would be the case if the model explicitly distinguished suspended load from bed load. The model, therefore, correctly focuses on the least mobile, most persistent component of the load.

5. **The application of the model to Lathrop Wells does not validate the model, but in fact proves that the model is incorrect.**

Originator Response:
Dr. Mayer states that the model "lacks a convincing downstream variation," and plots an alternative model based on two constant levels of concentration. The data from the western channel do, in fact, follow two populations because they are controlled by a single, large influx of nonbasaltic tributary sediments that leads to a single "step" change in concentration. In this sense, the eastern channel is a more rigorous test of the model because it includes several significant tributary inflows along its course. The key question is whether the model predicts the correct value of the *change* in concentration associated with the tributary influxes along both the western and eastern channels. It does. The model predicts the same overall trend as the observed data in both channels studied as well as the magnitude and locations of the discrete "jumps" associated with tributary influxes.

Dr. Mayer questions why samples acquired from upstream along the tributary to the western channel have high concentration values. A visit to the site confirms that there are several small outcrops along this tributary to the western channel that are being actively eroded, primarily by bank retreat. Two of the larger of these outcrops are readily visible in the images presented by Dr. Mayer. These small sources locally enrich the channel along short (10- to 100-m) sections of incomplete mixing. Upstream and downstream of these small outcrops the concentration values return to the background values within distances of 10-100 m from the sources. Samples were collected in the field before the resolution of the input data made it clear that these sources could not be resolved in the model. All of the data is presented for completeness. Given the limited resolution of the input data, however, the validation exercise was necessarily limited to the principal western and eastern channels draining the tephra sheet. A comment has been added in the report that clarifies this point. Finally it should be noted that the data from the eastern channel must be plotted on a log axis because the measured concentration values differ by two orders of magnitude. On a linear scale, the concentration values below 10% would not be easily read from a linear plot.

The fact that the Lathrop Wells study area is much smaller than Fortymile Wash is a compelling demonstration of the fact that dilution is effective even at distances of only 1 to 2 km from the contaminant source. The reviewer states general concerns about the sampling strategy, but he does not identify any specific weaknesses in the data beyond those issues are already addressed.

Originator Summary Statement:
In constructing any model of a system of this size and level of complexity, developers are required to compromise between model complexity and the availability of input data for calibrating the model. Dr. Mayer criticizes the model for "not actually routing sediment by

calculating sediment loads and mass balances during floods." Models of sediment transport during individual flood events that resolve a range of grain sizes are currently available, but such models require dozens of input parameters that are difficult to quantify even for a single flood event. Moreover, modeling a single flood event using a dynamic flood-wave model would be computationally challenging for a drainage basin as large as Fortymile Wash. Given that the modeling is over geologic time scales, the redistribution problem necessarily requires a substantial degree of process abstraction. The scour-dilution-mixing model, developed for the fluvial redistribution component of this work, represents the right compromise between complexity and availability of data. Although Dr. Mayer regards the model as "the simplest possible," it must be remembered that any model incorporated in YMP must be suitable for implementation in a system-level uncertainty analysis given a small number of input parameters that, in most cases, are readily measurable. The proposed model does that. Dr. Mayer's review contains no specific alternative models that could be used. The one page of text he uses to address alternative models is, in fact, mostly a restatement of the model under review.

The key issue is not whether the proposed model includes every process (it is fair to state that no model could represent all of the geomorphic processes occurring or that will occur in this system in the future), but whether the model adequately represents the range of system behaviors and resulting contaminant concentrations needed to estimate the range of doses experienced by the RMEI. This end goal was the paramount concern during model development. In cases where a significant process has been excluded from the model, it is argued that neglecting the process leads to conservative results. Given the efficacy of the dilution process under most wind direction and eruption scenarios, including eolian redistribution from channels to divides would decrease contaminant concentrations at the RMEI location in those scenarios in which contaminated tephra is deposited directly at the RMEI location because undiluted tephra on divides would be buried by diluted channel sediments. The decision not to explicitly distinguish suspended load from bed load transport is also consistent with the end goal of calculating concentrations at the RMEI location that adequately represent the range of values that can be expected. Fine-grained sediments that are transported as suspended load will be transported more readily past the RMEI location and into the Amargosa River. By considering all of the tephra as bed load, the model predicts that contaminants will persist longer in the system than would be the case if it explicitly distinguished suspended load from bed load.

It is further noted that even given Dr. Mayer's criticism of the over simplification of the model, he concluded that the model output, overall, seemed reasonable.

7.3.2.2 Originator's General Response to Dr. Hackett's Critical Reviews

It is clear from Dr Hackett's reviews that he had a generally positive opinion of the model presented in the report. Dr. Hackett reviewed the model in the larger context of its use in TSPA, specifically its relation to the other process models used to represent the volcanic eruption scenario in TSPA. Dr. Hackett's final review provides confidence that in the context of TSPA, the model is appropriate and valid for its intended use.

7.3.2.3 Summary of Critical Reviews

The first two critical reviews were done on the initial draft of the report and thus comments, suggestions, and criticisms could be addressed by making changes to the report in addition to directly responding to the reviews. Both of these reviews were done independently and without contact between reviewers, both reviewers received the same instructions, and Dr. Hackett's first review was completed before Dr Mayer's review. A comparison between the two critical reviews suggests that each reviewer had a different interpretation of their role in the critical review process. Dr. Hackett's second review discusses this issue in some detail. Dr. Mayer's review focused on details of the physical processes represented by the model, but did not focus on how the model fit into the TSPA system model. In contrast, Dr. Hackett reviewed the model in the larger context of its use in TSPA, and appeared to rely more on his experience as a volcanologist, than on a detailed examination of the mathematical relationships of the model. Both reviews offered informative and valuable observations. Dr. Mayer's detailed and probing review provided the authors a valuable opportunity to improve sections of the report and add additional model validation comparisons to the text. Perhaps the most significant comment made by Dr. Mayer regards the justification for excluding eolian transport of contaminants from the RMEI channels to the divides. The model makes an assumption that this process is insignificant in comparison to the other transport processes that are included in the model. As discussed in Section 5.2.2, uncertainty in the fraction of the RMEI location that is active channels is considered to implicitly account for uncertainty introduced by the decision not to explicitly model this process in FAR.

INTENTIONALLY LEFT BLANK

8. CONCLUSIONS

8.1 MODEL SUMMARY

The FAR tephra redistribution model quantifies the redistribution of volcanic tephra and associated waste within the Fortymile Wash drainage basin (the major drainage network in the western part of the Nevada Test Site) by hillslope and fluvial processes and quantifies diffusive redistribution of waste in soil profiles at the RMEI location on the Fortymile Wash alluvial fan. The model domain is divided into two sections: (1) an upper drainage basin, characterized by reasonably steep terrain draining into an incised and well-defined channel network, and (2) an alluvial fan downstream of the upper drainage basin having considerably less slope, and less deeply incised channels, representing the RMEI location.

The tephra redistribution model uses a spatially-distributed Geographic Information System (GIS) framework to calculate tephra redistribution in three steps. Specifically, the model calculates:

(1) **mobilization** by hillslope and fluvial processes of waste and tephra deposited in the upper drainage basin domain,

(2) **transport and mixing** (dilution) of waste-contaminated tephra within the channels of the upper drainage basin domain, and

(3) **emplacement and diffusion** of waste-contaminated sediments within the alluvial fan at the RMEI location.

The model assumes that tephra primary fallout is mobilized and transported toward the RMEI location if it falls on steep slopes or on active channels. The model performs a spatial analysis of the slopes and contributing areas (a proxy for stream power) for the entire basin using the input DEM. These values are then compared to critical slope (S) and drainage density (X) input values, on a grid cell-by-grid cell basis, to integrate the total mass of tephra and waste mobilized from the upper basin. If a given grid cell has a slope greater than the critical slope (S) or an inferred stream power greater than the reciprocal of drainage density ($1/X$), the tephra and waste in that grid cell is considered to be mobilized.

The mobilized tephra and waste are transported through the channel system of the upper drainage basin where mixing with uncontaminated channel sediments leads to dilution. Mixing occurs during flood events as sediment and tephra are entrained from the bed, mixed by turbulent flow, and redeposited on the bed. In addition, clean sediment transported from catchments with little to no tephrafall is added to the channel. The depth to which tephra and channel sediment are mixed is the scour depth. The dilution factor at each point (i.e., the fraction of channel sediment composed of tephra in each channel grid cell) is calculated using the local thickness of mobilized tephra and the local scour depth, calculated from the contributing area at each point. Contributing area is estimated using a divergent flow (bifurcation routing) algorithm that partitions the area of each upstream grid cell to each of the neighboring downstream grid cells in proportion to the local downstream slope between these grid cells. This same algorithm is used to route tephra thickness and scour depth downstream. The ratio of the routed tephra thickness

to the routed scour depth at the fan apex, which is just upstream from the RMEI location, is used to calculate the waste concentration in the channels at the RMEI location.

The spatially distributed model of tephra and waste transported from the upper basin channel network supplies contaminated tephra to the RMEI location on the upper Fortymile Wash alluvial fan. The model represents this large-scale transport and dilution as an instantaneous process occurring immediately after the eruption. At the RMEI location, the tephra redistribution model then considers the vertical migration of radionuclides within the soil as a time-dependent diffusion process. Vertical redistribution within the soil occurs primarily through suspension and redeposition of fine particles by infiltration, and physical mixing of soil particles by freeze-thaw cycles and bioturbation. Diffusion is assumed to occur within a finite thickness corresponding to the distance from the surface to a zone of reduced permeability at the base of the active zone (with different thicknesses for the divides and channels).

The FAR tephra redistribution model outputs time series results of relative waste concentrations at the surface and within a prescribed depth interval for the channel and inter-channel divide subdomains of the RMEI location.

8.1.1 Technical Product Output

Table 8.1-1 lists the product outputs from this model report intended for use in the TSPA model. Table 8.1-2 lists the product outputs from this model report that provide calculations and supporting information related to the model and associated parameters.

Table 8.1-1. Product Output Intended for Use in the TSPA Model

Description	Title	Product Output DTN
Files that document the generation of the input DEM	Input DEM for Fortymile Wash Drainage Basin	MO0605SPAFORTY.000
FAR model input parameter distributions	FAR Data	MO0702PAFARDAT.001
	Scour Depth	MO0704PASCOURD.000

Table 8.1-2. Product Output Not Directly Used by the TSPA Model

Description	Title	Product Output DTN
Files that document the development of the geomorphic map of the alluvial fan	Geomorphic Map of Alluvial Fan	SN0708GEOMOMAP.001
Files that document the calibration exercise that was performed in the development of the drainage density distribution	Drainage Density Calibration	SN0708DRAINDEN.001
Diffusivity values calculated from measured ^{137}Cs data	Diffusivity Parameter Calculation	SN0708DIFFRNGS.001

Table 8.1-2. Product Output Not Directly Used by the TSPA Model (Continued)

Description	Title	Product Output DTN
Example diffusion calculations for various scour depths, diffusion coefficients, etc	Example Diffusion Model Results	SN0708DIFFEXMP.001
Diffusivity values from sites used to validate the diffusion submodel in Section 7	Diffusivity Values Used for Model Validation	SN0708DIFFVALD.001
Files that document the sensitivity analysis performed on the FAR V.1.2 model and input parameters	FAR Sensitivity Analysis	SN0708FARSENSS.001

8.2 MODEL LIMITATIONS AND UNCERTAINTIES

Given uncertainties, lack of data, and the desire to minimize mathematical complexity that does not provide value commensurate with the model purpose, there are recognized limitations in the capabilities of the FAR tephra redistribution model. Model limitations are listed in Section 1.2 of this report.

In addition to the simplifying assumptions, there is uncertainty in the input parameters. Wherever practical, data specific to the model domain was measured. However, uncertainty exists associated with small sample populations, geomorphic differences across the site, and changing climates. A sensitivity analysis was performed in Section 6.6 to determine how uncertainty in input parameters affects the uncertainty in model results.

The sensitivity analysis focused on the uncertainty associated with those parameters describing the physical properties of the drainage system (epistemic uncertainty). The uncertain parameters that affect the transport and dilution of waste from the upper drainage basin include the critical slope, scour depth at the fan apex, and the drainage density. The analysis concluded that the variance in the initial waste concentration in the channels at the RMEI location was most sensitive to the value of the critical slope (S) (accounting for 47% of the variance in the results) and scour depth at the fan apex (H) (accounting for an additional 39% of the variance in the results). The drainage density (X) was the least sensitive of these parameters (accounting for only an additional 10% of the variance in the results). A further study analyzed the sensitivity of the time-dependent diffusion process to the input parameters, diffusivity and permeable depth. The results of this study confirmed that (1) the greater the diffusivity value the quicker the initial waste concentration declines and (2) the sensitivity to permeable depth is not apparent until later times (~60,000 years), when larger permeable depths result in slightly lower final concentrations.

8.3 YUCCA MOUNTAIN REVIEW PLAN CRITERIA ASSESSMENT

Yucca Mountain Review Plan, Final Report (YMRP) (NRC 2003 [DIRS 163274]) associates the integrated sub issue of redistribution of radionuclides in soil with the requirements listed in 10 CFR 63.114(a)-(c) and (e)-(g) [DIRS 180319]. The YMRP (NRC 2003 [DIRS 163274], Section 2.2.1.3.13.3) describes the acceptance criteria that the NRC will use to evaluate the adequacy of information addressing redistribution of radionuclides in soil in the license application. A listing of the acceptance criteria applicable to the tephra redistribution model

along with information addressing how these acceptance criteria are met is presented in Appendix B.

9. INPUTS AND REFERENCES

9.1 DOCUMENTS CITED

169793 Anspaugh, L.R.; Simon, S.L.; Gordeev, K.I.; Likhtarev, I.A.; Maxwell, R.M.; and Shinkarev, S.M. 2002. "Movement of Radionuclides in Terrestrial Ecosystems by Physical Processes." *Health Physics, 82,* (5), 669-679. Baltimore, Maryland: Lippincott Williams & Wilkins. TIC: 256136.

169673 BSC (Bechtel SAIC Company) 2004. *Agricultural and Environmental Input Parameters for the Biosphere Model.* ANL-MGR-MD-000006 REV 02. Las Vegas, Nevada: Bechtel SAIC Company. ACC: DOC.20040915.0007.

169989 BSC 2004. *Characterize Framework for Igneous Activity at Yucca Mountain, Nevada.* ANL-MGR-GS-000001 REV 02. Las Vegas, Nevada: Bechtel SAIC Company. ACC: DOC.20041015.0002; DOC.20050718.0007.

170002 BSC 2004. *Future Climate Analysis.* ANL-NBS-GS-000008 REV 01. Las Vegas, Nevada: Bechtel SAIC Company. ACC: DOC.20040908.0005.

172827 BSC 2005. *Characteristics of the Receptor for the Biosphere Model.* ANL-MGR-MD-000005 REV 04. Las Vegas, Nevada: Bechtel SAIC Company. ACC: DOC.20050405.0005.

175539 BSC 2005. *Q-List.* 000-30R-MGR0-00500-000-003. Las Vegas, Nevada: Bechtel SAIC Company. ACC: ENG.20050929.0008.

102040 Bull, W.B. 1991. *Geomorphic Responses to Climate Change.* New York, New York: Oxford University Press. TIC: 223847.

183192 Canfield, D.E. 2005. "The Early History of Atmospheric Oxygen: Homage to Robert M. Garrels." *Annual Review of Earth and Planetary Sciences*, *33*, 1-36. Palo Alto, California: Annual Reviews. TIC: 259729.

100968 Carslaw, H.S. and Jaeger, J.C. 1959. *Conduction of Heat in Solids.* 2nd Edition. Oxford, Great Britain: Oxford University Press. TIC: 206085.

108874 Crippen, J.R. and Bue, C.D. 1977. Maximum Floodflows in the Conterminous United States. Water-Supply Paper 1887. Washington D.C.: U.S. Geological Survey. TIC: 217532.

100973 Crowe, B.M. and Perry, F.V. 1990. "Volcanic Probability Calculations for the Yucca Mountain Site: Estimation of Volcanic Rates." *Proceedings of the Topical Meeting on Nuclear Waste Isolation in the Unsaturated Zone, FOCUS '89, September 17-21, 1989, Las Vegas, Nevada.* Pages 326-334. La Grange Park, Illinois: American Nuclear Society. TIC: 212738.

100116 CRWMS M&O 1996. *Probabilistic Volcanic Hazard Analysis for Yucca Mountain, Nevada.* BA0000000-01717-2200-00082 REV 0. Las Vegas, Nevada: CRWMS M&O. ACC: MOL.19971201.0221.

182051 DOE (U.S. Department of Energy) 2007. *Quality Assurance Requirements and Description.* DOE/RW-0333P, Rev. 19. Washington, D. C.: U.S. Department of Energy, Office of Civilian Radioactive Waste Management. ACC: DOC.20070717.0006.

183120 DOE 2007. *Software Validation Report for: FAR Version 1.2.* Document ID: 11190-SVR-1.2-00-Win2000. Las Vegas, Nevada: U.S. Department of Energy, Office of Repository Development. ACC: MOL.20070919.0334.

183116 DOE 2007. *User Information Document for: FAR Version 1.2.* Document ID: 11190-UID-1.2-00. Las Vegas, Nevada: U.S. Department of Energy, Office of Repository Development. ACC: MOL.20070919.0332.

174195 Freeman, T.G. 1991. "Calculating Catchment Area with Divergent Flow Based on a Regular Grid." *Computers & Geosciences, 17,* (3), 413-422. New York, New York: Pergamon Press. TIC: 257286.

169807 Gale, H.J.; Humphreys, D.L.O.; and Fisher, E.M.R. 1964. "Weathering of Caesium-137 in Soil." *Nature, 201,* (491), 257-261. London, England: Macmillan Magazines. TIC: 256310.

178708 Gellis, A.C.; Emmett, W.W.; and Leopold, L.B. 2005. *Channel and Hillslope Processes Revisited in the Arroyo de los Frijoles Watershed Near Santa Fe, New Mexico.* U.S. Geological Survey Professional Paper 1704. Reston, Virginia: U.S. Geological Survey. ACC: MOL.20060724.0001.

169808 Gilbert, R.O. and Eberhardt, L.L. 1976. "Statistical Analysis of 'A Site' Data and Interlaboratory Comparisons for the Nevada Applied Ecology Group." *Studies of Environmental Plutonium and Other Transuranics in Desert Ecosystems, Nevada Applied Ecology Group Progress Report (Workshop Session - May, 1975).* White, M.G. and Dunaway, P.B., eds. NVO-159. Pages 117-154. Las Vegas, Nevada: U.S. Energy Research and Development Administration, Nevada Operations Office. TIC: 201475.

178705 Graf, W.L. 1990. "Fluvial Dynamics of Thorium-230 in the Church Rock Event, Puerco River, New Mexico." *Annals of the Association of American Geographers, 80,* (3), 327-342. Washington, D.C.: Association of American Geographers. TIC: 259074.

164775 Harrington, C. 2003. Ash and Soil Redistribution Studies. Scientific Notebook SN-LANL-SCI-285-V1. ACC: MOL.20030411.0312.

174136 Hawkes, H.E. 1976. "The Downstream Dilution of Stream Sediment Anomalies." *Journal of Geochemical Exploration, 6,* 345-358. Amsterdam, The Netherlands: Elsevier. TIC: 257351.

178707 He, Q. and Walling, D.E. 1997. "The Distribution of Fallout ^{137}Cs and ^{210}Pb in Undisturbed and Cultivated Soils." *Applied Radiation and Isotopes, 48,* (5), 677-690. New York, New York: Pergamon. TIC: 257522.

107255 Heizler, M.T.; Perry, F.V.; Crowe, B.M.; Peters, L.; and Appelt, R. 1999. "The Age of Lathrop Wells Volcanic Center: An $^{40}Ar/^{39}Ar$ Dating Investigation." *Journal of Geophysical Research, 104,* (B1), 767-804. Washington, D.C.: American Geophysical Union. TIC: 243399.

174138 Helgen, S.O. and Moore, J.N. 1996. "Natural Background Determination and Impact Quantification in Trace Metal-Contaminated River Sediments." *Environmental Science & Technology, 30,* (1), 129-135. Easton, Pennsylvania: American Chemical Society. TIC: 257357.

182545 Hjulström, F. 1939. "Part 1. Transportation, Transportation of Detritus by Moving Water." *Recent Marine Sediments, A Symposium.* Trask, P.D., ed. Pages 5-31. Tulsa, Oklahoma: American Association of Petroleum Geologists. TIC: 259681.

174197 Jones, K.H. 1998. "A Comparison of Algorithms Used to Compute Hill Slope as a Property of the DEM." *Computers & Geosciences, 24,* (4), 315-323. New York, New York: Pergamon. TIC: 257285.

173899 Keefer, W.R.; Whitney, J.W.; and Taylor, E.M., eds. 2004. *Quaternary Paleoseismology and Stratigraphy of the Yucca Mountain Area, Nevada.* Professional Paper 1689. Reston, Virginia: U.S. Geological Survey. ACC: MOL.20050512.0077.

175456 Leopold, L.B.; Emmett, W.W.; and Myrick, R.M. 1966. "Channel and Hillslope Processes in a Semiarid Area, New Mexico." *Erosion and Sedimentation in a Semiarid Environment.* Geological Survey Professional Paper 352-G. Pages 193-253. Washington, D.C.: U.S. Government Printing Office. ACC: MOL.20050927.0277.

169810 Likhtarev, I.A.; Kovgan, L.N.; Jacob, P.; and Anspaugh, L.R. 2002. "Chernobyl Accident: Retrospective and Prospective Estimates of External Dose of the Population of Ukraine." *Health Physics, 82,* (3), 290-303. Baltimore, Maryland: Lippincott Williams & Wilkins. TIC: 256138.

183770 Lin, Zhou; Oguchi, Takashi 2004. "Drainage Density, Slope Angle, and Relative Basin Position in Japanese Bare Lands from High-resolution DEMs." *Geomorphology, 63,* pp. 159-173. Oxford, UK: Elsevier Science. TIC: 259819.

104660 Machette, M.N. 1985. "Calcic Soils of the Southwestern United States." *Soils and Quaternary Geology of the Southwestern United States.* Weide, D.L. and Faber, M.L., eds. Special Paper 203. Pages 1-21. Boulder, Colorado: Geological Society of America. TIC: 239387.

175455 Martz, L.W. and Garbrecht, J. 1999. "An Outlet Breaching Algorithm for the Treatment of Closed Depressions in a Raster DEM." *Computers and Geosciences, 25,* 835-844. New York, New York: Elsevier. TIC: 257726.

175760 Montgomery, D.R. and Dietrich, W.E. 1988. "Where Do Channels Begin?" *Nature, 336,* 232-234. New York, New York: Nature Publishing Group. TIC: 257986.

159538 NRC (U.S. Nuclear Regulatory Commission) 2002. *Integrated Issue Resolution Status Report.* NUREG-1762. Washington, D.C.: U.S. Nuclear Regulatory Commission, Office of Nuclear Material Safety and Safeguards. TIC: 253064.

163274 NRC 2003. *Yucca Mountain Review Plan, Final Report.* NUREG-1804, Rev. 2. Washington, D.C.: U.S. Nuclear Regulatory Commission, Office of Nuclear Material Safety and Safeguards. TIC: 254568.

100297 NRC 1998. *Issue Resolution Status Report Key Technical Issue: Igneous Activity.* Rev. 0. Washington, D.C.: U.S. Nuclear Regulatory Commission. ACC: MOL.19980514.0576.

174135 Pelletier, J.D. 2004. "Persistent Drainage Migration in a Numerical Landscape Evolution Model." *Geophysical Research Letters, 31,* (L20501), 1-4. Washington, D.C.: American Geophysical Union. TIC: 257363.

179612 Pelletier, J.D. 2007. Field Studies of Fortymile Wash Alluvial Fan in Support of Ash Redistribution Model Development [final submittal]. Scientific Notebook SN-M&O-SCI-050-V1. Pages i-120. ACC: LLR.20070601.0122.

175659 Pelletier, J.D. and Cook, J.P. 2005. "Deposition of Playa Windblown Dust Over Geologic Time Scales." *Geology, 33,* (11), 909-912. Boulder, Colorado: Geological Society of America. TIC: 257856.

175800 Pelletier, J.D.; Harrington, C.D.; Whitney, J.W.; Cline, M.; DeLong, S.B.; Keating, G.; and Ebert, K.T. 2005. "Geomorphic Control of Radionuclide Diffusion in Desert Soils." *Geophysical Research Letters, 32,* (L23401), 1-4. Washington, D.C.: American Geophysical Union. TIC: 257905.

182110 Pelletier, Jon D., DeLong, Stephen B., Cline, Michael L., Harrington, Charles D. 2007. "Dispersion of channel-sediment contaminants in distributary fluvial systems: Application to fluvial tephra and radionuclide redistribution following a potential volcanic eruption at Yucca Mountain." *Geomorphology - ScienceDirect,* . Amsterdam, Netherlands: Elsevier B.V. Awaiting Final Publication

183203 Pelletier, J.D. and DeLong, S. 2004. "Oscillations in Arid Alluvial-Channel Geometry." *Geology, 32,* (8), 713-716. Boulder, Colorado: Geological Society of America. TIC: 259730.

178706 Powell, D.M.; Brazier, R.; Wainwright, J.; Parsons, A.; and Kaduk, J. 2005. "Streambed Scour and Fill in Low-Order Dryland Channels." *Water Resources Research, 41,* (W05019), 1-13. Washington, D.C.: American Geophysical Union. TIC: 258347.

174134 Press, W.H.; Teukolsky, S.A.; Vetterling, W.T.; and Flannery, B.P. 2002. *Numerical Recipes in C, the Art Scientific Computing.* 2nd Edition. New York, New York: Cambridge University Press. TIC: 257274.

119693 Reamer, C.W. 1999. "Issue Resolution Status Report (Key Technical Issue: Igneous Activity, Revision 2)." Letter from C.W. Reamer (NRC) to Dr. S. Brocoum (DOE/YMSCO), July 16, 1999, with enclosure. ACC: MOL.19990810.0639.

180898 Reheis, M.C. 2006. "A 16-year Record of Eolian Dust in Southern Nevada and California, USA: Controls on Dust Generation and Accumulation." *Journal of Arid Environments, 67,* 487-520. New York, New York: Elsevier. TIC: 259394.

106658 Reheis, M.C.; Goodmacher, J.; Harden, J.; McFadden, L.D.; Rockwell, T.K.; Shroba, R.R.; Sowers, J.M.; and Taylor, E.M. 1995. "Quaternary Soils and Dust Deposition in Southern Nevada and California." *Geological Society of America Bulletin, 107,* (9), 1003-1022. Boulder, Colorado: Geological Society of America. TIC: 234884.

154124 Ritter, D.F. 1986. *Process Geomorphology.* Second Edition. Dubuque, Iowa: Wm. C. Brown Publishers. TIC: 224316.

145235 Sagar, B., ed. 1997. *NRC High-Level Radioactive Waste Program Annual Progress Report: Fiscal Year 1996.* NUREG/CR-6513, No. 1. Washington, D.C.: U.S. Nuclear Regulatory Commission. ACC: MOL.19970715.0066.

165740 Schlueter, J.R. 2003. "Igneous Activity Agreement 2.09, Additional Information Needed." Letter from J.R. Schlueter (NRC) to J.D. Ziegler (DOE/ORD), March 25, 2003, 0331036684, with enclosure. ACC: MOL.20031009.0249.

177358 Smith, B. and Sandwell, D. 2003. "Accuracy and Resolution of Shuttle Radar Topography Mission Data." *Geophysical Research Letters, 30*, (9), 20-1-20-4. Washington D.C.: American Geophysical Union. TIC: 258765.

177431 SNL (Sandia National Laboratories) 2007. *Atmospheric Dispersal and Deposition of Tephra from a Potential Volcanic Eruption at Yucca Mountain, Nevada.* MDL-MGR-GS-000002 REV 03. Las Vegas, Nevada: Sandia National Laboratories. ACC: DOC.20071010.0003.

177399 SNL 2007. *Biosphere Model Report.* MDL-MGR-MD-000001 REV 02. Las Vegas, Nevada: Sandia National Laboratories. ACC: DOC.20070830.0007.

177430 SNL 2007. *Dike/Drift Interactions.* MDL-MGR-GS-000005 REV 02. Las Vegas, Nevada: Sandia National Laboratories. ACC: DOC.20071009.0015.

177432 SNL 2007. *Number of Waste Packages Hit by Igneous Events.* ANL-MGR-GS-000003 REV 03. Las Vegas, Nevada: Sandia National Laboratories. ACC: DOC.20071002.0001.

182219 SNL 2007. *Technical Work Plan for: Igneous Activity Assessment for Disruptive Events.* TWP-WIS-MD-000007 REV 10. Las Vegas, Nevada: Sandia National Laboratories. ACC: DOC.20070830.0002.

179466 SNL 2007. *Total System Performance Assessment Data Input Package for Requirements Analysis for Subsurface Facilities.* TDR-TDIP-PA-000001 REV 00. Las Vegas, Nevada: Sandia National Laboratories. ACC: DOC.20070921.0007.

178871 SNL 2007. *Total System Performance Assessment Model/Analysis for the License Application.* MDL-WIS-PA-000005 REV 00. Las Vegas, Nevada: Sandia National Laboratories.

180001 Squires, R.R. and Young, R.L. 1984. *Flood Potential of Fortymile Wash and Its Principal Southwestern Tributaries, Nevada Test Site, Southern Nevada.* Water-Resources Investigations Report 83-4001. Carson City, Nevada: U.S. Geological Survey. ACC: NNA.19890511.0110; JQS.19880517.1933.

183748 Tarboton, David G.; Bras, Rafael. ; and Rodriguez-Iturbe, Ignacio. 1991. "On the Extraction of Channel Networks from Digital Elevation Data." *Hydrological Processes*, *5*, (1), 81-100. John Wiley & Sons, Ltd. TIC: 259816.

177782 Valentine, G.A.; Krier, D.; Perry, F.V.; and Heiken, G. 2005. "Scoria Cone Construction Mechanisms, Lathrop Wells Volcano, Southern Nevada, USA." *Geology, 33,* (8), 629-632. Boulder, Colorado: Geological Society of America. TIC: 258340.

107317 Whitney, J.W.; Taylor, E.M.; and Wesling, J.R. 1996. "Quaternary Mapping and Stratigraphy." Chapter 4.1 of *Seismotectonic Framework and Characterization of Faulting at Yucca Mountain, Nevada.* Whitney, J.W., ed. Milestone 3GSH100M. Denver, Colorado: U.S. Geological Survey. TIC: 237980. ACC: MOL.19970129.0041.

9.2 CODES, STANDARDS, REGULATIONS, AND PROCEDURES

180319 10 CFR 63. 2007. Energy: Disposal of High-Level Radioactive Wastes in a Geologic Repository at Yucca Mountain, Nevada. Internet Accessible.

IM-PRO-002, Rev. 001, ICN 0. *Control of the Electronic Management of Information*. Washington DC: U.S. Department of Energy, Office of Civilian Radioactive Waste Management. ACC: DOC.20070912.0012.

IM-PRO-003, Rev. 004, ICN 0. *Software Management*. Washington DC: U.S. Department of Energy, Office of Civilian Radioactive Waste Management. ACC: DOC.20071115.0005.

IM-PRO-004, Rev. 003, ICN 0. *Qualification of Software*. Washington DC: U.S. Department of Energy, Office of Civilian Radioactive Waste Management. ACC: DOC.20070918.0002.

SCI-PRO-002, Rev. 003, ICN 0. *Planning for Science Activities*. Washington DC: U.S. Department of Energy, Office of Civilian Radioactive Waste Management. ACC: DOC.20071009.0014.

SCI-PRO-006, Rev. 006, ICN 0. *Models*. Washington DC: U.S. Department of Energy, Office of Civilian Radioactive Waste Management. ACC: DOC.20071026.0003.

9.3 SOURCE DATA, LISTED BY DATA TRACKING NUMBER

107375 GS960908312121.001. Surface-Water Discharge Data for Yucca Mountain Area, Southern Nevada and Southern California, 1995 Water Year. Submittal date: 10/10/1996.

162863 LA0302CH831811.002. Ash Redistribution, Lava Morphology, and Igneous Process Studies SITP-02-DE-001, REV 00A. Submittal date: 02/18/2003.

179987 LA0612DK831811.001. Magma and Eruption Properties for Potential Volcano at Yucca Mountain. Submittal date: 03/23/2007.

181613 MO0706SPAFEPLA.001. FY 2007 LA FEP List and Screening. Submittal date: 06/20/2007.

182344 MO0708SCSOC137.000. Soil Characteristics, Sample and Observation Locations and Cesium-137 Abundance Values. Submittal date: 08/08/2007.

182108 SN0706DIGORTHO.001. Digital Orthophoto Quadrangles. Submittal date: 07/03/2007.

182111 SN0707DEMSOURC.001. Source DEM for the Forty Mile Wash Drainage Basin DEM. Submittal date: 07/05/2007.

183849 SN0711SCOURCHM.002. Scour Chain Measurements at the Fortymile Wash Narrows. Submittal date: 11/07/2007.

9.4 DEVELOPED AND PRODUCT OUTPUT DATA, LISTED BY DATA TRACKING NUMBER

MO0605SPAFORTY.000. Fortymile Wash Drainage Basin DEM. Submittal date: 05/23/2006.

SN0708GEOMOMAP.001. Geomorphic Characterization of the Fortymile Wash Alluvial Fan. Submittal date: 08/22/2007.

SN0708DIFFEXMP.001. Example Diffusion Model Results. Submittal date: 08/23/2007.

SN0708DIFFRNGS.001. Diffusivity Parameter Calculation. Submittal date: 08/23/2007.

SN0708DIFFVALD.001. Diffusivity Values used for Model Validation. Submittal date: 08/23/2007.

SN0708DRAINDEN.001. Drainage Density Calculation. Submittal date: 08/22/2007.

MO0702PAFARDAT.001. FAR Data. Submittal date: 02/22/2007.

MO0704PASCOURD.000. Scour Depth. Submittal date: 04/09/2007.

SN0708FARSENSS.001. FAR Sensitivity Analysis. Submittal date: 08/23/2007.

9.5 SOFTWARE CODES

182849 ArcGIS V. 9.2. 2007. Windows XP. STN: 11205-9.2-00.

178870 ASHPLUME_DLL_LA. V. 2.1. 2006. WINDOWS 2000/XP. STN: 11117-2.1-00.

182225 FAR V. 1.2. 2007. WINDOWS 2000 & WINDOWS 2003. STN: 11190-1.2-00.

181903 GoldSim V. 9.60.100. 2007. WINDOWS 2000, WINDOWS XP, WINDOWS 2003. STN: 10344-9.60-01.

173438 MVIEW V. 4.0. 2005. WINDOWS 2000. STN: 10072-4.0-00.

APPENDIX A
GEOMORPHIC CHARACTERIZATION OF THE FORTYMILE WASH ALLUVIAL FAN

A1. INTRODUCTION

Soil-geomorphic mapping of the Fortymile Wash fan was performed to provide inputs for the Yucca Mountain total system performance assessment (TSPA). Specifically, this mapping provides distributions for two model parameters: (1) the area of the Fortymile Wash alluvial fan representing the reasonably maximally exposed individual (RMEI) environment (*A*), and (2) the fraction of that area subject to fluvial deposition (*F*). This appendix describes the mapping activity and associated analyses performed to develop these two model parameters for use by TSPA.

The soil-geomorphic mapping activity used field observations of elevation above active channels, terrace dip, depth of dissection, degree of planarity, drainage pattern (tributary versus distributary), and the development of pavement, varnish, and calcic soils as relative-age indicators (Bull 1991 [DIRS 102040]). A total of five distinct units were mapped, ranging in ages from the oldest unit, Qa3 (middle to late Pleistocene), to the active channels (Qa7) that are recently formed. Holocene and Pleistocene units were readily distinguishable using pavement and varnish development, as is the case elsewhere in Amargosa Valley (Keefer et al. 2004 [DIRS 173899]). The degree of planarity was particularly useful for distinguishing between middle-to-late Pleistocene (Qa3) and late Pleistocene (Qa4) units on the Fortymile Wash fan. Drainage patterns were particularly useful for distinguishing between Qa4 (tributary drainage) and late Pleistocene to early Holocene (Qa5) surfaces (distributary drainage). Pelletier et al. (2005 [DIRS 175800]) use this map along with estimates of radionuclide diffusivities estimated from measured ^{137}Cs profiles in the soil to identify a correlation between surface age and diffusivity rates.

The area of the Fortymile Wash alluvial fan representing the RMEI environment (*A*) is physically bounded by large Qa3 (mid to late Pleistocene) terraces on either side of the active fan. The calculation of this area *A* is described in Section A4.

The fraction of the area subject to fluvial deposition (*F*) is assumed to be equal to the fraction of area deposited in the last 10,000 years. Since accurate age dating is not available for these units, an estimate of this areal fraction is bounded by calculating the areal fraction of the fan units deposited during the Holocene. However, the unit Qa5 spans the Pleistocene-Holocene boundary, and therefore including this unit in the areal fraction represents an upper bound on the value of *F*. Excluding Qa5 from the areal fraction represents the lower bound on the value of *F*. The calculation of these bounding values of *F* is described in Section A4.

A2. INPUTS

The inputs used for map development include the following two sources:

- Color digital orthophoto quarter quadrangles (DOQQs) (DTN: SN0706DIGORTHO.001 [DIRS 182108])
- Field observations from 265 locations on the Fortymile Wash alluvial fan from DTN: MO0708SCSOC137.000 [DIRS 182344], Table 4.

Three DOQQs were used to help identify the boundaries and extent of geomorphic units within the Fortymile Wash alluvial fan. Table A-1 lists these DOQQs. Figure A-1 displays the orthophotos.

Table A-1. DOQQs Used to Develop Geomorphic Map of the Fortymile Wash Alluvial Fan

Filename	USGS Quadrangle	Quadrant	Source (DTN)
36116F48.tif	Amargosa Valley	SW	SN0706DIGORTHO.001 [DIRS 182108]
36116F57.tif	Big Dune	SE	SN0706DIGORTHO.001 [DIRS 182108]
36116E45.tif	South of Amargosa Valley	NW	SN0706DIGORTHO.001 [DIRS 182108]

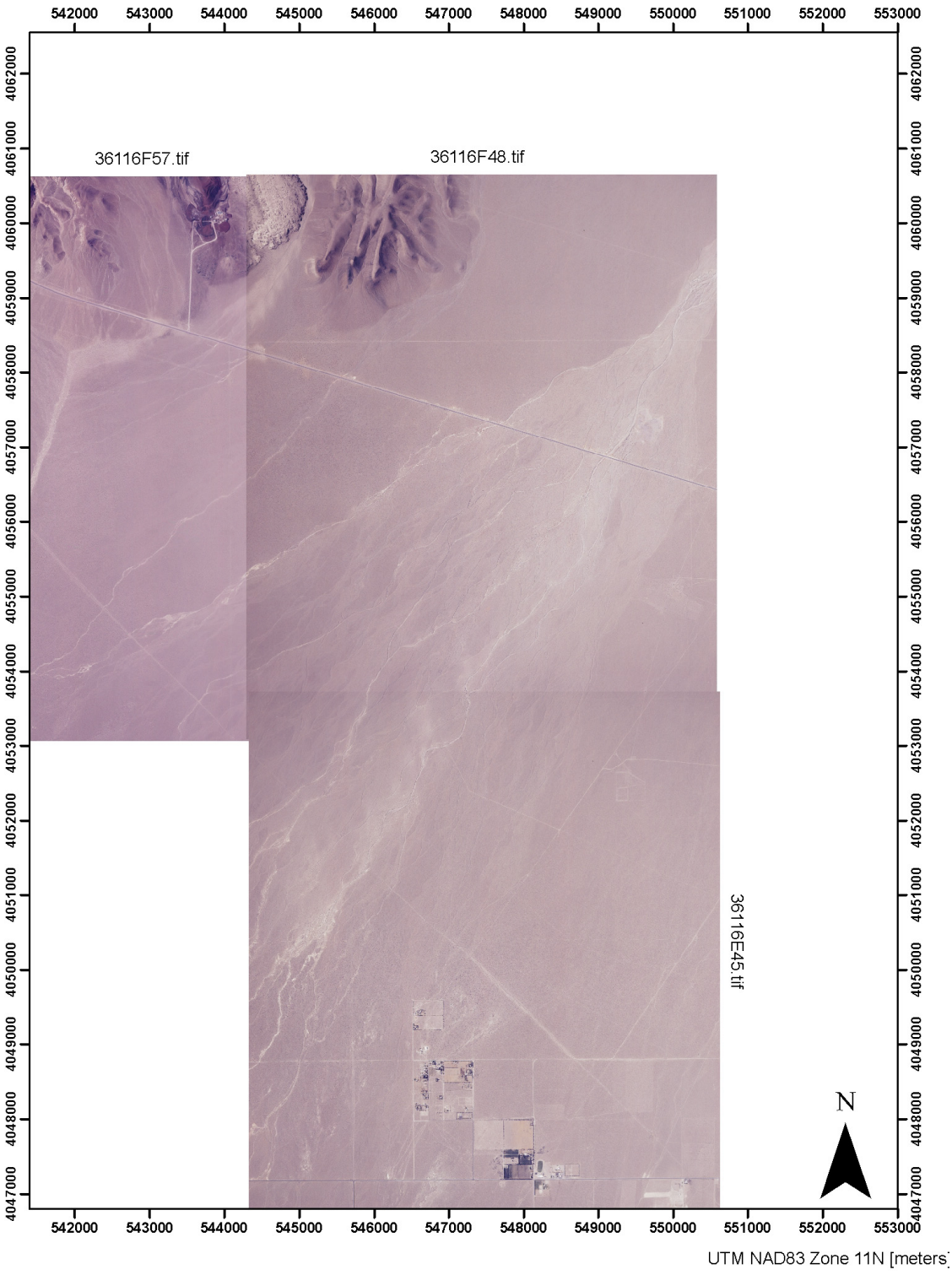

Source: DTN: SN0706DIGORTHO.001 [DIRS 182108].

Figure A-1. Fortymile Wash Alluvial Fan as Seen on Digital Orthophoto Quadrangles

Field observations of geomorphic indicators made during three field trips are found in DTN: MO0708SCSOC137.000 [DIRS 182344], Table 4. These observations are provided in Table 4-6. The observations consist of a station number, coordinates (UTM NAD 83, Zone 11N, meters), and field notes. In a number of cases there appear to be transcription errors in the original field scientific notebook entries (Pelletier 2007 [DIRS 179612], pp. 14-24, 29, 34-46, and 49-53) (e.g., coordinate is outside study area). In most cases such errors are easily fixed by an obvious substitution or correction. Table 4 of DTN: MO0708SCSOC137.000 [DIRS 182344] includes these corrections as table footnotes. Over the duration of the fieldwork, the naming conventions of the various units changed to bring the fieldwork into context with previous work in the Greater Yucca Mountain area. The field notes reported in Table 4 of DTN: MO0708SCSOC137.000 [DIRS 182344] and in Table 4-6 present the unit names as shown in the source for transparency. A full description of the final geomorphic units can be found in Section A3.

The measured field coordinates were overlaid onto orthophotos using Excel and ArcGIS software. The data were entered into Excel as a table. Then, within ArcMap, the XY data were imported using the Tools menu option: *Add XY Data*. Figure A-2 displays the points overlying the orthophoto imagery.

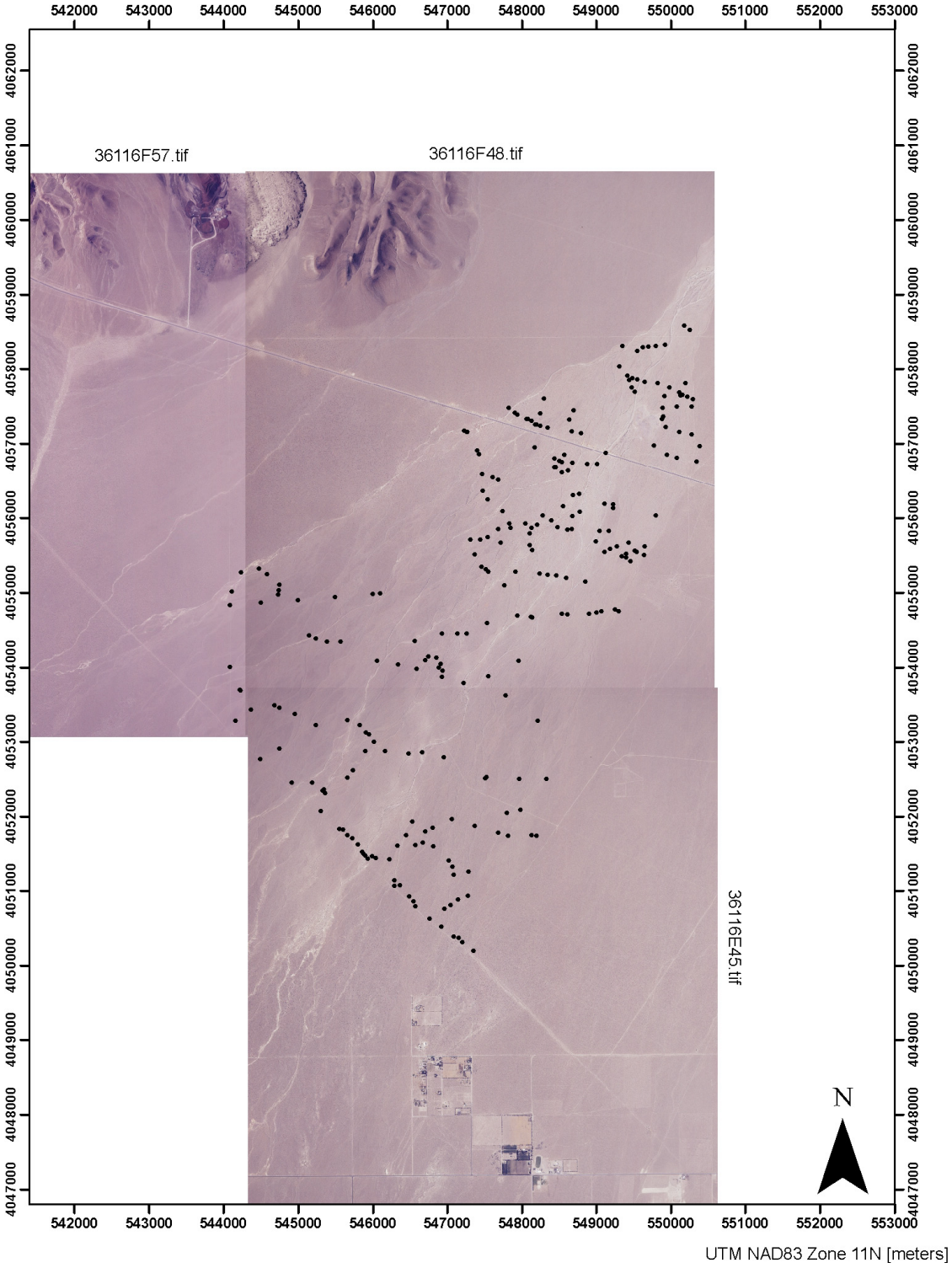

Sources: Orthophotos: DTN: SN0706DIGORTHO.001 [DIRS 182108]; field stations: DTN: MO0708SCSOC137.000 [DIRS 182344], Table 4.

Figure A-2. Locations of Field Observations Shown on Fortymile Wash Alluvial Fan (points) as Seen on Digital Orthophoto Quadrangles

A3. DEFINITION OF MAP UNITS

By combining the spatial and visual information provided in the orthophotos with the geomorphic information and interpretations provided by the field observations, a geomorphic soils map was generated. The units included on the map were defined based on the field observations and a regional chronology of Keefer et al. (2004 [DIRS 173899]), developed by integrating soil-geomorphic mapping and geochronology on nearby Yucca and Crater Flats.

The distribution, boundaries, and extent of the units across the entire fan were initially identified and delineated by drawing boundary lines on the DOQQs by hand and later were drawn digitally within ArcMap. The final digitized version of these hand-drawn lines is included as a geodatabase (*YMgeology.mdb*) in Output DTN: SN0708GEOMOMAP.001. The process of defining geomorphic units to the map required several iterations, with intermediate output used to guide where additional information was required. These data were collected on subsequent field trips, allowing the map to become more refined over time. Reproductions of the initial and intermediate hand-drawn field maps are included in "Oversized and Other Supplementary Material" for scientific notebook SN-M&O-SCI-050-V1 (Pelletier 2007 [DIRS 179612], supplement pp. 3 to 10). Field mapping, such as that done for this report, is not a precise science, but rather a subjective interpretation that relies on geological experience and judgment. No two geologists would create the exact same map given the same data, but there should be general agreement as to the reasonableness of the resulting maps based on the available observations and notes. It is the intent of this appendix and supporting output DTN to describe what was done to create the final map and to provide enough information such that an independent reviewer can judge the adequacy of the final product.

The following are complete unit descriptions for the soil-geomorphic units on the Fortymile Wash alluvial fan. Table A-2 summarizes and compares the main identifying features of the units.

- Qa7 is active alluvium in channels and recent flood deposits. Its age is historical. This unit locally includes narrow bars and late Holocene terrace remnants. Relief on these deposits tends to be <1 m locally. No significant soil development is apparent, though coppice dunes may be present and <1 cm cumulic eolian epipedon (sometimes referred to as an "A-horizon") may be present.

- Qa6 is the middle to late Holocene alluvium. This unit is dominated by bar and swale topography and often appears highly distributary on aerial photographs. It tends to be abandoned alluvial fan deposits preserved 0.5 to 1.5 m above active channels. This unit is distinguishable by prominent coarse bouldery bars that show little accumulation of eolian material. Soil development is minimal, with thin eolian epipedon and rare incipient petrocalcic coating on the undersides of clasts. No varnish development is observed.

- Qa5 unit is the latest Pleistocene to early Holocene alluvium and is the unit that is transitional for being considered part of the fraction of RMEI location that is subject to fluvial deposition. This unit tends to have distinct bar/swale topography with approximately 50 to 1 m relief between bars and swales. Bars tend to be bouldery up to

approximately 70 cm in diameter, though may become finer down-fan. Fine sandy and silty eolian epipedons are often present in swale areas with variable thickness from approximately 10 to 50 cm, with most thicknesses in the 20 to 35 cm range. Eolian epipedon thickness appears variable in relation to distance to active channels that appear to be the dominant source for windblown material. Surfaces show no-to-weak varnish development and weak pavement development. Gravel coverage on the surface is often about 40% with no interconnectedness. Gravel in the lower epipedon and below often shows incipient petrocalcic development with up to Stage I coating developed on the underside of clasts. Bar and swale texture is visible on aerial photos. Relief above active channel is commonly 0.5 to 1 m.

- Qa4 is a late Pleistocene alluvium. This unit generally shows subdued bar and swale topography and sub-planar relief, with weak to moderate varnish development (less than that of Qa3). Pavement is moderately developed, with 50% to 70% clast coverage though only rarely sutured. Eolian epipedon thickness is variable but usually greater than about 35 cm. Eolian epipedon thickness is most commonly 40 to 60 cm. Commonly a pure fine sand and silt, A1 (upper epipedon) horizon 20- to 30-cm thick is above another 20- to 30-cm-thick A2 (lower epipedon) horizon that has floating clasts of fluvial gravel present. Stage II petrocalcic horizon is present below about 80 cm. Relief above active channels is commonly 1 to 1.5 m. This unit tends to appear featureless or have some tributary drainage development on aerial photographs.

- Qa3 is the oldest unit in the field area. It is middle to late Pleistocene alluvium and flanks the active portion of the fan on both sides. It is also preserved as terrace remnants within the alluvial fan. It has well-varnished and well-developed pavement with moderate suturing. The surface clast coverage is up to approximately 80%. The bar and swale topography is extremely rare, and a strikingly planar surface is most common. The eolian epipedon is about 60 to 80 cm thick. A Btk horizon is present below around 55 cm. A well-cemented Stage III-IV, petrocalcic horizon is present below approximately 1.0 m. Relief above active channels is commonly 1.5 m but can be as little as 50 cm on the western portion of fan.

- Qd includes areas that are disturbed, and the surface geology is obscured. Usually these areas are obscured by recent surface mining activities (gravel pits).

Table A-2. Geomorphic Features of the Alluvial Units

Map Unit	Qa7	Qa6	Qa5	Qa4	Qa3
Pavement Development	None	Extremely weak	Weak	Moderate	Strong
Bar/Swale Relief, Drainage Pattern	Variable	1 m relief; distributary	0.5 to 1 m relief; distributary	Subdued, subplanar; <30 cm relief, tributary	Planar; indistinct drainage
Relief above Active Channel (m)	N/A	0.3 to 1	0.5 to 1	0.5 to 1	0.5 to 2.0
Rubifcation and Varnish	None	None	None	Weak to moderate	Moderate to strong
Maximum Soil Development	None	Rare incipient petrocalcic development on sands and some gravels	Stage I+ petrocalcic development	Stage II+ petrocalcic development at 0.5 m; B_{cambic} horizon below 60 cm	Stage IV petrocalcic K horizon at 1.2 m; incipient B_t horizon at 0.8 to 1 m
Eolian Epipedon Thickness (cm)	None	10	20 to 35	30 to 60	60 to 80
Epipedon Description	None	Rare, sandy	Loamy sand; floating clasts in lower epipedon	Loamy sand; floating clasts; discontinuous A_v with max thickness 10 mm	Loamy sand; floating clasts; discontinuous A_v with max thickness 50 mm

A4. RESULTS

This section presents the final soil geomorphic map and the associated calculations of the parameters *A* and *F*. The supporting file (*GeoMap-Area Calculation.xls*) is included in Output DTN: SN0708GEOMOMAP.001.

A4.1 DEVELOPMENT OF THE GEOMORPHIC MAP

Figure A-3 displays a transparent version of the final geomorphic map and field data locations overlain on the DOQQ imagery. Figure A-4 presents the entire geomorphic map and indicates the approximate locations of the large-scale versions of the maps presented in Figures A-5, A-6, and A-7. These large-scale maps show the position and identify the station number for each of the field observations so a more detailed examination of basis for assigning map units can be performed.

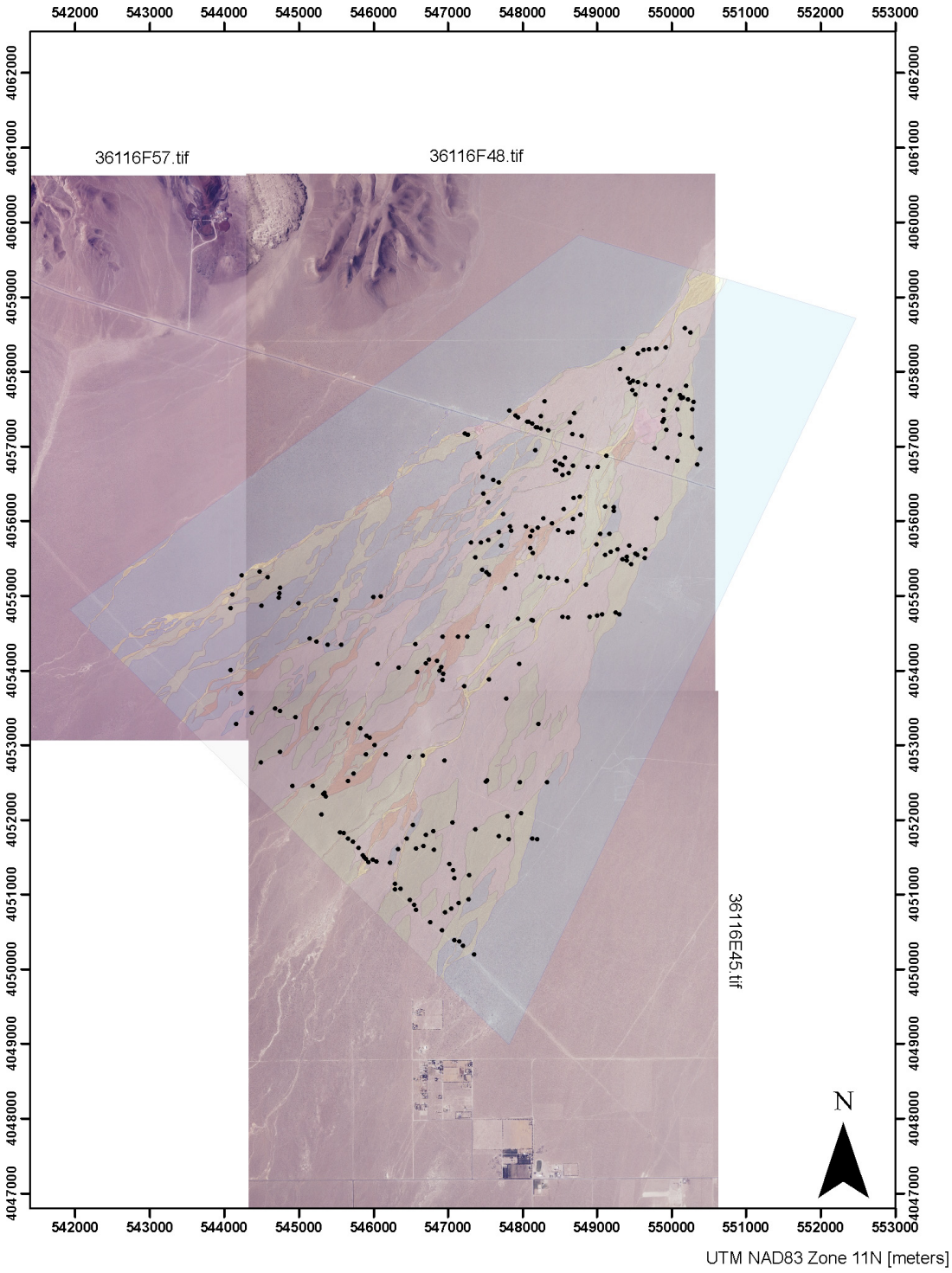

Sources: Orthophotos: SN0706DIGORTHO.001 [DIRS 182108]; field stations: DTN: MO0708SCSOC137.000 [DIRS 182344], Table 4; geomorphic map unit boundaries in Output DTN: SN0708GEOMOMAP.001.

Figure A-3. Transparent Geomorphic Map of the Fortymile Wash Alluvial Fan Shown with Field Observations (points) Overlain on Digital Orthophoto Quadrangles

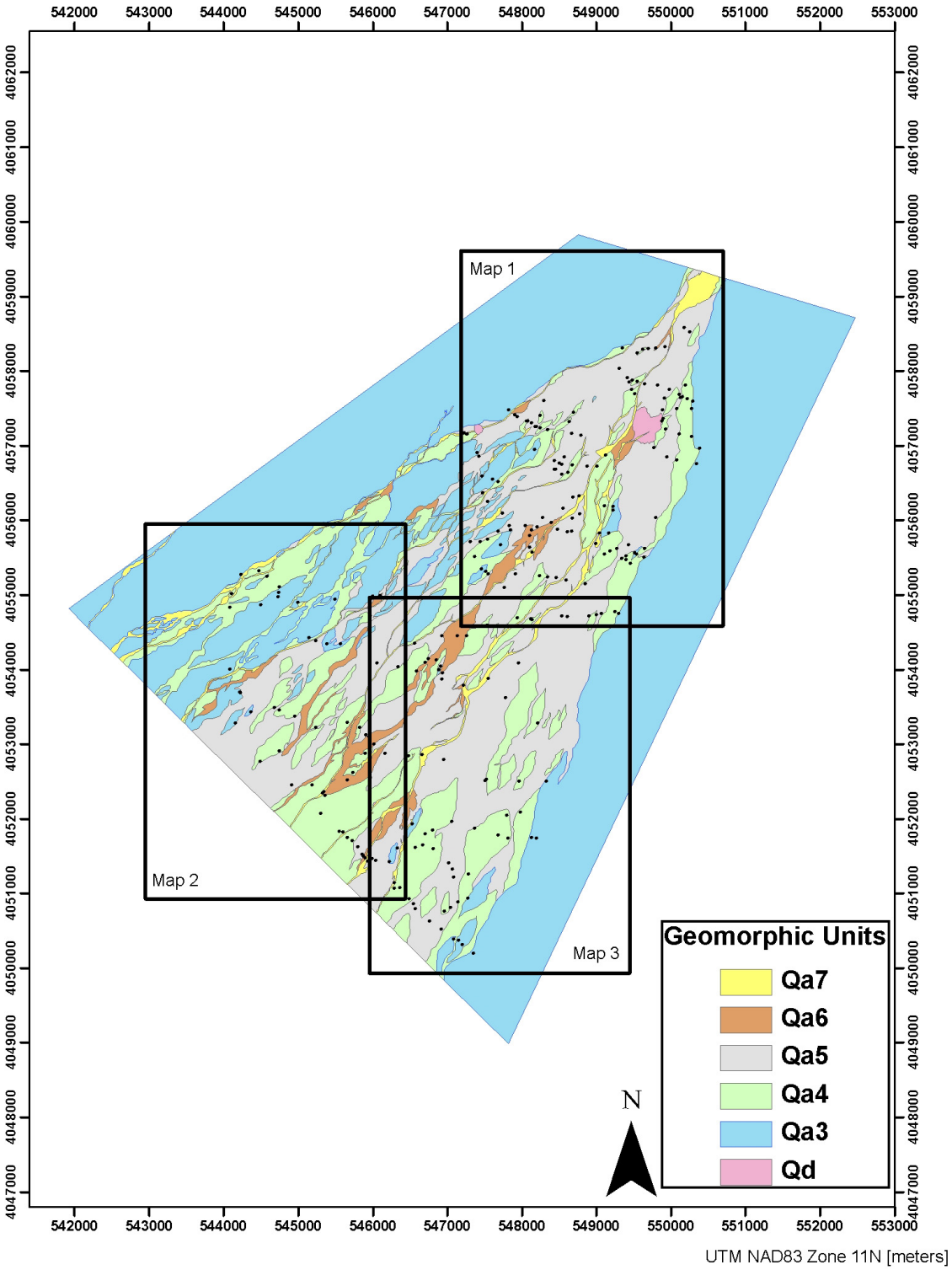

Sources: Field stations: DTN: MO0708SCSOC137.000 [DIRS 182344], Table 4; geomorphic map unit boundaries in Output DTN: SN0708GEOMOMAP.001.

Figure A-4. Geomorphic Map of the Fortymile Wash Alluvial Fan

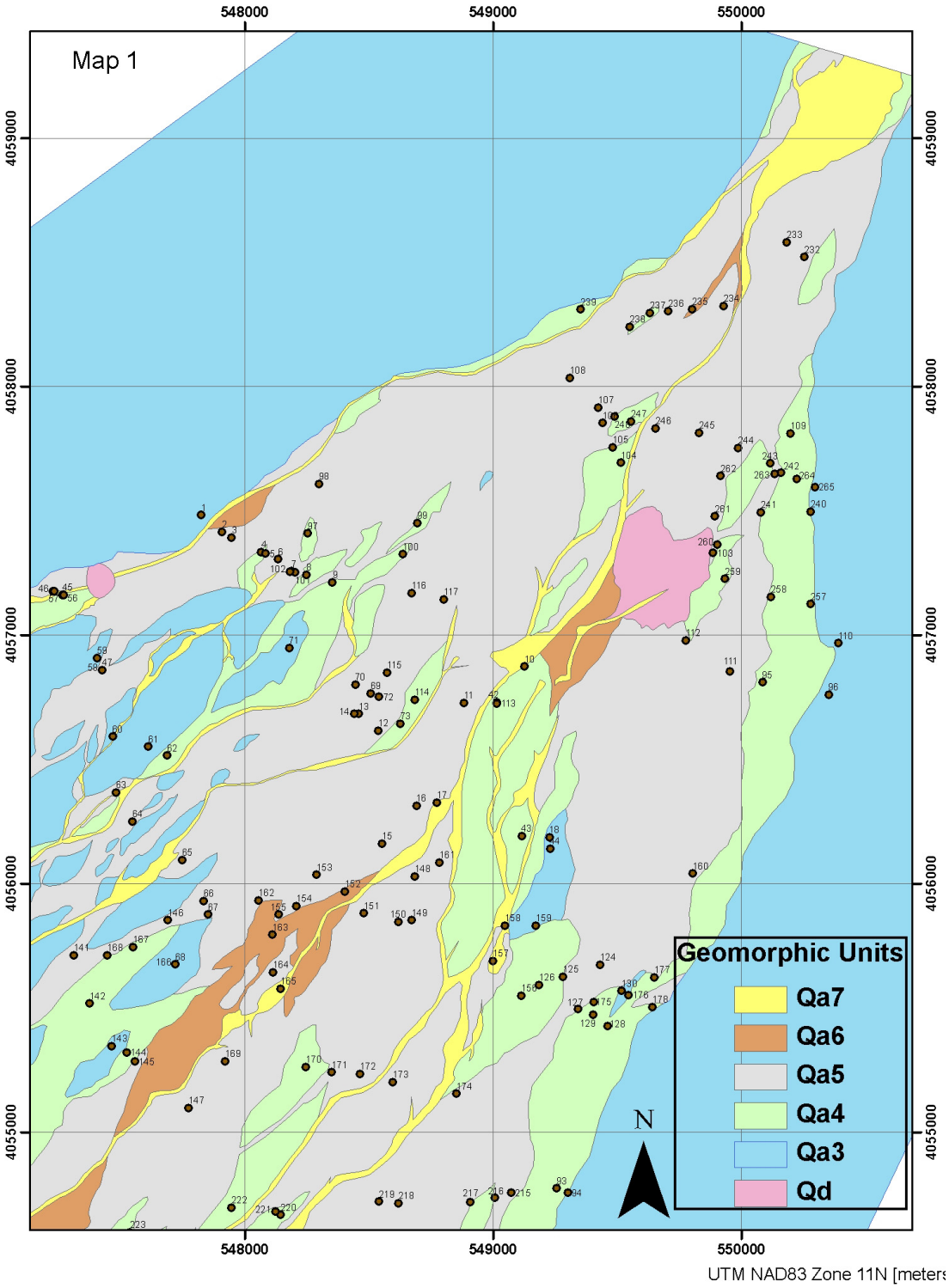

Sources: Field stations: DTN: MO0708SCSOC137.000 [DIRS 182344], Table 4; geomorphic map unit boundaries in Output DTN: SN0708GEOMOMAP.001.

Figure A-5. Detail Geomorphic Map 1 of the Fortymile Wash Alluvial Fan

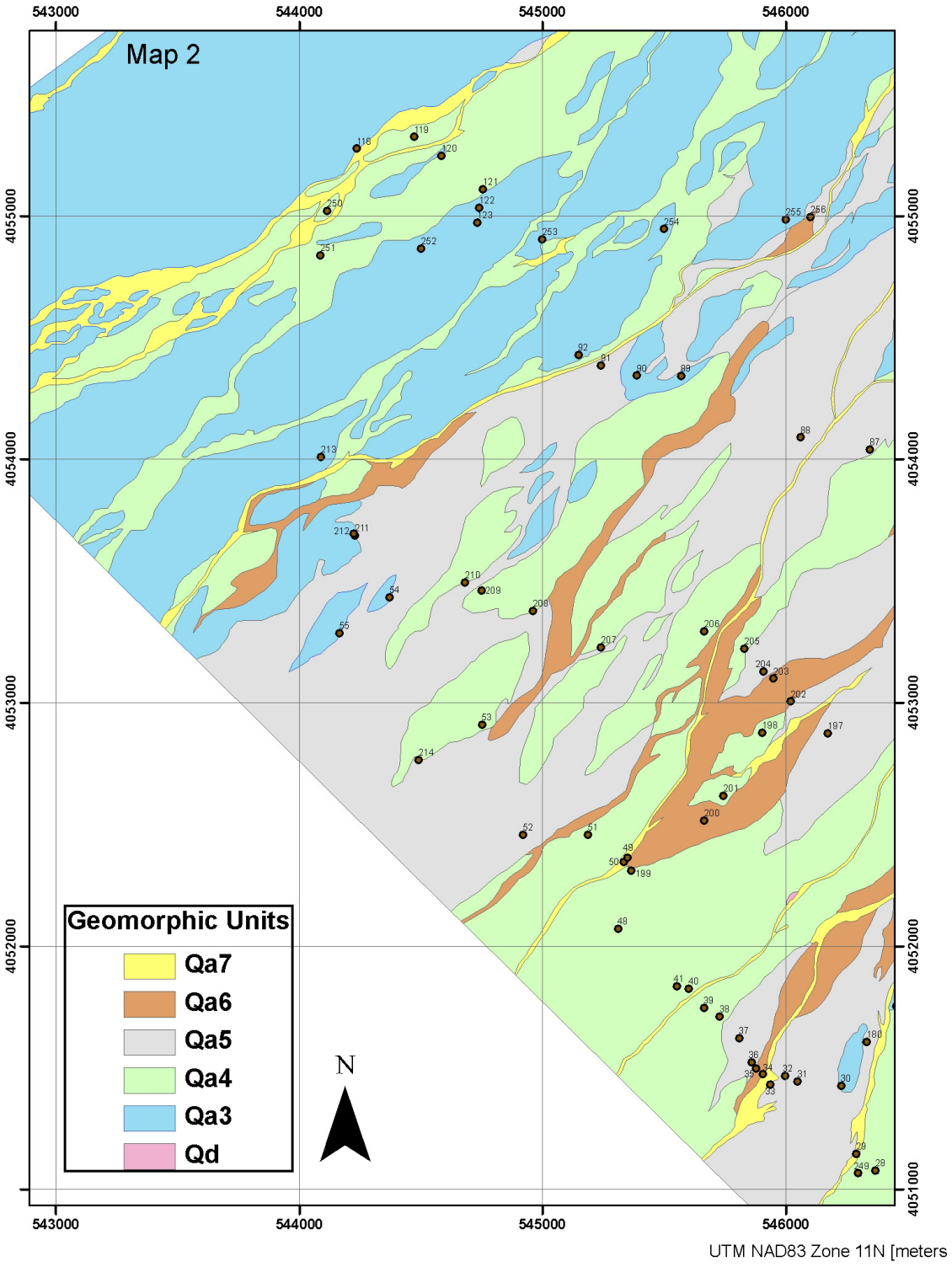

Sources: Field stations: DTN: MO0708SCSOC137.000 [DIRS 182344], Table 4; geomorphic map unit boundaries in Output DTN: SN0708GEOMOMAP.001.

Figure A-6. Detail Geomorphic Map 2 of the Fortymile Wash Alluvial Fan

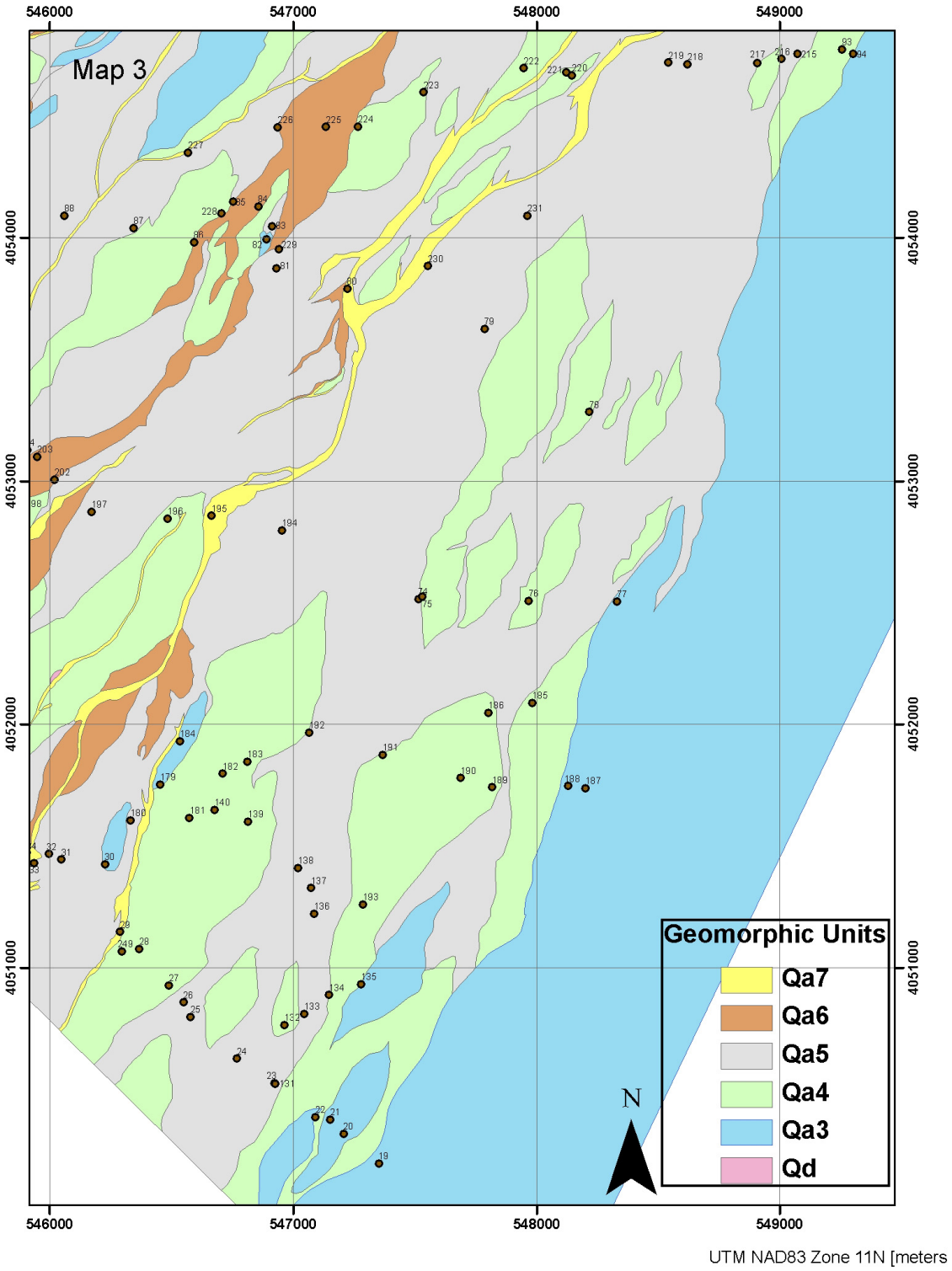

Sources: Field stations: DTN: MO0708SCSOC137.000 [DIRS 182344], Table 4; geomorphic map unit boundaries in Output DTN: SN0708GEOMOMAP.001.

Figure A-7. Detail Geomorphic Map 3 of the Fortymile Wash Alluvial Fan

A4.2 CALCULATION OF FAN AREA AND FRACTION SUBJECT TO FLUVIAL DEPOSITION

This section describes calculations performed to develop distributions for two model parameters: (1) the area of the Fortymile Wash alluvial fan representing the RMEI environment (A), and (2) the fraction of that area subject to fluvial deposition (F).

To develop these parameters, the areas covered by each of the mapped polygons were calculated using ArcGIS. Table A-3 lists the summed areas for each of the map units.

Table A-3. Combined Area of Each Geomorphic Map Unit

Map Unit	Area [m^2]	% of Total Area
Qa7	1,477,729	2.7
Qa6	1,396,815	2.5
Qa5	14,792,113	26.7
Qa4	9,367,721	16.9
Qa3 total	28,215,765	50.9
Qa3 largest polygon	*12,470,721*	*22.5*
Qa3 2nd largest polygon	*10,195,793*	*18.4*
Qd	148,150	0.3
Total Area	**55,398,293**	**100**

Source: Output DTN: SN0708GEOMOMAP.001, file: *GeoMap-Area Calculation.xls*.

NOTE: Qa3 total includes area of the two largest Qa3 polygons. Total area does not include the areas of the two largest Qa3 polygons.

The area of the Fortymile Wash alluvial fan representing the RMEI environment (A) is physically bounded by large Qa3 (mid- to late Pleistocene) terraces on either side of the active fan. The areas defined by these terraces are represented on the map as the two largest polygons in map unit Qa3. This area is calculated by subtracting the areas of Qd and Qa3 from the total area:

$$A = \text{Total area} - \text{Area(Qd)} - \text{Area(Qa3\_largest polygon)} - \text{Area(Qa3\_next largest polygon)}$$

$$A = 55398293 - 148150 - 12470721 - 10195793 = 32583629 \text{ m}^2$$

This value is then rounded to the nearest square kilometer, resulting in an area of 33 km^2.

The fraction of the area subject to fluvial deposition (F) is assumed to be equal to the fraction of area deposited in the last 10,000 years. Since accurate age dating is not available for these units, an estimate of this areal fraction is bounded by calculating the areal fraction of the fan units deposited during the Holocene. However, the unit Qa5 spans the Pleistocene-Holocene boundary and therefore including this unit in the areal fraction represents an upper bound on the value of F. Excluding Qa5 from the areal fraction represents the lower bound on the value of F.

Lower bound calculation of F:

$$F_{LB} = [\text{Area(Qa7)} + \text{Area(Qa6)}] / A$$

$$F_{LB} = [1477729 + 1396815] / 32583629 = \mathbf{0.09}$$

Upper bound calculation of F:

$$F_{UB} = [\text{Area(Qa7)} + \text{Area(Qa6)} + \text{Area(Qa5)}] / A$$

$$F_{UB} = [1477729 + 1396815 + 14792113] / 32583629 = \mathbf{0.54}$$

INTENTIONALLY LEFT BLANK

APPENDIX B
YUCCA MOUNTAIN REVIEW PLAN (NUREG-1804)
ACCEPTANCE CRITERIA

B1. BACKGROUND

Early in 1995, the U.S. Nuclear Regulatory Commission (NRC) recognized the need to refocus its prelicensing repository program on resolving issues most significant to repository performance. In 1996, the NRC identified 10 key technical issues (Sagar 1997 [DIRS 145235]) intended to reflect the topics that the NRC considered most important to repository performance. Nine of the issues were technical, and the tenth concerned the development of the dose standard for a repository at Yucca Mountain (see 40 CFR Part 197 [DIRS 173176]). The technical issues included igneous activity, and the status of resolution of each issue and associated open items were described by the NRC in a series of Issue Resolution Status Reports (e.g., Reamer 1999 [DIRS 119693]). In 2002, the NRC consolidated the subissues into a series of integrated subissues and replaced the series of nine issue resolution status reports with an Integrated Issue Resolution Status Report (NRC 2002 [DIRS 159538]). The Integrated Issue Resolution Status Report was based on the realization that the issue resolution process was "mature enough to develop a single Integrated Issue Resolution Status Report that would clearly and consistently reflect the interrelationships among the various key technical issue subissues and the overall resolution status" (NRC 2002 [DIRS 159538], pp. xviii and xix). The Integrated Issue Resolution Status Report and periodic letters from the NRC (e.g., Schlueter 2003 [DIRS 165740]) provide information about the resolution status of the integrated subissues that are described in *Yucca Mountain Review Plan, Final Report* (YMRP) (NRC 2003 [DIRS 163274]).

B2. IGNEOUS ACTIVITY KEY TECHNICAL ISSUE

The key technical issue for igneous activity was defined by the NRC staff as "predicting the consequence and probability of igneous activity affecting the repository in relationship to the overall system performance objective" (NRC 1998 [DIRS 100297], p. 3). Hence, the NRC defined two subissues for the igneous activity key technical issue: probability and consequences (NRC 1998 [DIRS 100297], p. 3). The probability subissue addresses the likelihood that future igneous activity would disrupt a repository at Yucca Mountain. The U.S. Department of Energy estimated the probability of future disruption of a repository at Yucca Mountain in *Probabilistic Volcanic Hazard Analysis for Yucca Mountain, Nevada* (CRWMS M&O 1996 [DIRS 100116]). For the total system performance assessment (TSPA), an analysis based on results from *Probabilistic Volcanic Hazard Analysis for Yucca Mountain, Nevada* and consideration of the repository design was updated and documented in *Characterize Framework for Igneous Activity at Yucca Mountain, Nevada* (BSC 2004 [DIRS 169989]).

The consequences subissue examined the effects of igneous activity on various engineered and natural components of the repository system. The consequences subissue comprises four integrated subissues: mechanical disruption of engineered barriers (NRC 2003 [DIRS 163274] Section 2.2.1.3.2); volcanic disruption of waste packages (NRC 2003 [DIRS 163274] Section 2.2.1.3.10); airborne transport of radionuclides (NRC 2003 [DIRS 163274] Section 2.2.1.3.11); and redistribution of radionuclides in soil (NRC 2003 [DIRS 163274] Section 2.2.1.3.13). This model report addresses the integrated subissue of redistribution of radionuclides in soil (NRC 2003 [DIRS 163274], Section 2.3.1.3.13). Mechanical disruption of engineered barriers and volcanic disruption of waste packages are addressed in *Dike/Drift Interactions* (SNL 2007 [DIRS 177430]) and *Number of Waste Packages Hit by Igneous*

Intrusion (BSC 2005 [DIRS 177432]). Airborne transport of radionuclides is addressed in *Atmospheric Dispersal and Deposition of Tephra from a Potential Volcanic Eruption at Yucca Mountain, Nevada* (SNL 2007 [DIRS 177431]).

For TSPA for the Site Recommendation, the U.S. Department of Energy defined two igneous modeling cases to evaluate the effects of igneous activity on the repository and its contents:

- A volcanic eruption or direct-release modeling case featuring penetration of the repository by an ascending basaltic dike followed by eruption of contaminated tephra at the surface and deposition of contaminated tephra downwind of the eruption site. This modeling case includes redistribution of the contaminated tephra by surface geological processes.

- An igneous-intrusion or indirect release modeling case featuring penetration of the repository by an ascending basaltic dike without surface eruption, followed by transport of mobilized radionuclides by groundwater flow processes.

Reworking of contaminated tephra deposits could increase the concentration of radioactive waste material at the reasonably maximally exposed individual (RMEI) location and, thereby, potentially increase the dose to the RMEI. For TSPA, mobilization of tephra deposited within the Fortymile Wash drainage basin following an eruption through the repository is the result of fluvial processes. Redistribution of tephra by eolian processes was considered, but based on regional evidence the amount of material redistributed by eolian processes is minor compared to that redistributed by fluvial processes. Hence, the redistribution model is based on fluvial and hillslope processes operating in the Fortymile Wash basin. Documentation of the redistribution model is provided in this report.

B3. YUCCA MOUNTAIN REVIEW PLAN ACCEPTANCE CRITERIA

The YMRP (NRC 2003 [DIRS 163274]) associates the integrated subissue of redistribution of radionuclides in soil with the requirements listed in 10 CFR 63.114(a)-(c) and (e)-(g) [DIRS 180319]. The YMRP (NRC 2003 [DIRS 163274], Section 2.2.1.3.13) describes the acceptance criteria that the NRC will use to evaluate the adequacy of information addressing the integrated subissue of redistribution of radionuclides in soil in the license application. The acceptance criteria may also be addressed in other analysis or model reports. The acceptance criteria will be considered fully addressed when this report is considered in conjunction with those reports. The following discussion provides a summary of how the information in this model report addresses those criteria that are associated with the development and use of the Fortymile Wash ash redistribution (FAR) model.

B4. YMRP SECTION 2.2.1.3.13.3: INTEGRATED SUBISSUE: REDISTRIBUTION OF RADIONUCLIDES IN SOIL

The YMRP (NRC 2003 [DIRS 163274]) associates the integrated subissue of redistribution of radionuclides in soil with the requirements listed in 10 CFR 63.114(a)-(c), (e)-(g), and 63.305 [DIRS 180319] as they relate to the redistribution of radionuclides in soil abstraction. The YMRP (NRC 2003 [DIRS 163274], Section 2.2.1.3.13.3) describes the acceptance criteria that

the NRC will use to evaluate the adequacy of information addressing the redistribution of radionuclides in soil in the license application. The following discussion provides a summary of how the information in this model report addresses those criteria that are associated with the development and use of the tephra redistribution conceptual model.

Acceptance Criterion 1: System Description and Model Integration Are Adequate

(1) Total system performance assessment adequately incorporates important features, physical phenomena and couplings between different models, and uses consistent and appropriate assumptions throughout the abstraction of redistribution of radionuclides in the soil abstraction process.

Information in this model report describes the conceptual model for tephra redistribution, the validity of the model, and model outputs for use in TSPA. Features, events, and processes included in the model are identified in Section 6.1. The purpose of the tephra redistribution model is described in Section 1.1. The tephra redistribution conceptual model is described in Section 6.2. Processes controlling tephra redistribution are described in Section 6.2.1, and the simplification and representation of these processes by the FAR model is discussed in Section 6.2.2. Assumptions associated with the use of the model are described in Section 5. A summary of the tephra redistribution model is provided in Section 8.1, and Section 8.1.1 lists the model outputs. Model uncertainties and limitations associated with the tephra redistribution model are described in Section 8.2. Sensitivity studies are described in Section 6.6.

Inclusion of FAR V.1.2 as a DLL in the TSPA model ensures that physical phenomena and couplings important to the analysis of redistribution of radionuclides in soil are consistently and appropriately treated in performance assessment.

(2) The total system performance assessment model abstraction identifies and describes aspects of redistribution of radionuclides in soil that are important to repository performance, including the technical bases for these descriptions. For example, the abstraction should include modeling of the deposition of contaminated material in the soil and the determination of the depth distribution of the deposited radionuclides.

The FAR tephra redistribution model outputs time series results of relative waste concentrations at the surface and within a prescribed depth interval for the channel and inter-channel divide subdomains of the RMEI location. The tephra redistribution model algorithm, along with example intermediate outputs, is described in Section 6.3.3. Model implementation with a list of input parameters is described in Section 6.4. Section 6.5 describes the development of parameter values for use by TSPA. Assumptions used in the model are documented in Section 5. A description of the mathematical model is provided in Section 6.3.

(3) Relevant site features, events, and processes have been appropriately modeled in the abstraction of redistribution of radionuclides, from surface processes, and sufficient technical bases are provided.

Site FEPs included in the model are identified in Section 6.1.

Acceptance Criterion 2: Data Are Sufficient for Model Justification

(1) Behavioral, hydrological, and geochemical values used in the license application are adequately justified (e.g., irrigation and precipitation rates, erosion rates, radionuclide solubility values, etc.). Adequate descriptions of how the data were used, interpreted, and appropriately synthesized into the parameters are provided.

Data sources that provide direct inputs for the development of parameters used in the tephra redistribution conceptual model are identified in Section 4.1. A general description of the tephra redistribution conceptual model and processes is provided in Section 6.2. The representation of rates of surficial processes that are needed to support model development and use is documented in Section 5, and the model inputs needed to implement the model are described in Section 6.5. Analogue studies to support the tephra redistribution conceptual model are described in Sections 7.1.2 and 7.1.3. The results of an independent review of the tephra redistribution model are described in Section 7.3 and Appendix C. Outputs from the tephra redistribution model are described in Section 8.1 and are listed in Table 6.5.10-1.

(2) Sufficient data (e.g., field, laboratory, and natural analog data) are available to adequately define relevant parameters and conceptual models necessary for developing the abstraction of redistribution of radionuclides in soil in the total system performance assessment.

Data sources that provide direct inputs for the development of parameters used in the tephra redistribution conceptual model are identified in Section 4.1. The model inputs needed to implement the model are described in Section 6.5. Tables 6.5.10-1 and 8.1-1 list the TSPA inputs that are provided by the tephra redistribution conceptual model.

Acceptance Criterion 3: Data Uncertainty Is Characterized and Propagated through the Model Abstraction

(1) Models use parameter values, assumed ranges, probability distributions, and bounding assumptions that are technically defensible, reasonably account for uncertainties and variabilities, do not result in an under-representation of the risk estimate, and are consistent with the characteristics of the reasonably maximally exposed individual in 10 CFR Part 63.

Inputs for the tephra redistribution conceptual model and the appropriateness of the inputs for use in the model are described in Section 4.1. Assumptions are described in Section 5. Analogue studies undertaken to ensure the model appropriately considers sedimentary processes that affect tephra sheets are described in Section 7. Section 6.5

discusses the development of input parameters and justifies these parameter ranges by showing that resulting model outputs to the TSPA do not result in an under-representation of risk. However, the representation of risk is a TSPA function that is beyond the scope of this report.

The development and use of the tephra redistribution conceptual model is not dependent on consideration of the characteristics of the RMEI. Characteristics of the RMEI are provided in *Characteristics of the Receptor for the Biosphere Model* (BSC 2005 [DIRS 172827]), which defines values for biosphere model parameters that are related to the dietary, lifestyle, and dosimetric characteristics of the receptor. Agricultural and environmental input parameters for the biosphere model are described in *Agricultural and Environmental Input Parameters for the Biosphere Model* (BSC 2004 [DIRS 169673], Section 6).

(2) *The technical bases for the parameter values and ranges in the TSPA abstraction are consistent with data from the Yucca Mountain region (e.g., Amargosa Valley survey, Cannon Center for Survey Research 1997), studies of surface processes in the Fortymile Wash drainage basin, applicable laboratory testing, or other valid sources of data. For example, soil types, crop types, plow depths, and irrigation rates should be consistent with current farming practices, and data on the airborne particulate concentration should be based on the resuspension of appropriate material in a climate and level of disturbance similar to that which is expected to be found at the location of the reasonably maximally exposed individual during the compliance time period*.

The tephra redistribution conceptual model is based on surficial-processes information, including tephra deposition and mobilization, tephra transport and mixing, and tephra emplacement and radionuclide diffusion, collected in the Yucca Mountain area, including sample locations in Fortymile Wash and surrounding the Lathrop Wells cone (Sections 6.2 and 6.5). The methods used to represent rates of surficial processes in Fortymile Wash are described in Section 5.

The development and use of the tephra redistribution conceptual model is not dependent on consideration of the characteristics of the RMEI. Characteristics of the RMEI are provided in *Characteristics of the Receptor for the Biosphere Model* (BSC 2005 [DIRS 172827]), which defines values for biosphere model parameters that are related to the dietary, lifestyle, and dosimetric characteristics of the receptor. Agricultural and environmental input parameters for the biosphere model are described in *Agricultural and Environmental Input Parameters for the Biosphere Model* (BSC 2004 [DIRS 169673]).

(3) Uncertainty is adequately represented in parameters for conceptual models, process models, and alternative conceptual models considered in developing the total system performance assessment abstraction of redistribution of radionuclides in soil, either through sensitivity analyses, conservative limits, or bounding values supported by data, as necessary. Correlations between input values are appropriately established in the total system performance assessment.

Product outputs that provide inputs for the TSPA are described in Table 6.5.10-1. As can be seen from Table 6.5.10-1, uncertainties in soil redistribution parameters are provided as uncertainty distributions for use in the TSPA. The tephra redistribution conceptual model is described in terms of its component processes in Section 6.2.

(4) Parameters or models that most influence repository performance based on the performance measure and time period of compliance, specified in 10 CFR Part 63, are identified.

Sensitivity analyses presented in Section 6.6 are used to identify and rank the uncertain input parameters by their importance and influence on model results.

Acceptance Criterion 4: Model Uncertainty is Characterized and Propagated through the Model Abstraction

(1) Alternative modeling approaches of features, events, and processes are considered and are consistent with available data, and current scientific understanding, and the results and limitations are appropriately considered in the abstraction.

The main process represented by the tephra redistribution model is referred to as the scour-dilution-mixing model in Sections 6.2.2 and 6.3.3 (STEP 4). This model is used to represent the process of tephra and clean sediment being mixed as they are transported down the drainage network. The result of this mixing process is that waste concentrations become diluted once sediment is deposited at the RMEI location. Sections 6.2.2 and 7.2.4 discuss the differences between alternative models widely used in the mining exploration and contaminant-transport literature and the one used in the tephra redistribution model.

Other alternative modeling approaches are described in Section 6.3.3 (e.g., bicubic versus bilinear interpolation schemes, steepest descent versus central differences for calculating slopes, steepest descent versus divergent flow (bifurcation) algorithm for calculating contributing area, etc.). These alternative approaches were considered in the development of the tephra redistribution model. The model validation presented in Section 7 provides confidence that the modeling approach taken is consistent with available data and current scientific understanding.

Sections 1.2 and 8.2 discuss the limitations of the tephra redistribution model.

(2) Sufficient evidence is provided that alternative conceptual models of features, events, and processes have been considered; that the preferred models (if any) are consistent with available data (e.g., field, laboratory, and natural analog) and current scientific understanding; and that the effect on total system performance assessment of uncertainties from these alternative conceptual models has been evaluated.

The main process represented by the tephra redistribution model is referred to as the scour-dilution-mixing model in Sections 6.2.2 and 6.3.3 (STEP 4). This model is used to represent the process of tephra and clean sediment being mixed as they are transported down the drainage network. The result of this mixing process is that waste concentrations become diluted once sediment is deposited at the RMEI location. Sections 6.2.2 and 7.2.4 discuss the differences between alternative models widely used in the mining exploration and contaminant-transport literature and the one used in the tephra redistribution model.

Other alternative modeling approaches are described in Section 6.3.3 (e.g., bicubic versus bilinear interpolation schemes, steepest descent versus central differences for calculating slopes, steepest descent versus divergent flow (bifurcation) algorithm for calculating contributing area, etc.). These alternative approaches were considered in the development of the tephra redistribution model. The model validation presented in Section 7 provides confidence that the modeling approach taken is consistent with available data and current scientific understanding.

(3) Consideration of conceptual model uncertainty is consistent with available site characterization data, laboratory experiments, field measurements, natural analog information and process-level modeling studies; and the treatment of conceptual model uncertainty does not result in an under-representation of the risk estimate.

The basis of the tephra redistribution conceptual model is described in Section 6.2; the description of the mathematical model and algorithm is included in Section 6.3. Direct inputs for the tephra redistribution model and the appropriateness of the inputs for use in the model are described in Section 4.1, and parameter inputs for TSPA are described in Section 6.5. Assumptions are described in Sections 5.1 through 5.7. Analogue studies undertaken in the Yucca Mountain area to ensure that the model appropriately considers sedimentary processes that affect tephra sheets are described in Section 7.

Conceptual model uncertainty is discussed with respect to model assumptions (Section 5) and with respect to post-development model validation (Section 7).

Acceptance Criterion 5: Model Abstraction Output Is Supported by Objective Comparisons

(1) Models implemented in the abstraction provide results consistent with output from detailed process-level models and/or empirical observations (e.g., laboratory testing, field measurements, and/or natural analogs).

Post-development model validation activities described in Section 7 provide comparison of model results with field data from analogue sites. This comparison demonstrates and provides confidence that the model adequately matches empirical observations.

APPENDIX C
CRITICAL REVIEWS

C1. INTRODUCTION

This appendix includes reviews from two independent critical reviewers. The selected reviewers were Dr. Larry Mayer and Dr. William Hackett. An initial critical review by Dr. Mayer (of Draft A of the report) was quite detailed and raised many specific as well as more general concerns and issues. This review is reproduced in Section C2 with inline comment responses (in blue italic font) below each specific comment. A scanned copy of Dr. Mayer's original review is included in Section C5. The initial critical review by Dr. Hackett (of Draft A of this report) is reproduced in Section C3. Section C4 reproduces Dr. Hackett's final critical review (of Draft D of this report).

Dr. Mayer is an accomplished geomorphologist who received his Ph.D. in 1982 from the University of Arizona, Department of Geosciences. He held the position of Professor in the Geology Department of Miami University from 1982 to 2000. He is the author/editor of several books and many peer-reviewed journal articles in the geosciences and has served on many distinguished national boards including as a panel member for the National Academy of Sciences and the National Science Foundation. Dr. Hackett's qualifications are included as part of the introduction to his final critical review (Section C4).

C2. CRITICAL REVIEW BY DR. LARRY MAYER

September 10, 2007

To: M. Kathryn Knowles

From: Larry Mayer

RE: Independent Critical Review of MDLMGRGS000006 REV 00A

This Independent Critical Review of "Post-development validation of a model describing Redistribution of Tephra and Waste by Geomorphic Processes Following a Potential Volcanic Eruption at Yucca Mountain, Nevada" will address the following six principal questions:

1. Is the conceptual model for tephra redistribution reasonable and appropriate for its intended use?

2. Are the mathematical relationships appropriate and representative of the scientific understanding of the geomorphic processes for the transport of sediment from the Fortymile drainage basin to the location of the RMEI on the Fortymile Wash alluvial fan?

3. Are the outputs of the model reasonable and representative?

4. Are there alternative models or approaches that should be considered?

5. Are the limitations of the model adequately described?

6. Are the model validation activities (in addition to validation by critical review) that have been planned in the TWP and reported in the model report appropriate and adequate, and adequately and correctly conducted and interpreted?

"Its *intended use* is to be integrated with the Ashplume and Biosphere models within the TSPA model to predict the waste concentration as a function of time since the eruption at a compliance point (RMEI) approximately 18 km south of the repository on the Fortymile Wash alluvial fan. Ashplume provides input (initial extent and thickness of contaminated tephra on the Fortymile Wash landscape) to the tephra redistribution model, which in turn provides input (waste concentration as a function of time since the eruption) to the Biosphere model that calculates radiological dose at the RMEI. NOTE: The Ashplume and Biosphere models have undergone separate validation and, therefore, are outside the scope of your critical review."

"Its *purpose* is to reasonably and appropriately represent the redistribution (mobilization, transport, dilution, deposition, and diffusion) of waste-contaminated tephra deposited in the Fortymile Wash drainage basin east and northeast of the Yucca Mountain, Nevada site by a low probability (mean annual frequency of intersection of a potential repository at Yucca Mountain by a volcanic event equal to 1.7×10^{-8}) volcanic eruption through the repository."

After making a few general comments regarding MDL-MGR-GS-000006 REV 00A, the review discusses sections of the report relevant to each question and answers each of the questions above sequentially.

General Comments

The version of the model report that I reviewed, MDL-MGR-GS-000006 REV 00A, is clearly a work in progress. The apparent quality and completeness, both technical/scientific and clarity, varied considerably throughout the document.

I have attempted to address the six questions required for Level II validation in a direct and formal manner. The probability of a volcanic event (provided in the statement of purpose above), only enters into the review as part of the discussion for question 4, alternative models. In this review, I may refer to the model for tephra redistribution as the FAR model and to data input into FAR coming from the ASHPLUME model.

I have made a conscious attempt to simplify the mathematics of MDL-MGR-GS-000006 for a non specialist, in order to make my technical review as transparent and easy to understand as possible. For this reason, and other reasons of clarity, I chose to include a number of figures that explain or demonstrate a specific point relevant to this review. Several of the figures are simply cartoons to help visualize the variables in the model. Several of figures are used to demonstrate and document how the model output was evaluated. Because of references to figures inside and outside of this review, I used the original report figure numbers. Figures in the MDL-MGR-GS-000006 report take a form reflecting their chapter and section location (e.g., Fig 6.5.3-3), while figures used in this review are simply labeled Fig. 1-12.

Some of the figures which represent model output were clipped directly from the electronic form of MDL-MGR-GS-000006 that I was sent. Others were provided by J.S. Stein at higher resolutions than in the PDF file of MDL-MGR-GS-000006 to allow for more detailed inspection.

Figures using overlays of model output with satellite or topographic data were done with Google Earth, and the projections of data onto the Lathrop Wells satellite image were also done in Google Earth.

The Lathrop Wells satellite image from Google Earth was used to help me understand the use of a validation study discussed in the MDL-MGR-GS-000006 report, to demonstrate the importance of eolian processes at the Lathrop Wells tephra sheet, and by inference, the adjacent Fortymile Wash alluvial fan. Note that all citations are from MDL-MGR-GS-000006 and are not reproduced here.

The scope of this technical review is largely determined by the request for the Independent Technical Review, which in turn is conditioned by regulatory requirements. I have tried to avoid extending the scope in any way.

Finally, this review was done within a limited period of time, allotted by Sandia National Laboratory, and as all technical reviews, may be in part dependent on that time period. However, I do believe that this review represents a broad identification and discussion of all critical points explicitly raised in the six principal questions.

Conceptual Model

The conceptual model presented in section 6.2 claims that it "integrates physically based submodels for hillslopes, fluvial, and soil redistribution processes". Further, the report claims that "the simplified approach taken is adequate for the intended purpose" (page 6-1).

Originator Response: A more detailed description of the conceptual model has been added (Section 6.2). It includes a clear description of the relevant geomorphic processes along with an explanation of how the model represents, simplifies, and approximates these processes. This description also includes references to related assumptions that are presented in Section 5. Most of this information was already included in Draft A of the report, but given the reviewer's comments, it was decided that this information needed to be discussed in the conceptual model description.

The conceptual model for the "hillslope submodel" is barely described in section 6.2.1. The description requires some development and clarity, but the text basically says that the hillslope submodel consists of a threshold calculation. If the slope upon which the tephra is deposited is greater than a threshold slope value, the "tephra and waste in that pixel is considered to be mobilized". First, the text should clarify whether the waste is uniformly distributed with the tephra and not partitioned according to particle size of the ejecta. But beyond this threshold calculation, there is no physical basis provided in the conceptual model description for this "submodel".

Originator Response: Clarifying descriptions of the way the model treats waste versus tephra have been added (Section 6.2). The conceptual model description of the "hillslope submodel" has been expanded (Section 6.2).

The conceptual model for the "fluvial submodel" is barely described in section 6.2.2. There is no discussion for the physical basis of the model in this section, although there is some description

of the method used to calculate dilution of tephra, which is further elaborated later in the mathematical model description. There is simply not enough description or background given in section 6.2.2 to consider this an adequate model of any kind. The reviewer is left wondering why this method was chosen and how it might relate to physical processes important for the intended purpose.

Originator Response: The conceptual model description of the "fluvial submodel" has been expanded (Section 6.2).

The final part of the conceptual model is described in section 6.2.3, the "soil redistribution process". Here the report considers two distinct surfaces separated by whether or not fluvial activity is "possible". On older fan surfaces or "interchannel divides" which have not been inundated by channel flow from the active main channels, the conceptual model considers only diffusion processes, and that diffusion will be limited to a zone physically constrained by calcretes. In the active channels, diffusion is also considered to be the sole process of redistribution, albeit at a higher effective diffusivity. The report also states that "additional mixing of sediments" in the fan channels can occur by flood events. This statement contradicts the conceptual model presented because there is a change in the concentration from outside the model unrelated to the one dimensional diffusion process.

Originator Response: The conceptual model description of the "soil redistribution process" has been expanded and clarified, and it is now clearly stated that although additional mixing during flood events is a reality, it is not included in the model (Section 6.2).

1. Is the conceptual model for tephra redistribution reasonable and appropriate for its intended use?

No, the conceptual model as presented in section 6.2 is neither reasonable nor appropriate for its intended use because a conceptual model is not developed or described. A conceptual model is largely absent from the reviewed version of the report. The context for its intended use is not explained in the brief sketch provided. I believe that it is the responsibility of the report author to develop, describe, and justify, a conceptual model that satisfies claims of being "physical based", and to demonstrate how this model is appropriate for intended use.

Originator Response: The conceptual model description has been expanded to address this reviewer's comment (Section 6.2).

The report also fails to document the conceptual models which are the basis of the mathematical model. The report does not satisfy its own claim to "integrate physically based submodels". The goal of a conceptual model is the explanation of the physical processes which are important for predicting tephra redistribution for the intended purpose and use and perhaps discounting those that are not important. Although this reviewer was able to reconstruct an algorithm-based conceptual model from the mathematical description below, it is the responsibility of the report author(s) to develop, document, and justify the conceptual model upon which the mathematical model is based. Lacking a conceptual model, there is no formal basis to accept or reject the underlying mathematics as conceptually appropriate or reasonable.

Originator Response: The conceptual model description has been expanded to address this reviewer's comment (Section 6.2).

Mathematical Model

The mathematical model is documented in section 6.3.

Initial Conditions: The initial conditions used in the FAR model are described in section 6.3.2. The tephra and waste concentrations from ASHPLUME. Any reviewer needs to understand whether the waste distribution is assumed to be uniformly distributed with the tephra, or partitioned in some way with particle size or other factor. That will also include the partitioning of radionuclides. Further, the reviewer needs to know whether the tephra thickness is given as a mean and standard deviation within each (concentration) isopach band, or as a simple thickness with no statistical variability within an isopach. Finally, the reviewer needs to know whether the likelihood of considerable accumulation in lower or wind shadow areas are part of the ASHPLUME model used for input into FAR.

Originator Response: Additional information about ASHPLUME output has been provided. In general it must be noted that the assumptions underlying the ASHPLUME model are presented and justified in that report, and it is not necessary to repeat in this report. As such, only the description of the output grids has been expanded upon. The FAR code, in turn, calculates based on the tephra and waste mass in each pixel. Tephra mass is converted to an effective thickness by dividing by tephra bulk density.

The 30 m resolution DEM needs to be validated in the low relief areas to make certain that there are no gross errors in the delineation of the drainage basin. I will revisit the DEM later in this section.

Originator Response: DEMs are standard, acceptable tools used for calculations similar to these (discussed in Section 7) and as such additional validation would be redundant. The DEM undergoes a "correction" (by filling "pit" artifacts) as part of the development of the watershed input file. This step ensures that all areas in the landscape drain to the watershed outlet.

The algorithm is delineated in section 6.3.3.

Step 1 is the interpolation of the ASHPLUME tephra output for use as input in FAR. This involves an interpolation from a polar grid to a Cartesian grid matching the DEM. I think that an estimate of the error in this method can be easily produced by comparison with the pre-transformed and rectified data, and would be useful to understand the sensitivity analyses.

Originator Response: Such a comparison is appropriate and an analysis and figure that compares ASHPLUME effective tephra thickness with interpolated values at the nearest DEM grid cell have been added (Figure 7.2.1-1).

Step 2 is taken to correct flaws in the DEM that are required for the subsequent calculations. It is unlikely that this method introduces serious error into the resultant calculations.

Originator Response: Nevertheless, a map and histograms that quantify both the location and magnitude of elevation changes made by applying this method have been added (Figures 7.2.2-1 and 7.2.2-2).

Step 3 computes slope, contributing area and scour depth. The slope computed in this step will be compared to a threshold value, the critical slope, to determine if the tephra stays on the hillslope or is transported to the adjacent channel. The method used here does not include diagonals in the slope calculation. The calculation also assumes that the grid is square.

Originator Response: It is true that diagonal gradients are not considered in the slope calculation. An additional validation analysis that compares the model-generated slopes to an alternative slope calculation (steepest descent) has been added along with a figure (Figure 7.2.3-1). The fact that the model uses a "square" grid is obvious and standard practice in numerical surface water hydrology analysis.

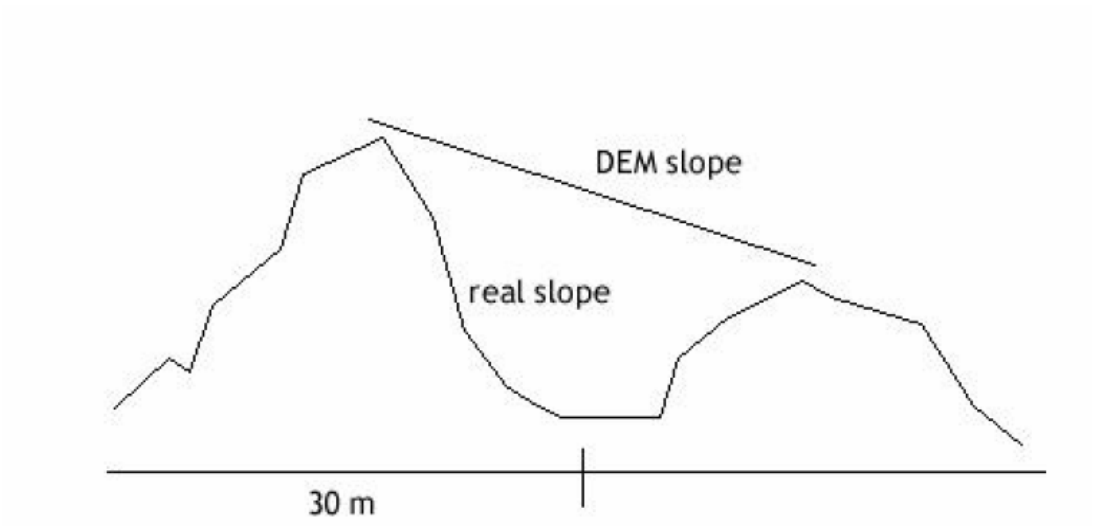

Figure 1: DEM slope compared to real world slope. The actual topographic profile may have a very different local slope in comparison to a 30-m DEM calculated slope.

The reviewer does not have a simple method to determine the relation between the DEM slope and the real Fortymile wash drainage basin slopes. Because it is conceivable that the two slope estimates diverge depending on the relief and roughness of the topographic surface (Fig. 1), perhaps the author should provide this comparison.

Originator Response: Such a comparison would require an independent measurement of slope throughout the drainage basin, which is not available. What's shown in Figure 1 is also unrealistic. On a 30 x 30m grid you will not typically have the type of peaks / valleys that the figure portrays, since such steep slopes would be unstable in this environment, unless composed of solid rock. In addition, DEM errors are considered random in space, and over large areas the general drainage directions therefore will be accurately represented. Errors in slope between the DEM and the reality on the ground may result in mobilized mass being routed to a place in the channel one (or even several) pixel from where it really would go, but on the spatial scale of the upper drainage basin any such errors are insignificant. Plus, because the FAR code uses essentially a "bulk" movement (not a finite difference element), as long as the mobilized

tephra reaches the correct channel, the actual location it enters the channel is of little consequence.

This is especially important as this calculation is used for an important step in the algorithm, calculating the area steeper than the critical slope, which in turn is the most sensitive model parameter.

Are the stream slopes calculated by this method comparable to the real world stream slopes measured in the field?

Originator Response: Alternative and independent measurements of stream slopes have not been made. Stream slope measurements are usually made from DEM or topographic maps and therefore would be consistent with the model results.

The report suggests that a 5x5 moving average is used to determine slope values for the stream power calculation. Is it really a moving average or just an average over a 5x5 grid? I can understand smoothing the values by averaging over 5x5 grids, but I cannot understand why a moving average would be used.

Originator Response: The description of this average has been modified and a figure (Figure 6.3.3-4) was added. The term "moving" is no longer used to describe this average.

Contributing area is calculated by progressively summing the upflow area, using the bifurcation routing method. The report claims that it provides an accurate method for mapping the channel area in a DEM, which is a critical calculation in this method, but does not explain how that claimed accuracy is validated in comparison to alternative methods, including manual channel delineation. I will return to this question in the model output section. The report also does not explain the selection of Freeman's "p" parameter in eq 6-5.

Originator Response: The report says that the bifurcation routing method is a better method than steepest descent, and provides a reference (Pelletier 2004 [DIRS 174135]). The equation (Equation 6.3-8) has been edited to show the "p" parameter and additional text has been added to explain that the model assumes "p" = 1, and thus flow is linearly weighted with directional slope.

Scour depth, another critical model parameter is calculated on the basis of only two studies. The first study, Squires and Young, 1984, estimated the maximum discharge as a function of contributing area for large floods. They suggest that they are describing floods with a recurrence interval of 100 years and 500 years, although there may be very large uncertainty associated with annual flood probabilities of rare floods. It should be noted that on Figure 13 of the Squire and Young study, there is an outlier.

*Originator Response: **Response to outlier in figure 13:** Figure 13 of Squires and Young (1984 [DIRS 180001], p. 21) is reproduced below. This figure is generated with data from another author (Crippen and Bue 1977 [DIRS 108874], Figure 18), who selected, compiled, and analyzed maximum observed flood peaks nationwide. The figure shown is a "boundary" curve for the five-state region that includes Yucca Mountain, from which the regional maximum flood discharge rates for the site were estimated. These regional discharge rates are significantly*

higher than the 100- and 500-year floods upon which the model is based. The regional maximum flood discharges at Fortymile Wash are estimated to have discharge rates on the order of 500,000 ft^3/s, whereas the 100- and 500-year floods have discharge rates of 12,000 and 55,000 ft^3/s, respectively. The boundary curve is defined to be greater than any of the measurements and its shape is somewhat arbitrary. The station AZ2 is furthest from the curve and could be considered an outlier, but since the boundary curve predicts a larger flood discharge the curve is still valid. Another point (labeled "NV 1 Data point and site number (table 4)") is actually not a data point, but rather shown as a legend for the figure, which might have confused the reviewer. This is confirmed by examining the source data being plotted.
Response to comment on uncertainty: *It is accepted that there is considerable uncertainty in the developed equations for the 100- and 500-year floods. The FAR model assumes that transport of the contaminated tephra will occur over multiple large floods. The overall mixing of the contaminated tephra with the channel bed sediment will be a function of all of these floods, with the final outcome being reasonably well mixed, diluted concentrations of radionuclides across the entire channel width to some depth. This depth as taken to be the scour depth, and is based on measured data from the Narrows. As discussed in the report, it is important to capture the lower bound of the scour depth (to be conservative); using a flood smaller than the 100- and 500-year floods predicted by Squires and Young (1984 [DIRS 180001], p. 16) (the measured flood at the Narrows) assures conservative results.*

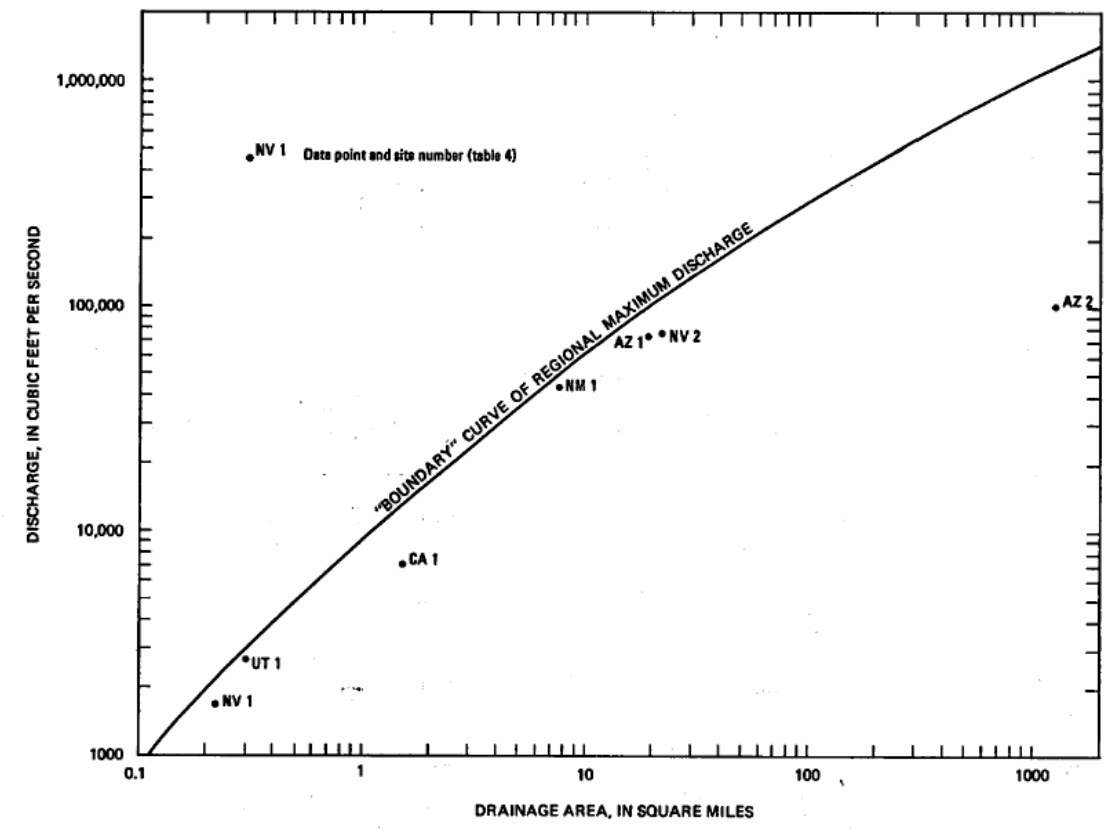

FIGURE 13.--Regional maximum discharge versus drainage area. "Boundary" curve was developed by Crippen and Bue (1977, figure 18) for maximum observed discharges in the flood region that includes the study area.

The second study is Leopold et al., 1966 which found a relationship between scour depth and unit width discharge. The Leopold study estimated that scour depth varies as a function of the square root of the unit width discharge.

Originator Response: This relationship was validated using data from Powell et al. (2005 [DIRS 178706]) in Section 7.2.3.

It should be pointed out, for example, that Leopold's study was based on a relatively short temporal record, and there was a great deal of scatter in his data. Leopold used linear regression to estimate the parameters B0 (intercept) and B1 (slope or exponent in the transformed data). They (Leopold et al, 1966) apparently did not force the regression through zero, so that the intercept is non zero. The intercept reflects what the predicted scour is when there is no discharge. In a process model, it makes no sense to have a non-zero intercept, and therefore the regression should probably be rerun forcing the intercept through zero. That will of course change the value of the B1 value. In addition, the regression can be used to estimate the confidence intervals on the parameter estimates.

Originator Response: It is true that the data were collected over a relatively short period of time (from 1958 through 1963). Over this time period, about a dozen different flood events were recorded. Most of these were small (discharge rates below 100 cfs); a few were larger (1,000 to 3,000 cfs). Resulting scour depths were less than a foot in all cases. The data, collectively, provide a general guide to scour depth as a function of discharge. While the figure in the study by Leopold et al. (1966 [DIRS 175456] makes it appear that the regression was not forced through 0, this is only a perception based on the axis scaling. The figure below shows the data, plotted as scour vs. the square root of the discharge per unit width. The resulting trendline (forced through zero) matches what is presented by Leopold et al. It is also true that there is considerable scatter in the data. However, the standard deviation in the differences between the regression and the measured scour data is only about 0.1 ft.

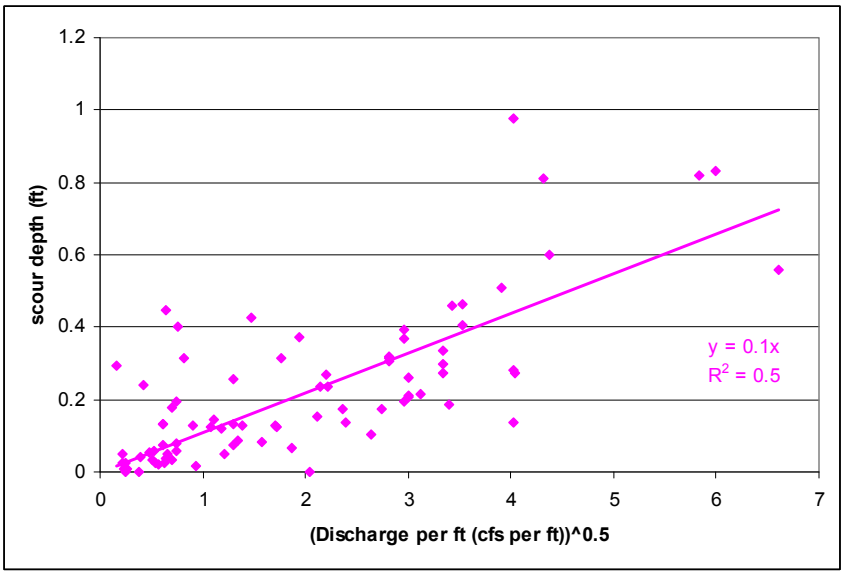

Figure shows data from Leopold et al. (1966 [DIRS 175456], pp. 215 to 218)

It seems illogical to me to use a single value when there is documented uncertainty in its value.

Originator Response: While a constant value for the exponent is used, the uncertainty is accounted for by incorporating a range for the base scour depth.

When you combine the uncertainties from the Squire and Young study with the Leopold et al study, it is likely that the uncertainty will be large. I also should note that the units (English versus metric) for the various studies are not equivalent, and the regression estimates could be sensitive to the units, and incorrectly applied.

Originator Response: Squires and Young (1984 [DIRS 180001], p. 16) use discharge in ft^3/s and contributing area in mi^2. If the equations from this report were converted to metric units, the proportionality constant would change as it has units associated with it, but the exponent would not. For example, for the 100-year flood, Squires and Young (1984 [DIRS 180001], p. 16) provide the equation as $Q_{100} = 482A^{0.57}$; converting this equation to metric units (discharge in units of m^3/s and contributing area in units of km^2) gives $Q_{100} = 7.9A^{0.57}$. Leopold et al. (1966 [DIRS 175456], pp. 215 to 218) use scour depth and channel width in ft and discharge in ft^3/s. The proportionality constant is in units of square seconds, and thus is the same for both English and metric units. Again, the exponent will not be impacted.

Scour chain data is of course serially dependent if the chains are not removed and reinstalled. In other words, once a scour chain is installed, the scour depth measured can be cumulative for several floods unless the measurements are made after each individual event and the chains reinstalled.

Originator Response: FAR assumes that the overall depth of mixing associated with the contaminant being transported downstream occurs over a number of flood cycles. Thus, the associated scour depth used in the model can be called a cumulative or effective scour. The overall magnitude associated with the effective scour is determined by the best measurement data available, the flood event of 1995. These data were measured with scour chains that were reset prior to the flood event.

On page 6-14, the author notes that this scour depth is a maximum value [caused] by "many large floods that will occur during the model duration". This statement seems wrong, in that it misstates how the scour value is used in comparison to "model duration". The scour depth is an instantaneous calculation and is not dependent on model duration. In fact the only section a "model duration" is used can be found in the diffusion calculations (later in the section).

Originator Response: The statement is not wrong, and additional text discussing this has been added in the conceptual model description (Section 6.2). In essence, the code does calculate scour depth "instantaneously" after the eruption. However, this is relative, where the model assumes that the time frame needed for enough 100-year, 500-year or larger floods to transport and mix the contaminated tephra is small when compared to the 10,000-plus-year model duration. This is conservative in that the model assumes that contaminant reaches the RMEI area more quickly than in reality, and allows a reasonable but low overall depth of mixing (which corresponds to a higher concentration of contaminant being entrained in the RMEI channels).

It appears that the author considers the scour depth to be a single scalable parameter for every channel in the entire drainage basin based on the scour depth estimated at the narrows. Using one point to calibrate scour depth for the entire area clearly can create enormous compound errors if the method is invalid or the estimate of scour at that one point is inaccurate.

Originator Response: It is true that there are many things that influence scour depth, and that scaling it throughout the entire drainage basin is extremely simplistic. However, given the large area of the drainage basin, difficulty in measuring the parameter, and overall lack of available measured data, the approach used provides a reasonable and conservative estimate of the parameter.

There is also field evidence (Fig. 2) that shows the channel does not simply fill with water in between the deep banks, but indicates that the channel is migrating like a wave form within the incised channel. Thus for those floods leaving a morphological record on the channel, the bank to bank use of scour depth does not seem justifiable.

Originator Response: The distinction between small ephemeral channels that meander within the main wash was not clearly explained in Draft A. A clearer explanation of these ephemeral channels has been added. In a large flood, bank-to-bank flow that inundates these ephemeral channels cannot be discounted (whereas flow on the divides ARE discounted, e.g., it is assumed in Section 5.1.3 that overbank flooding will not occur).

Trying to extract a conceptual context of this scour depth is difficult because the author did not provide that in the conceptual model section. But on page 6-15, the author assumes that the scaling factor for scour depth is constant because the drainage basin "as a whole experiences the same overall climatic conditions". I assume the author meant climate conditions. The author needs to justify the assumption that this is a simple scaling factor. Regarding climatic conditions, I will address that issue later.

Originator Response: Text regarding the approach used to estimate scour depth throughout the upper drainage grid has been added to the report. The magnitude of scour depth is primarily dependent upon hydraulic factors of individual flows, and these factors are related to the intensity and total amount of rainfall. While flood flows can be associated with intense storms over a localized area, maximum floods are generally caused by storms over larger areas. As it is these larger floods which are assumed to provide the mixing and transport of the contaminated tephra, the assumption of a constant scaling factor throughout the drainage area is reasonable.

Step 4 calculates the total mass of tephra that will be moved from hillslopes greater than a critical threshold onto adjacent channels "where it is added to the tephra deposited by primary fallout". The algorithm description on page 6-17 is not completely transparent. It seems as if the mathematical procedure is just a simple threshold and tephra is instantly removed if that threshold is exceeded. However later in section 6.5.2 where field measurements are discussed, the author suggests a range for critical slope is used and this range it a "uniform distribution between 0.21 and 0.47". I do not see how that "uniform distribution" is applied.

Originator Response: An explanation has been added to Section 6.4 that describes how TSPA incorporates parameter uncertainty in the calculation.

Figure 2: showing satellite image of Fortymile Wash just above the RMEI alluvial fan. Note the evidence of channel shifting within the overall incised banks. This evidence indicates that the interpretation of scour depth used in the model is questionable in larger channels.

Again, the author does not provide any real world conceptual understanding of this process, but the model calculation basically considers hillslopes whose slope is greater than a specified threshold to be perfectly frictionless, so that any tephra that falls on it will simply slide into the adjacent channel without requiring any precipitation or flow. Once the tephra has "slid" into the adjacent channels, the core calculation of the dilution model is performed.

Originator Response: The conceptual model description section has been completely rewritten to address this reviewer comment.

Eq. 6-14 reproduced from page 6-17.

$$dilution(i,j) = \frac{\left(\sum_{up} ashthickness(l,m)\right) + ashthickness(i,j)}{\left(\sum_{up} scourdepth(l,m)\right) + scourdepth(i,j)}$$

I have several concerns regarding the core algorithm of the dilution model, represented in equation 6-14 (p. 6-17). Please note that an independently reviewed peer-review publication,

which is used for corroboration and validation later in the report, uses a [**min**] function to select the numerator in the dilution equation (eq. 3 Pelletier et al., 2007, in press). The difference between the two equations needs to be resolved to reflect what the FAR code actually is computing. I proceed on the assumption that the code functions exactly as described in MDL-MGR-GS-000006 REV 00A as shown above. By the way, given the distinction between ash and tephra, the model should perhaps, have used the term ***tephrathickness*** to avoid confusion.

Originator Response: This section has been re-written so that the description is consistent with the FAR V. 1.2 software. Before tephra is routed, the software sets local tephra thickness to be the minimum of original tephra thickness and local scour depth. Therefore, the scenario where routed tephra thickness is greater than routed scour depth is precluded. This is now explained in the text. Code parameters cannot be renamed without re-qualifying the software.

First let's simplify the model's critical parameter calculation. Let's identify one particular pixel, which is the dilution at the outlet of the channel just before it supplies the fan with sediment. I must assume that this is a single pixel, as it is not identified explicitly in the text. Let's give the coordinates n,o for that pixel. If that pixel is the last pixel in the calculation of eq. 6-14, then we see that for that critical pixel, the dilution factor is a simple average of all the ash thickness and all of the presumed space for that ash to mix in the total channel scour depth for the entire drainage basin or:

$$Dilution(n,o) = \frac{\sum_{total} ashthickness(n,o)}{\sum_{total} scourdepth(n,o)}$$

As this is the governing equation for the dose calculations for the RMEI, it is this equation that requires particular scrutiny. This representation of eq 6-14 eliminates the misleading notion of tephra "routing". There is no dependence on any specific value upstream, rather it is a simple basin-wide average. Physically, it is the equivalent of taking a volume of ash and completely mixing it with a volume of uncontaminated sediment (which is calculated by assuming the accumulated basinwide scour depth is that volume).

Originator Response: A distinction has been made that the model does not use all of the mobilized tephra / waste for this calculation, but only that which can be routed continuously to the outlet cell. The text has been revised to explain this.

This calculation, for example, means that if a significant thickness of tephra fell directly on pixel n,o, as opposed to on the uppermost part of the basin, the concentration of the tephra in sediment at the fan apex would be very low even though the channel is buried by tephra.

Originator Response: "Significant" tephra can not fall on this pixel, given the way ASHPLUME calculates tephra distribution and the relative distance of this pixel from the vent location.

Recall that the basic model assumes an instantaneous mixing and redistribution of the upper basin channel sediments with tephra from hillslopes and channels and that the result of this instantaneous mixing is representative of the tephra concentrations in the channel at the fan apex for distribution to the RMEI fan channels. However, this method clearly takes an instantaneous spatial average over the entire basin and physically assumes that the undiluted tephra sitting on

the outlet waits (i.e., zero transport) until all the tephra and sediment from upstream are mixed and then mixed with the tephra on the outlet.

Originator Response: One should be careful not to equate the model algorithm with the conceptual model of the system. The dilution calculation uses the total mass of tephra and scoured material mobilized and transported from upstream of the outlet cell; however, this approach is meant to reproduce the resulting concentration at that location and not the transient nature of the process in a physical sense. The additions made to the conceptual model description and the improved clarity of the algorithm description address the reviewer's comment.

This result is confirmed in model output by Pelletier et al 2007, figure 9C. In particular, it assumes that during the "many floods" that accomplish the mixing, that no highly concentrated tephra from the basin outlet is transported to the RMEI. That does not seem reasonable given the process of stream flow and sediment transport, although the dilution factor at n,o might eventually either intersect or converge with the predicted value.

We can also look at the dilution model by examining the first stream (or the highest) channel cell where the dilution can also be simplified to:

$$Dilution(1,1)\frac{ashthickness(1,1)}{scourdepth(1,1)}$$

In this calculation, the description on page 6-17 indicates that the dilution is calculated according to this equation for the ashthickness ≤ scourdepth, otherwise dilution is set to 1.

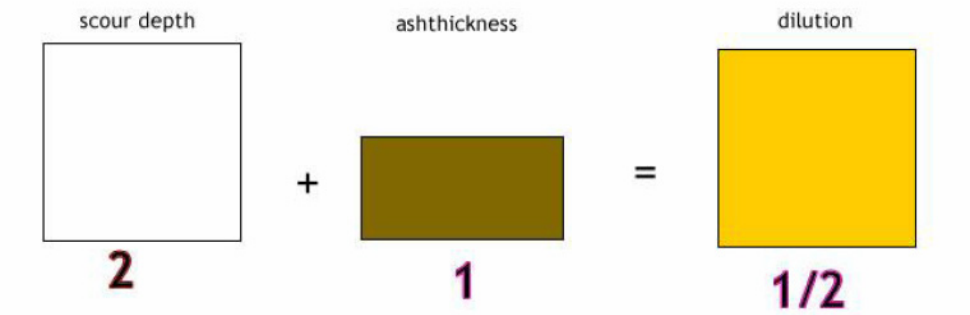

Figure 3: Dilution calculation where ashthickness < scourdepth.

We can visualize the quantities in Figure 3 above which shows the simple dilution calculation for the condition where ashthickness < 1. This calculation produces a sediment thickness equivalent to the original scour depth with half the original concentration of tephra. So for the first cell in the calculation in equation 6-14, this seems reasonable.

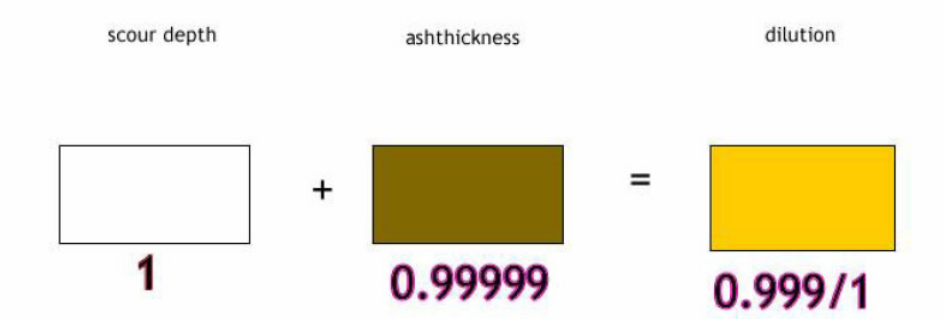

Figure 4: Dilution where ashthickness approaches scour depth.

However, as the ashthickness approaches and then exceeds the scour depth we see some problems concerning basic process assumptions. Figure 4 above shows at that as the tephra thickness approaches the scour depth, the channel is basically cutting or scouring in tephra. We must ask therefore, why the initial channel condition (grid) does not include the thickness of the direct tephra deposit and the hillslope contributions.

Originator Response: It is true that the assumption that the tephra deposit itself does not alter the drainage current drainage pattern was not stated in Draft A. An analysis has been added that looks at the distribution of tephra thickness greater than local scour depth and demonstrates that tephra thickness in excess of scour depth is not very common, and that the fraction of immobile tephra beneath the scour zone is very small when compared to the mobilized fraction (Sections 7.2.4 and 7.2.8) .

In fact, the channel configuration could be significantly affected by the distribution of tephra following the first part of Step 4.

Originator Response: An assumption that channel geomorphology is not significantly impacted by the initial tephra distribution has been added (Section 5.1.4).

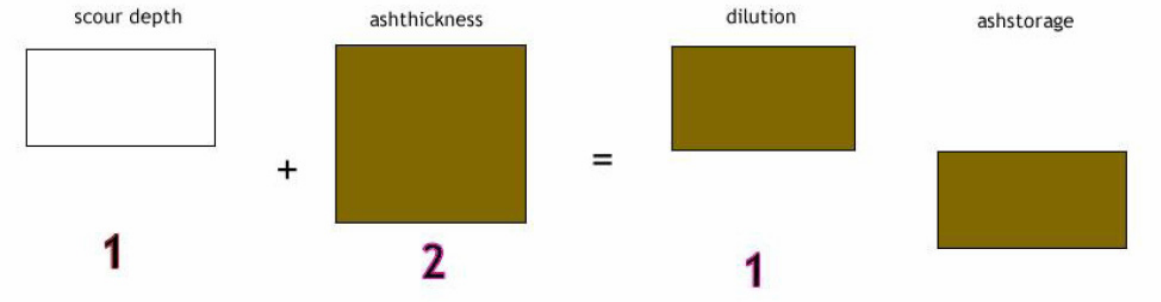

Figure 5: Dilution where ashthickness > scourdepth.

When the primary airfall and hillslope transported tephra in the channel exceeds the scour depth, we have a new set of inconsistencies appear. For this first cell we can easily see that the dilution is set to 1, or no dilution. However, we have excess tephra, indicated as ashstorage in Figure 5

above. The important question is what happens to this excess tephra? On the one hand, the model appears to state that the scour depth represents the maximum value of stream channel sediment in transport in any pixel and thus anything in excess of that value, ie scour depth, must be left behind. On the other hand, the "routing" equation actually sums the total tephra thickness, including the excess, which is made available for downstream transport and mixing. The model thus contradicts the physical assumptions upon which it was based. Please note that in Pelletier et al, 2007 in press, which is cited for validation, they identify the identical contradiction: "in the case of relatively thick (i.e. 1m) contaminant, however, some of the contaminant is stored indefinitely in channels of the source region because the scour depth is less than the contaminant thickness in some areas" but for Yucca Mountain it is assumed that all the tephra is mobilized regardless of thickness (Pelletier et al, 2007, in press preprint, page 9).

Originator Response: The reviewer is confusing tephra mobilization with mobilized tephra that affects the tephra concentration at the outlet. Only a portion of the mobilized tephra contributes to the calculation of the tephra concentration at the outlet. This explanation has been improved since the release of Draft A.

Step 5 estimates the initial concentration and thickness of tephra at the RMEI location, which is divided into "interchannel divides" and channels by mapping. The FAR model assumes that older fan surfaces are not subject to fluvial erosion or deposition. The thickness of tephra on these older surfaces is determined by converting tephra concentration (g/cm2) to an equivalent depth by using an estimate of tephra density (ρ) in equation 6-15a (p. 6-20). The tephra density is important because it is implicitly used to determine the concentration of waste as well (eq. 6-15b and 6-17). Should the author discuss what uncertainties are introduced as the density estimate changes?

Originator Response: The value (and uncertainty) of tephra bulk density is not developed in this model report, but is provided as input from another report. TSPA samples this parameter value in its analysis from a truncated normal distribution with a mean of 1,000 g/m^3, standard deviation of 100 g/m^3, maximum of 1,500 g/m^3, and minimum of 300 g/m^3, and thus the uncertainty in this value is included in the analysis.

Step 6 assumes a simple 1 D diffusion model represents the redistribution of radionuclides with the RMEI fan soils and channel sediments. The report states that "Field work was performed to measure the permeable soils thickness on divide surfaces". I am reasonably certain the author could use the same number of words to describe what was measured and how.

Originator Response: This measurement is detailed in Section 6.5.5. A pointer to that section has been included in the text.

This "measurement" is important because it is used to limit the depth of diffusion. A solution to the diffusion equation, taken from Carslaw and Jaeger (assumed validated), is used to solve for four output time series. Diffusivity was estimated by "fitting" with other data, but the method of that fit is not provided.

Originator Response: This measurement is detailed in Section 6.5.8. A pointer to that section has been included in the text.

By assuming a simple diffusion model for the redistribution of radionuclides in the RMEI over time, the model fails to provide (as it also failed in the section on conceptual models) of why this model is appropriate given other processes that are known to occur. These include vegetative recycling of radionuclides, adsorption and cation exchange with fine materials and clays, and eolian redistribution.

Originator Response: The validation for using a diffusion model is addressed in Section 7. In that section it is acknowledged that other processes occur, but and argument is made that, based on measured data from the literature, the shape of the concentration profiles with depth can be adequately represented using a diffusion model.

Other parameters

Section 6.5.3 describes drainage density which is used to "define" the channel system in the drainage basin (STEP 3). A pixel is defined as a channel "if the calculated stream power is greater than a threshold value equal to the inverse drainage density". A small number of channel heads are used in a method to optimize the drainage density. The optimization is based on a minimization of distance between the selected channel heads and the model channels. There is circularity to this reasoning, as drainage density a variable in the optimization procedure is then used to estimate drainage density. Furthermore, there is no guarantee that these 34 channels produce a basin wide optimum drainage density. Finally, drainage density can be relict, meaning that the current drainage density does not always reflect modern conditions.

Originator Response: First, there is no circularity in the reasoning. The method used to estimate drainage density is an example of a standard inverse calculation. Drainage density is directly related to the positions of channel heads relative to the ridge lines. The FAR model is run a number of times each with a different value of drainage density, and the run that best matches the set of channel head locations is chosen as the most appropriate value of drainage density. The decision to use only channel locations on the eastern slope of Yucca Mountain is reasonable because this drainage sub area is the closest to the vent location and therefore would have the thickest tephra deposit.

2. Are the mathematical relationships appropriate and representative of the scientific understanding of the geomorphic processes for the transport of sediment from the Fortymile drainage basin to the location of the RMEI on the Fortymile Wash alluvial fan?

No. As noted above lacking a conceptual model, there is no basis to accept or reject the underlying mathematics as conceptually appropriate or reasonable. The mathematics do not appear to be directly related to geomorphic processes of stream flow, sediment entrainment and transport, sediment deposition and storage, or even sediment mass balance. Also, there is no eolian component, despite field evidence for strong wind transport of sand size grains (and the eruption would produce silt-fine sand) from the RMEI channels onto the "interchannel divides".

Originator Response: The "strong evidence" of an eolian component the reviewer points to is from the Lathrop Wells lava sheet, not Fortymile Wash. Images of the Fortymile Wash area do NOT support this claim (this is presented in Section 5). The assumption dealing with eolian transport (Section 5.2.2) has been rewritten to clarify justification for excluding this process.

The FAR model belongs to class of models that might be called "reality conditioned lumped model" black-box algorithms. These are algorithms that work by using "cases" of logical if statements to work properly by conditioning output rather than process. For example, because the model does not actually route sediment by calculating sediment loads and mass balances during floods, it must rely on setting the condition that if the tephra is too thick (>scour depth) then it is just passed to the next channel pixel until it may finally be used in the dilution equation for the outlet.

Originator Response: The reviewer is correct in stating that FAR is not a time-dependent, sediment transport model such as a finite element code might be. In the re-written conceptual model description, this point has been clarified.

The model presented as equation 6-14 is almost identical to the residence time model with ideal mixing for a lake, rather than a process-based fluvial dilution model. In the lake system, pollutants enter the lake, mix rapidly so the concentration is effectively the sum of the total input divided by the total volume of the lake. That is exactly what this model does for the ***dilutionfactoroutlet*** pixel. Could that work for a fluvial system? Yes. Under the conditions where the supply of the contaminant was fixed spatially and temporally, and sufficient time was allowed for the system to possibly reach quasi equilibrium conditions, perhaps it could provide a reasonable dilution estimate. This model would still be vulnerable to large errors if the contaminant was spatially concentrated at the lake outlet which would make it harder to mix efficiently before exiting (the equivalent of thick tephra sitting on the pixel where the dilution factor for the fan is calculated).

Originator Response: Technically this is true, but there is no scenario under which this condition occurs since the vent location is quite far from the fan apex. It can also be pointed out that IF large quantities of tephra are deposited at the fan apex, there is also likely to be a large quantity of tephra directly deposited on the RMEI location, and these concentrations are directly included in the overall concentration calculations. In particular, the divides account for between 46% and 91% of the overall area in the RMEI location, and concentrations on the divides are initially set directly from ASHPLUME.

One key assumption is the requirement of hydraulic equivalency of the tephra load with the uncontaminated stream channel sediment load. Equivalency means that the two components would be affected by fluvial processes in exactly the same way. For example, if the tephra load is finer than the uncontaminated channel sediment, then it will be preferentially transported by floods, invalidating the ideal mixing model. If the tephra is very fine, it is likely that some of the contaminated tephra will be deposited in RMEI channels even before all of the hillsope tephra has "slid" into the channels. Each of these realization make the application of the ultimate time dependent portion of the model, i.e. diffusion of the radionuclides on RMEI surfaces, more difficult to apply because there is no simple initial condition.

Originator Response: This is true, but this is why assumptions are necessary. In reality, tephra will reach the RMEI location over time and any deposition there will depend on the physical properties of the material and on the size and timing of flood events. Radionuclide concentrations will initially be low, build to some peak value (corresponding to the period when the majority of the mobilized tephra has been removed from the hill slopes into the channels and

been transported through the channel system to the RMEI location), and then slowly decay, but likely not go to zero given late-stage hillslope and eolian processes. The FAR model is a simplification of this very complex process.

In particular, if the tephra includes silt, there will almost certainly be hydraulic sorting of the ash from the channel sediment, instead of mixing, and potential for actually concentration of radionculides through further chemical processes.

Originator Response: Silt is not present in the modern channel sediments on the alluvial fan, which means that it is effectively transported downstream (as suspended load) to Franklin Lake Playa, where it is deposited. Any hydraulic sorting that might occur prior to a large flood event would not persist for long. Chemical concentration process that would significantly increase the concentration at the RMEI location are not considered plausible. More than likely, some of the radionuclides (U, I, and Tc) would readily oxidize and dissolve in the flood waters and be transported far downstream and/or infiltrate deeper in the channel bottom.

The likelihood of contaminated silt size tephra, or ash, also increases the chances of redistribution from RMEI channels onto RMEI divides, at time scales outside the simple boundary conditions of the diffusion model.

Model Output

The model output can be evaluated in several ways, using intermediate outputs, the model results, and sensitivity analyses included in the report. By overlaying some of the intermediate results in Google Earth, I could determine whether there were obvious problems with the delineation of the drainage basin (Fig. 6), slopes, location of channels, etc. These all seemed reasonable, overall.

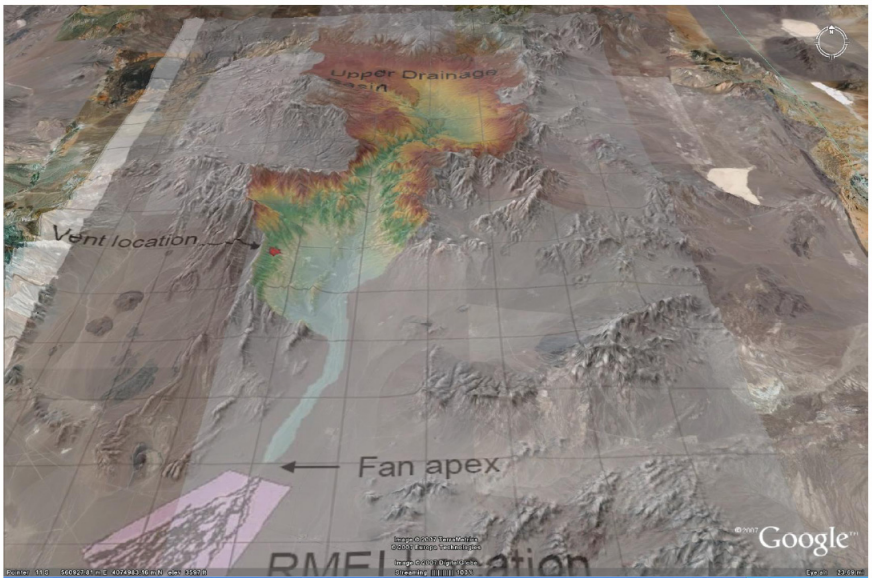

Figure 6, showing "upper" domain, the drainage basin, and the fan location, or RMEI location, projected onto an elevation and satellite base in Google Earth. There is an unfortunate gap between the drainage basin and the area identified as fan.

Originator Response: The "gap" is present in a short stretch of the Fortymile Wash between the outlet and the edge of the alluvial fan map area. The presence of this gap is not expected to alter the results of the model because the concentration in the channel near the outlet is quite homogeneous.

In examination of the slope grid (Fig. 7), there were features that seemed to be artifacts from either the DEM or the algorithm. The features included a "herringbone pattern" which also occurs in other parts of the upper basin, and lineaments that terminate slope classes. I am uncertain if these hold any significance in the overall performance of the algorithm.

Originator Response: The features identified by the reviewer in the flat area ("B") may be artifacts, since this is a flat area with small scale, topographic variability. It is worth noting that this entire area is characterized by slopes below the minimum value for critical slope (0.21), and therefore the slope patterns in this area have little influence on tephra mobilization. To provide more confidence in the slope calculation results, a comparison of slopes determined by the model to those calculated using an alternative method (steepest descent) has been added to Section 7. The differences are minor.

In examination of the "contributing area grid" (Fig. 8A), one finds channels that appear discontinuous and take the form of small fans. These channel "fans" are found throughout the drainage basin and suggest that these might indeed represent places where contaminant storage occurs.

Originator Response: These areas are indeed areas where the model "stores" tephra within the upper drainage basin. The description of this process in the conceptual model description and in the algorithm description has been improved. In addition, these unconnected channels are now shown on updated Figure 7.2.4-1.

Are these channels included in the "routing" and if so what happens to the upstream tephra load if a channel ends?

Originator Response: Tephra in unconnected channels is NOT included in the routing because the routing of tephra is only performed for channel cells moving downstream. Thus, material in unconnected channels is not available for the dilution calculation at the channel outlet. This explanation has been added to the report.

From a physical process perspective, it is clear that the tephra might be stored and therefore mixing is not complete, however, based on statements in Pelletier et al 2007, p. 9, it is also clear that the total cumulative tephra thickness is included in the calculation of dilution at the drainage basin outlet.

Originator Response: The model description has been edited to be consistent with the current version of the FAR model. The same mathematical model was used in the paper by Pelletier et al. (2007 [DIRS 182110]). The journal paper does not distinguish between tephra mobilized but not connected and all tephra mobilized. This distinction has been added to this report.

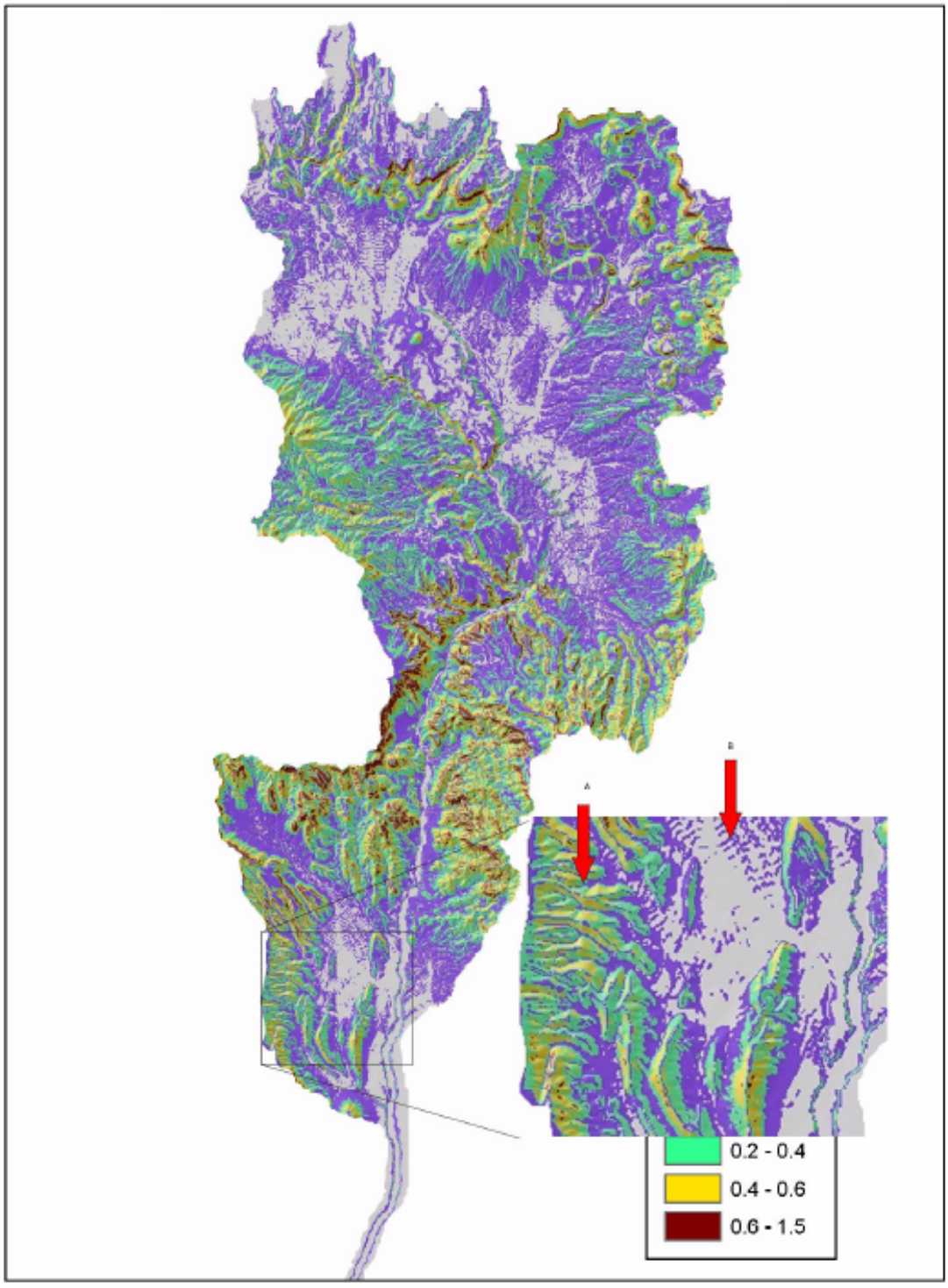

Figure 7, showing slope grid from section 6, figure 6.3.3-3, output from FAR, with arrows indicating features that seem anomalous.

Near the fan outlet, I examined how well the bifurcation method defined the main channel of Fortymile wash (Figure 8B). The resolution of the output I had did not allow precise comparison, however, I suggest a detailed comparison be made.

Originator Response: There is no expectation that the model, which is based on a 30-m DEM, would match the ephemeral channel pattern (within the main channel), which can be seen in high resolution imagery such as is available in Google Earth. Therefore, such a figure has not been added.

The model output for the dilution factor calculations highlight several relevant concerns regarding the model performance (Fig. 9). I focus on the lower part of the upper drainage basin just before the flow enters the RMEI location. This is the section of Fortymile wash where the dilution factor at the outlet is calculated. It would useful to identify the single pixel which is actually used for the initial RMEI concentration on that figure.

Note that in the inset (Fig. 9), that the dilution values appear to vary within the channel, in some places appear discontinuous, and for short reaches seems to be concentrated along a channel that is a single pixel wide. The fact that the channel appears to be a single pixel wide in this section of Fortymile wash suggests that the bifurcation method may not be entirely effective in distributing flow correctly for those 500-year floods, or that this figure is not showing the model results correctly.

Originator Response: A new figure (Figure 7.2.5-2) has been added that shows the exact location of the fan apex and example dilution factor results that show the spatial variability of this model output. The figure demonstrates that there is little variation in the dilution factor in this region of the wash, and therefore it is reasonable to use the value from a single grid cell in the middle of the channel to estimate dilution. The reviewer's observation about channel width oscillations is valid. Oscillations in channel width are features present in the natural arid alluvial channels (e.g., Pelletier and DeLong 2004 [DIRS 183203]).

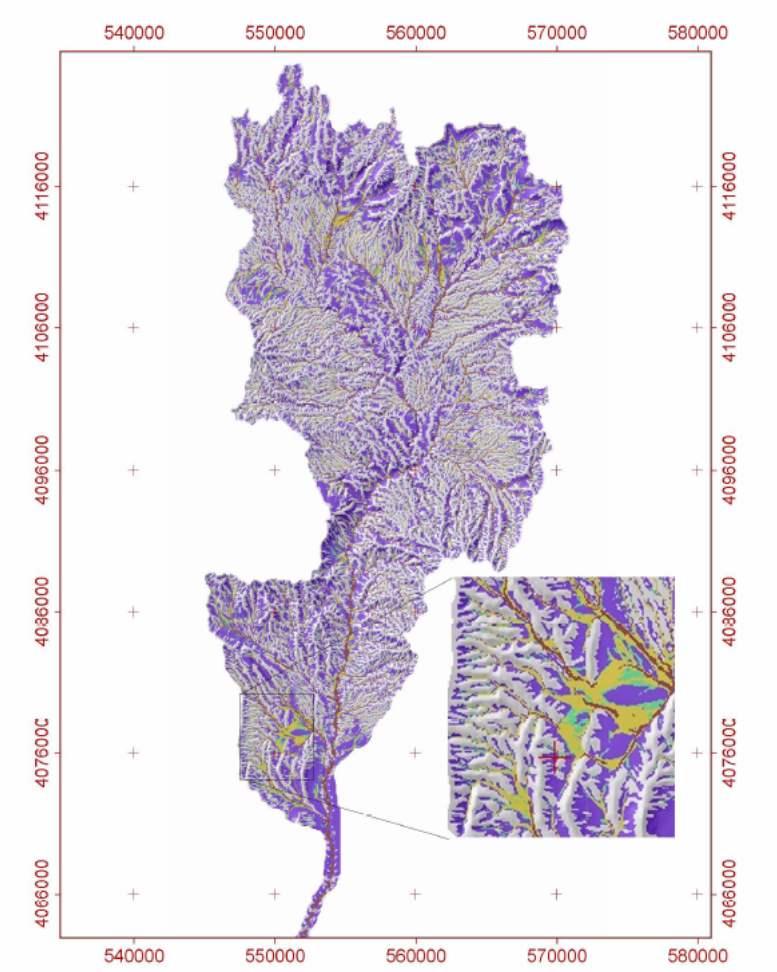

Figure 8: A) Above, showing contributing area output grid from FAR model. Note that in the inset, once can see that the channels are not always continuous, and appear to form fan shaped features. B) Below, channel definition near fan outlet compared to satellite image.

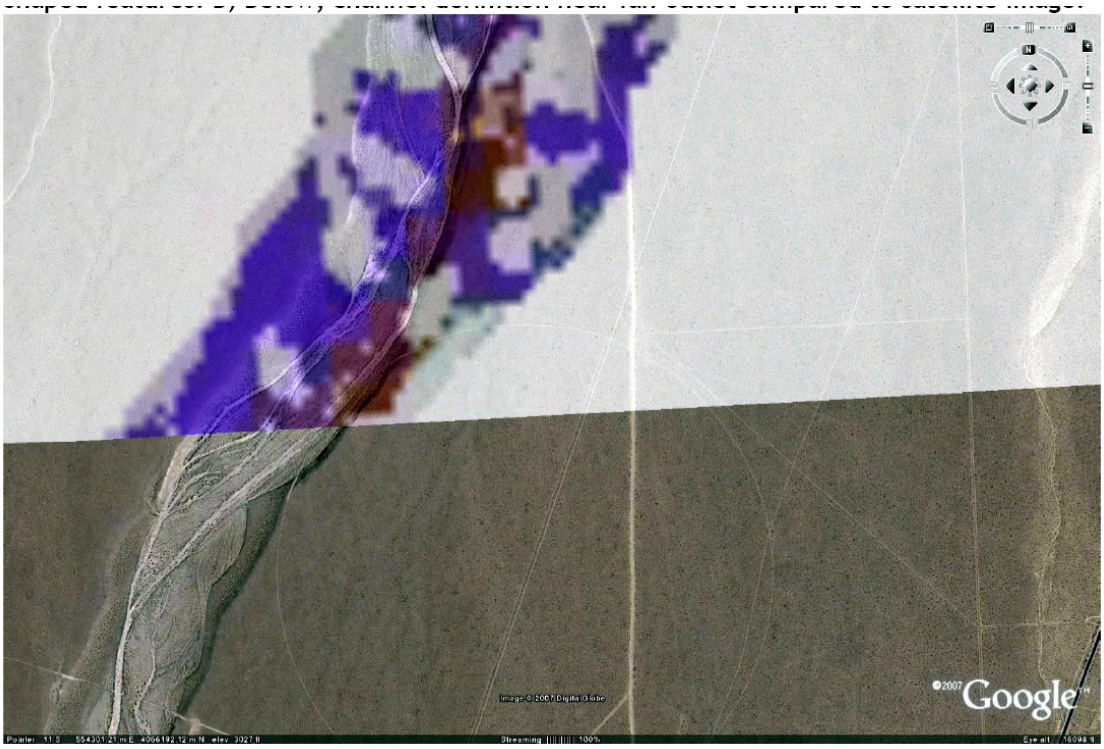

Also note that although the dilution factor for this model run was in the 0.3 – 0.1 range for most of this section of the wash, at the presumed outlet, the dilution was in the 0.01 - .1 range, or as much as a factor of 10 more dilute. Given the close proximity of these pixels, it would be useful to see what the actual range was, instead of the binned ranges, and to understand fully the impact of picking one particular pixel for the initial RMEI concentration.

Originator Response: See previous response.

The sensitivity analyses, section 6.6.2, explored some of the dependencies among the parameter variables and their impact on the dilution factor at the outlet pixel. The results are presented as a series of scattergrams with regression lines. I note that it is the convention to scale these plots according the data ranges rather than arbitrarily. The author should include the confidence intervals on the regression line slope estimate. For example, the scattergram of initial waste concentration versus drainage density (report figure 6.6.1-1 c?) does not appear to be statistically significant. In other words, the drainage density does not affect the dilution factor at the outlet. This confirms that the model itself is largely insensitive to factors that affect the primary geomorphic processes, which here is the density of stream channels carrying contaminated tephra towards the RMEI (channels) location.

Originator Response: First, the scatter plots are shown to illustrate the variability in the results and the overall character of the trends. The plots include the trendline equations and associated R^2 values. Calculating confidence bounds on the linear regressions used to illustrate the results of the sensitivity analysis is unnecessary. The sensitivity results generally agree with the reviewer's observation that the drainage density parameter does not significantly affect the results. It should be noted that this analysis was run using a single ASHPLUME result and therefore is not universally applicable; rather, it provides insight into the model behavior. A

new section (Section 7.2.8) that examines tephra mass distribution in the system has been added and this analysis generally confirms that the FAR model is "largely insensitive to factors that affect the primary geomorphic process."

In contrast, the sensitivity analysis identifies the model variable which is most significant, or highly weighted, in controlling the initial waste concentration, which is the critical slope. This is easily explained as this value is the largest part of the numerator in the governing equation for dilution, eq. 6-14. The estimated value for the slope of the regression line is about -2.0. In other words as the critical slope threshold increases, the initial waste concentration is halved. If the FAR report included the function that relates the area of the drainage basin to the DEM estimated slope, one could see how this dependency was related to the increases in tephra area.

Originator Response: Such a figure is included in the report (Figure 6.5.2-1).

Perhaps the author could produce a scattergram which relates initial waste concentration to area at or above the critical slope, which is a more understandable way of seeing the dependency. Unsurprisingly, the scour depth, the denominator in eq. 6-14 was the second most significant variable.

Originator Response: Critical slope is just one factor affecting the initial concentration. The text has been edited to add a discussion of the importance of whether channels are connected or disconnected from the main Fortymile Wash (Section 7.2.4).

The report concludes the sensitivity analysis section (p. 6-52) with the statement that the analyses "provide confidence that the model is functioning as expected and also provide information that could be used in the future to guide activities aimed at epistemic uncertainty". It would be useful if the author identified what epistemic uncertainty was considered important.

Originator Response: The sentence has been edited to clarify that the information could be used "to guide activities aimed at ***reducing*** *epistemic uncertainty* ***(e.g., making more field measurements)****." Section 6.6.3 identifies and ranks by importance the epistemic uncertainties.*

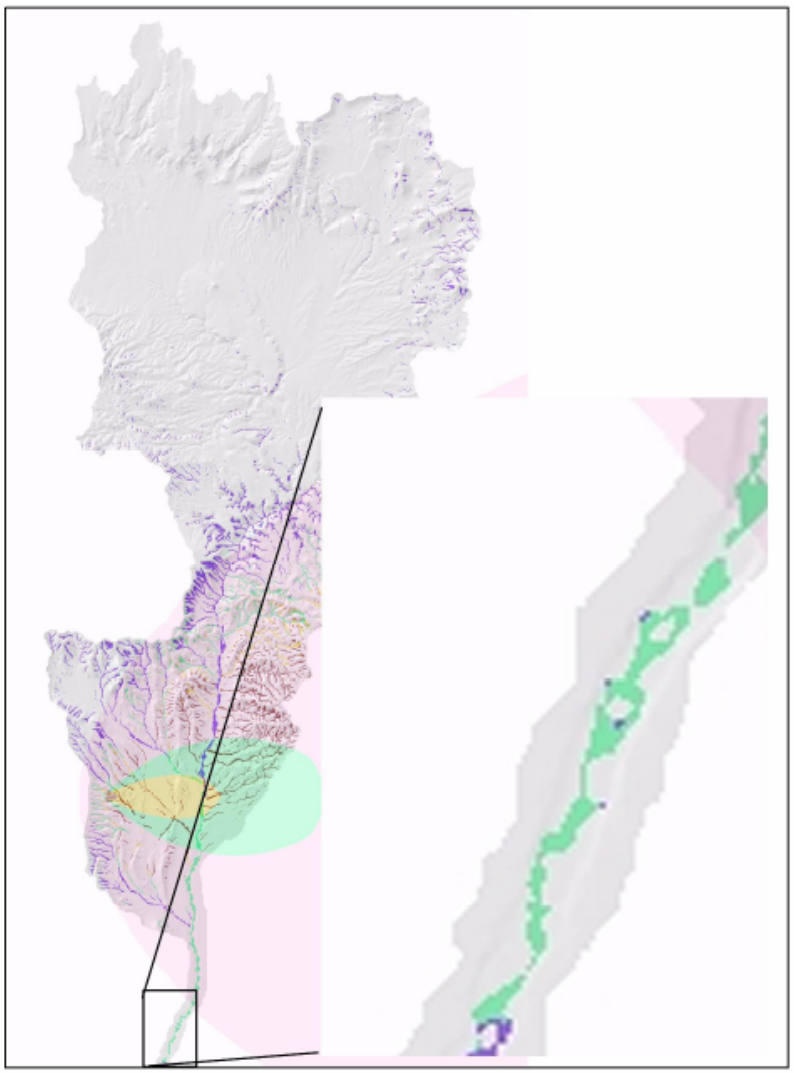

Figure 9, showing dilution factor output for one set of initial conditions, given in section 6 figure 6.3.3-6. The inset shows the part of the Fortymile wash channel that is used to provide the initial contaminant concentration to the RMEI channels.

3. Are the outputs of the model reasonable and representative?

Yes. The outputs of the model, specifically the intermediate outputs, the model results, and sensitivity analyses, are in general reasonable within the context of the model's implicit and explicit assumptions and mathematics.

With local exceptions that might highlight weaknesses in the possible robustness of the algorithms, including the core bifurcation routing algorithm, the output seems internally consistent and representative of the model assumptions and mathematics.

The results also seem representative of the realizations allowable under model conditions. The significance of local anomalies in the model output, specifically the ones cited above (slope, contributing area) is not known.

Originator Response: The purpose of this model is to provide input to TSPA. While local exceptions may exist, the assigned uncertainties in TSPA more than account for the variations.

4. Are there alternative models or approaches that should be considered?

The current model takes one of the simplest approaches possible to estimate the initial RMEI waste concentrations (note: the simplest approach is to assume undiluted tephra at all RMEI locations). For the channels it assumes perfect and instantaneous basin wide mixing independent of tephra location relative to the basin outlet.

Originator Response: This is not entirely true for the channels. To be included in the dilution calculation, the cells must be continuously connected via channels to the fan apex.

For the "inter-channel divides" the model assumes the initial waste concentration to be equal to the primary waste fallout which diffuses away with time. In this way, the current model will always predict a time dependent decrease in radionuclide concentration with time after the volcanic eruption. It might also be useful to allow the model to weight the dilution as a function of distance from the basin outlet with respect to tephra transport. In this way, one could at least see the importance of little time for mixing in the scenario where a significant thickness of tephra falls directly on the basin outlet.

In this reviewer's opinion, alternative models, specifically those that allow for post eruptive concentration of waste from the tephra by chemical and physical processes, might attenuate the decrease of radionuclide concentration with time, or modulate that function in a complicated way. The redistribution of ash by wind could be a significant factor where the volcanic eruption produces a sizable fine particle size fraction. Models that produce higher waste concentrations with time are, from a probabilistic point of view, the ones most worthy of considering given the estimate for the annual probability of a volcanic eruption (1.7×10^{-8}).

Originator Response: It is true that the actual redistribution of tephra following a potential eruption will be more complicated than any of the model scenarios might indicate. However, given that the purpose of this model is to provide input to the TSPA (a probabilistic performance assessment), the more important question is whether the model provides an adequate range of possible concentrations. Given the uncertainties, the model provides a reasonable range of results. Additional justification has been added to Section 5 discussing the reasons why it is acceptable to neglect eolian transport in the model.

Recall that the current model is assuming that current, very current in fact, stream channel conditions will persist throughout the performance period. If conditions change, periods of channel aggradation might occur, resulting in incomplete mixing and perhaps even long term storage.

Originator Response: Given enough time and changing climate and tectonic conditions, stream channels may migrate. However, the assumption that this process can be neglected from the model means that it is believed that the uncertainty associated by this possible change in the system is accounted for in the overall range in results provided to TSPA. For example, TSPA samples the fraction of the RMEI location that is active channels. Uncertainty in this fraction is

considerable and accounts for the uncertainty in exactly how the channel network may migrate in the future.

Those processes that allow for slower more efficient hydraulic sorting of the sediment load will produce excursions from the ideal mixing model presented.

The key logical argument made by the current model is that the tephra particle size distribution is equivalent to the channel sediment particle size distribution throughout the channel system, allowing the tephra to behave or be treated exactly like the existing bed load.

Originator Response: There is a possibility that the tephra may have a significantly different particle size distribution than the clean channel sediment and that this may cause a difference in the transport processes. However, the model may provide an upper bound to the concentration at the outlet because if the particle size is very small, most material will be transported well beyond the RMEI location as suspended load. If the particle size is larger, then most of the tephra will remain in the upper basin. By assuming that the size distribution is the same, the model will tend to overestimatew the time-integrated RMEI concentrations.

The current model does not actually model the transport of bed load in any way, while an alternative model might explore the impact on sediment yield of different tephra particle size distributions in order to determine the relative transport out of the drainage basin so that implication for dilution and mixing could be explicitly determined.

Originator Response: There are highly detailed sediment transport models in existence, but these models require dozens of parameters that are not known for this system. Furthermore, applying these models to such a large basin and for such a long time period would be impractical and unjustified. Model complexity should be commensurate with available data and ultimate purpose.

This basic logical branch is illustrated in Figure 10, indicates that where wind processes are potential transport agents of redistributed ash, the impact on RMEI dose estimates could be high.

Originator Response: The fact that silt-sized material is nearly absent from the modern channels supports the assumption that eolian processes can be neglected. The diagram presented in the reviewer's Figure 10 fails to show the fact that if particle size is very small, the fluvial system will transport material well beyond the RMEI location to Franklin Lake Playa. The fact is that there is no numerical model capable of accurately predicting the fate of fine-grained sediments in such a large area, over such a long time period, and considering variable eruption scenarios. The fact that the fraction of the RMEI area that is active channels is sampled implicitly accounts for the uncertainty in the role of eolian transport, since the tephra deposition on RMEI divides is based solely on the initial ashfall (see Section 5.2.2).

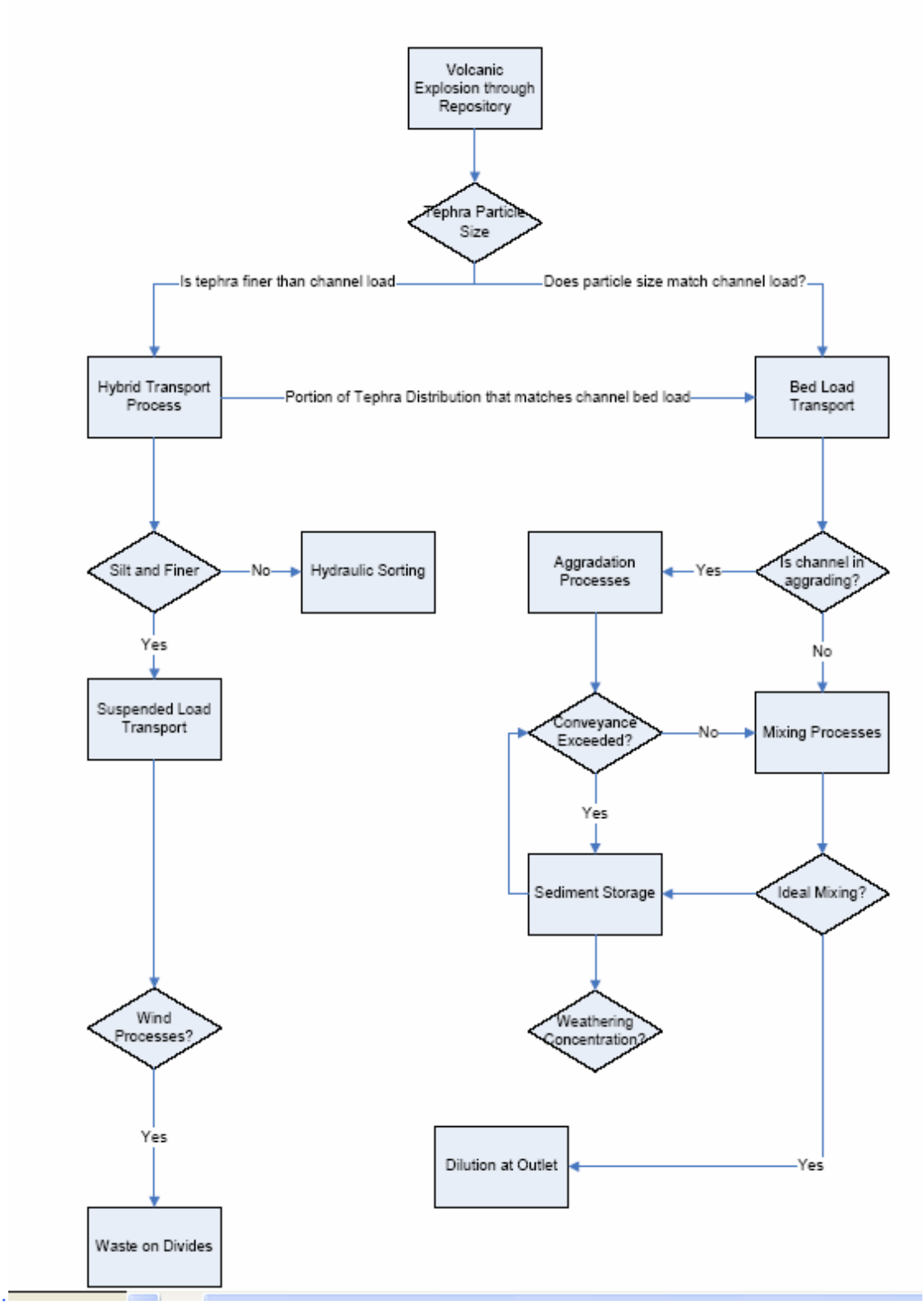

Figure 10, showing the main logical branch separating the current model from alternative models. That logical branch is the one regarding particle size.

Limitations

5. Are the limitations of the model adequately described?

Model limitations are listed in section 1.2 and further discussed in Section 5.

The basic assumption of the model is mixing of tephra and sediment in the channel during transport. This assumption is not stated in section 5.

Originator Response: Section 5.2.3, Mode of Sediment Transport, discusses the assumption that tephra and channel bed sediments are transported as bed-material load. Text has been added to include that this process will result in mixing.

The other assumption is the lack of any concentration processes.

Originator Response: An assumption has been added to the report discussing the lack of any concentration processes (e.g., placering, winnowing, chemical precipitation, reaction, etc) being considered in the model.

Each of the stated assumptions could be significantly elaborated however, a few require comment here.

Originator Response: Several assumptions have been expanded in response to this reviewer's comments and other comments. The current level of detail is sufficient for the intended purpose.

The model assumes no floodplain sedimentation (section 5.1.3). I interpret this mean that there is no significant channel storage of tephra which would affect the dilution calculations (reducing the numerator in eq 6-4). Although there maybe no visible floodplains, there could be significant storage if the channel experiences a period of aggradation, as might be expected following a pulse of sediment supply caused by the deposition of tephra in the channels

Originator Response: The reviewer's interpretation of this statement is incorrect. This assumption means that there will be no overbank flooding of the main wash (the conclusion of Squires and Young (1984 [DIRS 180001]) in their flood potential analysis of the Fortymile Wash). As pointed out, the channel morphology shows a meandering "channel within a channel." During large floods there may be bank-to-bank flow across the wash (not just within the meandering channel), which will result in scour / mixing and subsequent storage of the material in the wash bed sediment. The amount of material stored within the wash has been analyzed, and a section discussing this has been added to the report.

The model assumes that the rate of hillslope and fluvial redistribution is instantaneous (section 5.2.1). It also assumes that it occurs in two "instants" because the hillsope transport of tephra to the channels must occur before the channel redistribution. The model also assumes "dynamic equilibrium," an assumption with questionable authenticity[(1)]. Because the model assumes instantaneous mixing, it would also be plausible to assume instant mixing in the instant following the first instant when, the waste-contaminated tephra is washed out of the channels. Clearly, in a few "instants", there considerably less tephra in the channels as dilution progresses[(2)]. However, the author states that

> "it takes ≈ 10,000 yrs or greater for uncontaminated hillslope sediment to replace the quantity of contaminated sediment in the channel scour zone shortly following the eruption. This residence time implies that after the concentration in the RMEI peaks, values will decrease gradually as clean sediment is eroded from the hillslopes and mixed in the channels. Approximately 10,000 yrs after the eruption, clean sediment will have replaced the contaminated material in the RMEI channels to the scour depth." (3)

This logic contradicts the notion of mixing of sediments (the basic assumption of the model) versus replacement, and also is based on a maximum of rate hillslope erosion of 10cm/1000yr (p. 5-4) a rate that makes it impossible for the model to transport tephra (especially if the thickness is in excess of 10cm) from hillslopes to the channel instantly (4).

Originator Response: (1)The term "dynamic equilibrium" has been removed from the text. It implied the assumption that, in general, the initial tephra distributed across the upper drainage basin will not result in significant changes in the channel geomorphology. Fallout of ash from the plume forms a ground layer that generally thins with distance from the vent. The tephra deposited over the terrain after an eruption is unconsolidated, and the channel heads may be impacted by the deposition of the thick tephra layer very near the vent location. However, as discussed in Section 5.1.3, the alluvial channels in the Yucca Mountain region are entrenched into and bounded by early Holocene and older deposits. While the channel heads near the vent may move, the overall channel geomorphology likely will not be impacted due to the deep entrenchment of the channels. Those channels further from the vent will be less impacted by the initial tephra deposition given the thinner tephra layer in these areas. This assumption has been added to the text.

Originator Response: (2)The reviewer is associating a time step with the instantaneous hillslope and fluvial redistribution assumptions of the sediment redistribution portion of the model. Viewed in this manner, the reviewer is correct in saying that after several "instants" there will be considerably less contaminated tephra in the channels as dilution progresses. It is important to note that the overriding purpose of this model is to provide TSPA with a tool to aid in the estimation of dose, as a function of time, to the RMEI. In order to assure that dose is not underestimated, the model needs to be able to capture peak concentrations of the contaminant at the RMEI location. The assumptions of instantaneous hillslope and fluvial redistribution allow not only considerable simplification of the calculations, but also allow this peak concentration to be calculated, both because contaminant is applied to the RMEI location immediately after the eruptive event (earlier than it would be in "reality") and because it allows the maximum amount of contaminant which is mobilized to be redistributed to the RMEI location at that time. The model continues a conservative approach by not allowing further mixing and transport of the contaminant once it has been re-deposited to the RMEI (or, as the reviewer states, continuing "instants"). It is noted that there are plausible scenarios where higher concentrations than those calculated by the model could, in reality, occur within the RMEI location. However, there are no plausible scenarios where the entire region of the RMEI would see higher concentrations. TSPA calculates dose to the RMEI by essentially splitting the RMEI area into two sub-regions (channels and divides), and thus requires an average concentration for these RMEI domains. Because the model captures the peak mass of contaminant being applied to the RMEI location due to redistribution, it does provide conservative results.

Originator Response: (3)-(4) The paragraph marked has been deleted from the report. There was confusion in using the term "clean". The 10,000-year rough estimate was the overall timeframe of "instants" to clean the channels from the initial "pulse" (or "instant") of easily mobilized tephra. Given that much of the mass of tephra initially deposited in the upper drainage domain will not initially be mobilized, a contaminant source remains in the basin. Those processes moving the contaminant into the channels are considerably slower than the initial processes, which will result in lower concentrations in the channels. It is noted that the cited rate corresponds to this replacement rate. Because the model does not allow further dilution or "cleaning" of the initial mixed sediments, it provides conservative results (when compared to allowing the contaminant source to become depleted but then including the replacement processes).

The model assumes negligible eolian transport to the RMEI location. The author identifies a "third transport pathway" which is the transport from channels to the divide areas. I have already stated that given the particle size distribution from the ASHPLUME model, this will be a factor. The author noted sand streaks from the channels, which indicate that if silt mixed with fine sand was available, it would be entrained by winds and carried onto the divides. Also see Figure 11A.

Originator Response: The assumption discussing eolian redistribution to the RMEI location (Section 5.2.2) has been edited to both better clarify the underlying reasoning for the assumption, and to acknowledge the reviewer's comments. In essence, there are three potential pathways for eolian transport. The first pathway, inhalation by the RMEI of eolian entrainment from primary fallout at the RMEI location, is quantified in the biosphere model (SNL 2007 [DIRS 177399]). The second pathway, eolian entrainment from areas outside the RMEI location and inhalation by the RMEI, is considered to be negligible based on analogue studies. The final pathway, movement of contaminated tephra fluvially transported into the RMEI channels from the channels to the divides by eolian transport, was not fully addressed in the report. Eolian-deposited sand and silt is found within the top tens of centimeters on the older alluvial fan units (Qa4 and Qa3); however, these surfaces are significantly older than 10,000 years and deposition has occurred gradually over this time (Appendix A). In addition, since channel sediment is, by definition, already mixed and diluted, it is very unlikely that any such localized transport of contaminated tephra from the channels to the divides would make much difference to concentration, especially since in most scenarios the direct deposition on the divides is the most significant source of contaminated tephra to the RMEI location. In cases where the direct deposition is negligible, the concentration in the channels is very low and the uncertainty in the percent of the RMEI location that is composed of active channels implicitly accounts for the uncertainty associated with not explicitly including this process (Section 5.2.2).

The model assumes that transport will be bed load. Given the particle size distribution expected from the eruption (see revised section 5.2.3) it is almost certain that part of the tephra load will be transported as suspended load.

Originator Response: Material transported as suspended load will be carried high in the water column and will be transported past the RMEI location and into the Amargosa River more readily than coarse material. Silt-sized material is often transported as "wash load," meaning that it will be transported in the water column until the flood waters infiltrate completely. While some floods will infiltrate completely before they reach the RMEI location or the Amargosa

River downstream, the flood hydrology of large drainage basins in the western U.S. is dominated by frontal storms and tropical storms of significant duration (~1 to 3 days) that saturate channel sediments and result in continuous flood events throughout drainage basins of regional extent. The channels of the Fortymile Wash fan are almost completely devoid of silt, indicating that this drainage basin is, indeed, dominated by these types of storms. It is noted that Franklin Lake Playa is the primary depozone for silt-sized particles in the area.

By treating all of the tephra from the eruption as coarse-grained sediment for the purposes of fluvial transport, the model errs on the side of overestimating contaminant concentrations at the RMEI location. Fine-grained sediments that are transported as suspended load will be transported past the RMEI location and into the Amargosa River (based on the lack of silt currently stored in channel bed material and basic principles of sediment transport). By considering all of the tephra as bed load, the model predicts that more contaminants will persist in the system, resulting in higher concentrations in the RMEI channels.

The model assumes that the migration of all radionuclides can be modeled with same diffusivity. The differences in chemical characteristics between the various radionuclides suggest that is not strictly true. Cesium may tend to stay in the surface layer because of its binding with high cation exchange capacity minerals.

Originator Response: While it is not strictly true that all radionuclide species migrate into the subsurface at the same rate, the model makes this assumption (Section 5.3.3). There are three important points to note regarding this assumption. First, published data suggest that there is not a significant difference in the rate at which the radionuclides migrate into a particular soil. Second, the range of diffusivity values provided to TSPA will account for such differences between epistemic sample runs. And finally, if, as the reviewer suggests, cesium is inclined to remain in the surface layer, as opposed to other radionuclides that may be more mobile, the calculated diffusivity values used for TSPA will tend to overestimate contaminant concentrations at the RMEI location because diffusivity values are based on measured cesium concentrations from the site.

Unstated assumptions include the fact that the tephra particle size distribution will match the existing hydraulic characteristics of the channel bed load, which is unlikely.

Originator Response: As discussed above, by treating all of the tephra from the eruption as coarse-grained sediment for the purposes of fluvial transport, the model errs on the side of overestimating contaminant concentrations at the RMEI location. Fine-grained sediments that are transported as suspended load will be transported past the RMEI location and into the Amargosa River (based on the lack of silt currently stored in channel bed material and basic principles of sediment transport). By considering all of the tephra as bed load, the model predicts that more contaminants will persist in the system, resulting in higher concentrations in the RMEI channels.

It assumes that the scour depth is primarily a linear dependency, despite the fact that storm intensity and duration could be more important. It assumes that scour depth is non-zero everywhere in the drainage basin, which might require bedrock scour.

Originator Response: Additional text has been added to the sections discussing scour depth. The relationship between scour depth and discharge, and the relationship between discharge and contributing area are found in the literature, and fully developed and validated within the report. The scour depth is assumed to be non-zero throughout the channel network. There is no field evidence supporting significant areas within the channels where zero scour depths occur due to bedrock.

It assumes that the bifurcation routing method is adequate for delineating the channel boundaries (see Fig. 8B).

Originator Response: The report discusses the bifurcation routing method in Section 6. The bifurcation routing method was initially developed by Freeman (1991 [DIRS 174195]), as a method to more accurately estimate local values of contributing area in wide channels and low-relief areas (when compared to the simpler steepest descent method). It must be noted that the Freeman paper does question the use of the divergent method in all parts of the landscape and presents a "mixed" algorithm that tests whether a cell is in a convergent or divergent topography and applies either of the two methods. However, Pelletier (2004 [DIRS 174135]) compared results from the two methods to demonstrate the more realistic results obtained with the bifurcation routing method.

It assumes that the tephra deposit will not produce any dams in the stream channels, and it assumes that the channel configuration after the first instant (hillslope movement of tephra to channels on top of primary tephra fall) is reasonable, even though that channel configuration is not used for the actual "routing".

Originator Response: An assumption that channel geomorphology is not altered has been added.

It assumes that the present topographic surface represents the peak concentration of radionuclides with time. If for example radionuclides were concentrated with the calcium carbonate in the calcrete, and at a later time the divide was eroded down to that level, the maximum concentration would actually be higher than the present surface.

Originator Response: The authors considered a number of processes which might cause radionuclides to concentrate within the RMEI location (e.g. placering, winnowing, chemical precipitation, reaction). No plausible scenario was determined which would produce a higher concentration near the surface and throughout the RMEI location than that calculated by the model. It is acknowledged that fluvial concentration processes may occur shortly after the eruption, but that once the first large flood occurs, the scour-dilution-mixing process will overwhelm local concentrated deposits resulting in large scale mixing and dilution of contaminants.

It also assumes that the peak concentration in the surface at the RMEI location is the initial concentration. If wind processes, which are known to concentrate silts on these surfaces, were to occur, concentrations could increase with time.

Originator Response: The highest surface concentration which can occur in the RMEI area is from material directly placed on the RMEI divides during the eruption. An eolian process moving the diluted contaminated tephra from the RMEI channels onto the divides would result in

covering the higher-concentration material with a more dilute material. While the overall mass of contaminant would increase, the surface concentration would decrease. In cases where the direct deposition is negligible, the concentration in the channels is very low and the uncertainty in the percent of the RMEI location that is composed of active channels implicitly accounts for the uncertainty associated with not explicitly including this process (Section 5.2.2).

It assumes that no sediment concentration of radionuclides occurs, even though stream processes contribute to a significant part of the global resources of uranium, in conglomerates for example.

Originator Response: It is correct that significant amounts of ore-grade uranium occur as paleo-stream sediments. Uraninite placer deposits exist in the geologic record from early Precambrian metasedimentary rocks (older than approximately 2.3 billion years ago), but these deposits are interpreted as having formed in an atmosphere that was significantly less oxidizing than that of today (e.g., Canfield 2005 [DIRS 183192]). Uraninite is unstable in the present oxidizing atmosphere, and placer deposition is not a significant process for increasing the concentration of uranium-bearing minerals in the strongly oxidizing environment of an intermittent stream because the minerals themselves will not persist. Plutonium and other transuranic elements may form mineral phases that are stable in oxidizing environments and therefore may be transported with the bed load sediment; however, the mass of these radionuclides that remains after uranium is leached from the spent fuel particles incorporated in the tephra is very small compared to the mass of the tephra particles themselves. Density contrasts within the sediment will be small compared to those that created the Precambrian uraninite deposits or modern gold placers. Preferential separation of contaminated particles due to density contrasts will therefore be a minor effect. In addition, should any preferential increase in the concentration of contaminants occur, it will be balanced by a comparable decrease in concentration at other locations: mass can reasonably (and conservatively) be assumed to be conserved in the sediment transport process. Because the overall performance assessment is probabilistic, mean concentrations of nuclides at the location of the RMEI and the mean annual radiation doses that form the regulatory basis of the compliance evaluation will be insensitive to small-scale local variations in radionuclide concentrations.

Validation

6. Are the model validation activities (in addition to validation by critical review) that have been planned in the TWP and reported in the model report appropriate and adequate, and adequately and correctly conducted and interpreted?

The field data should be validated by a visit and inspection by an Independent Technical Reviewer.

Originator Response: The field data were collected under YMP procedures current at the time (LP-SIII.11Q-BSC). The data are qualified for use under SCI-PRO-006. Further validation of field data is outside the scope of this review.

The mapping of the alluvial fan can be somewhat subjective and requires validation.

Originator Response: This fact is acknowledged in Appendix A. Transcribed field notes are included in a qualified DTN, which is direct input to this report.

In addition, measurements of the wind blown contributions to the soil surface are needed

Originator Response: These data are reported in Appendix A. There is an eolian component of the fan surfaces that increases in thickness with age. This is discussed in the report.

There is no evidence that an impermeable layer exists under the channels.

Originator Response: It is true that the measurement locations did not show evidence of an impermeable layer in the channels, and this is clearly stated in the report. However, assigning a reasonable but constant value will result in overall conservative results because it will limit the predicted rate of diffusion.

The estimate of scour depth on the RMEI channels needs validation, especially if scour is being confused with incremental deposition.

Originator Response: The USGS did have scour chains in other parts of the Fortymile Wash drainage basin, at stations J-13 and Amargosa Valley. Both of these points are downstream from the Narrows, with the J-13 station being approximately 9 km south of the Narrows (about half-way between the Narrows and the fan apex) and the Amargosa Valley station being just below the fan apex. Mean scour measured at the J-13 location was 37 cm with a maximum scour of 61 cm (DTN: GS960908312121.001 [DIRS 107375]). A comparison of scour predicted by Equation 6.3-14 using the range of scour depths for the Narrows (73 to 122 cm) in the channel cells within a radius of 60 m from the measurement location resulted in average scour depth ranging from 49 to 81 cm. The mean scour depth at the Amargosa station was 12 cm (DTN: GS960908312121.001 [DIRS 107375]). While this station was outside the model domain, it supports that scour depth changes as a function of discharge area per unit width (the discharge area at this station is only slightly larger than at station J-13, while the channel width is greater, leading to smaller contributing areas on a pixel basis). This corroborating information has been added to the report.

The critical slope measurements came from the San Francisco Volcanic Field sitting on the already topographically high Colorado Plateau. I am unconvinced that these measurements are directly applicable to the very different weather conditions found in the Fortymile wash drainage basin.

Originator Response: The climate of Flagstaff is clearly different from Amargosa Valley. Here, again, the choice of study site was based on practical limitations not acknowledged by the reviewer and on conservatism. The wetter climate of Flagstaff can reasonably be assumed to result in lower critical slope values, thereby possibly overpredicting the volume of slope mobilized material in the eruptive case of Yucca Mountain.

Bulk ^{137}Cs concentration measurements were made in shallow pits to estimate or validate diffusivity estimates. It was unclear how these data were adjusted for multiple dosings caused by multiple above ground nuclear tests, or underground tests that leaked radionuclides to the surface through fractures and fissures.

Originator Response: Data were not adjusted for multiple dosings. Atmospheric tests were conducted at the site over a 10-year period, roughly 50 years prior to collection of the samples.

There is no clear way to determine how or when radionuclides were deposited at specific sample locations, and the impact of multiple dosings is considered to be one of the uncertainties in the data. Ranges for the diffusivity constants for both the divides and the channels were calculated with the intent of capturing the overall uncertainty in the parameter.

The square root dependence of scour depth with unit width discharge is accomplished with different units (metric versus English) than in the original Leopold study. Furthermore, the Leopold study did not force the regression through the origin, but the Powell et al. study citied, did force the regression through the origin (no intercept). Therefore they are not directly comparable until they are done the same way.

Originator Response: The difference in units used by the two studies does not impact the equations used in this report. As discussed above, the Leopold study did force the regression through the origin, and the data sets are comparable.

The report uses a simple Hjulstrom diagram (p. 7-17, fig 7.2.5-1) to assert that transport is dominant across the alluvial fan and therefore the fan is not a "perfect depozone" The problem with this application of the Hjulstrom diagram is that the alluvial fan is not an engineered structure where you can control which flow variable changes. The differences between the main channel in the drainage basin (upper domain) and the alluvial fan channels attest to the systematic adjustment to altered flow conditions. Specifically, in the very likely case where discharge decreases because stream flow is abstracted (lost by infiltration) through the channel floor, then the logic used in the report is clearly inadequate and inappropriate. While the fan may not be a "perfect depozone" its very existence suggests that it is a depozone, and many floods will not cross the entire fan without significant discharge loss and hence deposition. This again raises the points made earlier regarding significant accumulation of silts in the fan channels and wind redistribution onto the RMEI divide areas.

Originator Response: The report does not argue that the RMEI area is not a depozone, as pointed out; it clearly is. Rather, the report highlights the fact that it is not a perfect depozone, e.g., that the system is not closed. This argument is bolstered by the absence of silt within the RMEI area channels. Field observations have shown that Franklin Lake Playa is the primary depozone for silt-sized particles in the area. This is due to the dominating effect of large frontal and tropical storms of significant duration (on the order of 1 to 3 days) which control the flood hydrology of the area. These storms carry wash material through the RMEI area. They will also, over time, transport larger grained material as bed load. It is also noted that typical model cases result in very little (or no) contaminant leaving the RMEI area. Text describing these points has been added to the report.

Validation of diffusion constants is problematic due to the variability in soils and climate characteristics. Perhaps a term, "effective" diffusion constant might be more useful.

Originator Response: The diffusion constant is dependent on soil types and climate characteristics. In Section 7.2, the use of a diffusion process to accurately capture the migration of the contaminant into the soil was validated using data from the literature. The adequacy of the ranges chosen for the site-specific diffusion constants is discussed in Section 7.1. The word "effective" was added to the text.

Corroboration in Refereed Journal

Section 7.3.1 discusses the use of Pelletier et al 2007, a peer reviewed article to be published in the journal Geomorphology as a method for corroboration of model results. I will briefly discuss the data presented in this section that is relevant to usefulness of this journal article as corroboration.

There are significant differences between the two model scenarios. In the Lathrop Wells study, tephra thickness is not used for model input; rather measured concentrations are applied from field measurement. In addition, the stream system studied is small compared to Fortymile wash. In Lathrop Wells, the basaltic (tephra) and non-basaltic (clean) sediment are known to be of similar grain size

Originator Response: Text has been added to the report to point out the differences between the Lathrop Wells analogue study and the FAR model developed in the report. There is no reason why the smaller basin size in the Lathrop Wells study affects its use for model validation. In fact, the results at Lathrop Wells clearly demonstrate that dilution is effective even over small distances.

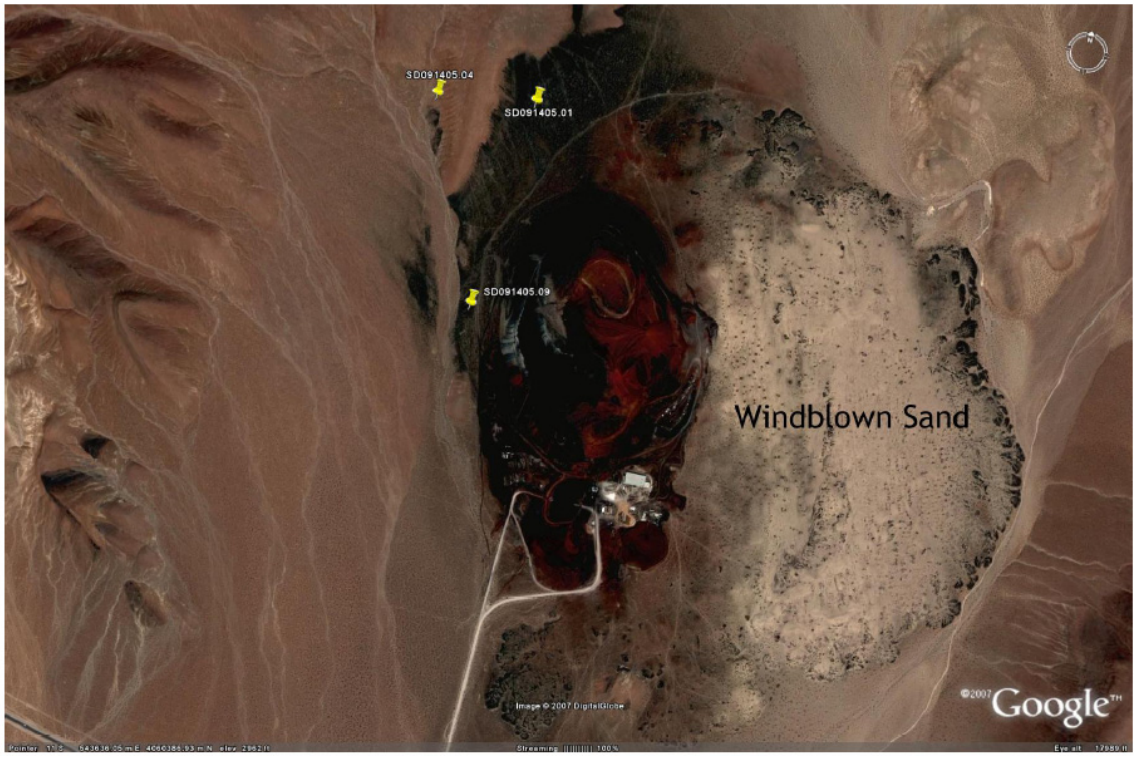

Figure 11: showing the Lathrop Wells cone: A) above the tephra sheet, and basalt flows. Note the accumulation of sand blown onto the tephra. B) Below the locations of data used in Lathrop Wells study. Note the area of stream confluence indicated by the white square.

I attempted to validate the locations of the samples in Google Earth using the data provided in Table 7.3.1-, but found that my plotted points did not apparently match exactly with those in figure 7.3.1-2. However, I was able to get a general sense of the locations, and the setting of these samples (see Fig. 11A).

The report notes that single samples were taken at single locations along the stream channels, but there is no information regarding amount of sample taken. I would note that coarse deposits require very careful sampling and could easily require multiple large samples at each channel location.

Originator Response: It is acknowledged that there is potential for error in any type of field sampling analysis. Samples collected for this work used standard field techniques and followed reasonable protocols. There is no reason to doubt results of the measured tephra concentrations.

A portion of the data collected is plotted on Figure 7.3.1-2 (p. 7-9), including a graph with a tephra concentration plotted on a log axis. This semi log plot is somewhat misleading, in as much as it gives large visual weight to the small differences in less concentrated samples. If you were to re-plot these data on linear axes (Fig. 12), you would basically see, as you can simply read from Table 7.3.1-1, that there appears to be two groups of concentrations in each of the streams studied. For example in the western stream one group of values ranges from between 70-80% and the other ranges from 36-47%. While you can perform a regression, and obtain a line showing decreasing concentration with distance, it seems simpler to say that there are two samples which vary in concentration. Thus I do not find any compelling data that corroborates the model. The photo presented in figure 7.3.1-3 showing the high and low concentration

channels probably represent the two classes of concentration. That area is shown in the white rectangle in Figure 11B and plotted in Figure 12 below.

Originator Response: The data from the western channel do, in fact, follow two populations because they are controlled by a single, large influx of nonbasaltic tributary sediments that leads to a single "step" change in concentration.

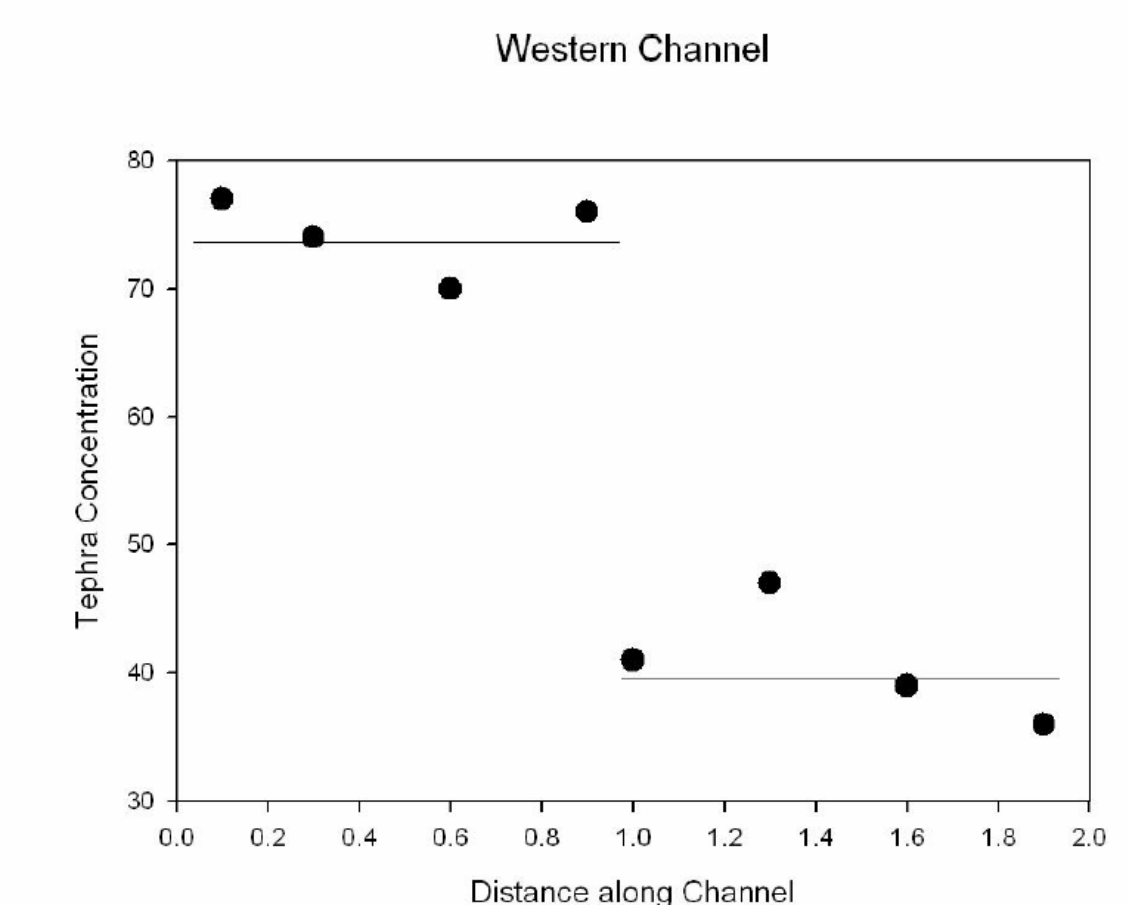

Figure 12: showing alternative model for data presented in Table 7.3.1-1 that indicates no downstream dependency, rather just two separate populations.

Perhaps more puzzling are the data that were not plotted from Table 7.3.1-1 (data numbers 1405.04-1405.07). These data represent concentration of the western stream flowing south, where it meets the stream that was flowing on the tephra sheet. Why are these concentrations so high? If they are coming from an area with a background concentration of 9%, and do not mix with other tephra draining streams, how did the concentrations get higher than the original source?

Originator Response: There are several small tephra outcrops along the tributary to the western channel that are being actively eroded, primarily by bank retreat. Two of the larger of these outcrops are readily visible in the images presented by the reviewer (see annotated figure below). These small sources locally enrich the channel along short (10- to 100-m) sections of incomplete mixing. Upstream and downstream of these small outcrops the concentration values

return to the background values within distances of 10 to 100 m from the sources. Samples were collected in the field before the resolution of the input data made it clear that these sources could not be resolved in the model. Given the limited resolution of the input data, however, the validation exercise was necessarily limited to the principal western and eastern channels draining the tephra sheet. A comment has been added to the report text to clarify this point.

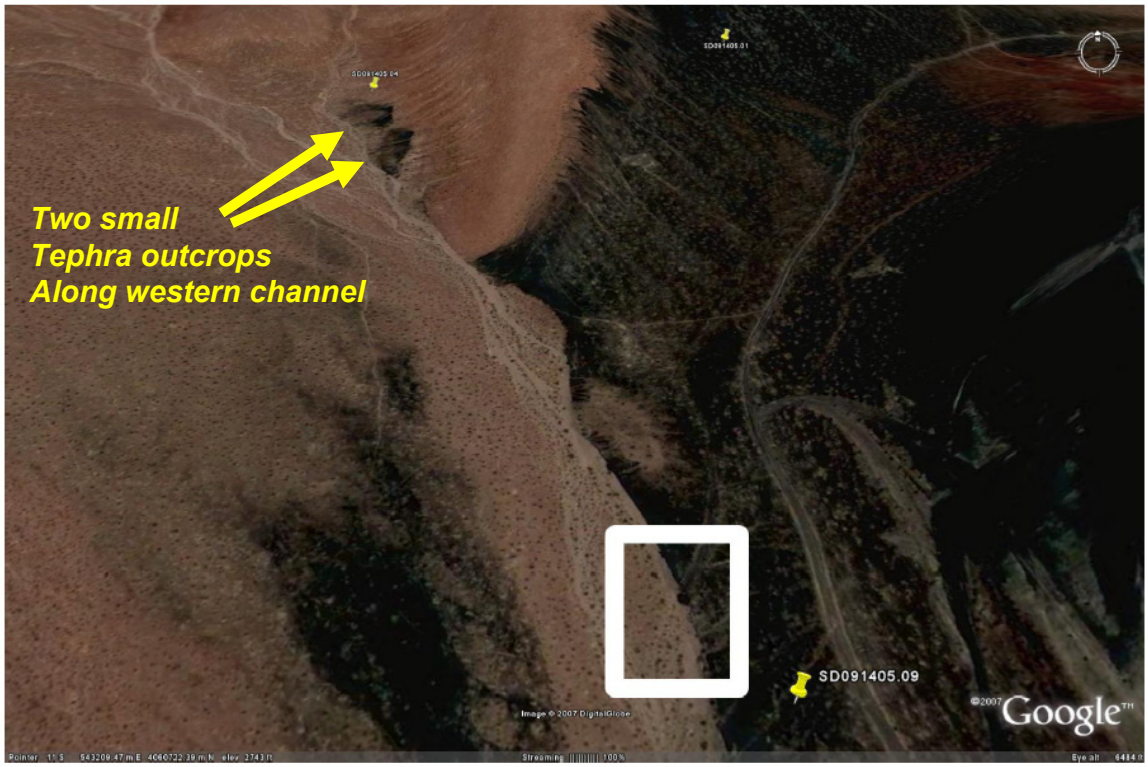

I also am confused by the model result shown as a line on the lower graph on Figure 7.3.1-2 B, labeled 3D model prediction which has a spike just upstream of data point 1405.11.

Originator Response: The model provides a prediction of tephra concentration taking into account the three-dimensional effects of scour depth changes along the channels. Areal characteristics of the grid are provided from the input DEM. The use of site-specific data on a pixel basis (rather than interpolating sparse populations of measured data) will lead to results that vary on a pixel basis. The spikes shown in Figure 7.3.1.-2B are the model response to real tephra outcrops through which the channel passes. These outcrops provide a small source for tephra, resulting in small increases in concentrations in the channel. It is also noted that data from the eastern channel must be plotted on a log axis because the measured concentration values differ by two orders of magnitude. On a linear scale, the concentration values below 10% would not be easily read from a linear plot.

Given the uncertainties associated with channel sampling and the lack of a convincing downstream variation, there is no strong case for corroboration of the mixing model here. On the contrary, the strong reversals in concentration downstream and in direct opposition to the model prediction, stresses the fact that ideal mixing and dilution is not occurring. Also note on Figure

11A, the blanket of windblown sand that could represent the level of eolian flux across the Fortymile wash fan.

Originator Response: The data from the western channel do, in fact, follow two populations because they are controlled by a single, large influx of nonbasaltic tributary sediments that leads to a single "step" change in concentration. In this sense, the eastern channel is a more rigorous test of the model because it includes several significant tributary inflows along its course. The key question is whether the model predicts the correct value of the change in concentration associated with the tributary influxes along both the western and eastern channels. It does. The model predicts the same overall trend as the observed data in both channels studied as well as the magnitude and locations of the discrete "jumps" associated with tributary in fluxes.

The sand present on the surface of the northeast lava field is visible because this late-stage lava flow did not contain lapilli-size fallout clasts that are necessary for desert pavement formation (Valentine and Harrington 2006 [DIRS 177271], p. 534). In fact, some eolian deposition probably occurs over the entire area, but as argued in Section 5.2.2, including such deposition in the model would only serve to further dilute waste concentrations at the RMEI location.

C3. CRITICAL REVIEW OF DRAFT A BY DR. WILLIAM R. HACKETT

MEMORANDUM

Date: September 5, 2007

To: Mr Tom Pfeifle

From: William R. Hackett

Subject: Internal Critical Review of

MDL-MGR-GS-000006 REV 00A
August 2007
Redistribution of Tephra and Waste by Geomorphic Processes Following a Potential Volcanic Eruption at Yucca Mountain, Nevada

INTRODUCTION AND BACKGROUND

This memorandum presents my internal critical review of MDL-MGR-GS-000006 REV 00A. In the mid-1990s I was a member of the Probabilistic Volcanic Hazards Analysis (PVHA) Expert Panel, and I am now a member of the Expert Panel that is currently updating the PVHA (PVHA-U). In 2004 I was a member of the Regulatory Integration Team (RIT), Igneous Events, for the Yucca Mountain Project. During that time I received training in the preparation and review of YMP documents in support of the License Application. My RIT responsibilities included checking and other activities for revising earlier versions of the Ash Redistribution Model Report. I have not been involved in the preparation of the current draft for which this review is given. The current draft is substantially different from earlier ones, and its authorship has changed. Following the instructions of Mr Tom Pfeifle (Responsible Manager/Lead), my review addresses the "strategic" questions listed below. My overall opinion of Draft A is entirely positive, as reflected in the itemized comments given below.

REQUIREMENTS FOR THE CRITICAL REVIEW

1. **Complete training in appropriate project procedures and processes.**

On August 30, 2007 I completed Lead Lab General Employee Training (GET). [Ref.: August 30 email received from Ms Cheryl Seminara, Project Lead, Training.

Although not required for the performance of this review, equivalency has been granted by Lead Lab for the following courses I took from BSC: YMP102 Ongoing Licensing Support Network

Obligations; YMP200 Analysis of Models and Calculations; YMP210 Managing Technical Product Inputs; YMP250 Checker Training. [Ref.: August 29, 2007 email received from Ms Cheryl Seminara, Project Lead, Training.]

2. **Review the draft model report, relevant reference material, and relevant sections of the technical work plan (TWP) that describes post-model development activities**

I have reviewed Draft A of the Model Report. I have also reviewed relevant sections of TWP-WIS-MD-000007 Rev 10, Technical Work Plan for Igneous Activity Assessment for Disruptive Events; relevant sections of SCI-PRO-006 Rev 5, Models; SCI-PRO-002 Rev 2, Planning for Science Activities; and TDR-TDIP-DE-000005 Rev 00, TSPA Data Input Package for Tephra Redistribution.

In addition I have reviewed the following reference materials:

Pelletier, J.D.; Harrington, C.D.; Whitney, J.W.; Cline, M.; DeLong, S.B.; Keating, G.; and Ebert, K.T. 2005. "Geomorphic Control of Radionuclide Diffusion in Desert Soils." *Geophysical Research Letters, 32,* (L23401), 1-4. Washington, D.C.: American Geophysical Union. TIC: 257905.

Jon D. Pelletier, Stephen B. DeLong, Michael L. Cline, Charles D. Harrington, Gordon N. Keating, in press, Dispersion of channel-sediment contaminants in distributary fluvial systems: Application to fluvial tephra and radionuclide redistribution following a potential volcanic eruption at Yucca Mountain

3. **Document your responses to the following questions:**

- Is the conceptual model for tephra redistribution reasonable and appropriate for its intended use?

Response: Yes. Not only is the conceptual model for tephra redistribution reasonable and appropriate for its intended use, but it also presents an elegant solution to a complex problem. By "elegant" I mean that the conceptual model successfully integrates the geomorphic processes relevant to tephra redistribution, presents them logically and comprehensively, and separates the key components of the process model such that those components are amenable to mathematical modeling. The overall model is clearly presented both verbally and mathematically.

- Are the mathematical relationships appropriate and representative of the scientific understanding of the geomorphic processes for the transport of sediment from the Fortymile Wash drainage basin to the location of the RMEI on the Fortymile Wash alluvial fan?

Response: Yes, in all cases. In Section 1. Purpose, it is stated that the model calculates:

(1) mobilization by hillslope and fluvial processes of waste-contaminated and uncontaminated tephra deposited in the upper drainage basin domain,
(2) transport and mixing (dilution) of waste-contaminated tephra within the channels of the upper drainage basin domain, and
(3) emplacement and diffusion of waste-contaminated sediments within the alluvial fan at the RMEI location.
These three steps are implemented in the FAR V. 1.2 software package, which is run within the Total Systems Performance Assessment (TSPA) GoldSim environment.

My opinion that the mathematical relationships are appropriate and representative stems from the following general observations: (A) The relationships are presented clearly and thoughtfully, such that readers (including this reviewer) can understand foundational principles of how the mathematical relationships are derived, how they are specifically applied to the problem, and the underlying assumptions and limitations of their application. (B) The mathematical models and relationships are clearly tied to the conceptual model and to the underlying geomorphic processes. Conceptual and mathematical models are in all cases defensible and credible because they stem from a thorough understanding of the geomorphic processes operating within the Yucca Mountain region. This Model Report represents not only the thorough understanding of discrete geomorphic processes, but also a thorough understanding of the interplay (synergy) of processes within a desert geomorphic system. (C) The mathematical relationships and models presented in this Model Report have also been published (or in press) by peer-reviewed scientific journals. Pelletier et al. (2005) "Geomorphic Control of Radionuclide Diffusion in Desert Soils" describes the conceptual and mathematical models used for the diffusion of radionuclides into soil. Pelletier et al. (2007 in press) "Dispersion of Channel-Sediment Contaminants…" describes the conceptual and mathematical models used for the mobilization, transport and mixing of waste-contaminated tephra and sediment, within both the upper drainage basin and the lower-basin alluvial fan at the RMEI location. The authors of these peer-reviewed publications include not only YMP personnel, but also eminent scientists from academia (Pelletier) and the USGS (Whitney). The lead authors of these papers are acknowledged experts in desert geomorphic systems and soils.

-Are the outputs of the model reasonable and representative?

The Model Report gives both Direct and Indirect Outputs to TSPA in Tables 8.1-1 and 8.1-2. The outputs in all cases are likely to be reasonable and representative, because the outputs have been developed using reasonable and representative analytical methods. These methods include the use of an up-to-date digital elevation model, regional mapping of geomorphic surfaces, data from soil pits, other field measurements from analog regions, trial runs of calculations and submodels, etc.

Results from the integrated model approach are not given in this Model Report. Rather, such results are to be calculated within TSPA, including additional inputs from Biosphere model(s), and ultimately reported as a radiation dose at the RMEI location at a given time. The results of twenty monte-carlo simulations of tephra eruption and redistribution are given in Fig. 10 of Pelletier et al. (2007 in press), wherein tephra concentrations in sediment are predicted by the scour-dilution-mixing model at the outlet of Forty Mile Wash. These results (in press) seem reasonable and representative because the underlying analysis and models are reasonable and representative.

- Are there alternative models or approaches that should be considered?

None that I can identify. My opinion of this Model Report is that it has considered and has built upon previous models and approaches, as found in earlier drafts of the conceptual and mathematical approaches to the problem of tephra redistribution. Furthermore, the scientific literature cited throughout the Model Report suggests to me that the authors have considered and have utilized all or most of the relevant information available for addressing the problem of tephra redistribution. I therefore consider the current Model Report to be state-of-the-art, and it presents no discernable conceptual or mathematical deficiencies.

- Are the limitations of the model adequately described?

The limitations and uncertainties are clearly and adequately described in Section 8.2 of the Model Report. The Assumptions of the model are clearly and adequately described in Section 5. Thorough justifications are given for the simplifying assumptions. The implications of the assumptions are explained, including the nature of specific conservatisms introduced by making the assumptions. The overall presentation presents the assumptions and limitations as being necessary and justifiable, in order to construct a workable and defensible model.

- Are the model validation activities that have been planned in the TWP and reported in the model report appropriate and adequate, and adequately and correctly conducted and interpreted?

This Model Report is very well validated. Level II Validation is required, as described in SCI-PRO-002, Attachment 3. In the Technical Work Plan, the two model validation methods selected are (1) technical review through publication in a refereed professional journal, and (2) independent critical review to evaluate whether the model is adequate for its intended use.

The critical review by an outside expert is planned but not yet completed.

The technical review through publication in a refereed professional journal has been partially completed. Pelletier et al. (2005) is a peer-reviewed publication that clearly presents the soil-diffusion aspects of the model. Pelletier et al. (2007 in press) was made available to me as a prepublication draft. If I were a peer reviewer of this draft, I would recommend its publication

with only minor modification. I therefore anticipate its timely publication, at which time the requirement for Level II Validation will be met.

It is my opinion that (1) Model validation during model development is adequately addressed in Section 7 of the Model Report; (2) The two peer-reviewed publications, together with the thorough treatment of the soil-diffusion and the scour-dilution-mixing models given in Section 7 of the Model Report, meet the specific validation requirements given in the Technical Work Plan, Section 2.6.5.2.3,for Confidence-Building After Model Development, and (3) That taken together, the Model Report and its supporting peer-reviewed publications adequately present and validate the general conceptual model, the detailed mathematical models and the numerical methods used in this Model Report.

Other points related to model validation that I wish to convey are: (1) The Model Report is exemplary in its attention to confidence-building during model development, including its examination of intermediate model outputs and the incorporation of thorough sensitivity analyses; (2) The Technical Work Plan is adequate, accurate and complete in its support of this scientific model. [SCI-PRO-002 Rev 2, Section 5.5 states, "The independent technical reviewer is responsible for confirming the adequacy, accuracy and completeness of the TWPs supporting scientific analyses and models."]

C4. CRITICAL REVIEW OF DRAFT D BY DR. WILLIAM R. HACKETT

MEMORANDUM

Date: November 7. 200~

To: Geoff Freeze

From: William R. Hackett

Subject: Critical Review of

MDL-MGR-GS-000006 REV 00D
October 2007
Redistribution of Tephra and Waste by Geomorphic Processes Following a Potential Volcanic Eruption at Yucca Mountain, Nevada

This memorandum constitutes my complete critical review of the subject document.

SUBJECT MATTER EXPERTISE AND QUALIFICATIONS

I earned a Ph.D. in 1985 from Victoria University of Wellington, New Zealand. My published research has addressed igneous processes, probabilistic volcanic-hazard analysis and physical volcanology. I have held positions as tenured Associate Professor of Geology and member of the Graduate Faculty at Idaho State University, Scientific Specialist at the Idaho National Laboratory, independent consulting geologist, and Principal Scientist with Integrated Science Solutions Inc. For the Yucca Mountain Project in the 1990s I was a member of the Probabilistic Volcanic Hazards Analysis (PVHA) Expert Panel for the Yucca Mountain Project. In 2004 I was a member of the Regulatory Integration Team (RIT), Igneous Disruptive Events. Recently I served as a member of the Expert Panel charged with updating the PVHA (PVHA-U).

REVIEW CRITERIA

I have been asked to provide answers to the following questions:

1. Is the conceptual model for tephra redistribution reasonable & appropriate for its intended use?

   Response: Yes, it is reasonable and appropriate for its intended use. I have a similar positive opinion of this model report to that given in my earlier review.

2. Are the mathematical relationships appropriate and representative of the scientific understanding of the geomorphic processes for the transport of sediment from the Fortymile drainage basin to the location of the RMEI on the Fortymile Wash alluvial fan?

   Response: Yes, per my earlier review in response to this question.

3. Are the outputs of the model reasonable and representative?

   Response: Yes, per my earlier review in response to this question.

4. Are there alternative models or approaches that should be considered?

   Response: None that I can identify, nor that have been identified by another critical reviewer, Dr Larry Mayer.

5. Are the limitations of the model adequately described?

   Response: Yes, the limitations and assumptions are thoroughly (not just adequately) described. This is a strong point of the model report.

6. Are the model validation activities that have been planned in the TWP and reported in the model report appropriate and adequate, and adequately and correctly conducted and interpreted?

   Response: Yes, per my earlier response to this question as a reviewer, conditional upon publication of Pelletier et al. (2007). Furthermore, I note in completing this review that I may be participating in a deviation from the YMP Level 2 Model Validation criteria. This is because I am being asked to complete the review of another critical reviewer who is unable to do so, specifically to provide concurrence that his comments have been adequately addressed by the authors of the model report. In doing this, I affirm the credibility of the reviewer's input, as well as the credibility of the responses to his input. My serving as proxy in the completion of the work of another critical reviewer calls into question the "independent" quality of his review. I give further context below.

7. Have the comments and concerns of Dr Larry Mayer, independent critical reviewer, been adequately addressed by the author(s) of this model report? This question is asked because Dr. Mayer is unavailable to concur with the responses to his comments.

   Response: Yes, it is my opinion that the comments and concerns of Dr Larry Mayer have been adequately addressed by the authors of this model report.
   I have reviewed the model report, Rev 00D, containing the written comments of the independent critical reviewer Dr Larry Mayer, and the authors' responses to Dr Mayer's comments. In providing my concurrence, I wish to make clear that Dr Mayer has not authorized me to speak for him. Rather, my role is similar to that of an editor of a peer-reviewed scientific journal who must judge the relevance of comments and the responses to them. Having served in this role before, I understand and accept it. In the absence of

Dr Mayer's concurrence, others will have to decide whether or not the strict validation criteria for this model report have been met.

Dr Mayer is an eminent geomorphologist with credentials well suited to serve as a critical reviewer. I acknowledge his expertise and reputation, and I am grateful to him for providing a very thorough review. His comments have led to substantial improvements in this model report. In my view, the authors of the model report have thoroughly addressed Dr Mayer's comments. The authors have provided direct written responses, embedded in the original text of Dr Mayer's review and included as part of the model report. In line with their responses, the authors have made substantial improvements by expanding and clarifying the text and graphics. In cases where the authors have declined to follow Dr Mayer's specific suggestions they have given adequate justification, but their general attitude has obviously been to accommodate Dr Mayer's criticisms to the extent possible, in the interest of improving the model report.

The comments I delivered in my earlier review, and those I give here, are substantially different from those of Dr Mayer. My comments are very general and very positive, in contrast to the detailed and constructively critical comments of Dr Mayer. Comparative readers of our comments may well ask, "Did they read the same document?" Yes we did, but with different backgrounds and perspectives. As a geomorphic specialist, Dr Mayer is well suited to give his thorough and detailed review. I on the other hand bring expertise as an applied geoscientist and specialist in igneous processes. I have worked on Yucca Mountain Project technical products for more than ten years and I therefore understand how these documents must be written, structured, and validated within the regulatory environment of the nuclear industry. I understand that complex problems must be made tractable, but not simplified to the extent that they lack credibility. I understand how the project documents must be integrated, how they must function together provide a defensible safety basis for the proposed repository. I understand that the models and documents must be efficiently produced in light of project resources and priorities. Most importantly, I understand that decisions I make today may affect the health and safety of future generations.

I strongly endorse the following statement from the summary response given by the authors near the end of the model report: "The key issue is not whether the proposed model includes every process (it is fair to state that no model could represent all of the geomorphic processes occurring or that will occur in this system in the future), but whether the model adequately represents the range of system behavior and resulting contaminant concentrations needed to estimate the range of doses experienced by the RMEI. This end goal has been our paramount concern during model development. In cases where a significant process has been excluded from the model, we have shown that neglecting the process leads to conservative results." Well said. My thoughts exactly.

From the outset, I have approached this critical review with an overriding question: "Are the conceptual and mathematical models for tephra redistribution REASONABLE AND APPROPRIATE FOR THEIR INTENDED USE?"

My answer is Yes.

My confidence in this has only been increased by the authors' thoughtful responses to Dr Mayer's review.

C5. CRITICAL REVIEW OF DRAFT A BY DR. LARRY MAYER (ORIGINAL SCAN)

September 10, 2007

To: M. Kathryn Knowles
From: Larry Mayer
RE: Independent Critical Review of MDL-MGR-GS-000006 REV 00A

This Independent Critical Review of "Post-development validation of a model describing Redistribution of Tephra and Waste by Geomorphic Processes Following a Potential Volcanic Eruption at Yucca Mountain, Nevada" will address the following six principal questions:

1. Is the conceptual model for tephra redistribution reasonable and appropriate for its intended use?
2. Are the mathematical relationships appropriate and representative of the scientific understanding of the geomorphic processes for the transport of sediment from the Fortymile drainage basin to the location of the RMEI on the Fortymile Wash alluvial fan?
3. Are the outputs of the model reasonable and representative?
4. Are there alternative models or approaches that should be considered?
5. Are the limitations of the model adequately described?
6. Are the model validation activities (in addition to validation by critical review) that have been planned in the TWP and reported in the model report appropriate and adequate, and adequately and correctly conducted and interpreted?

"Its *intended use* is to be integrated with the Ashplume and Biosphere models within the TSPA model to predict the waste concentration as a function of time since the eruption at a compliance point (RMEI) approximately 18 km south of the repository on the Fortymile Wash alluvial fan. Ashplume provides input (initial extent and thickness of contaminated ash on the Fortymile Wash landscape) to the ash redistribution model, which in turn provides input (waste concentration as a function of time since the eruption) to the Biosphere model that calculates radiological dose at the RMEI. NOTE: The Ashplume and Biosphere models have undergone separate validation and, therefore, are outside the scope of your critical review."

"Its *purpose* is to reasonably and appropriately represent the redistribution (mobilization, transport, dilution, deposition, and diffusion) of waste-contaminated tephra deposited in the Fortymile Wash drainage basin east and northeast of the Yucca Mountain, Nevada site by a low-probability (mean annual frequency of intersection of a potential repository at Yucca Mountain by a volcanic event equal to 1.7×10^{-8}) volcanic eruption through the repository."

After making a few general comments regarding MDL-MGR-GS-000006 REV 00A, the review discusses sections of the report relevant to each question and answers each of the questions above sequentially.

General Comments

The version of the model report that I reviewed, MDL-MGR-GS-000006 REV 00A, is clearly a work in progress. The apparent quality and completeness, both technical/scientific and clarity, varied considerably throughout the document.

I have attempted to address the six questions required for Level II validation in a direct and formal manner. The probability of a volcanic event (provided in the statement of purpose above), only enters into the review as part of the discussion for question 4, alternative models. In this review, I may refer to the model for tephra redistribution as the FAR model and to data input into FAR coming from the ASHPLUME model.

I have made a conscious attempt to simplify the mathematics of MDL-MGR-GS-000006 for a non specialist, in order to make my technical review as transparent and easy to understand as possible. For this reason, and other reasons of clarity, I chose to include a number of figures that explain or demonstrate a specific point relevant to this review. Several of the figures are simply cartoons to help visualize the variables in the model. Several of figures are used to demonstrate and document how the model output was evaluated. Because of references to figures inside and outside of this review, I used the original report figure numbers. Figures in the MDL-MGR-GS-000006 report take a form reflecting their chapter and section location (e.g., Fig 6.5.3-3), while figures used in this review are simply labeled Fig. 1-12.

Some of the figures which represent model output were clipped directly from the electronic form of MDL-MGR-GS-000006 that I was sent. Others were provided by J.S. Stein at higher resolutions than in the PDF file of MDL-MGR-GS-000006 to allow for more detailed inspection. Figures using overlays of model output with satellite or topographic data were done with Google Earth, and the projections of data onto the Lathrop Wells satellite image were also done in Google Earth.

The Lathrop Wells satellite image from Google Earth was used to help me understand the use of a validation study discussed in the MDL-MGR-GS-000006 report, to demonstrate the importance of eolian processes at the Lathrop Wells tephra sheet, and by inference, the adjacent Fortymile Wash alluvial fan. Note that all citations are from MDL-MGR-GS-000006 and are not reproduced here.

The scope of this technical review is largely determined by the request for the Independent Technical Review, which in turn is conditioned by regulatory requirements. I have tried to avoid extending the scope in any way.

Finally, this review was done within a limited period of time, allotted by Sandia National Laboratory, and as all technical reviews, may be in part dependent on that time period. However, I do believe that this review represents a broad identification and discussion of all critical points explicitly raised in the six principal questions.

Conceptual Model

The conceptual model presented in section 6.2 claims that it "integrates physically based submodels for hillslopes, fluvial, and soil redistribution processes". Further, the report claims that "the simplified approach taken is adequate for the intended purpose" (page 6-1).

The conceptual model for the "hillslope submodel" is barely described in section 6.2.1. The description requires some development and clarity, but the text basically says that the hillslope submodel consists of a threshold calculation. If the slope upon which the tephra is deposited is greater than a threshold slope value, the "tephra and waste in that pixel is considered to be mobilized". First, the text should clarify whether the waste is uniformly distributed with the tephra and not partitioned according to particle size of the ejecta. But beyond this threshold calculation, there is no physical basis provided in the conceptual model description for this "submodel".

The conceptual model for the "fluvial submodel" is barely described in section 6.2.2. There is no discussion for the physical basis of the model in this section, although there is some description of the method used to calculate dilution of tephra, which is further elaborated later in the mathematical model description. There is simply not enough description or background given in section 6.2.2 to consider this an adequate model of any kind. The reviewer is left wondering why this method was chosen and how it might relate to physical processes important for the intended purpose.

The final part of the conceptual model is described in section 6.2.3, the "soil redistribution process". Here the report considers two distinct surfaces separated by whether or not fluvial activity is "possible". On older fan surfaces or "interchannel divides" which have not been inundated by channel flow from the active main channels, the conceptual model considers only diffusion processes, and that diffusion will be limited to a zone physically constrained by calcretes. In the active channels, diffusion is also considered to be the sole process of redistribution, albeit at a higher effective diffusivity. The report also states that "additional mixing of sediments" in the fan channels can occur by flood events. This statement contradicts the conceptual model presented because there is a change in the concentration from outside the model unrelated to the one dimensional diffusion process.

1. Is the conceptual model for tephra redistribution reasonable and appropriate for its intended use?

No, the conceptual model as presented in section 6.2 is neither reasonable nor appropriate for its intended use because a conceptual model is not developed or described. A conceptual model is largely absent from the reviewed version of the report. The context for its intended use is not explained in the brief sketch provided. I believe that it is the responsibility of the report author to develop, describe, and justify, a conceptual model that satisfies claims of being "physical based", and to demonstrate how this model is appropriate for intended use.

The report also fails to document the conceptual models which are the basis of the mathematical model. The report does not satisfy its own claim to "integrate

physically based submodels". The goal of a conceptual model is the explanation of the physical processes which are important for predicting tephra redistribution for the intended purpose and use and perhaps discounting those that are not important. Although this reviewer was able to reconstruct an algorithm-based conceptual model from the mathematical description below, it is the responsibility of the report author(s) to develop, document, and justify the conceptual model upon which the mathematical model is based. Lacking a conceptual model, there is no formal basis to accept or reject the underlying mathematics as conceptually appropriate or reasonable.

Mathematical Model

The mathematical model is documented in section 6.3.

Initial Conditions: The initial conditions used in the FAR model are described in section 6.3.2. The tephra and waste concentrations from ASHPLUME. Any reviewer needs to understand whether the waste distribution is assumed to be uniformly distributed with the tephra, or partitioned in some way with particle size or other factor. That will also include the partitioning of radionuclides. Further, the reviewer needs to know whether the tephra thickness is given as a mean and standard deviation within each (concentration) isopach band, or as a simple thickness with no statistical variability within an isopach. Finally, the reviewer needs to know whether the likelihood of considerable accumulation in lower or wind shadow areas are part of the ASHPLUME model used for input into FAR.

The 30-m resolution DEM needs to be validated in the low relief areas to make certain that there are no gross errors in the delineation of the drainage basin. I will revisit the DEM later in this section.

The algorithm is delineated in section 6.3.3.
Step 1 is the interpolation of the ASHPLUME tephra output for use as input in FAR. This involves an interpolation from a polar grid to a Cartesian grid matching the DEM. I think that an estimate of the error in this method can be easily produced by comparison with the pre-transformed and rectified data, and would be useful to understand the sensitivity analyses.

Step 2 is taken to correct flaws in the DEM that are required for the subsequent calculations. It is unlikely that this method introduces serious error into the resultant calculations.

Step 3 computes slope, contributing area and scour depth. The slope computed in this step will be compared to a threshold value, the critical slope, to determine if the tephra stays on the hillslope or is transported to the adjacent channel. The method used here does not include diagonals in the slope calculation. The calculation also assumes that the grid is square.

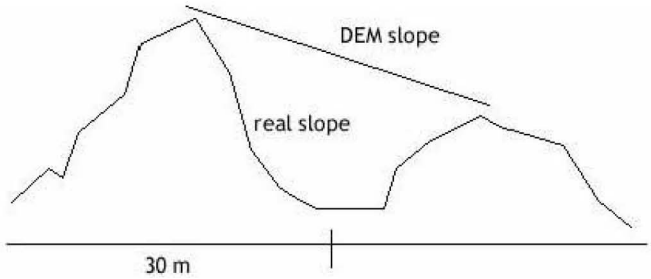

Figure 1: DEM slope compared to real world slope. The actual topographic profile may have a very different local slope in comparison to a 30-m DEM calculated slope.

The reviewer does not have a simple method to determine the relation between the DEM slope and the real Fortymile wash drainage basin slopes. Because it is conceivable that the two slope estimates diverge depending on the relief and roughness of the topographic surface (Fig. 1), perhaps the author should provide this comparison. This is especially important as this calculation is used for an important step in the algorithm, calculating the area steeper than the critical slope, which in turn is the most sensitive model parameter.

Are the stream slopes calculated by this method comparable to the real world stream slopes measured in the field?

The report suggests that a 5x5 moving average is used to determine slope values for the stream power calculation. Is it really a moving average or just an average over a 5x5 grid? I can understand smoothing the values by averaging over 5x5 grids, but I cannot understand why a moving average would be used.

Contributing area is calculated by progressively summing the upflow area, using the bifurcation routing method. The report claims that it provides an accurate method for mapping the channel area in a DEM, which is a critical calculation in this method, but does not explain how that claimed accuracy is validated in comparison to alternative methods, including manual channel delineation. I will return to this question in the model output section. The report also does not explain the selection of Freeman's "p" parameter in eq 6-5.

Scour depth, another critical model parameter is calculated on the basis of only two studies. The first study, Squires and Young, 1984, estimated the maximum discharge as a function of contributing area for large floods. They suggest that they are describing floods with a recurrence interval of 100 years and 500 years, although there may be very large uncertainty associated with annual flood probabilities of rare floods. It should be noted that on Figure 13 of the Squire and Young study, there is an outlier.

The second study is Leopold et al., 1966 which found a relationship between scour depth and unit width discharge. The Leopold study estimated that scour depth varies as a function of the square root of the unit width discharge.

It should be pointed out, for example, that Leopold's study was based on a relatively short temporal record, and there was a great deal of scatter in his data. Leopold used linear regression to estimate the parameters B_0 (intercept) and B_1 (slope or exponent in the transformed data). They (Leopold et al, 1966) apparently did not force the regression through zero, so that the intercept is non zero. The intercept reflects what the predicted scour is when there is no discharge. In a process model, it makes no sense to have a non-zero intercept, and therefore the regression should probably be rerun forcing the intercept through zero. That will of course change the value of the B_1 value. In addition, the regression can be used to estimate the confidence intervals on the parameter estimates. It seems illogical to me to use a single value when there is documented uncertainty in its value.

When you combine the uncertainties from the Squire and Young study with the Leopold et al study, it is likely that the uncertainty will be large. I also should note that the units (English versus metric) for the various studies are not equivalent, and the regression estimates could be sensitive to the units, and incorrectly applied. Scour chain data is of course serially dependent if the chains are not removed and reinstalled. In other words, once a scour chain is installed, the scour depth measured can be cumulative for several floods unless the measurements are made after each individual event and the chains reinstalled.

On page 6-14, the author notes that this scour depth is a maximum value [caused] by "many large floods that will occur during the model duration". This statement seems wrong, in that it misstates how the scour value is used in comparison to "model duration". The scour depth is an instantaneous calculation and is not dependent on model duration. In fact the only section a "model duration" is used can be found in the diffusion calculations (later in the section).

It appears that the author considers the scour depth to be a single scalable parameter for every channel in the entire drainage basin based on the scour depth estimated at the narrows. Using one point to calibrate scour depth for the entire area clearly can create enormous compound errors if the method is invalid or the estimate of scour at that one point is inaccurate.

There is also field evidence (Fig. 2) that shows the channel does not simply fill with water in between the deep banks, but indicates that the channel is migrating like a wave form within the incised channel. Thus for those floods leaving a morphological record on the channel, the bank to bank use of scour depth does not seem justifiable.

Trying to extract a conceptual context of this scour depth is difficult because the author did not provide that in the conceptual model section. But on page 6-15, the author assumes that the scaling factor for scour depth is constant because the drainage basin "as a whole experiences the same overall climactic conditions". I assume the author meant climate conditions. The author needs to justify the assumption that this is a simple scaling factor. Regarding climatic conditions, I will address that issue later.

Step 4 calculates the total mass of tephra that will be moved from hillslopes greater than a critical threshold onto adjacent channels "where it is added to the tephra deposited ... by primary fallout". The algorithm description on page 6-17 is not

completely transparent. It seems as if the mathematical procedure is just a simple threshold and tephra is instantly removed if that threshold is exceeded. However later in section 6.5.2 where field measurements are discussed, the author suggests a range for critical slope is used and this range it a "uniform distribution between 0.21 and 0.47". I do not see how that "uniform distribution" is applied.

Figure 2: showing satellite image of Fortymile wash just above the RMEI alluvial fan. Note the evidence of channel shifting within the overall incised banks. This evidence indicates that the interpretation of scour depth used in the model is questionable in larger channels.

Again, the author does not provide any real world conceptual understanding of this process, but the model calculation basically considers hillslopes whose slope is greater than a specified threshold to be perfectly frictionless, so that any tephra that falls on it will simply slide into the adjacent channel without requiring any precipitation or flow. Once the tephra has "slid" into the adjacent channels, the core calculation of the dilution model is performed.

Eq. 6-14 reproduced from page 6-17.

$$dilution(i,j) = \frac{\left(\sum_{up} ashthickness(l,m)\right) + ashthickness(i,j)}{\left(\sum_{up} scourdepth(l,m)\right) + scourdepth(i,j)}$$

I have several concerns regarding the core algorithm of the dilution model, represented in equation 6-14 (p. 6-17). Please note that an independently reviewed peer-review publication, which is used for corroboration and validation later in the report, uses a **[min]** function to select the numerator in the dilution equation (eq. 3 Pelletier et al., 2007, in press). The difference between the two equations needs to be resolved to reflect what the FAR code actually is computing. I proceed on the assumption that the code functions exactly as described in MDL-MGR-GS-000006 REV 00A as shown above. By the way, given the distinction between ash and tephra, the model should perhaps, have used the term *tephrathickness* to avoid confusion.

First let's simplify the model's critical parameter calculation. Let's identify one particular pixel, which is the dilution at the outlet of the channel just before it supplies the fan with sediment. I must assume that this is a single pixel, as it is not identified explicitly in the text. Let's give the coordinates n,o for that pixel. If that pixel is the last pixel in the calculation of eq. 6-14, then we see that for that critical pixel, the dilution factor is a simple average of all the ash thickness and all of the presumed space for that ash to mix in the total channel scour depth for the entire drainage basin or:

$$\text{Dilution (n,o)} = \frac{\sum_{total} ashthickness(n,o)}{\sum_{total} scourdepth(n,o)}$$

As this is the governing equation for the dose calculations for the RMEI, it is this equation that requires particular scrutiny. This representation of eq 6-14 eliminates the misleading notion of tephra "routing". There is no dependence on any specific value upstream, rather it is a simple basin-wide average. Physically, it is the equivalent of taking a volume of ash and completely mixing it with a volume of uncontaminated sediment (which is calculated by assuming the accumulated basin-wide scour depth is that volume).

This calculation, for example, means that if a significant thickness of tephra fell directly on pixel n,o, as opposed to on the uppermost part of the basin, the concentration of the tephra in sediment at the fan apex would be very low even though the channel is buried by tephra. Recall that the basic model assumes an instantaneous mixing and redistribution of the upper basin channel sediments with tephra from hillslopes and channels and that the result of this instantaneous mixing is representative of the tephra concentrations in the channel at the fan apex for distribution to the RMEI fan channels. However, **this method clearly takes an instantaneous spatial average over the entire basin and physically assumes that the undiluted tephra sitting on the outlet waits (i.e., zero transport) until all the tephra and sediment from upstream are mixed and then mixed with the tephra on the outlet.** This result is confirmed in model output by Pelletier et al 2007, figure 9C. In particular, it assumes that during the "many floods" that accomplish the mixing, that no highly concentrated tephra from the basin outlet is transported to the RMEI. That does not seem reasonable given the process of stream flow and sediment

transport, although the dilution factor at n,o might eventually either intersect or converge with the predicted value.

We can also look at the dilution model by examining the first stream (or the highest) channel cell where the dilution can also be simplified to:

$$\text{Dilution}\ (1,1)\ \frac{ashthickness(1,1)}{scourdepth(1,1)}$$

In this calculation, the description on page 6-17 indicates that the dilution is calculated according to this equation for the ashthickness ≤ scourdepth, otherwise dilution is set to 1.

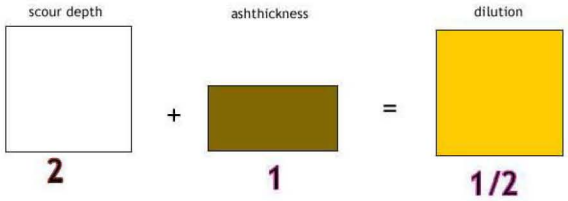

Figure 3: Dilution calculation where ashthickness < scourdepth.

We can visualize the quantities in Figure 3 above which shows the simple dilution calculation for the condition where ashthickness < 1. This calculation produces a sediment thickness equivalent to the original scour depth with half the original concentration of tephra. So for the first cell in the calculation in equation 6-14, this seems reasonable.

Figure 4: Dilution where ashthickness approaches scour depth.

However, as the ashthickness approaches and then exceeds the scour depth we see some problems concerning basic process assumptions. Figure 4 above shows at that as the tephra thickness approaches the scour depth, the channel is basically cutting or scouring in tephra. We must ask therefore, why the initial channel condition (grid) does not include the thickness of the direct tephra deposit and the hillslope contributions. In fact, the channel configuration could be significantly affected by the distribution of tephra following the first part of Step 4.

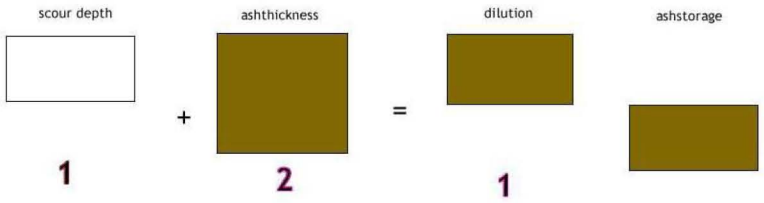

Figure 5: Dilution where ashthickness > scourdepth.

When the primary airfall and hillslope transported tephra in the channel exceeds the scour depth, we have a new set of inconsistencies appear. For this first cell we can easily see that the dilution is set to 1, or no dilution. However, we have excess tephra, indicated as ashstorage in Figure 5 above. The important question is what happens to this excess tephra? On the one hand, the model appears to state that the scour depth represents the maximum value of stream channel sediment in transport in any pixel and thus anything in excess of that value, ie scour depth, must be left behind. On the other hand, the "routing" equation actually sums the total tephra thickness, including the excess, which is made available for downstream transport and mixing. The model thus contradicts the physical assumptions upon which it was based. Please note that in Pelletier et al, 2007 in press, which is cited for validation, they identify the identical contradiction: "in the case of relatively thick (i.e. 1m) contaminant, however, some of the contaminant is stored indefinitely in channels of the source region because the scour depth is less than the contaminant thickness in some areas" but for Yucca Mountain it is assumed that all the tephra is mobilized regardless of thickness (Pelletier et al, 2007, in press preprint, page 9).

Step 5 estimates the initial concentration and thickness of tephra at the RMEI location, which is divided into "interchannel divides" and channels by mapping. The FAR model assumes that older fan surfaces are not subject to fluvial erosion or deposition. The thickness of tephra on these older surfaces is determined by converting tephra concentration (g/cm2) to an equivalent depth by using an estimate of tephra density (ρ) in equation 6-15a (p. 6-20). The tephra density is important because it is implicitly used to determine the concentration of waste as well (eq. 6-15b and 6-17). Should the author discuss what uncertainties are introduced as the density estimate changes?

Step 6 assumes a simple 1 D diffusion model represents the redistribution of radionuclides with the RMEI fan soils and channel sediments. The report states that "Field work was performed to measure the permeable soils thickness on divide surfaces". I am reasonably certain the author could use the same number of words to describe what was measured and how. This "measurement" is important because it is used to limit the depth of diffusion. A solution to the diffusion equation, taken from Carslaw and Jaeger (assumed validated), is used to solve for four output time series. Diffusivity was estimated by "fitting" with other data, but the method of that fit is not provided.

By assuming a simple diffusion model for the redistribution of radionuclides in the RMEI over time, the model fails to provide (as it also failed in the section on conceptual models) of why this model is appropriate given other processes that are known to occur. These include vegetative recycling of radionuclides, adsorption and cation exchange with fine materials and clays, and eolian redistribution.

Other parameters
Section 6.5.3 describes drainage density which is used to "define" the channel system in the drainage basin (STEP 3). A pixel is defined as a channel "if the calculated stream power is greater than a threshold value equal to the inverse drainage density". A small number of channel heads are used in a method to optimize the drainage density. The optimization is based on a minimization of distance between the selected channel heads and the model channels. There is circularity to this reasoning, as drainage density a variable in the optimization procedure is then used to estimate drainage density. Furthermore, there is no guarantee that these 34 channels produce a basin wide optimum drainage density. Finally, drainage density can be relict, meaning that the current drainage density does not always reflect modern conditions.

2. Are the mathematical relationships appropriate and representative of the scientific understanding of the geomorphic processes for the transport of sediment from the Fortymile drainage basin to the location of the RMEI on the Fortymile Wash alluvial fan?

No. As noted above lacking a conceptual model, there is no basis to accept or reject the underlying mathematics as conceptually appropriate or reasonable. The mathematics do not appear to be directly related to geomorphic processes of stream flow, sediment entrainment and transport, sediment deposition and storage, or even sediment mass balance. Also, there is no eolian component, despite field evidence for strong wind transport of sand size grains (and the eruption would produce silt-fine sand) from the RMEI channels onto the "interchannel divides". The FAR model belongs to class of models that might be called "reality conditioned lumped model" black-box algorithms. These are algorithms that work by using "cases" of logical if statements to work properly by conditioning output rather than process. For example, because the model does not actually route sediment by calculating sediment loads and mass balances during floods, it must rely on setting the condition that if the tephra is too thick (>scour depth) then it is just passed to the next channel pixel until it may finally be used in the dilution equation for the outlet.

The model presented as equation 6-14 is almost identical to the residence time model with ideal mixing for a lake, rather than a process-based fluvial dilution model. In the lake system, pollutants enter the lake, mix rapidly so the concentration is effectively the sum of the total input divided by the total volume of the lake. That is exactly what this model does for the ***dilutionfactoroutlet*** pixel. Could that work for a fluvial system? Yes. Under the conditions where the supply of the contaminant was fixed spatially and temporally, and sufficient time was allowed for the system to possibly reach quasi equilibrium conditions, perhaps it could provide a reasonable dilution estimate. This model would still be vulnerable to large errors if the contaminant was spatially concentrated at the lake outlet which would make it harder to mix efficiently before exiting (the equivalent of thick tephra sitting on the pixel where the dilution factor for the fan is calculated).

One key assumption is the requirement of hydraulic equivalency of the tephra load with the uncontaminated stream channel sediment load. Equivalency means that the two components would be affected by fluvial processes in exactly the same way. For example, if the tephra load is finer than the uncontaminated channel sediment, then it will be preferentially transported by floods, invalidating the ideal mixing model. If the tephra is very fine, it is likely that some of the contaminated tephra will be deposited in RMEI channels even before all of the hillsope tephra has "slid" into the channels. Each of these realization make the application of the ultimate time dependent portion of the model, i.e. diffusion of the radionuclides on RMEI surfaces, more difficult to apply because there is no simple initial condition.

In particular, if the tephra includes silt, there will almost certainly be hydraulic sorting of the ash from the channel sediment, instead of mixing, and potential for actually concentration of radionculides through further chemical processes. The likelihood of contaminated silt size tephra, or ash, also increases the chances of redistribution from RMEI channels onto RMEI divides, at time scales outside the simple boundary conditions of the diffusion model.

Model Output

The model output can be evaluated in several ways, using intermediate outputs, the model results, and sensitivity analyses included in the report. By overlaying some of the intermediate results in Google Earth, I could determine whether there were obvious problems with the delineation of the drainage basin (Fig. 6), slopes, location of channels, etc. These all seemed reasonable, overall.

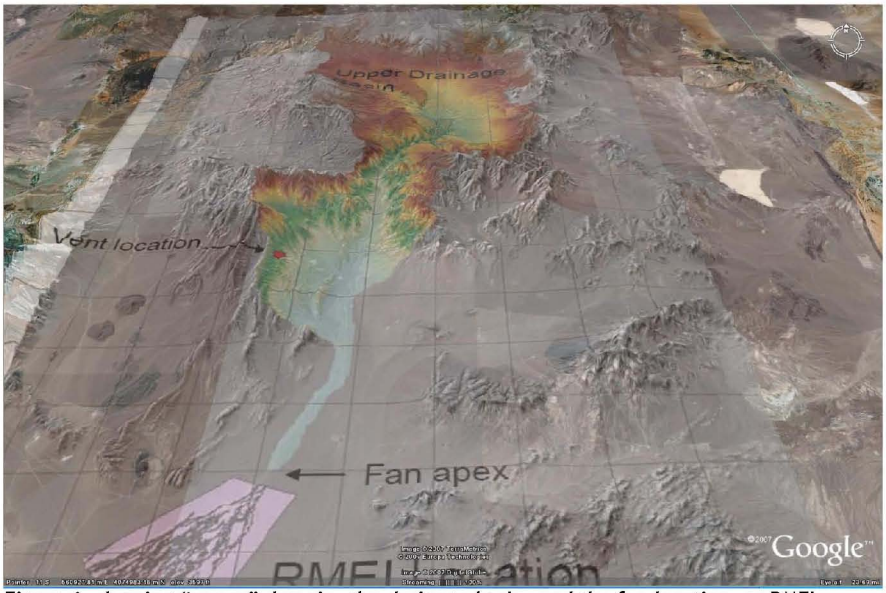

Figure 6, showing "upper" domain, the drainage basin, and the fan location, or RMEI location, projected onto an elevation and satellite base in Google Earth. There is an unfortunate gap between the drainage basin and the area identified as fan.

In examination of the slope grid (Fig. 7), there were features that seemed to be artifacts from either the DEM or the algorithm. The features included a "herringbone pattern" which also occurs in other parts of the upper basin, and lineaments that terminate slope classes. I am uncertain if these hold any significance in the overall performance of the algorithm.

In examination of the "contributing area grid" (Fig. 8A), one finds channels that appear discontinuous and take the form of small fans. These channel "fans" are found throughout the drainage basin and suggest that these might indeed represent places where contaminant storage occurs. Are these channels included in the "routing" and if so what happens to the upstream tephra load if a channel ends? From a physical process perspective, it is clear that the tephra might be stored and therefore mixing is not complete, however, based on statements in Pelletier et al 2007, p. 9, it is also clear that the total cumulative tephra thickness is included in the calculation of dilution at the drainage basin outlet.

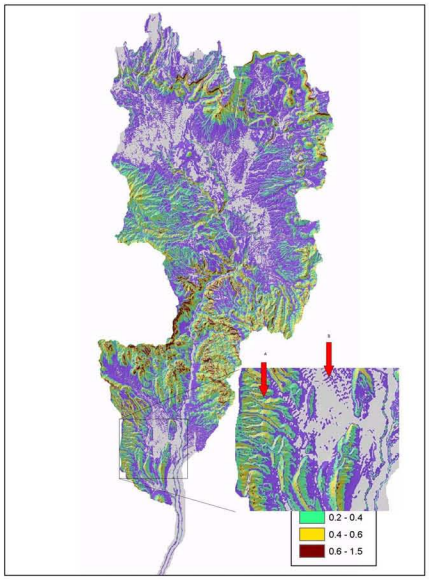

Figure 7, showing slope grid from section 6, figure 6.3.3-3, output from FAR, with arrows indicating features that seem anomalous.

Near the fan outlet, I examined how well the bifurcation method defined the main channel of Fortymile wash (Figure 8B). The resolution of the output I had did not allow precise comparison, however, I suggest a detailed comparison be made.

The model output for the dilution factor calculations highlight several relevant concerns regarding the model performance (Fig. 9). I focus on the lower part of the upper drainage basin just before the flow enters the RMEI location. This is the section of Fortymile wash where the dilution factor at the outlet is calculated. It would useful to identify the single pixel which is actually used for the initial RMEI concentration on that figure.

Note that in the inset (Fig. 9), that the dilution values appear to vary within the channel, in some places appear discontinuous, and for short reaches seems to be concentrated along a channel that is a single pixel wide. The fact that the channel appears to be a single pixel wide in this section of Fortymile wash suggests that the bifurcation method may not be entirely effective in distributing flow correctly for those 500-year floods, or that this figure is not showing the model results correctly.

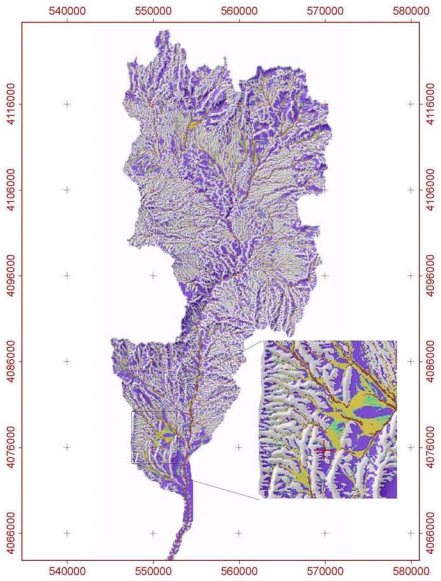

Figure 8: A) Above, showing contributing area output grid from FAR model. Note that in the inset, once can see that the channels are not always continuous, and appear to form fan shaped features. B) Below, channel definition near fan outlet compared to satellite image.

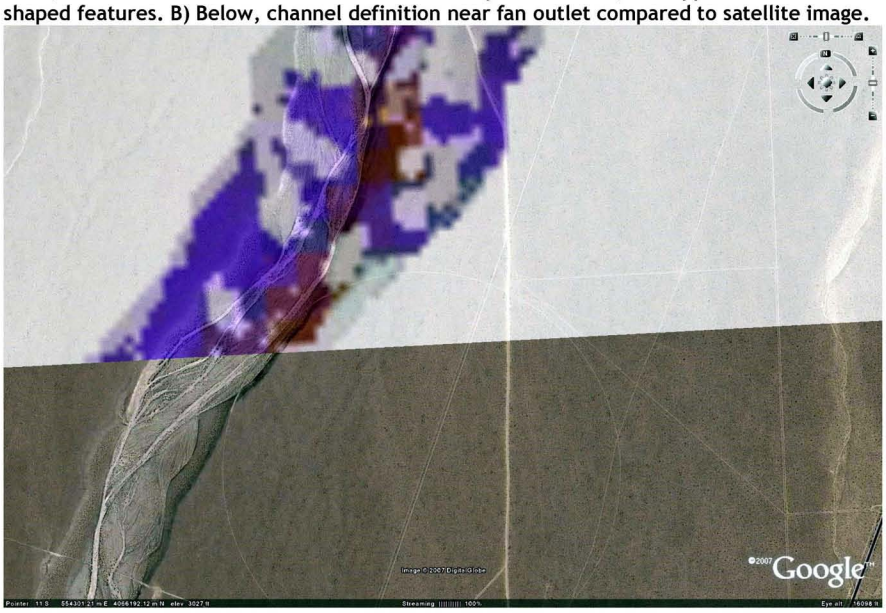

Also note that although the dilution factor for this model run was in the 0.3 - 0.1 range for most of this section of the wash, at the presumed outlet, the dilution was in the 0.01 - .1 range, or as much as a factor of 10 more dilute. Given the close proximity of these pixels, it would be useful to see what the actual range was, instead of the binned ranges, and to understand fully the impact of picking one particular pixel for the initial RMEI concentration.

The sensitivity analyses, section 6.6.2, explored some of the dependencies among the parameter variables and their impact on the dilution factor at the outlet pixel. The results are presented as a series of scattergrams with regression lines. I note that it is the convention to scale these plots according the data ranges rather than arbitrarily. The author should include the confidence intervals on the regression line slope estimate. For example, the scattergram of initial waste concentration versus drainage density (report figure 6.6.1-1 c?) does not appear to be statistically significant. In other words, the drainage density does not affect the dilution factor at the outlet. This confirms that the model itself is largely insensitive to factors that affect the primary geomorphic processes, which here is the density of stream channels carrying contaminated tephra towards the RMEI (channels) location.

In contrast, the sensitivity analysis identifies the model variable which is most significant, or highly weighted, in controlling the initial waste concentration, which is the critical slope. This is easily explained as this value is the largest part of the numerator in the governing equation for dilution, eq. 6-14. The estimated value for the slope of the regression line is about -2.0. In other words as the critical slope threshold increases, the initial waste concentration is halved. If the FAR report included the function that relates the area of the drainage basin to the DEM estimated slope, one could see how this dependency was related to the increases in tephra area.

Perhaps the author could produce a scattergram which relates initial waste concentration to area at or above the critical slope, which is a more understandable way of seeing the dependency. Unsurprisingly, the scour depth, the denominator in eq. 6-14 was the second most significant variable. The report concludes the sensitivity analysis section (p. 6-52) with the statement that the analyses “provide confidence that the model is functioning as expected and also provide information that could be used in the future to guide activities aimed at epistemic uncertainty”. It would be useful if the author identified what epistemic uncertainty was considered important.

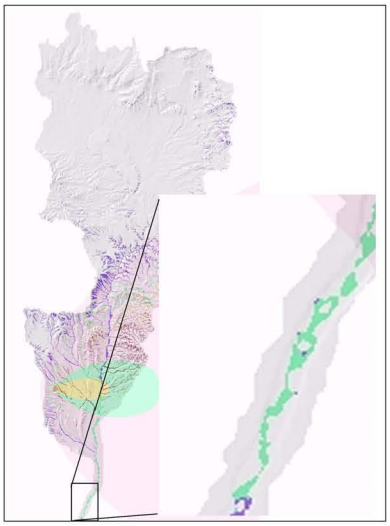

Figure 9, showing dilution factor output for one set of initial conditions, given in section 6 figure 6.3.3-6. The inset shows the part of the Fortymile wash channel that is used to provide the initial contaminant concentration to the RMEI channels.

3. Are the outputs of the model reasonable and representative?

Yes. The outputs of the model, specifically the intermediate outputs, the model results, and sensitivity analyses, are in general reasonable within the context of the model's implicit and explicit assumptions and mathematics.

With local exceptions that might highlight weaknesses in the possible robustness of the algorithms, including the core bifurcation routing algorithm, the output seems internally consistent and representative of the model assumptions and mathematics.

The results also seem representative of the realizations allowable under model conditions. The significance of local anomalies in the model output, specifically the ones cited above (slope, contributing area) is not known.

4. Are there alternative models or approaches that should be considered?

The current model takes one of the simplest approaches possible to estimate the initial RMEI waste concentrations (note: the simplest approach is to assume undiluted tephra at all RMEI locations). For the channels it assumes perfect and instantaneous basin wide mixing independent of tephra location relative to the basin outlet. For the "inter-channel divides" the model assumes the initial waste concentration to be equal to the primary waste fallout which diffuses away with time. In this way, the current model will always predict a time dependent decrease in radionuclide concentration with time after the volcanic eruption. It might also be useful to allow the model to weight the dilution as a function of distance from the basin outlet with respect to tephra transport. In this way, one could at least see the importance of little time for mixing in the scenario where a significant thickness of tephra falls directly on the basin outlet.

In this reviewer's opinion, alternative models, specifically those that allow for post eruptive concentration of waste from the tephra by chemical and physical processes, might attenuate the decrease of radionuclide concentration with time, or modulate that function in a complicated way. The redistribution of ash by wind could be a significant factor where the volcanic eruption produces a sizable fine particle size fraction. Models that produce higher waste concentrations with time are, from a probabilistic point of view, the ones most worthy of considering given the estimate for the annual probability of a volcanic eruption (1.7×10^{-8}).

Recall that the current model is assuming that current, very current in fact, stream channel conditions will persist throughout the performance period. If conditions change, periods of channel aggradation might occur, resulting in incomplete mixing and perhaps even long term storage. Those processes that allow for slower more efficient hydraulic sorting of the sediment load will produce excursions from the ideal mixing model presented.

The key logical argument made by the current model is that the tephra particle size distribution is equivalent to the channel sediment particle size distribution throughout the channel system, allowing the tephra to behave or be treated exactly like the existing bed load. The current model does not actually model the transport of bed load in any way, while an alternative model might explore the impact on sediment yield of different tephra particle size distributions in order to determine the relative transport out of the drainage basin so that implication for dilution and mixing could be explicitly determined.

This basic logical branch is illustrated in Figure 10, indicates that where wind processes are potential transport agents of redistributed ash, the impact on RMEI dose estimates could be high.

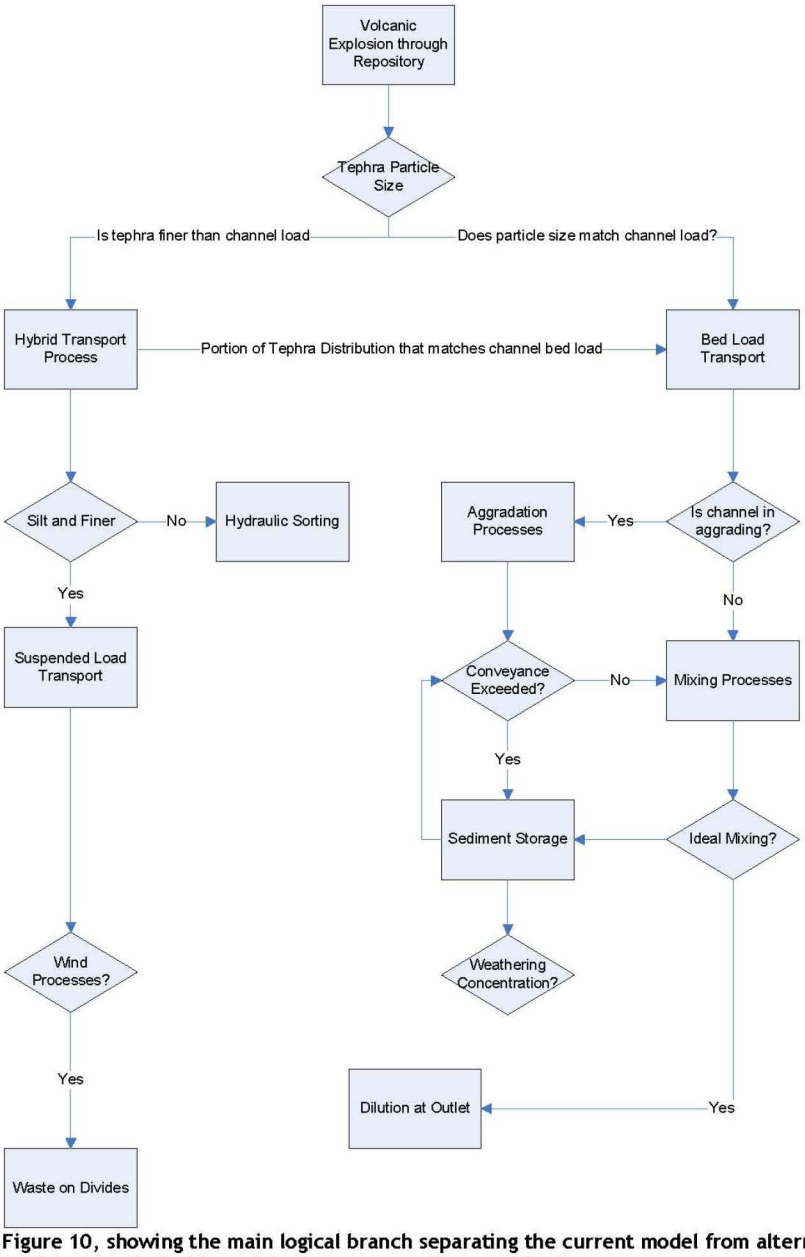

Figure 10, showing the main logical branch separating the current model from alternative models. That logical branch is the one regarding particle size.

Limitations

5. Are the limitations of the model adequately described?

Model limitations are listed in section 1.2 and further discussed in Section 5.

The basic assumption of the model is mixing of tephra and sediment in the channel during transport. This assumption is not stated in section 5. The other assumption is the lack of any concentration processes.

Each of the stated assumptions could be significantly elaborated, however, a few require comment here. The model assumes no floodplain sedimentation (section 5.1.3). I interpret this mean that there is no significant channel storage of tephra, which would affect the dilution calculations (reducing the numerator in eq 6-14). Although there maybe no visible floodplains, there could be significant storage if the channel experiences a period of aggradation, as might be expected following a pulse of sediment supply caused by the deposition of tephra in the channels. The model assumes that the rate of hillslope and fluvial redistribution is instantaneous (section 5.2.1). It also assumes that it occurs in two "instants" because the hillsope transport of tephra to the channels must occur before the channel redistribution. The model also assumes "dynamic equilibrium", an assumption with questionable authenticity. Because the model assumes instantaneous mixing, it would also be plausible to assume instant mixing in the instant following the first instant when, the waste-contaminated tephra is washed out of the channels. Clearly, in a few "instants", there considerably less tephra in the channels as dilution progresses. However, the author states that

> "it takes ≈ 10,000 yrs or greater for uncontaminated hillslope sediment to replace the quantity of contaminated sediment in the channel scour zone shortly following the eruption. This residence time implies that after the concentration in the RMEI peaks, values will decrease gradually as clean sediment is eroded from the hillslopes and mixed in the channels. Approximately 10,000 yrs after the eruption, clean sediment will have replaced the contaminated material in the RMEI channels to the scour depth."

This logic contradicts the notion of mixing of sediments (the basic assumption of the model) versus replacement, and also is based on a maximum of rate hillslope erosion of 10cm/1000yr (p. 5-4) a rate that makes it impossible for the model to transport tephra (especially if the thickness is in excess of 10cm) from hillslopes to the channel instantly.

The model assumes negligible eolian transport to the RMEI location. The author identifies a "third transport pathway" which is the transport from channels to the divide areas. I have already stated that given the particle size distribution from the ASHPLUME model, this will be a factor. The author noted sand streaks from the channels, which indicate that if silt mixed with fine sand was available, it would be entrained by winds and carried onto the divides. Also see Figure 11A.

The model assumes that transport will be bed load. Given the particle size distribution expected from the eruption (see revised section 5.2.3) it is almost certain that part of the tephra load will be transported as suspended load.

The model assumes that the migration of all radionuclides can be modeled with same diffusivity. The differences in chemical characteristics between the various radionuclides suggest that is not strictly true. Cesium may tend to stay in the surface layer because of its binding with high cation exchange capacity minerals.

Unstated assumptions include the fact that the tephra particle size distribution will match the existing hydraulic characteristics of the channel bed load, which is unlikely.

It assumes that the scour depth is primarily a linear dependency, despite the fact that storm intensity and duration could be more important. It assumes that scour depth is non-zero everywhere in the drainage basin, which might require bedrock scour.

It assumes that the bifurcation routing method is adequate for delineating the channel boundaries (see Fig. 8B).

It assumes that the tephra deposit will not produce any dams in the stream channels, and it assumes that the channel configuration after the first instant (hillslope movement of tephra to channels on top of primary tephra fall) is reasonable, even though that channel configuration is not used for the actual "routing".

It assumes that the present topographic surface represents the peak concentration of radionuclides with time. If for example radionuclides were concentrated with the calcium carbonate in the calcrete, and at a later time the divide was eroded down to that level, the maximum concentration would actually be higher than the present surface.

It also assumes that the peak concentration in the surface at the RMEI location is the initial concentration. If wind processes, which are known to concentrate silts on these surfaces, were to occur, concentrations could increase with time.

It assumes that no sediment concentration of radionuclides occurs, even though stream processes contribute to a significant part of the global resources of uranium, in conglomerates for example.

Validation

6. Are the model validation activities (in addition to validation by critical review) that have been planned in the TWP and reported in the model report appropriate and adequate, and adequately and correctly conducted and interpreted?

The field data should be validated by a visit and inspection by an Independent Technical Reviewer. The mapping of the alluvial fan can be somewhat subjective and requires validation. In addition, measurements of the wind blown contributions to the soil surface are needed. There is no evidence that an impermeable layer exists under the channels. The estimate of scour depth on the RMEI channels needs validation, especially if scour is being confused with incremental deposition.

The critical slope measurements came from the San Francisco Volcanic Field sitting on the already topographically high Colorado Plateau. I am unconvinced that these measurements are directly applicable to the very different weather conditions found in the Fortymile wash drainage basin.

Bulk 137Cs concentration measurements were made in shallow pits to estimate or validate diffusivity estimates. It was unclear how these data were adjusted for multiple dosings caused by multiple above ground nuclear tests, or underground tests that leaked radionuclides to the surface through fractures and fissures.

The square root dependence of scour depth with unit width discharge is accomplished with different units (metric versus English) than in the original Leopold study. Furthermore, the Leopold study did not force the regression through the origin, but the Powell et al. study citied, did force the regression through the origin (no intercept). Therefore they are not directly comparable until they are done the same way.

The report uses a simple Hjulstrom diagram (p. 7-17, fig 7.2.5-1) to assert that transport is dominant across the alluvial fan and therefore the fan is not a "perfect depozone" The problem with this application of the Hjulstrom diagram is that the alluvial fan is not an engineered structure where you can control which flow variable changes. The differences between the main channel in the drainage basin (upper domain) and the alluvial fan channels attest to the systematic adjustment to altered flow conditions. Specifically, in the very likely case where discharge decreases because stream flow is abstracted (lost by infiltration) through the channel floor, then the logic used in the report is clearly inadequate and inappropriate. While the fan may not be a "perfect depozone" its very existence suggests that it is a depozone, and many floods will not cross the entire fan without significant discharge loss and hence deposition. This again raises the points made earlier regarding significant accumulation of silts in the fan channels and wind redistribution onto the RMEI divide areas.

Validation of diffusion constants is problematic due to the variability in soils and climate characteristics. Perhaps a term, "effective" diffusion constant might be more useful.

Corroboration in Refereed Journal

Section 7.3.1 discusses the use of Pelletier et al 2007, a peer reviewed article to be published in the journal Geomorphology as a method for corroboration of model results. I will briefly discuss the data presented in this section that is relevant to usefulness of this journal article as corroboration.

There are significant differences between the two model scenarios. In the Lathrop Wells study, tephra thickness is not used for model input, rather measured concentrations are applied from field measurement. In addition, the stream system studied is small compared to Fortymile wash. In Lathrop Wells, the basaltic (tephra) and non-basaltic (clean) sediment are known to be of similar grain size.

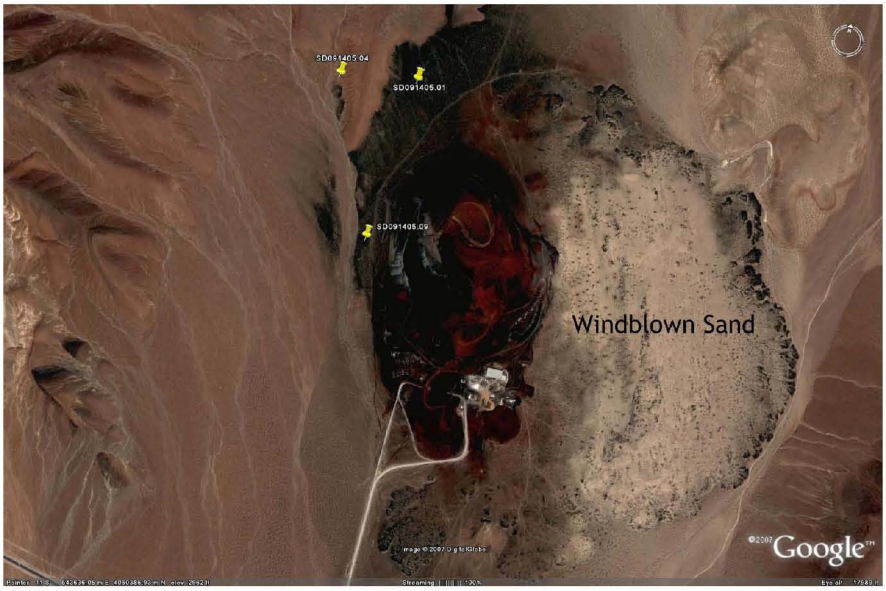

Figure 11: showing the Lathrop Wells cone: A) above the tephra sheet, and basalt flows. Note the accumulation of sand blown onto the tephra. B) Below the locations of data used in Lathrop Wells study. Note the area of stream confluence indicated by the white square.

I attempted to validate the locations of the samples in Google Earth using the data provided in Table 7.3.1-1, but found that my plotted points did not apparently match exactly with those in figure 7.3.1-2. However, I was able to get a general sense of the locations, and the setting of these samples (see Fig. 11A).

The report notes that single samples were taken at single locations along the stream channels, but there is no information regarding amount of sample taken. I would note that coarse deposits require very careful sampling and could easily require multiple large samples at each channel location.

A portion of the data collected is plotted on Figure 7.3.1-2 (p. 7-29), including a graph with a tephra concentration plotted on a log axis. This semi log plot is somewhat misleading, in as much as it gives large visual weight to the small differences in less concentrated samples. If you were to re-plot these data on linear axes (Fig. 12), you would basically see, as you can simply read from Table 7.3.1-1, that there appears to be two groups of concentrations in each of the streams studied. For example in the western stream one group of values ranges from between 70-80% and the other ranges from 36-47%. While you can perform a regression, and obtain a line showing decreasing concentration with distance, it seems simpler to say that there are two samples which vary in concentration. Thus I do not find any compelling data that corroborates the model. The photo presented in figure 7.3.1-3 showing the high and low concentration channels probably represent the two classes of concentration. That area is shown in the white rectangle in Figure 11B and plotted in Figure 12 below.

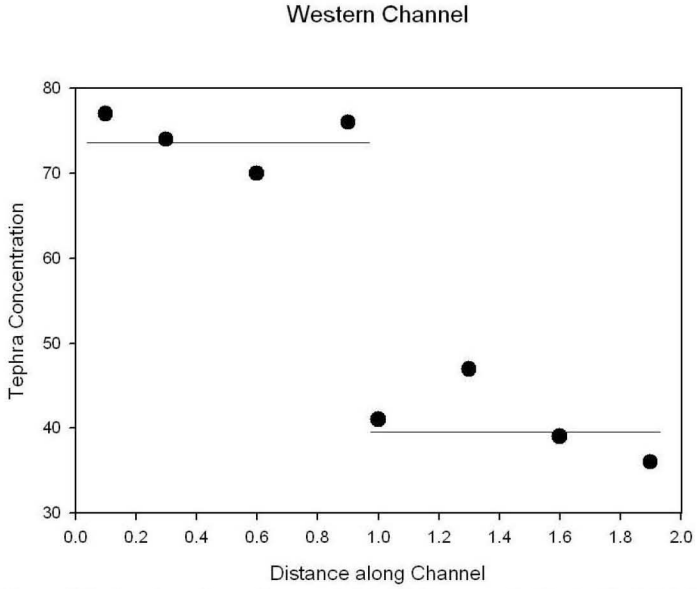

Figure 12: showing alternative model for data presented in Table 7.3.1-1 that indicates no downstream dependency, rather just two separate populations.

Perhaps more puzzling are the data that were not plotted from Table 7.3.1-1 (data numbers 1405.04-1405.07). These data represent concentration of the western stream flowing south, where it meets the stream that was flowing on the tephra sheet. Why are these concentrations so high? If they are coming from an area with a background concentration of 9%, and do not mix with other tephra draining streams, how did the concentrations get higher than the original source?

I also am confused by the model result shown as a line on the lower graph on Figure 7.3.1-2 B, labeled 3D model prediction which has a spike just upstream of data point 1405.11.

Given the uncertainties associated with channel sampling and the lack of a convincing downstream variation, there is no strong case for corroboration of the mixing model here. On the contrary, the strong reversals in concentration downstream and in direct opposition to the model prediction, stresses the fact that ideal mixing and dilution is not occurring. Also note on Figure 11A, the blanket of windblown sand that could represent the level of eolian flux across the Fortymile wash fan.

APPENDIX D
NOMENCLATURE USED

D. BACKGROUND

All of the parameters / symbols / terms used in the report are defined within the report text, in the section where they are first introduced. As a reference, those parameters / symbols / terms used in multiple sections of the report are also defined here.

D1. INPUT PARAMETERS FOR THE TEPHRA REDISTRIBUTION MODEL

Developed input parameters

S	Critical slope for tephra mobilization from hillslopes (dimensionless)
X	Average drainage density [the ratio of the total length of channels in a drainage basin to the basin area] in the Fortymile Wash drainage basin (km^{-1})
H ($scourdepth_{narrows}$, $scourdepthoutlet$)	Depth of scour in Fortymile Wash at the fan apex (cm)
F	Decimal fraction of the area of the Fortymile Wash alluvial fan subject to fluvial activity (channels) (dimensionless)
A	Area of the Fortymile Wash alluvial fan (the RMEI domain) potentially subject to redistributed tephra deposition (km^2);
L	Depth of permeable soil (channels or interchannel divides) at the RMEI location (cm)
D	Diffusivity of waste in soil (channels or interchannel divides) at the RMEI location (cm^2/yr)

Subscripts for developed input parameters:

c	Channels
d	Interchannel divides

General input parameters

Δt	The output time step (yr)
T	The model duration (yr)
rvent	The radius below which no tephra is mobilized (m). For example, if *rvent* = 500 m, all tephra that is deposited between the vent location and a 500 m radius is assumed to remain on the landscape.

oflag — The output grids flag; this variable indicates whether spatial grids (elevation, slope, contributing area, and pre-processed tephra and waste grids) should be output. This flag can be set to 1 for testing [send grids to output file], or 0 for use within the total system performance assessment (TSPA) [do not send grids to output file] (dimensionless).

Input that is directly taken from BIOSPHERE output:

B — The biosphere depth (cm); FAR outputs the areal (depth-integrated) radionuclide concentration between the surface and depth *B*, which represents a critical depth in the biosphere model

Input that is either directly taken from ASHPLUME output, or a function of ASHPLUME output:

ρ *(ashsettleddensity)* — Tephra settled density (g/cm^3)

xvent — The easting coordinate location of the vent in UTM zone 11S, NAD 27 datum (m) [NOTE: The default vent location is the center of the drift area (i.e., the mean value of the minimum and maximum drift boundaries in the N-S and E-W directions).]

yvent — The northing coordinate location of the vent in UTM Zone 11, NAD 27 datum (m)

gridflag — This variable indicates whether a Cartesian or a polar grid is input from ASHPLUME. If *gridflag* = 0, a Cartesian grid is used. If *gridflag* = 1, a polar grid is used.

minx — The distance between the western boundary of the input ASHPLUME grid and the vent location (km). Used only if *gridflag* = 0.

maxx — The distance between the eastern boundary of the input ASHPLUME grid and the vent location (km). Used only if *gridflag* = 0.

miny — The distance between the southern boundary of the input ASHPLUME grid and the vent location (km). Used only if *gridflag* = 0.

maxy — The distance between the northern boundary of the input ASHPLUME grid and the vent location (km). Used only if *gridflag* = 0.

N_x — The number of columns in the input ASHPLUME grid (dimensionless). Used only if *gridflag* = 0.

N_y — The number of rows in the input ASHPLUME grid (dimensionless). Used only if *gridflag* = 0.

minrad	The smallest radius of the input ASHPLUME grid (m). Used only if *gridflag* = 1.
rfactor	The radial multiplicative factor for the input ASPLUME grids. Radial coordinates within the ASHPLUME input grids are not linear, but increase geometrically with *rfactor*. For example, if *rfactor* = 2.0, each radial sample is greater than the last by a factor of 2.0 (dimensionless). Used only if *gridflag* = 1.
N_r	The number of radial samples of the ASHPLUME grid (dimensionless). Used only if *gridflag* = 1.
N_θ	The number of azimuthal samples of the input ASHPLUME grid (dimensionless). Used only if *gridflag* = 1. Note: The polar coordinate system is defined with $\theta = 0$ being due north and values of θ increasing in a clockwise direction. This definition is equivalent to most of the igneous models within TSPA but differs from the input wind data for ASHPLUME.
ashdepositionRMEI	The tephra concentration at the RMEI location output by ASHPLUME (g/cm^2)
fueldepositionRMEI	The waste concentration at the RMEI location output by ASHPLUME (g/cm^2)

D.2 TEPHRA REDISTRIBUTION MODEL VARIABLES

The following variables are used within FAR V.1.2 and appear within the mathematical model. In some cases, multiple variable names are given. In these cases, the first variable is the mathematical symbol used in the equations of this document. The second variable is the variable name used in the FAR source code. In rare instances, the third variable name is that used in Section 7.

ashthickness(i,j)	The local tephra thickness at each channel pixel in the basin (cm), designated by d_{df} in the equations
C_d	The radionuclide concentration in the soil profile on interchannel divides at the RMEI location (includes temporal effects of diffusion) (g/cm^3)
C_c	The radionuclide concentration in the soil profile in channels at the RMEI location (includes temporal effects of diffusion) (g/cm^3)
C_{d0} *(fueldivideinit)* *(fuelinitsurfacedivide)*	Initial radionuclide concentration for the depth of tephra and contaminant initially deposited on the interchannel divides at the RMEI location (g/cm^3); calculated as *fueldepositionRMEI*/ *primaryashthickness*

C_{c0} *(fuelchannelinit)* *(fuelinitsurfacechannels)*	Initial radionuclide concentration in the soil profile in channels at the RMEI location (g/cm^3); calculated as: $\frac{fueldepositionRMEI}{scourdepthoutlet} + \frac{\rho \bullet dilutionfactoroutlet \bullet fyeknibukuzed}{ashmobilized}$
concentration(i,j)	The decimal fraction of channel sediment composed of tephra at each channel pixel in the basin (dimensionless)
contribarea(i,j)	The contributing area upstream of each pixel in the basin (km^2)
d_{df} *(primaryashthickness)*	The primary tephra and associated waste thickness on interchannel divides at the RMEI location (cm); calculated as *ashdepositionRMEI*/ρ.
d_{cf} *(depthfuelchannel)*	The total tephra and associated waste thickness (including both primary tephra/waste and redistributed tephra/waste) in channels at the RMEI location (cm); equal to *scourdepthoutlet*
dilution(i,j)	dilution factor at each channel grid cell (dimensionless)
dilutionfactoroutlet	The decimal fraction of channel sediment composed of tephra at the fan apex [also called the basin outlet] (dimensionless)
fueldepthBdivide	depth-integrated concentration (from the surface to the biosphere depth, *B*) in the divides (g/cm^2)
fueldepthBchannel	depth-integrated concentration (from the surface to the biosphere depth, *B*) in the channels (g/cm^2)
fuelsurfacedivide	waste concentration in the surface soils on the interchannel divides of the RMEI location (g/cm^3)
fuelsurfacechannel	waste concentration in the surface soils in the channels of the RMEI location (g/cm^3)
ashmobilized	The total mass of tephra mobilized from steep slopes and active channels in the upper basin of Fortymile Wash (g) which influences the concentration at the outlet
fuelmobilized	The total mass of waste mobilized from steep slopes and active channels in the upper basin of Fortymile Wash (g) which influences the concentration at the outlet
power(i,j)	The product of an average of the local of the local slope and the square root of contributing area of each pixel in the basin (km)

routedscour(i,j)	The routed scour depth of each channel pixel in the basin (cm)
routedash(i,j)	The routed tephra depth of each channel pixel in the basin (cm)
scourdepth(i,j)	The local scour depth of each channel pixel in the basin (cm)
slope(i,j)	slope (dimensionless)
slopeavg(i,j) ($slope_{avg}$)	The 5 × 5-grid cell average of the local slope (dimensionless)
t	Time following the simulated eruption (yr)
z	Depth in the soil profile below the surface (cm)

INTENTIONALLY LEFT BLANK

APPENDIX E
VERIFICATION OF THE SOLUTION TO AN INITIAL-VALUE PROBLEM

Section 6.5.8 states that

$$\frac{C(z,t)}{C_0 d_w} = \frac{1}{\sqrt{\pi D t}} \exp(-z^2/4Dt), z \geq 0, t \geq 0 \quad \text{(Eq. E-1)}$$

is a solution to the equation

$$\frac{\partial C(z,t)}{\partial t} = D \frac{\partial^2 C(z,t)}{\partial z^2}; z \geq 0, \quad t \geq 0 \quad \text{(Eq. E-2)}$$

subject to the boundary condition

$$\frac{\partial C(z,t)}{\partial z} = 0, z = 0, t \geq 0 \quad \text{(Eq. E-3)}$$

and the initial condition of a mass $C_0 d_w$ concentrated at z=0 (a delta function). The initial condition is that

$$C(z,0) = 0, z > 0 \quad \text{(Eq. E-4)}$$

and

$$\int_0^\infty C(z,0) dz = C_0 d_w \quad \text{(Eq. E-5)}$$

This appendix first develops the partial derivatives of the solution given in Equation E-1 and then shows that the solution satisfies, respectively, Equations E-2, E-3, E-4, and E-5. The time derivative is

$$\frac{1}{C_0 d_w} \frac{\partial C(z,t)}{\partial t} = -\frac{1}{\sqrt{\pi D t}} \left(\frac{1}{2t} - \frac{z^2}{4Dt^2} \right) \exp(-z^2/4Dt), z \geq 0, t \geq 0 \quad \text{(Eq. E-6)}$$

The first spatial derivative is

$$\frac{1}{C_0 d_w} \frac{\partial C(z,t)}{\partial z} = -\frac{1}{\sqrt{\pi D t}} \left(\frac{2z}{4Dt} \right) \exp(-z^2/4Dt), z \geq 0, t \geq 0 \quad \text{(Eq. E-7)}$$

The second spatial derivative is

$$\frac{1}{C_0 d_w} \frac{\partial^2 C(z,t)}{\partial z^2} = -\frac{1}{\sqrt{\pi D t}} \left(\frac{2}{4Dt} - \frac{4z^2}{(4Dt)^2} \right) \exp(-z^2/4Dt), z \geq 0, t \geq 0 \quad \text{(Eq. E-8)}$$

Therefore,

$$\frac{D}{C_0 d_w}\frac{\partial^2 C(z,t)}{\partial z^2}\begin{cases} = -\dfrac{1}{\sqrt{\pi D t}}\left(\dfrac{1}{2t}-\dfrac{z^2}{4Dt^2}\right)\exp(-z^2/4Dt) \\ = \dfrac{1}{C_0 d_w}\dfrac{\partial C(z,t)}{\partial t} \end{cases}, z \geq 0, t \geq 0 \qquad \text{(Eq. E-9)}$$

so that Equation E-2 is satisfied.

Evaluating Equation E-7 at z=0,

$$\frac{1}{C_0 d_w}\frac{\partial C(z,t)}{\partial z} = 0\exp(0) = 0, z = 0, t \geq 0 \qquad \text{(Eq. E-10)}$$

so that Equation E-3 is satisfied.

The quotient on the right-hand side of Equation E-1 becomes an indeterminate form as t approaches zero, both the numerator and denominator approaching zero. Therefore, it is necessary to take the limit as t approaches zero. For $z > 0$,

$$\frac{C(z,0)}{C_0 d_w} = \lim_{t\to 0}\frac{\exp(-z^2/4Dt)}{\sqrt{\pi D t}} = 0, z > 0 \qquad \text{(Eq. E-11)}$$

and Equation E-4 is satisfied.

Finally, integrating Equation E-1 for $t > 0$,

$$\frac{1}{C_0 d_w}\int_0^\infty C(z,t)dz = \int_0^\infty \frac{1}{\sqrt{\pi D t}}\exp\left(-z^2/4Dt\right)dz = \operatorname{erf}(\infty) = 1, t > 0 \qquad \text{(Eq. E-12)}$$

so that the total mass is always $C_0 d_w$. Therefore, the solution satisfies Equation E-5 in the limit as t approaches zero.

Because the function in Equation E-1 satisfies the differential equation in Equation E-2, the boundary condition in Equation E-3, and the initial conditions of Equations E-4 and E-5, it is a valid solution of the stated initial-value problem.